LIBRARY VOLUME 40

Copy 2

THE PHYSICAL REVIEW

PUBLISHED BY THE

AMERICAN INSTITUTE OF PHYSICS

INCORPORATED

UNDER THE EDITORIAL SUPERVISION OF THE

AMERICAN PHYSICAL SOCIETY

BOARD OF EDITORS

Managing Editor, JOHN T. TATE, University of Minnesota, Minneapolis

Assistant Editor, J. W. BUCHTA, University of Minnesota, Minneapolis

K. F. HERZFELD, A. W. HULL, F. W. LOOMIS, A. J. DEMPSTER, DAVID M. DENNISON, J. C. SLATER, R. C. GIBBS, E. O. LAWRENCE, J. M. VAN VLECK

AUGUST 1, 1932

On the Effect of a Secondary Structure upon the Interference of Xrays — H. M. Evjen 333
Analysis of the (0, 0) $^1\Pi \rightarrow {}^1\Sigma$ CN Band at 3182Å — Allan E. Pearson 338
Dirac Electron in Simple Fields — Milton S. Plesset 353
Infrared Absorption Spectrum of Carbon Dioxide — E. H. Hulburt and R. F. Barrow 364
Vibrational Levels of Linear Symmetrical Triatomic Molecules — David M. Dennison 378
Two-Minima Problem and the Ammonia Molecule — David M. Dennison and G. E. Uhlenbeck 379
Nuclear Moment of Barium as Determined from the Hyperfine Structure of the Ba II Lines — P. Gerald Kruger, E. C. Kemble and R. C. Williams 387
Elimination of One Boundary Condition for a Sphere in Radiative Equilibrium by a Layer in Adiabatic Equilibrium — Harold Bondi 398
Magnetic Susceptibilities of Alpha- and Beta-Manganese — Mary A. Weinstein 401
Magnetic Susceptibility of Nitrogen Dioxide — Glenn G. Haven 407
Barkhausen Effect. III. Nature of Change of Magnetization in Elementary Domains — Richard M. Bozorth and Joy F. Dillinger 408
Variation with Temperature of the Thermoelectric Power of Nickel and Some Copper-Nickel Alloys — E. R. Grew 422
Diamond Windows for Withstanding Very High Pressures — Thos. C. Poulter and Francis Buckley 429
Effect of Pressure on the Index of Refraction of Paraffin Oil and Glycerine — Thos. C. Poulter, Carter Ritchey and Carl A. Rees 434
Letters to the Editor — 435
Probable Values of e, h, e/m and e/h—A Reply to R. T. Birge — W. N. Rose 435
Relation of Relative Humidity to the Absorption of Supersonic Waves in Various Mixtures of CO_2 — Harry E. Bodine 440
Constants of the N_2O Molecule — E. F. Barker 442
Raman Effect of Methyl Acetylene — Geo. Glockler and H. M. Davis 446
Structure of Atomic Nuclei — James H. Bartlett, Jr. 450
Reciprocal Effect as a Special Case of the Barrier-layer Photoelectric Cell — R. H. Muller and A. Schuster 451
Note on the Hyperfine Structure of Rhodium Lines — P. Gerald Kruger and R. C. Williams 454
Newton's Rings in Transparent Metallic Films — J. R. Nathanson 457
Total Secondary Electron Emission from Metal Foils — S. Ramachandra Rao 459
Theory of the Ozone of the Lower Atmosphere and its Relation to the General Problem of Atmospheric Ozone — Oliver R. Wulf 465
Surface Tension of Two Liquid Phases of Nitrobenzene — A. M. Thomas and F. L. Bailey 467
Raie Band System of Barium Hydride in the Infrared — William W. Watson 467
Raman Effect and Perturbations in the CO Analyzers and the H_2 Bands — Wyman W. Watson 468
Rate of Gas Absorption in Counting Chambers — L. V. Compton 470

Book Reviews — 471

Proceedings of the American Physical Society — 475

Current Literature of Physics

THE AMERICAN PHYSICAL SOCIETY

OFFICERS OF THE SOCIETY

President:	W. F. G. Swann	Bartol Research Foundation, Philadelphia, Pa.
Vice-President:	Paul D. Foote	The Gulf Companies, Pittsburgh, Pa.
Secretary:	W. L. Severinghaus	Columbia University, New York City
Treasurer:	G. B. Pegram	Columbia University, New York City
Editor:	John T. Tate	University of Minnesota, Minneapolis, Minn.
Local Secretary for the Pacific Coast:	L. B. Loeb	University of California, Berkeley, Calif.

THE PHYSICAL REVIEW

Published by the American Institute of Physics under the editorial supervision of the American Physical Society. Four volumes annually, six issues per volume.

First series. From July 1, 1893, to January 1, 1913, the Review was conducted by Edward L. Nichols, Ernest Merritt and Frederick Bedell, with the financial support of Cornell University. The first four volumes were issued annually; subsequent volumes, semi-annually; thirty-five volumes in all.

Second series. On January 1, 1913, the Review was transferred to the American Physical Society as announced on the first page of the new series which was then begun. Since then it has been conducted by a Board of Editors elected by the Society. Volumes 1-38 are semi-annual, beginning in January and July of each year from 1913 to 1931. Volumes 1-33 contain six issues each. Volumes 34-38 twelve issues. Beginning with Volume 39 there will be four volumes per year of six issues each.

Contributors are referred to page 2 of the advertisements for further information.

Annual subscription, throughout the Postal Union, $12.00 in advance.

General index, 1893-1920, $4.00 in advance.

Back Volumes. Volumes 1-38, $9.00 per volume; Volume 39, $4.50; Back Numbers, $1.50 per copy for issues prior to July 1, 1929 (Vols. 1-33), $.75 per copy for issues subsequent thereto. Postage is free if remittance accompanies order; otherwise postage is extra. No bound volumes can be supplied. The Review offers to purchase a limited number of First Series, Vol. 1, No. 1 (at $2.00 each); Second Series, Vol. 7, No. 1, January 1916; Vol. 7, No. 2, February 1916; Vol. 7, No. 4, April 1916; and Vol. 7, No. 5, May 1916 (at $2.00 each).

Advertisements. Rates will be supplied by the Editor on request. Copy for each number must be received at Minneapolis two weeks prior to the dates of issue; old copy is used until new copy is received. Send electrotypes direct to printers, George Banta Publishing Co., Menasha, Wis.

Discount of ten percent is allowed to members of the American Physical Society on purchase of back numbers.

Changes of Address and Complaints of failure to receive the Review, in the case of members of the Physical Society, should be addressed to the Treasurer; in the case of other subscribers, to the Editorial Secretary. New copies can be sent free in response to complaints of non-delivery only if notice of non-delivery is received within three months of date of issue.

Manuscripts for publication should be submitted to the Editor, Physical Review, University of Minnesota, Minneapolis, Minn.

Proof and all correspondence concerning papers in process of publication should be addressed to the Editorial Secretary, American Institute of Physics, 11 East 38th Street, New York, New York.

Subscriptions, renewals, and orders for back numbers should be addressed to the Editorial Secretary, American Institute of Physics, 11 East 38th Street, New York, New York.

Entered at the post office at Menasha, Wis., as second class matter.
Acceptance for mailing at special rate of postage provided for in section 1103, Act of October 3, 1917, authorized September 6, 1926.

Second Series *August 1, 1932* *Vol. 41, No. 3*

THE

PHYSICAL REVIEW

On the Effect of a Secondary Structure upon the Interference of X-rays

By H. M. EVJEN*

Norman Bridge Laboratory of Physics, California Institute of Technology

(Received June 17, 1932)

Laue's dynamic theory of x-ray interference is shown to be applicable, with only a few minor changes, to crystals having a very general type of secondary structure. It is thus applied for the purpose of obtaining a quantitative estimate of the effect of such a structure upon the nature of the x-ray interference maxima. The estimate is relative insofar as it compares the intensities of respectively the "secondarily" and the "primarily" reflected interference beams and applies only in the region where the latter have been, or can be observed. In this region the "two-dimensional lattice" type of secondary structure is found to give rise to a fine structure which, with the present insufficient resolving power, would be manifested experimentally as a weak, diffuse background. The secondary structure of this type produces *no broadening* of the primary lines. The existence of this type of structure, therefore, is not inconsistent with the sharpness of the interference maxima obtained from such crystals as calcite, and a possible objection to the existence of the secondary structure in such crystals is removed. The extinction effect is briefly considered, but absorption is not taken into account, except with a few qualitative remarks.

ARGUMENTS against the existence of a secondary structure[1] in crystals have been raised from time to time in the literature on the basis of the nature of the x-ray interference patterns. For instance,[2] it has been argued that the sharpness of the x-ray interference lines from such crystals as calcite is not consistent with the presence of a secondary structure. This argument, if theoretically tenable, would be very weighty on account of the reliability and great accuracy of the x-ray spectroscopy; and its consequences would be far reaching in the theory of the solid state.[3] For this reason, and also in view of the possibility of enlisting the aid of the x-ray spectroscopist in the detection and analysis of secondary structures, it is desirable to obtain a quan-

* National Research Fellow.

[1] Not to be confused with a "mosaic structure." For the sense in which these terms are here used, see F. Zwicky, Phys. Rev. **40**, 63 (1932).

[2] M. Siegbahn, *Spektroskopie d. Röntgenstrahlen*, 2d Ed., p. 60 (1931).

[3] As pointed out by Siegbahn, in reference 2, we would have as an immediate effect that Zwicky's explanation of the discrepancy between the values of the electronic charge obtained respectively by direct measurement and by x-ray analysis would be rendered unsatisfactory. (See F. Zwicky, Proc. Nat. Ac. **16**, 211 (1930)). There is, however, at present some controversy as to whether or not this discrepancy is significant.

titative estimate of the effect of such structures upon the interference of x-rays.[4]

Laue's dynamic theory of x-ray interference[5] is directly applicable to crystals having a very general type of secondary structure. In fact, the formulae developed by Laue remain formally the same when his theory is applied to crystals having such a structure; only the symbols involved must be given a slightly different interpretation. In order to prove this proposition we shall have to review briefly the physical background of Laue's theory.

Laue's theory in contradistinction to Ewald's[6] earlier theory and Waller's[7] modification thereof, is based on the supposition that the negative electric charges are distributed in an arbitrary manner over the entire lattice cell. It contains Ewald's theory as a special case when certain restrictions are placed on a group of symbols whereby the concentration of the said charges at the lattice points is accomplished.

His theory owes its simplicity and elegance to the following ingenious considerations.

First he shows that it is permissible to assume that for small displacements the displacement of the negative charges at any point in the lattice cell is proportional to the electric field strength at that point. The proportionality factor is calculable in principle, but since it does not enter directly into the theory, it is not necessary to go into the question as to how this factor may be calculated.

Secondly, on account of the large masses with which the positive charges are associated, these do not take any appreciable part in the scattering of the x-rays. They may therefore be distributed in any manner whatsoever over the lattice cell, provided we specify that they shall not be displaced by the electric vector. The positive charges, in fact, may be distributed in such a way that when there is no disturbing field they exactly neutralize everywhere the negative charges. A field then produces in every point of space a polarization which is proportional to the field strength at that point. The magnitude of the polarization is characterized by a proportionality factor varying from point to point within the crystal. By thus distributing the positive charges we therefore arrive at a fictitious body whose dielectric constant varies with the coordinates. In the real body, with its positive charges concentrated in the immediate neighborhood of the lattice points, the electromagnetic wave field is exactly the same. The fact that the two bodies differ electrostatically is of no consequence for our purpose.

In order to obtain the solution of the interference problem it is now only

[4] Darwin, (See reference 15), has already calculated the effect of one type of imperfections in crystals. The type of secondary structure which will be considered here, however, is essentially different from Darwin's imperfections.

[5] M. v. Laue, Erg. d. ex. Naturwiss **10,** 133 (1931).

[6] P. P. Ewald, Series of papers starting with Ann. d. Physik **54,** 519 (1917). The general method embodied in Ewald's and Laue's works is more convenient for our purpose than the method employed by Darwin in a still earlier paper, C. G. Darwin, Phil. Mag. **27,** 315, 675 (1914).

[7] J. Waller, Uppsala Universitets Aarsskrift (1925).

necessary to solve Maxwell's equations for a medium having a triply periodic dielectric constant. In the case of the ideal crystal, as treated by Laue, the periodicities of the dielectric constant, ϵ, must conform with the periodicities of the primary lattice of the crystal. In the case of the crystal having a secondary structure, on the other hand, the *periodicities of* ϵ *must conform with the periodicities of the secondary structure.* The primary structure here appears as a very prominent higher harmonic. Instead of representing ϵ itself as a triply periodic Fourier summation it is more convenient for the purpose of calculation thus to represent the factor $\psi = 1 - 1/\epsilon$ which determines the polarization, $\mathcal{D}(1 - 1/\epsilon)$, $\mathcal{D}$ being the electric displacement vector of the electromagnetic field. If we understand by, $(\boldsymbol{a}_1^0, \boldsymbol{a}_2^0, \boldsymbol{a}_3^0)$ the primitive translations of the primary lattice, and by $(\boldsymbol{b}_1^0, \boldsymbol{b}_2^0, \boldsymbol{b}_3^0)$ the corresponding elementary vectors of the reciprocal lattice, we have for the ideal crystal:

$$1 - 1/\epsilon = \psi = \sum \psi_m e^{-j(\boldsymbol{b}_m \cdot \boldsymbol{r})} \tag{1}$$

where

$$\boldsymbol{b}_m = \sum_{\alpha=1}^{3} m_\alpha \boldsymbol{b}_\alpha^0; \; j = 2\pi(-1)^{1/2}.$$

m_α is an integer, and $\boldsymbol{r}$ is the independent variable radius vector measured from an arbitrary lattice point.

From the definition,

$$\boldsymbol{b}_k^0 = [\boldsymbol{a}_i^0 \times \boldsymbol{a}_j^0]/(\boldsymbol{a}_i^0 \boldsymbol{a}_j^0 \boldsymbol{b}_k^0) \tag{1a}$$

it follows immediately that each term in the series (1) is periodic with the three periods $(\boldsymbol{a}_1^0, \boldsymbol{a}_2^0, \boldsymbol{a}_3^0)$.

This is the starting point for Laue's theory. For crystals having a secondary structure Eq. (1) must be slightly modified. Let the periodicities of the secondary structure be $(\boldsymbol{D}_1^0, \boldsymbol{D}_2^0, \boldsymbol{D}_3^0)$. Let the corresponding reciprocal lattice be defined by,

$$\boldsymbol{B}_k^0 = [\boldsymbol{D}_i^0 \times \boldsymbol{D}_j^0]/(\boldsymbol{D}_i^0 \boldsymbol{D}_j^0 \boldsymbol{D}_k^0). \tag{2}$$

The polarization factor[8] now must be represented as follows:

$$1 - 1/\epsilon' = \phi = \sum \phi_m e^{-j(\boldsymbol{B}_m \cdot \boldsymbol{r})} \tag{3}$$

where

$$\boldsymbol{B}_m = \sum_{\alpha=1}^{3} m_\alpha \boldsymbol{B}_\alpha^0.$$

By the definition (2) we are assured that each term in the series (3) is periodic with the three periods $(\boldsymbol{D}_1^0, \boldsymbol{D}_2^0, \boldsymbol{D}_3^0)$.

[8] This factor, as Laue points out, is akin to, and takes the place of the structure factor of the elementary theory; but only in so far as the polarization is proportional to the density of charge with a *constant* proportionality factor can it be said to be a measure of the distribution of charge.

Eq. (3) is formally the same as Eq. (1), the only differences being that ϕ and ϕ_m have replaced ψ and ψ_m, and $\boldsymbol{B}_m$ has replaced $\boldsymbol{b}_m$. From this it follows that any subsequent formula that may be derived on the basis of Eq. (3), in conjunction with Maxwell's questions, must be formally the same as the corresponding one derived by Laue on the basis of Eq. (1), since any subsequent development is of a purely mathematical nature. We can therefore write immediately in the place of Laue's fundamental Eqs. (I):[9]

$$\frac{K_m'^2 - k^2}{K_m'^2} \mathfrak{D}_m = \sum \phi_{m-q} \mathfrak{D}_{q[m]} \tag{I'}$$

where $\mathfrak{D}_m$ represents the electric displacement of the plane wave propagated in the direction of K_m' given by,

$$K_m' = K_0 + \boldsymbol{B}_m \tag{4}$$

and $\mathfrak{D}_{q[m]}$ represents the component of $\mathfrak{D}_q$ perpendicular to K_m'. k is the reciprocal of the vacuum wave-length.

When these conditions are fulfilled the solution of Maxwell's equations for a medium having the dielectric constant specified in Eq. (3) is given by,

$$\begin{aligned} \mathfrak{D} &= e^{i\nu t} \sum \mathfrak{D}_m e^{-i(\boldsymbol{K}_m' \cdot \boldsymbol{r})} \\ \mathfrak{H} &= e^{i\nu t} \sum \mathfrak{H}_m e^{-i(\boldsymbol{K}_m' \cdot \boldsymbol{r})} \end{aligned} \tag{5}$$

$\mathfrak{H}$ being the magnetic field strength.

Each member of this triple sum represents a plane wave propagated in the direction of K_m' with the phase velocity

$$v = \mathbf{v} / \left| K_m' \right|$$

ν being the frequency of the wave field which is assumed to be monochromatic. The index of refraction of the plane wave therefore is given by:

$$n = c/v = c \left| K_m' \right| / \nu. \tag{6}$$

It follows moreover from Maxwell's equations that the electric vector $\mathfrak{D}_m$ is perpendicular to the vector K_m' as well as to $\mathfrak{H}_m$. Hereby the number of unknowns, (components of $\mathfrak{D}_m$ perpendicular to K_m'), as well as the number of algebraic equations in (I') is reduced to $2N$ where N is the total number of vectors $\mathfrak{D}_m$, in general infinity.

Now to solve the infinite set of linear, homogeneous Eqs. (I') in general, not only is impracticable by the methods of existing mathematics but also is useless, since as Laue points out, only a finite number of the plane waves have an appreciable intensity. If, therefore, we follow the example set by Laue and neglect all the vectors $\mathfrak{D}_m$ except those that have an appreciable absolute value, the fundamental Eqs. (I') reduce to a finite set of linear, homogeneous equations which can be solved by ordinary methods. The criterion by which this reduction is brought about is the same as that employed by Laue in the case of the ideal crystal, and for practical purposes is

[9] See reference 5, p. 139.

most easily obtained by geometrical considerations in the reciprocal space. For a detailed account of the method, however, we shall refer to Laue's admirable paper.[5] Here we shall only consider the changes brought about in the reciprocal lattice by the introduction of the secondary structure. Although the following assumption is not necessary, we shall for simplicity assume that the secondary structure belongs to the same crystallographic group as the primary structure. Then we have:

$$\boldsymbol{D}_i^0 = M_i \boldsymbol{a}_i^0; \qquad (i = 1, 2, 3) \quad (7)$$

where

$$M_1 \sim M_2 \sim M_3 \sim M \qquad (7a)$$

are integral numbers all of the same order of magnitude. From Eqs. (1a) and (2) it then follows that,

$$\boldsymbol{B}_i^0 = \boldsymbol{b}_i^0 / M_i \qquad (8)$$

By this equation the relation between respectively the primary and the secondary reciprocal lattice is determined.

Now in order to obtain a quantitative estimate of the effect of the secondary structure it is necessary first to derive the relative magnitudes of the Fourier coefficients ψ_m and ϕ_m appearing respectively in Eqs. (1) and (3). From the general theory it is known that the secondary structure must be considered as a very slight modulation of the primary structure. In other words,

$$\psi_P > \phi_\pi$$

provided the triplet $\pi = (\pi_1, \pi_2, \pi_3)$ does not represent an integral multiple of the triplet $M = (M_1, M_2, M_3)$. In the latter case, that is when $\pi = Mq = (q_1 M_1, q_2 M_2, q_3 M_3)$, the exponential function by which ϕ_π is multiplied in the summation (3) is the same as the exponential function by which ψ_q is multiplied in the summation (1), and we have,

$$\psi_q \sim \psi_P \sim \phi_{Mq}.$$

A closer estimate is possible by sacrificing some of the generality. That is, if we exclude the type of secondary structure in which the individual blocks are tilted with respect to each other, it is clear that the ratio ϕ_π / ψ_P must be of the order of magnitude of the relative amplitude of deviation in lattice constant from the primary value. This amplitude of deviation is given particularly on the basis of the one,[10] but also on the basis of the other,[11] of the two general types of secondary structure lately propounded in the literature, as follows:

$$\Delta/a \sim a/D \sim 1/M.$$

Consequently the relative order of magnitude of the two Fourier coefficients is given by,

[10] F. Zwicky, Helv. Phys. Acta **3**, 287 (1930).
[11] F. Zwicky, Phys. Rev. **38**, 1772 (1931).

$$\phi_\pi/\psi_P \sim 1/M; \qquad (\pi \neq M_q) \quad (9)$$

where M usually is of the order of 50 or larger.

Eqs. (8) and (9) in conjunction with the formulae derived by Laue enable us to arrive at the desired estimates. The constructions in the reciprocal space are the same as those employed by Laue except that a number of lattice points are added in accordance with Eq. (8) as illustrated in Fig. 1.

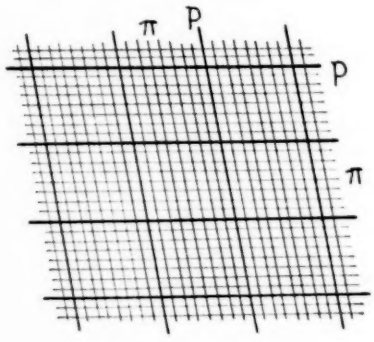

Fig. 1. Reciprocal lattice.

Associated with these additional lattice points are structure factors ϕ_π which bear the relation (9) to the factors ψ_P of the primary lattice points.

In the simplest possible case, that is when only one of the vectors $\mathcal{D}_m$, namely $\mathcal{D}_0$, has an appreciable absolute value, we obtain:

$$\mathcal{D}_\pi = (\phi_\pi/2\epsilon_\pi)\mathcal{D}_{0[\pi]}$$

$$\mathcal{D}_P = (\psi_P/2\epsilon_P)\mathcal{D}_{0[P]}.$$

Therefore, when the quantities ϵ_π and ϵ_P are roughly the same,[12] that is, when the "propagation sphere" passes at roughly the same distance from the secondary lattice point π as from the primary point p, and the geometrical status of the two points is otherwise roughly the same, our theory yields,

$$\mathcal{D}_\pi/\mathcal{D}_P \sim \phi_\pi/\psi_P$$

or by Eq. (9):

$$(\mathcal{D}_\pi/\mathcal{D}_P)^2 \sim 1/M^2. \qquad (10)$$

For the order of magnitude of M which we have indicated this ratio is very small. Nevertheless, when we consider the total or integrated energy scattered by the secondary structure we may arrive at a very sizable figure since the density of the secondary scattering centers in the reciprocal space is M^3 greater than that of the primary scattering centers. For the ordinary experimental setup, however, it is clear that this scattering from the secondary structure could be manifested only as an apparently diffuse background of radiation.

[12] See reference 5, Eq. (14a).

When more than one of the vectors $\mathfrak{D}_m$ have an appreciable absolute value we can usually write down relations similar in context to Eq. (10). Only in very particular cases do situations arise in which the plane wave created by interference from the secondary scattering centers is comparable in intensity with those produced under similar circumstances from the primary scattering centers. In these cases, however, the solid angular regions over which this intensity prevails is of the order $1/M^2$ for the secondary interference beams as compared with the primary ones. Therefore, again the experimental detection of the secondary interference beams would be very difficult.

We shall consider one such case somewhat more in detail, namely the practically very important Bragg reflection. This we shall do only in the symmetrical case, that is when the reflecting planes are parallel to the surface of the crystal. The more general case, where this condition is not fulfilled, presents no principally greater difficulties, but neither does it add any essentially novel features, so nothing is gained by its inclusion.

In the crystal of infinite thickness perpendicular to the reflecting planes the secondary as well as the primary structure will give rise to total reflection over certain angular regions. These angular regions are defined by the Eqs. IIIa and IVa derived by Laue,[13] equations which we shall reproduce here:

$$\chi_m = \chi_B + \psi_0/\sin 2\chi_B \tag{11}$$

$$\Delta\chi = 2(\psi_m\psi_{-m})^{1/2}/\sin 2\chi_B \tag{12}$$

where χ_B is the Bragg angle defined by the equation,

$$n\lambda = 2d\cos\chi_B$$

χ_m is the midpoint of the region of total reflection, and $\Delta\chi$ is the width of this region. In order to obtain the corresponding quantities for the reflection from the secondary structure it is only necessary to substitute ϕ_m for ψ_m and $D\sim Md$ for d. It follows immediately that,

$$\Delta\chi_\pi/\Delta\chi_P \sim |\phi_\pi| / |\psi_P| \sim 1/M. \tag{13}$$

For a somewhat divergent beam of incident, the apparent intensities of reflection are proportional to these widths. Again the intensity of reflection from the secondary structure is small compared with the intensity of reflection from the primary structure. Moreover, the interference maxima from the two structures ordinarily do not overlap[14] since ψ_P is of the order of magnitude 10^{-6} which hence is also the order of magnitude of the width $\Delta\chi_P$, whereas the distance between neighboring midpoints of the interference maxima is of the order $\lambda/2Md$ which is ordinarily very much larger than 10^{-6}. This type of secondary structure consequently produces no apparent widening of the primary lines, in contradistinction to the mosaic structure introduced by Darwin[15] to explain certain anomalies of x-ray reflection. Dar-

[13] See reference 5, p. 157.

[14] This is a point of considerable importance since otherwise it would be necessary to consider not only two of the rays K_m' simultaneously but three.

[15] C. G. Darwin, Phil. Mag. **43**, 800 (1922).

win's type of mosaic structure is characterized by an angle of tilt between the elementary blocks. Such a contingency has not been taken into account in the present theory, and our results represent not a contradiction but rather a complement to those of Darwin. Whereas such an angle of tilt is apparently, in most cases, a necessary result of the energetic considerations which led to the second type of secondary structure,[11] the angle of tilt is not an adjunct of the secondary structure of the first kind.[1] In other words, our theory applies to the latter type of structure. Incidentally this was the type of structure employed by Zwicky[3] to explain the discrepancy between the values for the electronic charge obtained respectively by direct measurement and by x-ray analysis. If this discrepancy should turn out to be significant, Zwicky's explanation consequently will remain consistent with the great sharpness of the interference lines obtained from such crystals as calcite.

In spite of the weakness of the individual interference maxima arising from the secondary structure the total or integrated intensity obtained from this source when the crystal is turned through a certain finite angle may be quite appreciable, since the number of secondary interference maxima by the Bragg arrangement in general is M times greater than that of the primary maxima. Again, however, this "secondarily" reflected radiation would be manifested for experimental purposes, (with the employment of hard x-rays), as a diffuse background. This would be particularly true when the secondary structure is no longer ideal, but is degenerated into a mosaic structure, which is to be expected unless the crystal is grown under very carefully controlled conditions; for it is clear that the mosaic structure, in its effects, would bear a somewhat analogous relation to the ideal secondary structure, as the thermally agitated lattice, in its effects, bears to the ideal static one.

To complete the theory we shall consider briefly the effect of the finite thickness of the crystal. Total reflection, strictly speaking, is only obtained when the crystal is nonabsorbing and has an infinite thickness. When the crystal has a finite thickness some of the energy in the angular regions defined by Eqs. (11) and (12) is transmitted through the crystal. The energy of the transmitted beam drops off exponentially from the reflecting surface. The rapidity with which the intensity drops off depends on the coefficient in the exponent of the exponential factor. This coefficient, κ, which may be called the extinction coefficient varies from zero at one extremity of the angular region defined by Eqs. (11) and (12) through a maximum and back to zero at the other extremity. This maximum is given to a sufficiently close approximation by Laue's theory as follows:

$$\kappa_{\max} = k(\psi_m \psi_{-m})^{1/2}. \tag{14}$$

From this it is seen that the extinction coefficient is of the order M times greater for the primary interference beams than for the secondary ones. For crystals of finite thickness, therefore, the efficiency of reflection from the primary structure may be enormously greater than the efficiency of reflection from the secondary structure. Thus the relative intensity of the secondary interference beams is no longer given by the ratio $1/M$; this ratio now must

be multiplied by a factor containing exponential terms depending on the thickness of the crystal, and this factor may be very small when the crystal is thin although it reaches a value of unity asymptotically as the thickness is increased. Incidentally these considerations show that the intensity of the interference beams from the secondary structure must be reduced more by absorption than the primary beams, since the former traverse more of the crystal before they are reflected than the latter.

It should be noted that the present theory is only concerned with the *relative* intensities of the interference maxima for x-rays of the same wavelength. Nothing has been said about the absolute value of the Fourier coefficients involved, except in so far as they are known from measurements on the primary interference beams. It is therefore quite conceivable that measureable interference maxima from the secondary structure will be obtained when x-rays of sufficient softness to exclude the primary lines are employed. In this case, moreover, it is doubtful whether or not Laue's theory is applicable since the boundary solution, (i.e., the interference pattern from the cross grating forming the boundary of the crystal), might be expected to come within the region of observables.

Analysis of the (0,0) $^2\Pi \rightarrow {}^2\Sigma$ CN Band at 9168A

By ALLAN E. PARKER
Sloane Physics Laboratory, Yale University

(Received June 8, 1932)

The rotational structure of the 0,0 band of the red CN system has been analyzed by means of spectrograms taken in the first order of a 21-foot grating. The values obtained for the various constants are $B_0'' = 1.8906$ cm^{-1}, $B_0' = 1.6907$ cm^{-1}, $D_0' = -6.07 \times 10^{-6}$ cm^{-1}, $A = -53.3$ cm^{-1}, $p_0 = 0.009$ cm^{-1} and $q_0 = -0.0008$ cm^{-1}. These are in agreement with the values obtained by Jenkins, Roots and Mulliken for transitions which involve higher vibrational levels of the $^2\Pi$ state. The origin of the band is at 10905.12 cm^{-1}.

INTRODUCTION

RECENTLY Kiess[1] has reported the existance of strong carbon bands in the infrared beyond 9000A. It seemed desirable to photograph these as they might or might not be the 0, 0 and 1, 1 bands of the $^2\Pi \rightarrow {}^2\Sigma$ CN band system whose position has been determined by Asundi and Ryde.[2] Analysis of the bands shows them to be these transitions. The results obtained are in agreement with those of Jenkins, Roots and Mulliken[3] who have analyzed transitions involving higher vibrational levels of the $^2\Pi$ state.

EXPERIMENTAL PROCEDURE

The source used was a 220 volt d.c. arc drawing 9 amperes. Spectrograms were obtained upon xenocyanine plates recently developed by the Eastman Kodak Company. These plates were hypersensitized with ammonia and exposed for nine hours in order to obtain sufficiently strong spectrograms. The dispersive apparatus was a 21-foot grating mounted stigmatically. Plates were taken in the first order, the dispersion for this region being 4.78A per mm. Second and third order iron lines were used for the comparison spectrum.

ROTATIONAL ANALYSIS

The rotational analysis of the 0, 0 band yields the six main branches. The satellite, ${}^oP_{12}$ and ${}^pR_{21}$, branches are not strong enough to permit of identification. In the region to the violet of the 1, 1 band, the six principal branches of the 0, 0 band account for virtually all the lines observed. For the equations giving the term values and for the combination relations reference is made to the article of Jenkins, Roots and Mulliken. Table I gives the wave-numbers of the various branches of the 0, 0 band. The appearance of the bands is quite similar to that of the 8, 3 band of which a reproduction is shown in reference three.

[1] C. C. Kiess, Bureau of Standards, Journal of Research **8,** 393 (1932).
[2] R. K. Asundi and J. W. Ryde, Nature **124,** 57 (1929).
[3] F. A. Jenkins, Y. K. Roots and R. S. Mulliken, Phys. Rev. **39,** 16 (1932).

TABLE I.

K''	R_2	Q_2	P_2	R_1	Q_1	P_1
0	10,931.83					
1	33.62	10,929.69			10,878.25	
2	35.05	27.10			79.08	
3	36.13	24.42			79.48	
4	36.82	21.48			79.08	
5	37.27	18.26			78.05	
6	37.27	14.97		10,901.80	76.62	
7	36.82	10.89		02.90	74.65	
8	36.13	06.59		03.71	72.44	
9	35.05	02.02		04.18	69.59	
10	33.62	897.19		04.18	66.43	
11	31.83	92.02		03.71	62.65	
12	29.77	86.39		02.72	58.56	
13	27.27	80.42		01.17	53.89	
14	24.42	74.28		899.64	48.86	
15	21.23	67.66		97.77	43.37	
16	17.63	60.73		95.11	37.55	
17	13.69	53.38		92.02	31.02	
18	09.35	45.67		88.36	24.20	
19	04.66	37.55		84.60	17.01	
20	899.60	29.18	10,762.19	80.42	09.39	
21	94.08	20.35	50.06	75.49	01.20	
22	88.36	11.19	37.44	70.21	792.72	
23	82.09	01.57	24.54	64.60	83.80	10,705.83
24	75.49	791.71	11.36	58.56	74.38	693.19
25	68.48	81.37	697.39	52.05	64.62	80.09
26	61.07	70.69	83.49	45.15	54.44	66.59
27	53.38	59.62	68.99	37.55	43.87	52.63
28	45.15	48.16	54.20	30.15	32.86	38.17
29	36.63	36.30	38.94	21.98	21.44	23.46
30	27.68	24.01	23.46	13.40	09.64	08.35
31	18.31	11.36	07.43	04.45	697.39	592.74
32	08.66	698.33	591.11	795.07	84.78	76.78
33	798.50	84.78	74.37	85.32	71.65	60.52
34	88.00	77.16	57.36	75.04	58.13	43.72
35	77.11	56.95	39.69	64.62	44.27	26.46
36	65.76	42.41		53.33	29.97	08.89
37		27.41		41.93	15.28	490.72
38		12.13		30.03	00.25	71.89
39		596.31		17.60	584.76	
40		80.22		05.10	68.81	
41		63.68		692.07	52.60	
42		46.68		78.62	35.86	
43		29.34		64.60	18.76	
44		11.64		50.31	01.27	
45		493.61		35.56	483.32	
46		75.08		20.50	65.03	
47		56.13		04.94	46.31	
48		36.92		589.16	27.23	
49		17.24		72.73	07.66	
50		397.09		55.98	387.78	
51		76.79		38.76	67.51	
52		55.89		21.16	46.77	
53		34.60			25.67	
54		12.98			04.17	

TABLE I. (*Cont.*)

K''	R_2	Q_2	P_2	R_1	Q_1	P_1
55		290.91			282.27	
56		68.54			60.05	
57		45.77			37.30	
58		22.51			14.27	
59		198.90			190.77	
60		74.90			66.89	
61		50.53			42.60	
62		25.76			17.95	
63		00.63			092.84	

The combination differences for the $^2\Sigma$ state have been computed from the expression

$$R_1(K-1) - P_1(K+1) = \Delta_2 F_1''(K).$$

The values obtained have been compared with those for the 0, 0 transition of the violet CN band system as determined by Uhler and Patterson.[4] Unfortunately the greater portion of the $\Delta_2 F_1''(K)$ values available from the $^2\Pi \rightarrow {}^2\Sigma$ transition are not obtainable from the violet band. The reason for this is that the P lines necessary for the determination of the combination differences are, for the most part, those in the immediate vicinity of the head of the band and Uhler and Patterson were unable to resolve them. There is good agreement between those values of $\Delta_2 F_1''(K)$ which are available from both band systems. The value of B_0'' obtained is 1.8906 cm^{-1} which is to be compared with 1.8904 cm^{-1}, the value predicted from the B_v'' equation given by Jenkins, Roots and Mulliken.

TABLE II. *Combination differences $\Delta_2 F_i'$ for the $v=0$ level of the $^2\Pi$ state.*

J	$R_2(J)-P_2(J)$	$R_1(J)-P_1(J)$
$19\frac{1}{2}$	137.41	
$20\frac{1}{2}$	144.02	
$21\frac{1}{2}$	150.92	
$22\frac{1}{2}$	157.55	
$23\frac{1}{2}$	164.13	158.77
$24\frac{1}{2}$	171.09	165.37
$25\frac{1}{2}$	177.58	171.90
$26\frac{1}{2}$	184.39	178.56
$27\frac{1}{2}$	190.95	
$28\frac{1}{2}$	197.69	191.98
$29\frac{1}{2}$	204.22	198.52
$30\frac{1}{2}$	210.88	205.05
$31\frac{1}{2}$	217.55	211.71
$32\frac{1}{2}$	224.13	218.29
$33\frac{1}{2}$	230.64	224.80
$34\frac{1}{2}$	237.42	231.32
$35\frac{1}{2}$		238.16
$36\frac{1}{2}$		244.44
$37\frac{1}{2}$		251.21
$38\frac{1}{2}$		258.14

[4] H. S. Uhler and R. A. Patterson, Astrophys. J. **42,** 434 (1915).

Table II contains the combination differences for the $^2\Pi$ state. By means of these values the various constants have been determined by the same methods as those used by the above mentioned authors. The values are

$$B_0^*{}_{,-1/2} = 1.7404 \text{ cm}^{-1}$$
$$B_0^*{}_{,1/2} = 1.6410 \text{ cm}^{-1}$$
$$B_0' = 1.6907 \text{ cm}^{-1}$$
$$D_0' = -6.07 \times 10^{-6} \text{ cm}^{-1}$$
$$A = -53.3 \text{ cm}^{-1}$$
$$p_0 = 0.009 \text{ cm}^{-1}$$
$$q_0 = -0.0008 \text{ cm}^{-1}$$
$$\nu_0 = 10905.12 \text{ cm}^{-1}.$$

The value of B_0' is in excellent agreement with the value, 1.6903 cm^{-1}, obtained by extrapolation from the results of the analysis of other bands of this system. There is considerable inaccuracy in the determination of the values of p_0 and q_0 as the P branches could not be measured in the region of low K values. Furthermore the value of A is slightly higher than that obtained from the higher vibrational levels of this electronic state.

The analysis of the 1, 1 band has not been carried out due to the fact that the lines of low K value were absent from the spectrograms obtained. The two Q branches are easily identified and may be followed to quite high K values. There is also evidence of the R branches.

The author wishes to thank Professor W. W. Watson for his generous assistance and advice.

The Dirac Electron in Simple Fields*

By MILTON S. PLESSET
Sloane Physics Laboratory, Yale University

(Received June 6, 1932)

The relativity wave equations for the Dirac electron are transformed in a simple manner into a symmetric canonical form. This canonical form makes readily possible the investigation of the characteristics of the solutions of these relativity equations for simple potential fields. If the potential is a polynomial of any degree in x, a continuous energy spectrum characterizes the solutions. If the potential is a polynomial of any degree in $1/x$, the solutions possess a continuous energy spectrum when the energy is numerically greater than the rest-energy of the electron; values of the energy numerically less than the rest-energy are barred. When the potential is a polynomial of any degree in r, all values of the energy are allowed. For potentials which are polynomials in $1/r$ of degree higher than the first, the energy spectrum is again continuous. The quantization arising for the Coulomb potential is an exceptional case.

1.

IN HIS treatment of the reflection of the relativity electron at a potential jump Klein[1] found a paradoxical behavior of the Dirac electron associated with the possibility of the existence of states of negative kinetic energy. He showed by an ingenious treatment that the reflection coefficient for electrons incident upon a discontinuous potential jump of height P varied with P from the value zero for $P=0$ to the value unity for $P=W-mc^2$ (W being the energy of the incident electrons). For this last value of P the momentum p associated with the transmitted beam had the value zero, and as P was increased beyond $W-mc^2$ this momentum became imaginary and the reflection coefficient remained unity until P attained the value $W+mc^2$. The results thus far are exactly what would be expected. If P is increased further one enters the domain of negative kinetic energy wherein the group velocity and the momentum in the transmitted beam are oppositely directed; also the reflection coefficient falls off from the value unity and approaches the value $(W-cp)/(W+cp)$ as P is indefinitely increased. Thus by a transition to a state of negative kinetic energy the Dirac electron has apparently an appreciable probability of penetrating a barrier of infinite height. Bohr suggested that this peculiar result might be due to a jump in potential of the order of mc^2 over a region of the order of the Compton wave-length h/mc. It is within a region of the order of h/mc that the internal structure of the Dirac electron and the accompanying "trembling" phenomenon[2] manifests itself. This supposition of Bohr was verified by Sauter[3] who treated the problem of the

* The results of this paper were presented at the Washington meeting of the American Physical Society (April, 1932).

[1] O. Klein, Zeits. f. Physik **53**, 157 (1929).

[2] E. Schrödinger, Preuss. Akad. Wiss. Berlin, Ber. **24**, 418 (1930).

[3] F. Sauter, Zeits. f. Physik **69**, 742 (1931).

Dirac electron passing through a potential barrier in which the rise of potential was taken to be linear. Sauter then showed that the transmission coefficient was very small for a rise in potential $P > W + mc^2$.

Here we shall discuss analytically the nature of the stationary solutions of Dirac's equations for continuous potential functions of a more general type than those heretofore considered. A simple familiar method of treating these equations will be used. The results secured are perhaps unexpected on the basis of the corresponding results for the nonrelativistic treatment.

2.

The relativistic equation of Dirac[4] for an electron of charge $-e$ is

$$\left\{\frac{W}{c} + \frac{e}{c}A_0 + \alpha_x\left(p_x + \frac{e}{c}A_x\right) + \alpha_y\left(p_y + \frac{e}{c}A_y\right) + \alpha_z\left(p_z + \frac{e}{c}A_z\right) + \rho_3 mc\right\}\Psi = 0. \tag{1}$$

We shall suppose that $\boldsymbol{A} = 0$; then Eq. (1) may be expanded as follows

$$\begin{aligned}
(W/c - V/c + mc)\Psi_1 + (p_x - ip_y)\Psi_4 + p_z\Psi_3 &= 0 \\
(W/c - V/c + mc)\Psi_2 + (p_x + ip_y)\Psi_3 - p_z\Psi_4 &= 0 \\
(W/c - V/c - mc)\Psi_3 + (p_x - ip_y)\Psi_2 + p_z\Psi_1 &= 0 \\
(W/c - V/c - mc)\Psi_4 + (p_x + ip_y)\Psi_1 - p_z\Psi_2 &= 0
\end{aligned} \tag{2}$$

where we have put V for the potential energy $-eA_0$. The expansion of (1) into (2) corresponds to these choices of the α's and ρ_3

$$\alpha_x = \begin{pmatrix} 0 & 0 & 0 & 1 \\ 0 & 0 & 1 & 0 \\ 0 & 1 & 0 & 0 \\ 1 & 0 & 0 & 0 \end{pmatrix}, \quad \alpha_y = \begin{pmatrix} 0 & 0 & 0 & -i \\ 0 & 0 & i & 0 \\ 0 & -i & 0 & 0 \\ i & 0 & 0 & 0 \end{pmatrix},$$

$$\alpha_z = \begin{pmatrix} 0 & 0 & 1 & 0 \\ 0 & 0 & 0 & -1 \\ 1 & 0 & 0 & 0 \\ 0 & -1 & 0 & 0 \end{pmatrix}, \quad \rho_3 = \begin{pmatrix} 1 & 0 & 0 & 0 \\ 0 & 1 & 0 & 0 \\ 0 & 0 & -1 & 0 \\ 0 & 0 & 0 & -1 \end{pmatrix}.$$

We shall consider first the case for which V is a polynomial[5] of any degree in x,

$$V = \sum_{n=0}^{q} a_n x^n, \qquad (0 < q < \infty) \tag{3}$$

[4] P. A. M. Dirac, *The Principles of Quantum Mechanics*, p. 243.

[5] The case of a uniform field, $V = ax$, has been treated by Sauter, Zeits. f. Physik **69**, 742 (1931), and that of the simple harmonic oscillator, $V = ax^2$, by K. Nikolsky, Zeits. f. Physik **62**, 677 (1930); the methods used in these cases differ from that used here and are perhaps not so readily capable of generalization as the present method.

and we shall seek solutions of the form

$$\Psi = (\exp 2\pi i(p_y y + p_z z - Wt)/h)\psi(x) \tag{4}$$

so that the components of $\psi(x)$ satisfy these differential equations

$$\begin{aligned}
\frac{d\psi_1}{dx} &= -\frac{2\pi i}{h}\left\{ip_y\psi_1 - p_z\psi_2 + \left(\frac{W}{c} - \frac{V}{c} - mc\right)\psi_4\right\};\\
\frac{d\psi_2}{dx} &= -\frac{2\pi i}{h}\left\{p_z\psi_1 - ip_y\psi_2 + \left(\frac{W}{c} - \frac{V}{c} - mc\right)\psi_3\right\};\\
\frac{d\psi_3}{dx} &= -\frac{2\pi i}{h}\left\{\left(\frac{W}{c} - \frac{V}{c} + mc\right)\psi_2 + ip_y\psi_3 - p_z\psi_4\right\};\\
\frac{d\psi_4}{dx} &= -\frac{2\pi i}{h}\left\{\left(\frac{W}{c} - \frac{V}{c} + mc\right)\psi_1 + p_z\psi_3 - ip_y\psi_4\right\}.
\end{aligned} \tag{5}$$

In view of (3) it may be said that every finite value of x corresponds to an ordinary point of the system of differential equations (5); hence for all finite values of x the solutions of (5) are not only finite but analytic. The points at infinity, $x = \pm\infty$, are, however, irregular singular points of Eqs. (5) of rank $q+1$. The behavior of the solutions of (5) in the neighborhood of these singular points will now be investigated.

We consider the possibility of formally satisfying Eqs. (5) by a set of normal solutions of the type

$$\psi_i = e^{Q(x)}u_i(x), \qquad (i = 1, \cdots 4) \tag{6}$$

where $u_i(x)$ is assumed to be regular in the neighborhood of $|x| = \infty$, and

$$Q(x) = \alpha x^{q+1}/(q+1) + \beta x^q/q + \cdots + \lambda x. \tag{7}$$

The permissible values of α are determined by the characteristic equation

$$\begin{vmatrix} -\alpha & 0 & 0 & a \\ 0 & -\alpha & a & 0 \\ 0 & a & -\alpha & 0 \\ a & 0 & 0 & -\alpha \end{vmatrix} = 0; \quad a = 2\pi i a_q/hc. \tag{8}$$

The roots of this equation, which are both double, are

$$\alpha = \pm a = \pm 2\pi i \cdot a_q/hc; \tag{9}$$

the fact that there are only two distinct roots of Eq. (8) indicates that there are only two independent sets of solutions of the system of Eqs. (5). We transform Eqs. (5) into an analytically symmetrical form by the simple transformation

$$\begin{aligned}
\psi_1' &= (1/2^{1/2})(\psi_1 + \psi_4);\\
\psi_2' &= (1/2^{1/2})(\psi_2 + \psi_3);\\
\psi_3' &= (1/2^{1/2})(\psi_2 - \psi_3);\\
\psi_4' &= (1/2^{1/2})(\psi_1 - \psi_4).
\end{aligned} \tag{10}$$

The matrix of the constants in the linear transformation (10)

$$C = \begin{pmatrix} 1/2^{1/2} & 0 & 0 & 1/2^{1/2} \\ 0 & 1/2^{1/2} & 1/2^{1/2} & 0 \\ 0 & 1/2^{1/2} & -1/2^{1/2} & 0 \\ 1/2^{1/2} & 0 & 0 & -1/2^{1/2} \end{pmatrix} = C^{-1} \tag{11}$$

generates a unitary transformation of the matrix of the determinant of the characteristic equation into the diagonal form

$$\begin{pmatrix} -\alpha + a & 0 & 0 & 0 \\ 0 & -\alpha + a & 0 & 0 \\ 0 & 0 & -\alpha - a & 0 \\ 0 & 0 & 0 & -\alpha - a \end{pmatrix}. \tag{12}$$

The "canonical" form of the system of Eqs. (5) is

$$\begin{aligned}
\frac{d\psi_1'}{dx} &= -\frac{2\pi i}{h}\left\{\left(\frac{W}{c} - \frac{V}{c}\right)\psi_1' - p_z\psi_3' + (mc + ip_y)\psi_4'\right\}; \\
\frac{d\psi_2'}{dx} &= -\frac{2\pi i}{h}\left\{\left(\frac{W}{c} - \frac{V}{c}\right)\psi_2' + (mc - ip_y)\psi_3' + p_z\psi_4'\right\}; \\
\frac{d\psi_3'}{dx} &= -\frac{2\pi i}{h}\left\{p_z\psi_1' - (mc + ip_y)\psi_2' - \left(\frac{W}{c} - \frac{V}{c}\right)\psi_3'\right\}; \\
\frac{d\psi_4'}{dx} &= -\frac{2\pi i}{h}\left\{(ip_y - mc)\psi_1' - p_z\psi_2' - \left(\frac{W}{c} - \frac{V}{c}\right)\psi_4'\right\}.
\end{aligned} \tag{13}$$

We are assuming solutions of this system of Eqs. (13) of the form (an additional subscript s is introduced to distinguish the two sets of solutions)

$$\begin{aligned}
\psi_{1s}' &= e^{Q_s(x)}x^{\mu_s}B_{1s}(x); \quad \psi_{2s}' = e^{Q_s(x)}x^{\mu_s}B_{2s}(x); \\
\psi_{3s}' &= e^{Q_s(x)}x^{\mu_s}B_{3s}(x); \quad \psi_{4s}' = e^{Q_s(x)}x^{\mu_s}B_{4s}(x);
\end{aligned} \qquad (s = 1, 2) \tag{14}$$

where

$$Q_s(x) = \alpha_s x^{q+1}/(q+1) + \beta_s x^q/q + \cdots + \lambda_s x; \tag{15}$$

and

$$B_{rs}(x) = B_{rs}^{0} + B_{rs}^{(1)}x^{-1} + B_{rs}^{(2)}x^{-2} + \cdots. \tag{16}$$

The constants of the solutions (14) are evaluated by direct substitution into Eqs. (13). Of the two sets of formal solutions the first may be written as

$$\begin{aligned}
\psi_{11}' &= e^{Q_1(x)}\left\{B_{11}^{0} + B_{11}^{(q-1)}/x^{q-1} + \cdots\right\} \\
\psi_{21}' &= e^{Q_1(x)}\left\{B_{21}^{0} + B_{21}^{(q-1)}/x^{q-1} + \cdots\right\} \\
\psi_{31}' &= e^{Q_1(x)}\left\{B_{31}^{(q)}/x^{q} + \cdots\right\} \\
\psi_{41}' &= e^{Q_1(x)}\left\{B_{41}^{(q)}/x^{q} + \cdots\right\}
\end{aligned} \tag{17}$$

where

$$Q_1(x) = \frac{2\pi i}{hc} \sum_{n=0}^{q} \frac{a_n x^{n+1}}{n+1} - \frac{2\pi i W x}{hc}. \tag{17a}$$

It may be shown by examination of the recurrence relations which determine the B's that ψ'_{11} and ψ_{21}' are linearly dependent as are also ψ'_{31} and ψ'_{41}. The second set of solutions is

$$\begin{aligned}
\psi_{12}' &= e^{Q_2(x)} \{ B_{12}^{(q)}/x^q + \cdots \} \\
\psi_{22}' &= e^{Q_2(x)} \{ B_{22}^{(q)}/x^q + \cdots \} \\
\psi_{32}' &= e^{Q_2(x)} \{ B_{32}^{0} + B_{32}^{(q-1)}/x^{q-1} + \cdots \} \\
\psi_{42}' &= e^{Q_2(x)} \{ B_{42}^{0} + B_{42}^{(q-1)}/x^{q-1} + \cdots \}
\end{aligned} \tag{18}$$

where

$$Q_2(x) = -\frac{2\pi i}{hc} \sum_{n=0}^{q} \frac{a_n x^{n+1}}{n+1} + \frac{2\pi i W x}{hc}. \tag{18a}$$

Again ψ_{12}' and ψ_{22}' are linearly dependent as are also ψ_{32}' and ψ_{42}'. We have further that only the constants B_{11}^{0}, B_{21}^{0}, B_{32}^{0}, B_{42}^{0} are arbitrary.

We wish to use the solutions (17) and (18), which we have found to satisfy the canonical equations (13) formally, to discuss the behavior of the true solutions for values of x numerically large; this use requires a rigorous justification since it follows from the recurrence relations for the B's that the infinite series $B_{rs}(x)$ do not in general converge for finite values of x. This justification might be carried out by eliminating as follows from the canonical Eqs. (13). Put

$$\begin{aligned}
\psi_1' &= e^{Q_1(x)} u_1(x); \quad & \psi_2' &= e^{Q_1(x)} u_2(x); \\
\psi_3' &= e^{Q_1(x)} u_3(x); \quad & \psi_4' &= e^{Q_1(x)} u_4(x);
\end{aligned} \tag{19}$$

where $Q_1(x)$ is the polynomial given above in (17a). Then the simultaneous Eqs. (13) give readily

$$\frac{d^2 u_3}{dx^2} + \frac{4\pi i}{hc} \{ V(x) - W \} \frac{du_3}{dx} + \frac{4\pi}{hc} \left\{ i \frac{dV}{dx} - \frac{\pi c}{h} (p_y^2 + p_z^2 + m^2 c^2) \right\} u_3 = 0; \tag{20}$$

u_4 satisfies the same equation as u_3. We get also

$$\frac{d^2 u_1}{dx^2} + \frac{4\pi i}{hc} \{ V(x) - W \} \frac{du_1}{dx} - \frac{4\pi^2}{h^2} \{ p_y^2 + p_z^2 + m^2 c^2 \} u_1 = 0; \tag{21}$$

and u_2 satisfies the same equation as u_1. The symmetry and simplicity with which elimination can be accomplished to give Eqs. (20) and (21) show the analytical advantage of working with the canonical form of Dirac's equations. If elimination were attempted directly upon Eqs. (5), the result would be an extremely unsymmetrical set of equations.[6] Eqs. (20) and (21) show that the

[6] This analytical lack of symmetry holds also for Weyl's expansion of Dirac's equation.

points $x = \pm \infty$ are irregular singular points of the functions $u_i(x)$ as well as of the functions $\psi_i'(x)$. Instead of proceeding further with Eqs. (20) and (21), it is more convenient to treat the canonical Eqs. (13) directly. These equations, now considered in the complex plane, have as solutions the generalized Laplace contour integrals

$$\psi_{rs}' = (\exp \beta_s z^q/q + \cdots + \lambda_s z) \int_{C_s} (\exp z^{q+1}) \left(\zeta - \frac{\alpha_s}{q+1}\right)^{-(\mu_s+1)/(q+1)} \sum_{k=0}^{q} z^k \phi_{rk}^{(s)}\left(\zeta - \frac{\alpha_s}{q+1}\right) d\zeta. \tag{22}$$

The contour C_s is a loop circuit about $\zeta = \alpha_s/(q+1)$ such that the real part of $[z^{q+1}\{\zeta - \alpha_s/(q+1)\}]$ is negative along its ray. The functions $\phi_{rk}^{(s)}$ are analytic functions (determined by (13)) in the neighborhood of $\zeta = \alpha_s/(q+1)$. These contour integrals (22) are precise solutions of the canonical equations; the asymptotic expansions[7] of these contour integrals, valid in certain sectors of the z-plane which may be so taken as to include the real axis, are exactly the formal solutions (17) and (18) written above.[8] Therefore these formal solutions have significance as the asymptotic solutions of Eqs. (13). Their use in discussing the behavior of the solutions of (13) for numerically large values of x is thus justified. The importance of using the canonical form of Dirac's equations is here apparent; for, if formal solutions of the type (6) were attempted with the original Eqs. (5), a divergent expansion would result which would be meaningless.

We may now say from Eqs. (17), (17a) and (18), (18a) that the components of the Dirac wave function, remain finite as x becomes infinite; further we have

$$\int_{-a}^{a} \sum_{1}^{4} \psi_i \psi_i^* dx < c(a), \tag{23}$$

where c is a finite number, since the functions ψ_i are finite and analytic for all finite values of x. And if the constant a is sufficiently large $(b > a)$,

$$\int_{a}^{b} \sum_{1}^{4} \psi_i \psi_i^* dx \propto (b-a); \qquad \int_{-a}^{-b} \sum_{1}^{4} \psi_i \psi_i^* dx \propto -(b-a); \tag{24}$$

that is, the integral square becomes proportional to the domain of integration. The wave functions exhibit, therefore, quite common characteristics of the wave functions associated with a continuous energy spectrum. It is thus clear that the Dirac electron possesses a continuous spectrum with all values of W allowed for a potential field which is a polynomial of any degree in x.

3.

Let us now consider potential fields which are polynomials in $1/x$,

$$V(x) = \sum_{n=0}^{q} a_n x^{-n}. \qquad (0 < q < \infty) \tag{25}$$

[7] Asymptotic expansions in the sense of Poincaré.

[8] Cf. E. L. Ince, *Ordinary Differential Equations* p. 484.

It is evident from the discussion given above that we may make the simplifying assumption $p_y = p_z = 0$ in Eqs. (5) without affecting the generality of the results secured. Then Eqs. (5) become

$$\frac{d\psi_1}{dx} = -\frac{2\pi i}{hc}(W - mc^2 - V)\psi_4; \tag{26a}$$

$$\frac{d\psi_2}{dx} = -\frac{2\pi i}{hc}(W - mc^2 - V)\psi_3; \tag{26b}$$

$$\frac{d\psi_3}{dx} = -\frac{2\pi i}{hc}(W + mc^2 - V)\psi_2; \tag{26c}$$

$$\frac{d\psi_4}{dx} = -\frac{2\pi i}{hc}(W + mc^2 - V)\psi_1. \tag{26d}$$

The complete behavior of this system of equations may be determined by considering only Eqs. (26a) and (26d) since this pair of equations has the same form as the pair of Eqs. (26b) and (26c). For the potential function given in (25) the system of Eqs. (26) has an irregular singularity at $x = \pm\infty$ of rank unity and an irregular singularity at $x = 0$ of rank $q - 1$.

To investigate the behavior of the solutions in the neighborhood of the origin we proceed by the method given in §2 above. The transformation to the canonical form of (26a) and (26d) is given by

$$\begin{aligned} \psi_1' &= (1/2^{1/2})(\psi_1 + \psi_4), \\ \psi_2' &= (1/2^{1/2})(\psi_1 - \psi_4), \end{aligned} \tag{27}$$

so that Eqs. (26a) and (26d) become

$$\begin{aligned} \frac{d\psi_1'}{dx} &= -\frac{2\pi i}{hc}\{[W - V(x)]\psi_1' + mc^2\psi_2'\}; \\ \frac{d\psi_2'}{dx} &= \frac{2\pi i}{hc}\{mc^2\psi_1' + [W - V(x)]\psi_2'\}. \end{aligned} \tag{28}$$

To make the analytical procedure of §2 completely applicable we need only put $x = 1/y$ in Eqs. (28) to get

$$\begin{aligned} \frac{d\psi_1'}{dy} &= \frac{2\pi i}{hc}\frac{1}{y^2}\left\{\left[W - V\left(\frac{1}{y}\right)\right]\psi_1' + mc^2\psi_2'\right\}; \\ \frac{d\psi_2'}{dy} &= -\frac{2\pi i}{hc}\frac{1}{y^2}\left\{mc^2\psi_1' + \left[W - V\left(\frac{1}{y}\right)\right]\psi_2'\right\}. \end{aligned} \tag{29}$$

We now consider the behavior of the solutions of Eqs. (29) for values of y numerically large. We assume, as before, formal solutions of the normal type

$$\psi_{rs}' = e^{Q_s(y)}y^{\mu_s}B_{rs}(y) \qquad (r, s = 1, 2) \tag{30}$$

where now

$$Q_s(y) = \frac{\alpha_s y^{q-1}}{q-1} + \frac{\beta_s y^{q-2}}{q-2} + \cdots + \lambda_s y$$

and as before

$$B_{rs}(y) = B_{rs}^{0} + B_{rs}^{(1)} y^{-1} + \cdots .$$

By direct substitution it is found that the asymptotic solutions have the form

$$\psi_{rs}'(y) \cong \delta_{rs} \exp\left\{(-1)^{s}\frac{2\pi i}{hc}\left[\frac{a_q}{q-1}y^{q-1} + \frac{a_{q-2}}{q-2}y^{q-2} + \cdots + a_1 \log y\right]\right\} \quad (31)$$

where δ_{rs} is the Kronecker delta. From Eq. (31) it is clear that the solutions of Eqs. (29) remain finite as y approaches infinity for all values of W; that is, the solutions of Eqs. (28) remain finite in the neighborhood of $x=0$. The origin, $x=0$, does not, therefore, give any limitations on possible allowed solutions of Eqs. (28) or (26).

We must now investigate the behavior of the solutions of Eqs. (26a) and (26d) near $x = \pm\infty$. The characteristic equation for (26a) and (26d) is

$$\begin{vmatrix} -\alpha & -\frac{2\pi i}{hc}(W - mc^2 - a_0) \\ -\frac{2\pi i}{hc}(W + mc^2 - a_0) & -\alpha \end{vmatrix} = 0; \quad (32)$$

so that

$$\alpha = \pm (2\pi/hc)\{m^2c^4 - (W - a_0)^2\}^{1/2}. \quad (33)$$

We may secure a canonical form of Eqs. (26a) and (26d) by putting

$$\begin{aligned} \psi_1 &= a_1^{1/2}(\psi_1' - \psi_2') \\ \psi_4 &= a_2^{1/2}(\psi_1' + \psi_2') \end{aligned} \quad (34)$$

where

$$\frac{1}{a_1} = (W + mc^2 - a_0); \quad \frac{1}{a_2} = (W - mc^2 - a_0).$$

Eqs. (26a) and (26d) then become

$$\frac{d\psi_1'}{dx} = -\frac{2\pi}{hc}\left\{[m^2c^4 - (W - a_0)^2]^{1/2} + \frac{(W - a_0)}{[m^2c^4 - (W - a_0)^2]^{1/2}}(V - a_0)\right\}\psi_1'$$
$$-\frac{2\pi}{hc}\frac{mc^2}{[m^2c^4 - (W - a_0)^2]^{1/2}}(V - a_0)\psi_2'; \quad (35a)$$

$$\frac{d\psi_2'}{dx} = \frac{2\pi}{hc}\frac{mc^2}{[m^2c^4 - (W - a_0)^2]^{1/2}}(V - a_0)\psi_1'$$
$$+\frac{2\pi}{hc}\left\{[m^2c^4 - (W - a_0)^2]^{1/2} + \frac{(W - a_0)}{[m^2c^4 - (W - a_0)^2]^{1/2}}(V - a_0)\right\}\psi_2'. \quad (35b)$$

The formal substitution into Eqs. (35) of solutions of the normal type gives the asymptotic solutions of these equations. The asymptotic solutions are readily found to be

$$\psi_{rs}' \cong c^{\alpha_s x} x^{\mu_s} \delta_{rs} \qquad (r, s = 1, 2) \quad (36)$$

where

$$\alpha_1 = -\frac{2\pi}{hc}\left[m^2c^4 - (W' - a_0)^2\right]^{1/2} = -\alpha_2, \quad (37)$$

and

$$\mu_1 = -\frac{2\pi}{hc}\frac{(W' - a_0)a_1}{\left[m^2c^4 - (W' - a_0)^2\right]^{1/2}} = -\mu_2. \quad (38)$$

If $(W'-a_0)^2 > m^2c^4$, it is evident from Eq. (36) that the solutions of Eqs. (35) are all finite at infinity; all such values of W' are allowed so that a continuous spectrum arises. If, however, $(W'-a_0)^2 < m^2c^4$, Eq. (36) shows that it is not possible to find solutions of (35) which remain finite both at $x=+\infty$ and at $x=-\infty$. Hence there are no proper solutions in this band; these energy values are barred.

4.

We now turn to the case in which the potential function depends on r alone. To examine the characteristics of the Dirac equations for this case we may begin with the radial equations in the form in which they are given by Dirac[9]

$$\frac{dR_a}{dr} = \frac{j}{r}R_a + \left(b_2 + \frac{2\pi}{hc}V(r)\right)R_b \quad (39a)$$

$$(j = \pm 1, \pm 2, \cdots)$$

$$\frac{dR_b}{dr} = -\frac{j}{r}R_b + \left(b_1 - \frac{2\pi}{hc}V(r)\right)R_a \quad (39b)$$

where

$$b_1 = 2\pi(mc^2 + W)/hc; \quad b_2 = 2\pi(mc^2 - W)/hc.$$

The type of potential to be considered first is that for which V is a polynomial of any degree in r

$$V = \sum_{n=0}^{q} a_n r^n. \qquad (0 < q < \infty) \quad (40)$$

With $V(r)$ given by (40) Eqs. (39) for R_a and R_b have an irregular singularity at $r=\infty$ of rank $q+1$; the origin, $r=0$, is a regular singular point; and all other points are ordinary points. We consider first the nature of the solutions in the neighborhood of $r=\infty$. The characteristic equation is

[9] Dirac, *The Principles of Quantum Mechanics*, p. 252.

$$\begin{vmatrix} -\alpha & 2\pi a_q/hc \\ -2\pi a_q/hc & -\alpha \end{vmatrix} = 0; \quad \alpha = \pm \frac{2\pi i}{hc} a_q. \tag{41}$$

The transformation to a canonical form is given by

$$\begin{aligned} R_a &= (1/2^{1/2})(\psi_1 - i\psi_2) \\ R_b &= (1/2^{1/2})(-i\psi_1 + \psi_2) \end{aligned} \tag{42}$$

and the canonical form of Eqs. (39) is

$$\frac{d\psi_1}{dr} = \frac{2\pi i}{hc}\{W - V\}\psi_1 + \left\{\frac{2\pi mc}{h} - i\frac{j}{r}\right\}\psi_2; \tag{43a}$$

$$\frac{d\psi_2}{dr} = \left\{\frac{2\pi mc}{h} + i\frac{j}{r}\right\}\psi_1 - \frac{2\pi i}{hc}\{W - V\}\psi_2. \tag{43b}$$

The asymptotic solutions of Eqs. (43) may be readily found to be

$$\psi_{ms} \backsimeq \delta_{ms} \exp\left\{(-1)^s \frac{2\pi i}{hc}\left[\sum_{n=0}^{q} \frac{a_n}{n+1} r^{n+1} - Wr\right]\right\}. \quad (m, s = 1, 2). \tag{44}$$

From (44) it is seen that the solutions of Eqs. (43) remain finite as r approaches infinity and exhibit an integral square behavior like that discussed above. The irregular singular point at infinity, therefore, does not contribute any limitation on permitted energy values.

The singularity at the origin is regular so that in the neighborhood of the origin solutions of the form

$$R_{as} = r^{\alpha_s}(B_{as}{}^0 + B_{as}{}^{(1)}r + B_{as}{}^{(2)}r^2 + \cdots) \tag{45a}$$

$$R_{bs} = r^{\alpha_s}(B_{bs}{}^0 + B_{bs}{}^{(1)}r + B_{bs}{}^{(2)}r^2 + \cdots) \tag{45b}$$

satisfy the radial Eqs. (39). From the permissible values of α_s as determined by the characteristic equation for this case, $\alpha = \pm j$, it is evident that there is always one solution finite at the origin. Combining this result with that given in (44) we may say that there is always a solution of the radial equations which for all values of W is finite everywhere and which possesses in addition a well behaved integral square for large values of r. Hence for potential functions which are polynomials of any degree in r the equations of Dirac give a continuous spectrum with all values of W allowed.

5.

Let us consider finally the case for which the potential function $V(r)$ is a polynomial in $1/r$

$$V(r) = \sum_{n=0}^{q} a_n r^{-n}. \qquad (0 < q < \infty) \tag{46}$$

With this potential function the radial Eqs. (39) have an irregular singularity at $r = \infty$ of rank unity; the roots of the characteristic equation are

$$\alpha_1 = (2\pi/hc)\left[m^2c^4 - (W - a_0)^2\right]^{1/2} = -\alpha_2. \tag{47}$$

The transformation

$$R_a = (b_2 + 2\pi a_0/hc)^{1/2}(\psi_1 - \psi_2)$$
$$R_b = (b_1 - 2\pi a_0/hc)^{1/2}(\psi_1 + \psi_2) \tag{48}$$

gives the canonical form

$$\frac{d\psi_1}{dr} = \frac{2\pi}{hc}\left\{[m^2c^4 - (W - a_0)^2]^{1/2} + \frac{(W - a_0)}{[m^2c^4 - (W - a_0)^2]^{1/2}}(V - a_0)\right\}\psi_1$$
$$+ \left\{-\frac{j}{r} + \frac{2\pi}{h}\frac{mc}{[m^2c^4 - (W - a_0)^2]^{1/2}}(V - a_0)\right\}\psi_2; \tag{49a}$$

$$\frac{d\psi_2}{dr} = -\left\{\frac{j}{r} + \frac{2\pi}{h}\frac{mc}{[m^2c^4 - (W - a_0)^2]^{1/2}}(V - a_0)\right\}\psi_1$$
$$- \frac{2\pi}{hc}\left\{[m^2c^4 - (W - a_0)^2]^{1/2} + \frac{(W - a_0)}{[m^2c^4 - (W - a_0)^2]^{1/2}}(V - a_0)\right\}\psi_2; \tag{49b}$$

and the asymptotic behavior of the solutions of Eqs. (49) is given by

$$\psi_{rs} \cong e^{\alpha_s r} r^{\mu_s}\delta_{rs} \qquad (r, s = 1, 2) \tag{50}$$

where

$$\mu_1 = \frac{2\pi}{hc}\frac{(W - a_0)}{[m^2c^4 - (W - a_0)^2]^{1/2}}a_1 = -\mu_2. \tag{51}$$

It is evident from (47) and (51) that for $(W-a_0)^2 > m^2c^4$ all the solutions remain finite as r approaches infinity; and for $(W-a_0)^2 < m^2c^4$ there is one finite and one infinite solution at $r = \infty$.

To investigate the singularity at the origin, $r=0$, it is only necessary to make the transformation $r = 1/y$ in the canonical Eqs. (43). If $q = 1$, that is to say, if the potential is a Coulomb potential, $y = \infty$ is a regular singular point and regular solutions may be found as follows

$$\psi_{rs} = y^{\alpha_s}(B_{rs}^{0} + B_{rs}^{(1)}y^{-1} + B_{rs}^{(2)}y^{-2} + \cdots) \tag{52}$$

where the exponent α_s is fixed by the characteristic equation

$$\begin{vmatrix} -\alpha - 2\pi i a_1/hc & -ij \\ ij & -\alpha + 2\pi i a_1/hc \end{vmatrix} = 0; \quad \alpha = \pm (j^2 - 4\pi^2 a_1^2/h^2c^2)^{1/2}. \tag{53}$$

These values of the exponent α are, of course, precisely those found in the treatment of the hydrogen atom.[10] From (53) it is evident that there is one finite and one infinite solution at $r=0$; also for $r=\infty$ there is one finite and one infinite solution for $(W-a_0)^2 < m^2c^4$ (by Eq. (50)). These are exactly the conditions which lead to quantization.

[10] Dirac, p. 253.

Such is not the case, however, when $q>1$. For these potential functions the origin, $r=0$, is an irregular singularity. The behavior of the solutions may be investigated by means of Eqs. (43) by the same methods as those used previously. The asymptotic solutions are readily found to be

$$\psi_{rs}(y) \cong \delta_{rs} \exp\left\{(-1)^{s+1}\frac{2\pi i}{hc}\left[\frac{a_q}{q-1}y^{q-1} + \frac{a_{q-1}}{q-2}y^{q-2} + \cdots + a_1 \log y\right]\right\}. \quad (y = 1/r) \quad (54)$$

From (54) it is clear that when $q>1$ all the solutions of (43) remain finite in the neighborhood of $r=0$ for all values of W. From Eq. (50) it was seen that there is always one solution finite at infinity for all values of W. Combining (50) and (54), we see that a continuous energy spectrum always arises when the potential function is of the form

$$V(r) = a_0 + a_1/r + a_2/r^2 + \cdots + a_q/r^q. \qquad (q > 1)$$

We may discuss briefly the analytical source of the difference in the results found for the potentials $V=1/x$ and $V=1/r$. We note that for the potential $1/x$ Eqs. (29) retain their canonical form; that is, the highest power of y in the expression for $d\psi_i'/dy$ occurs in the coefficient of ψ_i'. The general result (31), therefore, remains applicable to this case also. For the potential $V=1/r$, however, Eqs. (43) (transformed by $r=1/y$ and considered for $y\sim\infty$) do not have the canonical form because of the presence of the terms involving j; thus, this potential must be considered apart from those which contain powers of $1/r$ beyond the first. The general result (54) is not at all applicable to the Coulomb potential.

We may note further here that, if the potential function $V(x)$ is of the form

$$V(x) = \sum_{n=-p}^{q} a_n x^n, \qquad (0 < p, q < \infty)$$

a continuous spectrum arises with no values of W barred. Similarly, if the potential $V(r)$ contains direct as well as inverse powers of r, all values of W are allowed.

6.

By writing the relativity equation of Dirac in a symmetrical canonical form it has been possible to make deductions of a quite general nature regarding the characteristics of the stationary solutions for simple potential fields. The results here presented for the potential fields which are polynomials in x or r give an analytic generalization of the Klein paradox. We may note also that these potential functions will rise by more than mc^2 over a region of the order of h/mc if sufficiently large values of x or r are taken.[11] Hence the hypothesis of Bohr advanced to explain the results of Klein is analytically verified for these general cases also.

[11] We are referring now to polynomial potentials of degree higher than the first.

Such an argument cannot perhaps be so clearly applied to explain the results here presented for potential fields which are polynomials in $1/x$ or $1/r$ since with these potentials the steep rises occur toward the origin. For the Coulomb potential by taking sufficiently small values of r a rise in potential of mc^2 in a region of the order of a Compton wave-length may be secured, and yet this potential gives eminently satisfactory agreement with experiment. If the potential contains higher powers of $1/r$ as well as $1/r$, then, as was stated above, continuous spectra result. Here there is striking disagreement with the results of the nonrelativistic Schrödinger theory; for example potentials of the type $a/r-b/r^2$ applied to oscillating rotator models have been shown[12] to give a discrete spectrum in satisfactory agreement with observed spectra.

We may observe, however, from a purely classical point of view that none of the potentials here discussed (except the Coulomb potential and the linear potential ax) satisfy Laplace's equation. Classically, then, these potentials correspond to a continuous distribution of charge. The relativity theory of the electron is not sufficiently advanced, possibly, to deal with such a complicated physical situation. It should perhaps not be held at fault for giving peculiar results for potential functions which are over-simplified and in that over-simplification correspond to an over-complicated electromagnetic mechanism.

In conclusion the writer takes pleasure in expressing his appreciation to Professor Page for his kind interest in this work.

[12] Cf. A. Sommerfeld, *Wellenmechanischer Ergänzungsband*, p. 24 ff.

The Infrared Absorption Spectrum of Carbon Dioxide

By P. E. MARTIN AND E. F. BARKER
University of Michigan

(Received June 17, 1932)

The complete infrared spectrum of CO_2 may consistently be explained in terms of a linear symmetrical model, making use of the selection rules developed by Dennison and the resonance interaction introduced by Fermi. The inactive fundamental ν_1 appears only in combination bands, but ν_2 at 15μ and ν_3 at 4.3μ absorb intensely.

Resolution of the fundamentals ν_2 and ν_3.—The 15μ band has been resolved into several constituent bands corresponding to absorption by the normal molecule, and by molecules in the first and second excited states. Each band consists of a narrow and intense zero branch, with equally spaced rotation lines on either side. The 4.3μ band has also been resolved, best results following a material reduction in the CO_2 content of the atmospheric path. The line spacing is the same as in the 15μ band, and there is no zero branch. In each case alternate rotation lines are absent, the J values for the normal state all being even. The computed moment of inertia is 70.8×10^{-40} gr cm^2.

Harmonic and combination bands.—No first harmonic bands appear, either for ν_2 or ν_3, but the second harmonic has been observed in each case. The strong pair of doublet bands at 2.7μ are interpreted as combination bands corresponding to $\nu_3+\{\nu_1,2\nu_2\}$ and the bands at 2.0μ and 1.6μ are higher members of the same sequence. The differences $\nu_3-\{\nu_1,2\nu_2\}$ explain the weak absorption maxima observed by Schaefer and Philipps at 9.4μ and 10.4μ. The difference bands $\nu_1-\nu_2$ form a part of the 15μ pattern.

Correlation with Raman spectra.—The Raman lines corresponding to the transitions $0\rightarrow\{\nu_1,2\nu_2\}$ and the weaker pair originating in the first excited state 1_1 of ν_2 fit precisely into the energy level diagram obtained from infrared measurements.

MEASUREMENTS of the absorption due to carbon dioxide were among the earliest observations in infrared spectroscopy,[1] and, as apparatus and methods have gradually improved, these bands have been repeatedly re-examined.[2] Resolution of the rotational structure has not been achieved, however, and even the character of the vibrations has been in doubt until quite recently. Three regions of fairly intense absorption are known; those at 2.7μ and 4.3μ were discovered by Langley, while the band at 14.9μ was first observed by Rubens and Aschkinass. The most complete map of the spectrum from 1μ to 15μ is given by Schaefer and Philipps, and includes many bands of low intensity. These show the curious property that none of the frequencies are either sums or differences of others in the set, which, according to Dennison,[3] indicates a linear symmetrical molecule. Other evidence also suggesting that the three atoms of CO_2 lie on a line has been presented by Eucken[4] from

[1] Langley, Phil. Mag. **15,** 153 (1883). Rubens and Aschkinass, Astrophys. J. **8,** 176 (1898).

[2] Coblentz, Carnegie Inst. Pub. **35** (1905); Burmeister, Verh. d. D. Phys. Ges. **15,** 589 (1913); E. v. Barh, Verh. d. D. Phys. Ges. **15,** 1150 (1913); Barker, Astrophys. Jour. **55,** 391 (1922); Ellis, Phys. Rev. **26,** 469 (1925); Schaefer and Philipps, Zeits. f. Physik **36,** 641 (1926).

[3] Dennison, Rev. Mod. Phys. **3,** 280 (1931).

[4] Eucken, Zeits. f. Physik **37,** 714 (1926).

a consideration of specific heats, and by Stuart[5] who found no permanent electric moment. However, not all of the experimental evidence has seemed to be consistent with this model. The lowest frequency fundamental, though unresolved, was observed as a broad doublet, instead of a triplet as would have been expected from linear molecules vibrating normally to their axes. Also the 2.7μ band appeared as a pair of doublets of almost equal intensity, the explanation for which has not been obvious.

We are now able to present observations on the two active fundamental bands at resolutions sufficient to reveal the rotational structure. These indicate that the molecule is in fact linear and symmetrical. Moreover, they may be satisfactorily correlated with the Raman lines and the whole series of combination bands, including the pair at 2.7μ, in such a manner as to leave no further doubt about the conclusion.

The mechanical problem of the vibrations and rotations of a symmetrical linear triatomic molecule has been discussed in detail by Dennison.[3] The symmetrical vibration ν_1 of the two extreme atoms along the line connecting them is optically inactive, since no change in electric moment results; it is not observed in the infrared. The symmetrical vibration ν_2 normal to the linear axis necessarily involves changes in electric moment having components along the axis of rotation, and must exhibit P, Q and R branches. It should correspond to the lowest fundamental frequency, observed at 14.9μ. Heretofore this has been reported as a broad doublet band, except in the recent observations by Sleator.[6] The third fundamental vibration ν_3 is an unsymmetrical one involving changes of electric moment normal to the axis of rotation, and giving rise to an intense absorption band at 4.3μ with P and R branches only. On the basis of these assignments the approximate numerical value of ν_1 may be computed. It should lie between ν_2 and ν_3, at a wave-length of about 8μ. The combination relations are particularly characteristic. While $\Delta\nu_1$ may be any integer, the value of $\Delta\nu_2+\Delta\nu_3$ must always be odd. Many possibilities are thus excluded, among them the first harmonic bands. Q branches occur only when $\Delta\nu_2$ is odd. The most intense of the combination bands to be expected are $\nu_3+2\nu_2$ and $\nu_3+\nu_1$, both doublets falling in the neighborhood of 2.7μ.

Most of the equipment used in this investigation has already been described. The grating spectrometer of highest resolution is the one recently used for observations on N_2O.[7] Although very effective for measurements with small absorption cells it cannot conveniently be used with long gas paths for detecting weak bands, nor is it so arranged as to be easily cleared of atmospheric components which absorb very strongly, making observations at certain wave-lengths almost impossible. Fortunately a second instrument was available which could be completely enclosed from source to thermopile. Although equipped with mirrors of shorter focus it gave a resolution sufficient to show the rotational structure of the 4.3μ band when the concentration of

[5] Stuart, Zeits. f. Physik **47**, 457 (1928).
[6] Sleator, Phys. Rev. **38**, 147 (1931).
[7] Plyler and Barker, Phys. Rev. **38**, 1827 (1931).

CO_2 was considerably reduced. This instrument could be filled with almost pure CO_2, or with air practically free of CO_2 as required, though it could not be evacuated. No absorption cells were used. The thermopile was a particularly good one, kindly supplied to us by Dr. Hardy, and, when connected with the Firestone amplifier and recording apparatus,[8] made continuous photographic records possible. We are indebted to Professor Randall for a thin KBr prism (angle 10°) made from a crystal grown under his direction and especially useful for observations beyond 15μ.

The Low-Frequency Fundamental ν_2

In determining the form of the CO_2 molecule a study of the lowest frequency fundamental band is crucial. Fig. 1 shows a series of energy curves for this region traced from the photographic records obtained with a com-

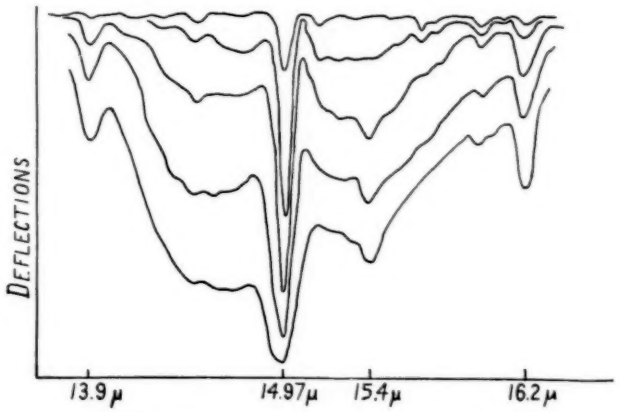

Fig. 1. Development of the 15μ band with increasing amounts of CO_2. Equivalent path lengths in cm at 76 cm pressure: 0.004, 0.05, 0.23, 0.68, 1.58.

pletely enclosed spectrometer using a coarse grating (960 lines per inch) and 1 mm slits. The narrow and intense zero branch is most striking. The whole case was washed for many hours with air from which the CO_2 had been removed, but a trace of this central maximum still persists in the upper curve. Small measured additions of gas very rapidly increase the intensity of the absorption. The estimated percentage absorbed at the peak has been plotted in Fig. 6 as a function of the equivalent length of path. The curves of Fig. 1 also show the development of the three secondary maxima described by Sleator, which lie at 13.9μ, 15.4μ and 16.2μ.

Energy curves for this same region under higher resolution are shown in Fig. 2. These were taken with a grating having 1200 lines per inch, used with a thin KBr foreprism. The slits included about 0.45 cm^{-1}. For the central portion the absorbing medium was about six meters of ordinary atmosphere, the equivalent path length in CO_2 being approximately 0.25 cm. The two lateral portions were obtained by increasing the quantity of CO_2 about one hundredfold. The structure of this absorption region is clearly revealed, and

[8] Firestone, Rev. Sci. Inst. **3**, 163 (1932).

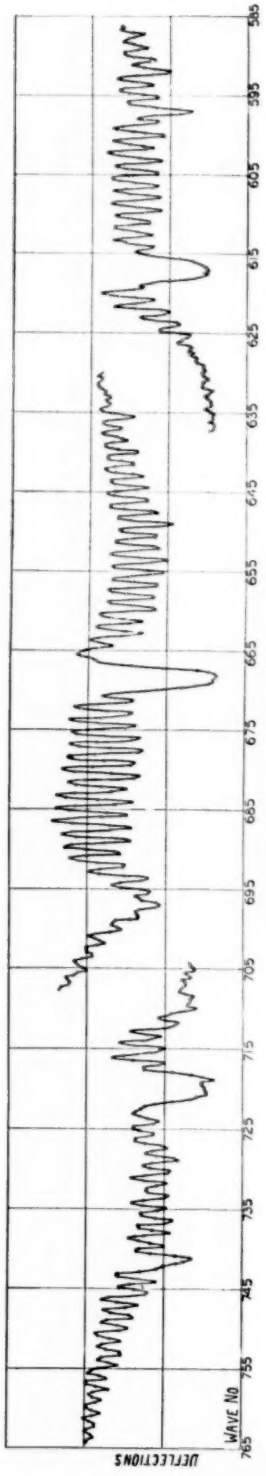

Fig. 2. Fine structure of the 15μ band.

though relatively simple, it is somewhat unusual. In addition to the strong central band with its P, Q and R branches, we find two of the secondary bands already mentioned, similar in structure and symmetrically placed at about ± 50 cm^{-1} from the center. Beyond these on either side and about 20 cm^{-1} farther out another sharp maximum of lesser intensity is found. The symmetry in arrangement and intensities is most striking, and assumes particular interest when the pattern is compared, as in Fig. 3A with the Raman spectrum observed by Dickinson, Dillon and Rasetti.[9] In fact this comparison provides an important means of checking the final interpretation. It should be remarked that the curious dip in the curve at about 697 cm^{-1} upon which the rotation lines are superposed, is not characteristic of CO_2, as it does not appear in the curves of Fig. 1.

Dennison's analysis of the motion associated with the frequency ν_2 assigns to each level two quantum numbers, of which V, the principal one, refers to the vibration state, while the subsidiary number L measures (in units

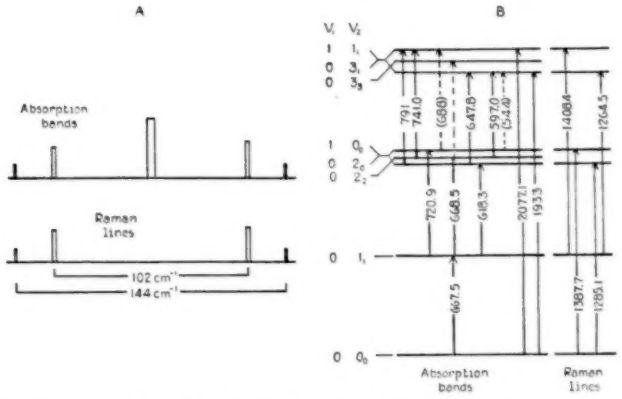

Fig. 3. Vibration levels and transitions involving ν_1 and ν_2.

of $h/2\pi$) the angular momentum about the linear axis which is introduced by the two dimensional vibration. Any transition in V is permitted, but L must change by ± 1 when ΔV is odd, and by 0 when ΔV is even. Combinations of these transitions with ν_1 are also possible, and in particular $\nu_1 - \nu_2$ may lie very close to ν_2. As has been shown[10] it is possible to interpret all of the observed CO_2 bands by this scheme, but not without certain curious intensity relations, and no explanation of the symmetry of the pattern is thus provided. Recently a modification has been introduced by Fermi[11] to take account of the interaction between the levels ν_1 and $2\nu_2$. This has been further developed by Dennison,[12] and in his notation has been introduced in the level

[9] Dickinson, Dillon and Rasetti, Phys. Rev. **34,** 582 (1929).

[10] This analysis of the absorption bands and its correlation with the observed Raman spectra, including the weaker transitions originating in the first excited state 1_1, were first reported at the Washington meeting of the Am. Physical Society in May, 1931. Phys. Rev. **37,** 1708 (1931).

[11] Fermi, Zeits. f. Physik **71,** 250 (1931).

[12] Dennison, Phys. Rev. **41,** 304 (1932).

diagram of Fig. 3B. When the carbon atom vibrates along a line normal to the molecular axis it is clear that the two oxygen atoms must swing along arcs so that the distance between them changes slightly, with two minima and two maxima per oscillation; i.e., the motion has a symmetrical component parallel to the axis, with frequency $2\nu_2$. This component alone is, of course, optically inactive. For CO_2 it happens that the frequencies ν_1 and $2\nu_2$ are almost exactly identical, so that a resonance interaction between them produces a pair of combined states (states whose wave functions are linear combinations of those appropriate to ν_1 and $2_0\nu_2$) separated rather widely and almost symmetrically with respect to their unperturbed position, which, of course, would not have been far from the level 2_2. A similar coupling occurs between succeeding pairs of states of like character, such as $3_1\nu_2$ and $\nu_1+1_1\nu_2$.[13]

The motion in the states designated 1_1, 2_2, 3_3 etc., is peculiar since it does not involve changes in the distances between atoms; the molecule is no longer linear but forms a very obtuse triangle which rotates without deformation about an axis parallel to its base. This motion is not coupled with ν_1, for no longitudinal oscillation accompanies it. Further, since there is no change in polarizability of the molecule during the motion, there can be no Raman transitions terminating at these levels.[14] Thus, none of the transitions $0_0\rightarrow1_1$, $0_0\rightarrow2_2$ or $1_1\rightarrow3_3$ is represented in the Raman spectrum.

The explanation of the patterns in Fig. 3A follows at once from this scheme of levels. The two strong Raman lines originate in the state 0_0, and the two weaker ones in the first excited state, as previously suggested.[10] The relative populations of these levels are as 13 to 1 (state 1_1 has a double weight). Infrared transitions to the same final states occur from 1_1 and 2_2 as common initial levels, the population ratio here being 26 to 1. The line $0_0\rightarrow1_1$ lies almost exactly at the midpoint, its frequency practically coinciding with that determined for $1_1\rightarrow2_2$ by subtracting 741.0 ($2_2\rightarrow3_1$) from the Raman frequency 1408.4. This indicates that for ν_2 the anharmonic term is very small, and also that ν_1 and $2\nu_2$ must coincide very exactly. It is not possible to locate the level 3_3 experimentally since the only line in which it is involved ($2_2\rightarrow3_3$) is completely masked.

The precise determination of the frequencies corresponding to the transitions indicated in Fig. 3 is rendered somewhat difficult by differences in convergence, which shift slightly the maxima of the observed zero branches, sometimes toward higher and sometimes toward lower frequencies. However, utilizing the combination principle, a consistent set of term values has been selected in which the errors probably do not exceed one half of a wave number (except for the level 3_3 which is not observed directly). These term values are listed in Table I, column 3. The positions of the vibration bands computed from them appear in column 4, while columns 5 and 6 show the observed

[13] As a result of discussions with Professor Kramers during the 1931 Summer Symposium in Ann Arbor we had already reached the conclusion before Fermi's paper appeared, that an interaction of this sort must be invoked to explain the infrared and Raman lines, but details had not been worked out.

[14] Placzek, Zeits. f. Physik **70**, 84 (1931).

wave numbers and the estimated relative intensities. A precise determination of intensities is not possible, for many of the lines are superposed upon a strong background, as in the case of 668.5 and 647.8. Furthermore, the differences in degree of convergence change the contours of the bands sufficiently so that some appear narrow and correspondingly more intense, while others are appreciably broadened. There is a tendency, also, to underestimate the absorption coefficient in regions which are almost opaque, as at the central maximum. It is somewhat surprising that the line at 688.7 has not been clearly revealed, when the corresponding one at 647.7 shows so distinctly. Both lie in regions of strong absorption due to rotation lines of the principal band. The line at 545.1 has also eluded observation although a search for it was made with the coarse grating and a path length of 200 cm of CO_2.

TABLE I. *Term values and vibrational transitions involving v_2.*

Initial state			Vibration frequency		Relative
V_1	V_2	term value	computed	observed	intensities
			Fundamental bands		
0	0_0	0	667.5	667.5	10,000
			720.9	720.9	250
0	1_1	667.5	668.7	668.5	—
			618.3	618.3	250
			740.9	741.0	10
0	2_2	1336.2	669.5	—	—
			597.3	597.0	10
			791.3	791	1
1	0_0	1285.8	647.7	647.8	7
0	2_0	1388.4	688.7	—	—
			545.1	—	—
0	3_3	2005.7			
1	1_1	1933.5			
0	3_1	2077.1			
			Harmonic bands		
0	0_0		2077.1	2077.1	7
			1933.5	1933	1
			Raman lines		
0	0_0		1388.4	1387.7	15
			1285.8	1285.1	10
0	1_1		1409.6	1408.4	1
			1266.0	1264.5	1

The two second harmonic bands listed in Table I form a part of the absorption region near 4.9μ observed by Schaefer and Philipps. The trace of an energy curve for this region recorded automatically with a 200 cm path of CO_2 is shown in Fig. 5B. In addition to the two maxima listed, other absorption lines appear, probably due to transitions originating in excited states. A further study of this region is contemplated.

The agreement between the Raman frequencies observed by Dickinson, Dillon and Rasetti, and those computed from the term values in Table I

may be considered fairly satisfactory, though the differences are somewhat larger than our estimated errors. A better correspondence would result if our frequency scale were uniformly contracted about seven parts in ten thousand. This difference we believe to be considerably greater than our error of calibration.

Rotational Structure of the Bands at 15μ

As is well known, a necessary symmetry property of the wave function Ψ for a diatomic or a linear triatomic molecule with identical extreme atoms excludes either those alternate rotation states for which ψ_R is symmetrical, or those for which it is antisymmetrical, ψ_R being the factor of Ψ affected by an interchange of the identical atoms. It is to be expected, then, that for those vibration states of CO_2 in which $L=0$ the rotational quantum number J may assume only even or only odd values. Which of these sets is excluded depends upon the symmetry properties of the remaining factors of Ψ. When

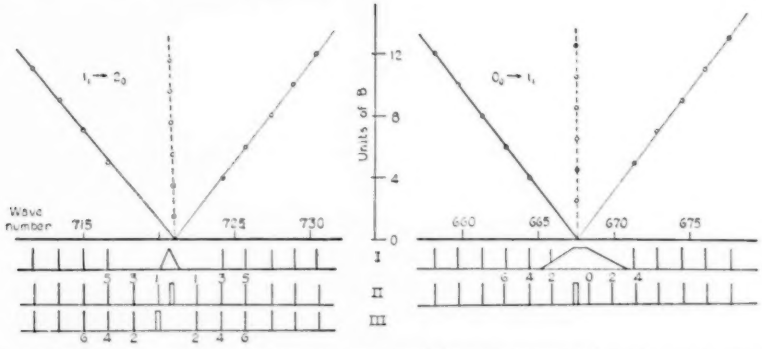

Fig. 4. Comparison of observed and predicted band patterns for $\Delta L = \pm 1$. I. Observed positions of the lines. II. Predicted positions for $\psi_R{}^0$ symmetrical. III. Predicted positions for $\psi_R{}^0$ antisymmetrical.

L is not zero the molecule is no longer precisely linear, and J may assume all integral values equal to or greater than L. In those bands involving the transitions $0\rightarrow1$ or $1\rightarrow0$ in L alternate rotation lines will be completely suppressed and the proper J transitions may be assigned only after it has been decided which are the missing levels. In the absence of zero branches this decision would not be difficult as the frequency interval between the first lines of the positive and negative series would be different for the two cases, but the zero branches are always present, and ordinarily are so broad as to obscure several of the neighboring rotation lines. If their positions could be determined precisely a criterion would be provided for assigning odd and even J values, as is indicated by the band patterns in the lower section of Fig. 4. The band centers at 13.9μ and 16.2μ are particularly favorable for observations of this sort, since, with atmosphere of normal CO_2 content, the central maxima appear weak and very narrow. The adjacent rotation lines are then too weak to be measured, but their positions can be determined, with higher concentrations of CO_2. We find the two zero branches to lie at 720.6 cm^{-1} and 617.9 cm^{-1}, with displacements toward lower frequencies as the concentrations are

increased. The rotation lines adjacent to the former, taken from Fig. 2, have been plotted in the upper section of Fig. 4 just above the characteristic band pattern for $\Delta L = -1$, and the position of the zero branch shows clearly that even numbers must be used for the J values of the upper state ($L = 0$); hence also for the normal state. This is in contrast with the molecule O_2 which, for the nonvibrating state, has only odd J values. It indicates that for CO_2 ψ_R must have the same symmetry as ψ_V. The intersection of the two straight lines falls at 720.9, which is the value given in Fig. 3 as the vertex of the zero branch, and in Table I as the band center. For the other band the coincidence is equally good, the indicated center being 618.3 cm^{-1}. Because of its great intensity we have not determined the position of the strongest zero branch at 14.9μ with equal precision, but since in the initial state (0_0) the J values are even, its frequency may be obtained graphically as on the right of Fig. 4, from the positions of the observed rotation lines. The value so obtained is 667.5 cm^{-1}.

TABLE II. *Wave numbers and wave-number differences in the band at 14.9μ.*

Initial J	Observed frequencies $\Delta J=+1$	$\Delta J=-1$	D	D'	$h/4\pi^2cI$	$h/4\pi^2cI'$	ν computed $\Delta J=0$
4	671.3	664.4	8.4	6.9	0.762	0.765	667.5
6	672.8	662.9	11.5	9.9	0.767	0.762	667.5
8	674.5	661.3	14.8	13.2	0.778	0.777	667.5
10	676.0	659.7	17.8	16.3	0.774	0.777	667.5
12	677.6	658.2	20.9	19.4	0.774	0.776	667.5
14	679.2	656.7	24.1	22.5	0.777	0.777	667.6
16	680.8	655.1	27.2	25.7	0.777	0.778	667.6
18	682.5	653.6	30.4	28.9	0.780	0.781	667.7
20	684.1	652.1	33.6	32.0	0.782	0.780	667.7
22	685.7	650.5	36.7	35.2	0.781	0.783	667.7
24	687.3	649.0	39.8	38.3	0.780	0.782	667.8
26	689.0	647.5	43.0	41.5	0.782	0.783	667.9
28	690.6	646.0	46.2	44.6	0.782	0.783	667.9
30	692.1	644.4	49.0	47.7	0.778	0.783	667.9
32	693.7	643.1	52.2	50.6	0.780	0.780	668.0
34	695.3	641.5	55.4	53.8	0.780	0.780	668.1
36	697.0	639.9	58.5	57.1	0.780	0.783	668.1
38	698.6	638.5	61.6	60.1	0.780	0.781	668.2
40	700.1	637.0	64.6	63.1	0.780	0.780	668.2
42	701.8	635.5		66.3		0.780	668.3
44	703.3						
46	705.2						
48	706.7						

The wave numbers as measured for the various rotation lines are shown in Table II with this assignment of J values. Frequency differences characteristic of the upper and lower vibration states have been obtained in the usual way, i.e.,

$$[J \to J'] - [(J+2) \to J'] = [J \to (J+2)] = (2J'+1)B$$

and

$$[J \to J'] - [J \to (J'-2)] = [J' \to (J'-2)] = (2J+1)B'.$$

These are tabulated under the headings D and D', the primes referring to the upper state. The half interval between rotation lines, $B = h/4\pi^2cI$, is obtained

by dividing these differences by the appropriate integers, the results appearing in the 6th and 7th columns. The 8th column shows the positions of the zero branch lines as determined by subtracting $h/8\pi^2cI$ from the corresponding means of columns 2 and 3. The effect of rotation upon the vibration frequency is seen to be very small. Within the limits of experimental error the positions of the zero branch lines are represented by the formula

$$\nu = 667.5 + 0.00045J^2.$$

Clearly the moment of inertia is affected very little by the change in state of vibration. The mean value of $h/4\pi cI$ is practically 0.780, and consequently $I = 70.8\times10^{-40}$ gr. cm^2. Here a little less weight has been assigned to the low rotation states, where larger errors are to be expected. In the same way we find the value $I' = 70.7\times10^{-40}$. These results agree very well with the value $I = 70.2\times10^{-40}$ obtained from measurements upon rotational Raman spectra by Houston and Lewis.[15] It is to be noted that these authors also reach the conclusion that the J's must be even for the nonvibrating molecule.

Since each of the bands corresponding to absorption from the first vibration state is at least partially obscured by the more intense fundamental, a similar treatment may be applied to them only for the lower rotation states, and much smaller precision is to be expected. The resulting moments of inertia, computed from the wave numbers appearing in Table III are 67.3×10^{-40} for the 13.9μ band, and 73.6×10^{-40} for the 16.4μ band.

TABLE III. *Wave numbers of rotation lines in the bands at 13.9μ and 16.2μ.*

Band at 13.9μ		Initial	Band at 16.2μ	
$\Delta J=+1$	$\Delta J=-1$	J	$\Delta J=+1$	$\Delta J=-1$
—	—	1	—	—
724.2	—	3	620.9	—
725.7	716.6	5	622.8	614.1
727.4	715.0	7	623.9	612.7
728.9	713.5	9	625.3	611.2
730.4	711.7	11		609.6
731.8		13		607.9
733.4		15		606.4
734.9		17		604.8
736.5		19		603.3
738.0		21		601.6
739.5		23		600.1
741.2		25		598.4
744.1		27		596.9
745.5		29		595.3
747.0		31		593.7
748.5		33		592.0
749.9		35		590.5
751.5		37		589.0
753.1		39		587.2
754.6		41		

THE FUNDAMENTAL BAND AT 4.3μ

The absorption associated with the other active fundamental is so intense that near the center of the band observations through ordinary atmos-

[15] Houston and Lewis, Proc. Nat. Acad. **17**, 229 (1931).

phere are difficult and show very little contrast. Fig. 5C represents a typical set of absorption measurements for this region, plotted against frequencies. The rotation lines are fairly obvious on the low-frequency side of the center, but on the high-frequency side where they are closer together and the absorption is stronger, their positions can be determined only in rough approximation. Table IV shows the average values taken from this and several similar curves, and the corresponding values of $h/4\pi^2cI$ and $h/4\pi^2cI'$. The precision is much less than for the observations given in Table II, but the indicated value for the moment of inertia is practically the same. The values of ν_3 com-

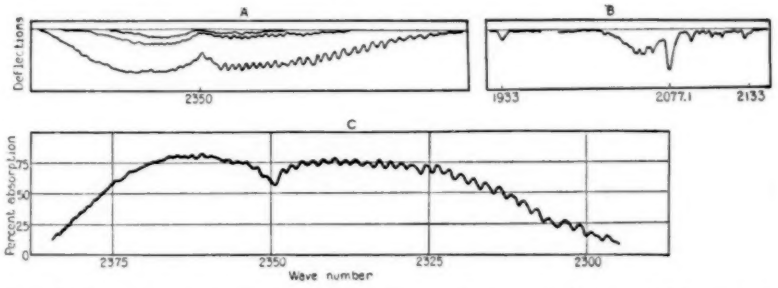

Fig. 5. *A* and *B:* Energy curves traced from automatic records for ν_3 at 4.3μ and $3\nu_2$ at 5μ; *C:* Absorption curve for ν_3 from point by point observations.

TABLE IV. *Wave numbers and wave-number differences in the band at 4.3μ.*

Initial J	Observed frequencies $\Delta J=+1$	$\Delta J=-1$	D	D'	$h/4\pi^2cI$	$h/4\pi^2cI'$	ν computed $\Delta J=0$
0	2350.9	—	2.6		0.867		
2	2352.7	2348.3	5.9	4.3	0.843	0.860	2350.1
4	2354.0	2346.8	8.7	7.2	0.791	0.800	2350.0
6	2355.5	2345.3	12.0	10.2	0.800	0.786	2350.0
8	2356.9	2343.5	15.0	13.4	0.789	0.787	2349.8
10	2358.1	2341.9	18.0	16.2	0.784	0.771	2349.6
12	2359.6	2340.1	21.2	19.5	0.785	0.780	2349.5
14	2361.0	2338.4	24.3	22.6	0.785	0.780	2349.3
16	2362.7	2336.7	27.8	26.0	0.794	0.787	2349.3
18	2364.0	2334.9	31.0	29.1	0.795	0.787	2349.1
20	2365.2	2333.0	33.8	32.2	0.786	0.785	2348.7
22	2366.4	2331.4	36.7	35.0	0.781	0.779	2348.5
24	2367.7	2329.7	40.1	38.0	0.787	0.776	2348.3
26	2369.0	2327.6	43.5	41.4	0.790	0.780	2347.9
28	2370.2	2325.5	46.7	44.7	0.790	0.784	2347.5
30	2371.2	2323.5	49.6	47.7	0.787	0.782	2347.0
32	—	2321.6					
34	—	2319.8					
36	—	2317.9					
38	2375.3	2315.7	61.5	59.6	0.780	0.776	2345.1
40	2376.3	2313.8	64.5	62.5	0.777	0.772	2344.6
42	2377.2	2311.8	67.5	65.4	0.776	0.770	2344.1
44	2378.0	2309.7	70.3	68.3	0.774	0.768	2343.5
46	2378.7	2307.7		71.0		0.765	2342.8

puted as before by averaging the numbers in columns 2 and 3 and subtracting $h/8\pi^2cI$ are shown in column 8. These may be satisfactorily represented by the equation

$$\nu_3 = 2350.1 - 0.0035J^2.$$

The convergence is larger than for the other band, but not extremely large, and hardly explains the great asymmetry of the emission band. The very strong emission observed beyond 4.4μ[16] is doubtless due in large measure to transitions between states both of which are vibrationally excited.

With the enclosed spectrometer it was possible to remove all traces of this band by washing for many hours with air from which the CO_2 had been removed. A small amount of gas was replaced, and records run with the 7200 line grating and very narrow slits. The rotation structure then showed up clearly on the low-frequency side, but on the high-frequency side was scarcely more distinct than in the plotted curve. Envelopes traced from the photographic records are shown in Fig. 5A, for quantities of CO_2 equivalent to 0.01, 0.02 and 0.11 cm path length at normal pressure. A number of such curves were obtained after adding successively measured amounts of pure CO_2, and

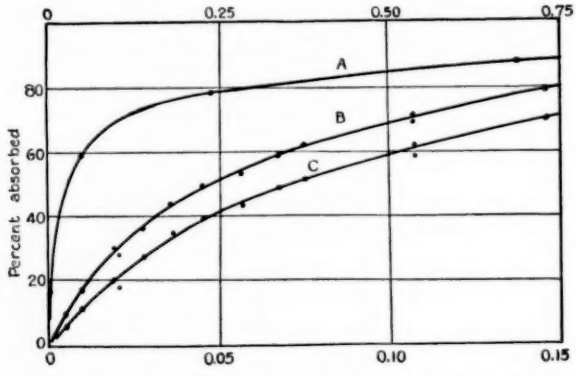

Fig. 6. Dependence of absorption upon path length. Abscissae are equivalent lengths in cm of CO_2 at one atmosphere. *A:* Zero branch of 15μ band, 668 cm^{-1} (upper scale). *B* and *C:* Maxima of 4.3μ band at 2365 and 2340 cm^{-1} (lower scale).

from each the percentage absorption at the two maxima was determined. These values are plotted in Fig. 6, curves *B* and *C*.

Harmonic and Combination Bands

The preliminary measurements upon the second harmonic of ν_2 in the region near 4.8μ have already been mentioned. These provide precise term values for the pair of interacting levels $\{(\nu_1+1_1\nu_2),3_1\nu_2\}$. With better resolution it may also be possible to identify lines originating in the level 1_2, thus determining the positions of the various compound levels involving 4_0 and 4_2. No first harmonic of ν_3 appears, but the selection rules permit the transition $\Delta V_3=3$, and a weak band has been observed in the proper position, 1.4μ, by Schaefer and Philipps.

The strong double band at 2.7μ has not yet been remeasured, but its character and position are well known. It corresponds to the allowed transitions $\nu_3+\{\nu_1,2\nu_2\}$ where the bracket represents the pair of interacting states at 1285 and 1388 cm^{-1}. Both components are doublet bands, in agreement with the

[16] Cf. Barker, reference 1.

prediction for $\Delta L = 0$. The fact that their intensities are almost equal again indicates the close resonance between ν_1 and $2\nu_2$, for both of the compound levels must partake about equally of the two component motions. A considerably weaker group of bands appears in the neighborhood of 2μ, and is doubtless to be interpreted as

$$\nu_3 + \{2\nu_1, \nu_1 + 2_0\nu_2, 4_0\nu_2\}$$

but this also remains to be examined in detail. The next member of the same sequence, obtained by adding $\{\nu_1, 2\nu_2\}$ would account for the observed bands near 1.6μ.

With very large amounts of absorbing gas Schaefer and Philipps have also located a pair of bands at 9.4μ and 10.4μ absorbed by molecules already excited to the first pair of interacting levels, and corresponding to the transitions $\nu_3 - \{\nu_1, 2_0\nu_2\}$. There remains the very weak band at 3.28μ, in a position corresponding to $\nu_2 + \nu_3$, a combination which is in apparent contradiction with the rule that $\Delta V_2 + \Delta V_3$ must be odd. If further observation definitely confirms this absorption, and if no other interpretation appears, then the question must be raised whether or not the restriction is absolute.

Thus with one possible exception every observed band is in complete accord with the vibration spectrum predicted by Dennison's rules for a linear symmetrical molecule. The fine structure of the fundamental bands leads also to the conclusion that the molecule must have the linear form O:C:O. Finally the Raman spectra, both vibrational and rotational, may be explained only in terms of the same model. All existing observational data seem now to be consistently correlated.

The Vibrational Levels of Linear Symmetrical Triatomic Molecules

By DAVID M. DENNISON
University of Michigan

(Received June 17, 1932)

The theory proposed by E. Fermi of the energy levels of molecules of the CO_2 type is discussed. It is shown that this assumes a particularly simple form when expressed in the coordinates used by Dennison for describing such molecules. When there exist no integral or nearly integral relations between the vibrational frequencies the first order energy correction λW_1 caused by the anharmonic forces vanishes leaving only the second order term $\lambda^2 W_2$. When, however, two of the fundamental frequencies are commensurable, certain of the energy levels coincide thus becoming degenerate. This degeneracy may be removed by the anharmonic forces in which case there appears a first order energy constant λW_1 different from zero. The value of λW_1 is computed explicitly for certain of the lower energy states and it appears that the only levels which interact under the influence of the resonance are those having the same value of the azimuthal quantum number l. From this it follows that the selection rules are not affected by the existence of the resonance. Finally it is shown how the first order term λW_1 goes over into the second order term $\lambda^2 W_2$ as the resonance between the frequencies becomes less and less exact. When these results are applied to the CO_2 spectrum it is found that the resonance between ν_1 and $2\nu_2$ is almost perfect and consequently the energy levels can only be ordered with the help of the first order term λW_1. For CS_2 on the other hand the difference between ν_1 and $2\nu_2$ is so large that the effect of the resonance on the positions of the energy levels may be disregarded.

WITHIN the last few months two important contributions have been made to our knowledge of the carbon dioxide molecule and its infrared spectrum. The first of these was contained in a paper by E. Fermi[1] and was intended in the first instance to explain the Raman spectrum of CO_2. The second, by P. E. Martin and E. F. Barker,[2] is reported in the foregoing paper and consists of an experimental study of the fine structure of certain of the infrared bands. It is proposed in the present paper to discuss Martin and Barker's results in the light of Fermi's theory and to relate both to the earlier work of Dennison[3] on the general properties of symmetrical molecules of the type YX_2.

It can no longer be doubted that the carbon dioxide molecule in its normal electronic state possesses a form which is both linear and symmetrical. Two sets of independent data prove this. The fact that the fine structure lines of the parallel type band at 4.3μ and of the perpendicular type band at 15μ both are linearly spaced in frequency and have the same spacing constant shows that the CO_2 molecule must be linear. The fact that alternate fine structure lines of these bands have zero intensity shows that the mole-

[1] F. Fermi, Zeits. f. Physik **71**, 250 (1931).
[2] P. Martin and E. F. Barker, Phys. Rev. **41**, 291 (1932).
[3] D. M. Dennison, Rev. Mod. Phys. **3**, 280 (1931).

cule must have the form O=C=O and not O=O=C. The second reason for believing that CO_2 is both linear and symmetrical is that it has been shown that the vibrational levels of such molecules are connected by rather unusual selection rules which permit only certain of the overtone bands to appear. A study of all the known infrared bands of CO_2 reveals that just the permitted overtones and no others are observed.

In discussing the positions of the vibrational levels of the molecule YX_2, the notation proposed by Dennison[3] will be used as well as the same coordinates. The internal or vibrational degrees of freedom are four in number since of the total $3n$ or 9 degrees of freedom, three may be associated with translation of the system as a whole and two (not three, since the molecule is linear) with rotation of the system. The coordinates of the vibrational motion are chosen as z, q, r and ϕ. z is the displacement of the Y atom along the figure axis relative to the center of gravity of the X atoms. q is the displacement of the X atoms, from their equilibrium position, relative to each other. r is the displacement of the Y atom $\perp$ to the figure axis relative to the line joining the X atoms and ϕ is the angle this latter displacement makes in a plane $\perp$ to the figure axis.

The kinetic energy of the system (internal) may be readily computed and is,

$$T = (m/4)\dot{q}^2 + (\mu/2)(\dot{z}^2 + \dot{r}^2 + r^2\dot{\phi}^2)$$

where m is the mass of an X atom and μ is the reduced mass $2mM/(M+2m)$.

We assume that the potential energy U possesses a symmetry which corresponds with the geometric symmetry of the molecule. That is, U must be an even function of z, an even function of r and independent of the angle ϕ.

We assume that the potential function may be developed after λ, a parameter of smallness so that $U = U_0 + \lambda U_1 + \lambda^2 U_2$. The function U_0 contains all the permissable terms which are quadratic in the coordinates, U_1 all the cubic terms and U_2 all the quartic terms. It is usual to let the constants of U_0 contain the normal frequencies ν_1, ν_2 and ν_3 so that it has the form,

$$U_0 = \pi^2\nu_1^2 m q^2 + 2\pi^2\nu_2^2\mu r^2 + 2\pi^2\nu_3^2\mu z^2.$$

The wave function which results from using a wave equation based on T and U_0 has been already described by Dennison.

$$\psi = \psi_{(\sigma)}{}^{V_1}\psi_{(\xi)}{}^{V_3}R_{(\rho)}{}^{V_2 l}e^{\pm il\phi}$$

where $\psi_{(\sigma)}{}^{V_1}$ and $\psi_{(\xi)}{}^{V_3}$ are the well-known Hermitian orthogonal functions.

$$R_{(\rho)}{}^{V_2 l} = \rho^l e^{-\rho^2/2}\sum_{k=0}^{V_2 - l} a_k \rho^k$$

where

$$a_{k+2} = \frac{2k + 2l - 2V_2}{(k+2)(k+2+2l)}\, a_k.$$

The dimensionless variables σ, ξ and ρ, replace the coordinates q, z and r and are related to them by the following expressions,

$$\sigma = 2\pi[\nu_1 m/2h]^{1/2} q$$
$$\xi = 2\pi[\nu_3 \mu/h]^{1/2} z$$
$$\rho = 2\pi[\nu_2 \mu/h]^{1/2} r.$$

It will prove convenient to write the energies T and U in terms of these variables.

$$T = (h/8\pi^2)\{\dot{\sigma}^2/\nu_1 + \dot{\xi}^2/\nu_3 + (\dot{\rho}^2 + \rho^2\dot{\phi}^2)/\nu_2\}$$
$$U_0 = (h/2)\{\nu_1\sigma^2 + \nu_3\xi^2 + \nu_2\rho^2\}$$
$$\lambda U_1 = \lambda h(a\sigma^3 + b\sigma\rho^2 + c\sigma\xi^2)$$
$$\lambda^2 U_2 = \lambda^2 h(d\sigma^4 + e\rho^4 + f\xi^4 + g\sigma^2\rho^2 + i\xi^2\sigma^2 + j\rho^2\xi^2).$$

The quantities λ, $a, \cdots j$ are constants which characterize the anharmonic nature of the potential function. It will be noted that the condition that U must possess a symmetry which corresponds to the geometric symmetry of the molecule, greatly reduces the number of terms appearing in U_1 and U_2. Thus of the ten cubic terms which may be formed with three variables, only three actually appear in U_1.

The energy constant W of the system may be developed in powers of λ so that $W = W_0 + \lambda W_1 + \lambda^2 W_2$. The zeroth order term W_0 has of course the form,

$$W_0/h = \nu_1(V_1 + \tfrac{1}{2}) + \nu_2(V_2 + 1) + \nu_3(V_3 + \tfrac{1}{2})$$

where V_1, V_2, and V_3 are the quantum numbers appearing in the expression for the wave function. Since the number l does not appear in W_0, the system is in this approximation (V_2+1) fold degenerate.

The terms W_1 and W_2 which arise from the anharmonic nature of the potential function may be readily computed using perturbation theory methods. In the usual case when the frequencies ν_1, ν_2 and ν_3 are incommensurable, this leads to the following result.

$$\lambda W_1 = 0$$
$$\lambda^2 W_2/h = x_0 + x_1 V_1 + x_2 V_2 + x_3 V_3 + x_{11} V_1^2 + x_{22} V_2^2 + x_{ll} l^2 + x_{33} V_3^2 + x_{12} V_1 V_2 + x_{13} V_1 V_3 + x_{23} V_2 V_3$$

$x_0, \cdots x_{23}$ are a set of constants[4] which are related to the anharmonic constants $a, \cdots j$.

The important contribution of Fermi consists in an investigation of the system when two of the frequencies bear a commensurable or nearly commensurable relation to each other. He has been able to show that when $\nu_1 \cong 2\nu_2$ the first order energy constant λW_1 no longer vanishes and may exert a very considerable influence in the energy levels. We propose to make clear just how this result obtains and how it may be correlated with the observed infrared spectrum of CO_2.

[4] Dennison (reference 3) in giving the formula for $\lambda^2 W_2$ stated that the constant x_{ll} was equal to $-\frac{1}{3}x_{22}$. Unfortunately this statement is incorrect except in the special case where $\lambda U_1 = 0$. In general an independent constant x_{ll} must be introduced.

It will become evident from the analysis that when $\nu_1 \cong 2\nu_2$, λW_1 depends solely upon the anharmonic term $b\sigma\rho^2$ while if ν_1 were approximately twice ν_3, λW_1 would depend entirely upon $c\sigma\xi^2$. For CO_2 as well as CS_2 it is the former condition which holds and we may therefore confine our attention to the term $b\sigma\rho^2$.

We shall first carry out the computation, assuming first that no commensurable relation exists between ν_1 and ν_2. It is possible to ignore the existence of the vibration ν_3 since its coordinate ξ does not enter the part of U_1 we are considering. In fact we may without loss of generality confine ourselves to the case where $\lambda U_1 = \lambda hb\sigma\rho^2$ and $\lambda^2 U_2 = 0$. The usual methods of perturbation theory then give

$$\lambda W_1 = \lambda U_{1V_1V_2l}^{V_1V_2l}$$

$$\lambda^2 W_2 = \lambda^2 \sum_{V_1'V_2'} \left(U_{1V_1'V_2'l}^{V_1V_2l} \right)^2 \Big/ \left(W_0^{V_1V_2} - W_0^{V_1'V_2'} \right)$$

where $U_{1\,V_1'V_2'l}^{\,V_1V_2l}$ is the matrix element of U_1.

The general expression for the perturbation energy has been slightly simplified since we take only those matrix elements of U_1 which are diagonal in l and omit the corresponding integration over ϕ. This is permissible since the function U_1 is independent of ϕ and therefore all the matrix elements which are nondiagonal in l automatically vanish. It is supposed that ψ^{V_1} and $R^{V_2\,l}$ are properly normalized.

It is clear that the matrix elements of U_1 which are diagonal in V_1 must vanish since $(\psi^{V_1})^2$ is an even function of σ while the function U_1 is odd. Evidently then $\lambda W_1 = 0$. The computation of $\lambda^2 W_2$ is somewhat tedious but quite straight-forward and leads to the following result.

$$\lambda^2 W_2 = -\frac{\lambda^2 b^2 h}{8} \left\{ \frac{V_2^2 + 4V_1V_2 - l^2 + 4V_1 + 4V_2 + 4}{\nu_1 + 2\nu_2} + \frac{V_2^2 - 4V_1V_2 - l^2 - 4V_1}{\nu_1 - 2\nu_2} + \frac{4(V_2 + 1)^2}{\nu_1} \right\}.$$

The expression for $\lambda^2 W_2$ which has been obtained is valid except in the region where ν_1 and $2\nu_2$ are approximately equal. In this case $\lambda^2 W_2$ becomes of higher order of magnitude and the whole method of the perturbation theory which has been used breaks down. A new method must then be employed which leads to the result that when $\nu_1 \cong 2\nu_2$, a first order perturbation energy λW_1 exists.[5]

We begin by letting the unperturbed system be one where ν_1 and $2\nu_2$ are exactly equal, thus making a number of the previously distinct energy levels coincide. It is possible as before to ignore the vibration ν_3 and its coordinate ξ and to introduce the single anharmonic term $\lambda U_1 = \lambda hb\sigma\rho^2$. To this however

[5] We may remark that λW_1 and $\lambda^2 W_2$ will be given by the above expressions even when $\nu_1 \cong 2\nu_2$ for the particular states where the quantum numbers bear the relation $V_2^2 - 4V_1V_2 - l^2 - 4V_1 = 0$. This conclusion is borne out by the results of the ensuing investigation.

must be added a term involving $\Delta = \nu_1 - 2\nu_2$ to take account of the fact that in the final or perturbed system ν_1 is only of the same order but not necessarily equal to $2\nu_2$. The problem may then be treated in a manner similar to that used by Fermi, namely by the standard method of perturbations of a degenerate system.[6]

The unperturbed system may be characterized by T_0 and U_0 and the effect of the perturbation grouped into the two terms T_1 and λU_1.

$$T_0 = (h/8\pi^2\nu_2)(\dot{\sigma}^2/2 + \dot{\rho}^2 + \rho^2\dot{\phi}^2)$$
$$U_0 = (h\nu_2/2)(2\sigma^2 + \rho^2)$$
$$T_1 = (\Delta h/32\pi^2\nu_2^2)\dot{\sigma}^2 = -(\Delta h/2)(\partial^2/\partial\sigma^2)$$
$$\lambda U_1 = \lambda hb\sigma\rho^2 + \Delta h\sigma^2/2.$$

The unperturbed system having the kinetic and potential energies T_0 and U_0 respectively possesses an energy constant $W_0/h = \nu_2(2V_1 + V_2 + 2)$. The unperturbed system is thus degenerate in two ways, first because as before W_0 is independent of the quantum number l and second because the energy does not depend upon V_1 and V_2 separately but only upon the function $2V_1 + V_2$.

To find the first order perturbed energy of a degenerate system, the secular determinant must be constructed and set equal to zero.

$$\left| A_s^r - \lambda W_1 \delta_s^r \right| = 0.$$

The roots of this determinant λW_1 furnish the required perturbed energies. The quantity A_s^r is the matrix element of the perturbing function $T_1 + \lambda U_1$.

The quantum numbers for any one secular determinant must belong to the same value of W_0, that is $2V_1 + V_2 =$ a constant. We may simplify the expression for A_s^r by noting two properties of the system. (a) All the elements which are nondiagonal in l vanish since $T_1 + \lambda U_1$ is independent of the angle ϕ. (b) The wave function ψ^{V_1} satisfies the differential equation $(d^2\psi^{V_1}/d\sigma^2) + (2V_1 + 1 - \sigma^2)\psi^{V_1} = 0$ and therefore $(T_1 + \lambda U_1)\psi^{V_1} = \{\lambda hb\sigma\rho^2 + \Delta h(V_1 + \frac{1}{2})\}\psi^{V_1}$. Combining these properties with the other known properties of the unperturbed wave functions, we may express all the nonvanishing elements of A_s^r as follows,

$$A^{V_1 V_2 l}_{V_1 V_2 l} = \Delta h(V_1 + \tfrac{1}{2})$$
$$A^{V_1 \quad V_2 \quad l}_{V_1 - 1 \quad V_2 + 2 \quad l} = -\lambda hb(V_1)^{1/2}\left[(V_2 + 2)^2 - l^2\right]^{1/2}/2^{3/2}.$$

The secular determinant may now easily be constructed for any value of $2V_1 + V_2$. The coordinate system we have used allows the determinant to be evaluated very simply since, because the elements A_s^r which are nondiagonal in l all vanish, the determinant may be factored into a set of determinants each corresponding to a particular value of l. Thus if $2V_1 + V_2$ equals 4, the

[6] While our computation is quite equivalent to that performed by Fermi and leads to the same result we feel that a real advantage is secured by our use of the coordinates σ, ρ and ϕ. Not only is the calculation much simpler but it is found that the final results may be presented in a very natural form which allows a clear understanding of their interrelations.

original determinant is of 9th order. It can be factored into three determinants of order 3, 2, 2, 1 and 1 corresponding to $l=0$, $+2$, -2, $+4$ and -4 respectively.

The explicit solutions of the secular determinant for the smaller values of the quantum members are presented in Table I.

TABLE I.

V_1	V_2	l	$\lambda W_1/h$
0	0	0	$\Delta/2$
0	1	±1	$\Delta/2$
1	0	0	$\Delta\pm[\Delta^2/4+(\lambda b)^2/2]^{1/2}$
0	2	0	
0	2	±2	$\Delta/2$
1	1	±1	$\Delta\pm[\Delta^2/4+(\lambda b)^2]^{1/2}$
0	3	±1	
0	3	±3	$\Delta/2$
2	0	0	$(\lambda W_1)^3-(9/2)\Delta h(\lambda W_1)^2$
1	2	0	$-[3(\lambda hb)^2-(2\ 3/4)\ (\Delta h)^2]\lambda W_1$
0	4	0	$-(1\ 5/8)\ (\Delta h)^3+(1\ 1/2)\ (\lambda bh)^2\Delta h=0$
1	2	±2	$\Delta\pm[\Delta^2/4+(3/2)\ (\lambda b)^2]^{1/2}$
0	4	±2	
0	4	±4	$\Delta/2$

The degeneracy that originally existed in the unperturbed system has been to a considerable extent removed by the perturbing potential and the identities of the levels have been somewhat changed. When two or more levels are connected by lines in the above table, we mean that the original degeneracy of the levels has been removed. The wave functions which are appropriate for describing these new undegenerated levels are linear combinations of the wave functions of the degenerate levels. The coefficients in the linear combinations are given by the first minors of the secular determinant in question.

We should now like to show how the energy constant of second order $\lambda^2 W_2$ which is appropriate for the case $\nu_1 \neq 2\nu_2$ goes over into the first order constant λW_1 when $\nu_1 \doteqdot 2\nu_2$. In order to compare these two expressions, values of $\Delta=\nu_1-2\nu_2$ must be chosen which are small compared with $\nu_1+2\nu_2$ but which are large compared with the anharmonic constant λb. The leading term of $\lambda^2 W_2$ is then $-\lambda^2 b^2 h(V_2^2-4V_1V_2-4V_1-l^2)/\Delta$ while the expressions for λW_1 may be developed. Thus the energy levels of the states (100) and (020) become $(3/2)\Delta h+\lambda^2 b^2 h/2\Delta$ and $(1/2)\Delta h-\lambda^2 b^2 h/2\Delta$. The terms $(3/2)\Delta h$ and $(1/2)\Delta h$ when added to the W_0 of the degenerate system ($\nu_1=2\nu_2$) are just equal to the W_0 of the undegenerate system and the remaining terms $\pm\lambda^2 b^2 h/2\Delta$ are just equal to $\lambda^2 W_2$ when we substitute the appropriate values of the quantum numbers. A similar agreement is found between λW_1 and $\lambda^2 W_2$ for all the other levels which have been computed.

This analysis leads to a criterion as to the method to be used in correlating the energy levels of such a system. When $|\Delta| \leq |\lambda b|$ we must treat the system as degenerate and use the first order energy constant λW_1. A second

order constant $\lambda^2 W_2$ could also be added and would probably have the usual form (i.e., a quadratic function of the quantum numbers). When $|\Delta| \gg |\lambda b|$, λW_1 becomes equal to one of the terms of $\lambda^2 W_2$ and consequently we may order the levels with the aid of the second order constant $\lambda^2 W_2$ alone. The difference between these cases will be brought out in our discussion of the CO_2 and CS_2 spectra.

Finally it will be observed that the selection rules proposed by Dennison for the symmetrical triatomic molecules apply equally well to the degenerate system and to the nondegenerate system for which they were derived. The states of the degenerate system which combine and lose their identity possess wave functions having the same quantum numbers l and V_3 and having numbers V_2 which differ by an even integer. The selection rules depend upon whether the changes ΔV_2, ΔV_3 and Δl are odd or even integers and these changes will be the same (i.e., odd or even) for all the levels of a related group. The wave functions of a related group all have the same symmetry character with regard to an interchange of the two equal atoms.

Discussion of the CO_2 Spectrum

Let us now consider the energy levels of the CO_2 molecule as determined by the observations of Martin and Barker. If the assumption is made that the system is nearly degenerate ($|\Delta| \ll |\lambda b|$), the energy may be expressed as $W_0 + \lambda W_1$ and the second order terms $\lambda^2 W_2$ may be neglected. This identification will allow us to compute from three of the levels Δ and λb (thus checking the assumption as to the degeneracy) and then to predict the positions of the remaining levels. The difference between the predicted and observed positions of these levels will be a measure of the neglected term $\lambda^2 W_2$. The results of this correlation are collected in Table II where the lowest state (000) is taken to have zero energy.

Table II.

V_1	$\nu_2 = 667.5$ cm^{-1} V_2	l	$\lambda b = \pm 72.5$ cm^{-1} Observed level	$\Delta = +4.2$ cm^{-1} Computed level
0	0	0	0	0
0	1	1	667.5 cm^{-1}	—
1	0	0	1285.8	—
0	2	0	1388.4	—
0	2	2	1336.2	1335.0
1	1	1	1933.5	1932.1
0	3	1	2077.1	2077.1
0	3	3	—	2004.6
2	0	0	—	2548.0
1	2	0	—	2675.6
0	4	0	—	2799.0

It appears that in CO_2 the resonance between ν_1 and $2\nu_2$ is almost exact so that their difference is small, $\Delta = 4.2$ cm^{-1}. The accuracy with which this constant has been determined is not great. We estimate the error to be of the order of 50 to 100 percent. The value of $|\lambda b|$ on the other hand may be fixed with considerable precision since it depends essentially on the distance

between the two strong Raman bands or between certain of the infrared bands. It is probably accurate to at least 1 percent. It will be noted that the sign of λb cannot be determined through the positions of the energy levels.

The overtone bands of CO_2 which have been observed by Barker[7] and others to lie in the region of 2.7μ must be correlated with the sum of the levels (100), (020) and the level $\nu_3 = 2350$ cm^{-1}. The computed values of these overtone frequencies are therefore 3636 and 3738 cm^{-1} while their observed positions are 3610 and 3717 cm^{-1}. The differences, 24 and 21 cm^{-1}, are due to the fact that in the computation we have neglected the second order energy constant $\lambda^2 W_2$. In a similar way the three overtone bands observed by Schaefer and Philipps[8] at about 2μ arise from a combination of the level ν_3 with the levels (200), (120), (040). The computed values of the frequencies are 4898, 5026 and 5149 cm^{-1}, while their observed positions are 4780, 4890 and 5010 cm^{-1}. The differences, which are also due to the neglected second order terms, are 118, 136 and 139 cm^{-1} respectively. We should expect these differences to be larger than those for the lower overtone bands but only by a factor of about two. The solution of this difficulty must await the results of further analysis.

Discussion of the CS_2 Spectrum

According to Krishnamurti[9] the Raman spectrum of CS_2 gas consists principally of two strong lines with an intensity ratio of about 5:1 lying at 655.5 and 795.0 cm^{-1} respectively. These may be identified with transitions from the normal state to the two combined levels (100), (020). The frequency ν_1 has been found by Dennison and Wright[10] to lie at 396.8 cm^{-1}. Combining these three data and neglecting as before the second order constant $\lambda^2 W_2$ we may compute $\lambda b = \pm 19.7$ cm^{-1} and $\Delta = -136.7$ cm^{-1}.

These results for λb and Δ show that we are in the region where the resonance between ν_1 and $2\nu_2$ is very poor and where λW_1 is equivalent to one of the terms of $\lambda^2 W_2$. (Since for these values of λb and Δ, the expression $[\Delta^2/4 + (\lambda b)^2/2]^{1/2}$ does not differ appreciably from $\Delta/2 + (\lambda b)^2/2\Delta$.) Consequently we may not neglect $\lambda^2 W_2$ in computing the energy levels. In fact we may consider that λW_1 is included among the terms of $\lambda^2 W_2$ and thus use the general expression $W_0 + \lambda^2 W_2$ alone for correlating the energy levels. This expression involves ten constants while there have been observed only eight Raman and infrared bands. Thus only certain of the anharmonic constants may be obtained and no independent relations are available with which to check the theoretical formula. (Those constants which may be computed are all small and of the correct order of magnitude). These considerations show that our initial computation of λb and Δ was somewhat meaningless. That is to say, while we can determine with accuracy the value of Δ, the difference between ν_1 and $2\nu_2$, the positions of the levels will not furnish us with any clear information as to the value of λb other than its order of magnitude.

[7] E. F. Barker, Astrophys. J. **55,** 391 (1922).
[8] Cl. Schaefer and B. Philipps, Zeits. f. Physik **36,** 641 (1926).
[9] Krishnamurti, Ind. Journ. Phys. **5,** 109 (1930).
[10] D. M. Dennison and N. Wright, Phys. Rev. **38,** 2077 (1931).

In a recent note S. Bhagavantam[11] calls attention to the fact that the Raman line at 795.0 cm^{-1} possesses properties which are characteristic of the inactive frequency ν_1 and which have nothing in common with the frequency ν_2. He therefore prefers to designate this level with the symbol ν_1' rather than with $2\nu_2$ as do Dennison and Wright. This remark by Bhagavantam illustrates very clearly the nature of the line in question. As a Raman line its existence depends wholly on the fact that the level must be described partly with the wave function (100) of the unperturbed inactive frequency ν_1. Thus its character in the Raman spectrum must be similar to ν_1 and there is some justification for calling it ν_1'. However, in ordering all the vibrational levels of the molecule, we have shown that since $|\Delta|$ is large compared with $|\lambda b|$ we may disregard the fact that $\nu_1 \leqq 2\nu_2$. Therefore in speaking of the positions of the levels it is more appropriate to speak of this level as $2\nu_2$. The level possesses a wave function partly characteristic of ν_1 and partly characteristic of $2\nu_2$ and consequently its proper designation will depend upon what properties of the spectrum are being considered.

[11] S. Bhagavantam, Phys. Rev. **39**, 1020 (1932).

The Two-Minima Problem and the Ammonia Molecule

By DAVID M. DENNISON AND G. E. UHLENBECK
University of Michigan

(Received June 8, 1932)

The system of a particle moving in a potential field containing two equal minima is treated by the Wentzel-Kramers-Brillouin method of approximation. The energy levels are grouped in pairs and the object of the computation is to find the separation between two levels forming a pair. This is accomplished by connecting the oscillatory and exponential approximate solutions of the wave equation by means of the Kramers connection formulae. If Δ is the separation of a pair and $h\nu$ the distance between two pairs $\Delta/h\nu=1/\pi A^2$ where $A=\exp\left[(2\pi/h)\int_0^{x_1}[2m(V-E)]^{1/2}dx\right]$. A particular potential curve is chosen consisting of two equal parabolae connected by a straight line. The expression for Δ may then be evaluated explicitly as a function of the length of the joining line, $2(x_0-\alpha)$ and the distance between two minima, $2x_0$. These formulae may be applied to determining the form of the ammonia molecule. Substituting the experimental values for Δ_0 and Δ_1, it is found that $x_0=3.161$ and $\alpha=1.916$. An exact solution for this particular potential curve may be found by joining Weber's function $D_n(x-x_0)$ and $D_n(x+x_0)$ to a hyperbolic sine or cosine. This process also leads to expressions for Δ which may be equated to the experimental values yielding $x_0=3.182$ and $\alpha=1.930$, in good agreement with the earlier determination. Finally x_0 is used to compute $2q_0=0.760\times10^{-8}$ cm, the distance between the two potential minima, and the following dimensions of the ammonia molecule, $H-H=1.64\times10^{-8}$, $N-H=1.02\times10^{-8}$ cm.

§1.

THE one-dimensional system of a particle moving in a potential field consisting of two equal minima was first treated qualitatively by Hund[1] who showed that the vibrational energy levels which lie below the potential maximum will occur in pairs. The distance between two pairs is roughly equal to $h\nu_0$ where ν_0 is the normal frequency of oscillation, while the separation of the two levels forming a pair depends upon the height and nature of the barrier between the minima and is in general very small. We propose to compute the level separation using the Wentzel-Kramers-Brillouin method of approximation and then to compare this solution with an exact solution based on a particular potential field. Finally an application of the results will be made to the ammonia molecule.

§2.

The W. K. B. method yields an approximate solution of the wave equation whose form depends essentially upon whether the region being considered lies within or without the region in which the classical motion might take place, that is, the region where the kinetic energy is positive. In the first case the solution is oscillatory and has the form

$$\psi_{(x)} = (c/P^{1/2}) \cos\left[(2\pi/h)\int^x Pdx + \gamma\right]$$

[1] F. Hund, Zeits. f. Physik **43**, 805 (1927).

where x is the coordinate of the system, c and γ are arbitrary constants, and

$$P = + \left[2m \left| E - V \right| \right]^{1/2}.$$

In the second or non-classical region the solution consists of a linear combination of an increasing and a decreasing exponential[2] which has the form

$$\psi_{(x)} = (a/P^{1/2}) \exp\left[(2\pi/h)\int^{x} Pdx\right] + (b/P^{1/2}) \exp\left[-(2\pi/h)\int^{x} Pdx\right].$$

At each boundary or critical point there will exist two conditions upon the arbitrary constants c, γ, a and b which arise from the fact that each function must approximate the *same* exact solution of the wave equation. These relations between the constants are the so-called Kramers connection formulae.[3] The increasing exponential connects with the oscillatory solution so that $c=a$ and $\gamma=+\pi/4$ while for the decreasing exponential $c=2b$ and $\gamma=-\pi/4$.

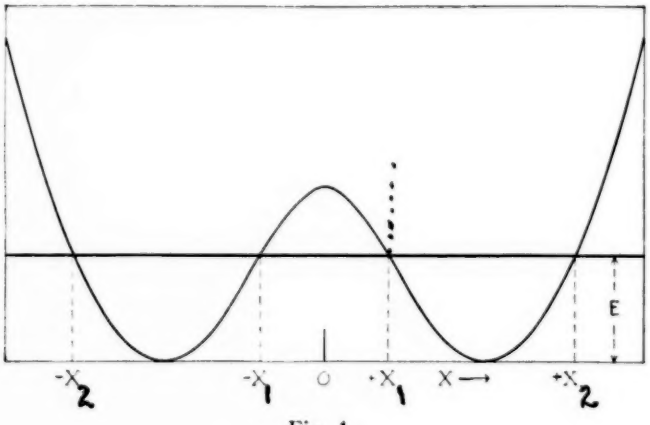

Fig. 1.

These formulae furnish a method by which we may approximate to any solution of the wave equation. When however one wishes to approximate the *eigenfunctions*, namely those functions for which $\int_{-\infty}^{+\infty}\bar{\psi}\psi dx$ is finite, one must let ψ be represented only by the *decreasing* exponential as x approaches + or − infinity. Thus in a region from $+\infty$ to $-\infty$ which has n critical points, there will exist $2n+2$ conditions arising from the connection formulae.

The $n+1$ regions will furnish $2n+2$ constants but one of these, the multiplicative one, must be kept arbitrary in order later to normalize the wave

[2] By increasing or decreasing exponential we will always mean increasing or decreasing when we proceed *away* from the boundary point between the classical and non-classical regions *into* the non-classical region.

[3] H. A. Kramers, Zeits. f. Physik **39**, 828 (1926), H. A. Kramers and G. P. Ittmann, Zeits. f. Physik **58**, 217 (1929), A. Zwaan, Utrecht Diss., 1929. These formulae are collected in a paper by L. A. Young and G. Uhlenbeck, Phys. Rev. **36**, 1154 (1930).

function. Thus there is one condition remaining and this just serves to fix the value of E, that is to determine the eigenvalues of the problem. When we have a system in which the potential has only a single minimum this procedure leads to the well-known half integer quantization of the phase integral.

$$\oint P dx = (n + \tfrac{1}{2})h. \tag{1}$$

§3.

Let us now consider the case of two equal minima, (illustrated in Fig. 1) where the energy level E is assumed to lie below the potential barrier at $x=0$. Since the potential is an even function of x the wave functions will be divided into two classes, those which are even functions of x and those which are odd functions. We begin by assuming that the level in question corresponds to an even eigenfunction, ψ_+, and we denote the energy by E_+.

In the region from $-x_1$ to $+x_1$ the wave function will have the character of an hyperbolic cosine and may be written in the following manner where C is the multiplicative constant mentioned earlier.

$$\psi_+ = (C/P^{1/2}) \cosh\left[(2\pi/h)\int_0^x P dx\right] \quad -x_1 < x < x_1.$$

It is now convenient to write $\int_0^x P dx = \int_0^{x_1} P dx - \int_x^{x_1} P dx$. Further let $A = \exp\left[(2\pi/h)\int_0^{x_1} P dx\right]$. We may then express ψ_+ as

$$\psi_+ = (C/2P^{1/2})\left\{A \exp\left[-(2\pi/h)\int_x^{x_1} P dx\right] + (1/A)\exp\left[(2\pi/h)\int_x^{x_1} P dx\right]\right\}$$

$$-x_1 < x < x_1.$$

Applying now the connection formulae between the regions $-x_1$ to x_1 and x_1 to x_2, we obtain the following oscillatory solution for the latter region.

$$\psi_+ = \frac{R_+ C}{\sqrt{P}} \cos\left[(2\pi/h)\int_{x_1}^x P dx - \theta_+\right] \tag{2}$$

where

$$\tan\theta_+ = (2A^2 - 1)/(2A^2 + 1) \tag{3}$$

and

$$R_+ = (4A^4 + 1)^{1/2}/2A.$$

Now in the region $x > x_2$ we must have the decreasing exponential, that is,

$$\psi_+ = (\alpha C/P^{1/2}) \exp\left[-(2\pi/h)\int_{x_2}^x P dx\right]$$

where α is a new constant as yet undetermined. This connects in the region x_1 to x_2 with

$$\psi_+ = (2\alpha C/P^{1/2}) \cos\left[(2\pi/h)\int_x^{x_2} Pdx - \pi/4\right]. \tag{4}$$

Eqs. (2) and (4) must give identical values for ψ_+ as a function of x and consequently also of the first derivative of ψ_+. We may thus eliminate α by requiring that ψ_+'/ψ_+ as determined from (2) shall be the same as ψ_+'/ψ_+ determined from (4). This gives immediately

$$\tan\left[(2\pi/h)\int_{x_1}^{x} Pdx - \theta_+\right] = \tan\left[(2\pi/h)\int_{x_1}^{x} Pdx + \pi/4\right].$$

The two angles whose tangents are equal must differ by $n\pi$ where n is an integer and this leads to the result,

$$\oint Pdx = (n + \tfrac{1}{4} + \theta_+/\pi)h. \tag{5}$$

From (3) one sees that $\theta_+ < \pi/4$ and in the limit of an infinite barrier where $A \to \infty$, $\theta_+ \to \pi/4$ and (5) reduces to (1).

The foregoing calculation is appropriate for a discussion of one of the levels E_+ where ψ_+ is an even function of x. For the remaining levels E_- where ψ_- is an odd function of x we must start in the region $-x_1$ to x_1 with the hyperbolic sine. We obtain in a similar manner,

$$\oint Pdx = (n + \tfrac{1}{4} + \theta_-/\pi)h \tag{6}$$

where

$$\tan\theta_- = (2A^2 + 1)/(2A^2 - 1),$$

thus $\theta_- \geq \pi/4$.

Let us now consider a pair of levels E_+ and E_- which are defined by the same value of n. Subtracting (6) from (5) and writing out $\oint Pdx$ we find.

$$2\int_{x_1}^{x_2} \{[2m(E_- - V)]^{1/2} - [2m(E_+ - V)]^{1/2}\} dx = (\theta_- - \theta_+)h/\pi. \tag{7}$$

A is usually a large quantity and when this is the case it will be seen that θ_+ is nearly equal to θ_- and consequently we may develop both and obtain to a high degree of approximation,

$$\theta_- - \theta_+ = 1/A^2.$$

Where $\theta_- - \theta_+$ is small, both E_- and E_+ must lie very close to the energy E of a corresponding one minimum potential system. Calling the difference $E_- - E_+$ for the nth pair of levels Δ_n, we find by developing (7)

$$\Delta_n = h/2\pi m A_n^2 \int_{x_1}^{x_2} \frac{dx}{[2m(E_n - V)]^{1/2}}.$$

This expression may be somewhat simplified by remembering that

$$2m\int_{x_1}^{x_2}\frac{dx}{[2m(E-V)]^{1/2}}=\oint dt=\frac{1}{\nu}$$

where ν is the classical frequency of oscillation. When the potential V between x_2 and x_1 does not deviate too greatly from a parabolic form, $h\nu$ may be identified with the distance between neighboring pairs of levels.

$$\Delta_n/h\nu = 1/\pi A_n^2 \tag{8}$$

where

$$A_n = \exp\left[+(2\pi/h)\int_0^{x_1}[2m(V-E_n)]^{1/2}dx\right].$$

The expression (8) shows that the relative separation of a pair of levels does not depend upon the form of the curve but only upon a square root area

$$(2\pi/h)\int_0^{x_1}[2m(V-E_n)]^{1/2}dx$$

in the non-classical region. This result might have been expected from considerations analogous to the Gamow, Condon, Gurney theory of radioactive disintegration.

§4.

The infrared spectrum of the ammonia molecule exhibits features which may be directly related to the one dimensional problem of two equal minima. The parallel type vibration bands for example are observed to be composed of two nearly superimposed bands; a phenomenon whose existence depends upon the fact that there are two equivalent positions of equilibrium for the nitrogen nucleus. This problem has been treated by Dennison and Hardy,[4] who show that the normal coordinate x_3 which is to be correlated with the band at 10.5μ, may be identified with the coordinate x which we have been using. (For a more exact discussion, see the paper just cited.)

The experimental work so far done on the ammonia spectrum presents us with three data, the frequency ν_0 and the separation between the two lowest pairs of levels.

$$\nu_0 = 950\ \text{cm}^{-1},\quad \Delta_0 = 0.8\ \text{cm}^{-1},\quad \Delta_1 = 32.2\ \text{cm}^{-1}.$$

The estimated error of ν_0 and Δ_1 is less than a percent but the error in Δ_0 may be as high as 10 or 20 percent.

We should of course like to be able to reconstruct the potential V as a function of x using the known experimental data. Of the three facts we possess, ν_0 is needed to determine the curvature in the region of the minima which we designate by $x=\pm x_0$. Formula (8) now shows that if we know Δ_0 and Δ_1 we can impose two and only two conditions on the curve, namely we can de-

[4] D. M. Dennison and J. D. Hardy, Phys. Rev. **39**, 938 (1932).

termine the square root area from $x=0$ to $x=(x_1)_0$ and from $x=0$ to $x=(x_1)_1$ where $(x_1)_0$ and $(x_1)_1$ are the critical points for the two states $n=0$ and 1 respectively.

We shall therefore choose a very simple curve with two parameters which will allow us to correlate the observed data. Let this curve be formed by two equal parabolae joined by a straight line as illustrated in Fig. 2. The two pairs of levels corresponding to $n=0$, 1 are shown in the figure but since the drawing is to scale the separations Δ_0 and Δ_1 are much too small to be represented. The two parameters are $(x_0-\alpha)$, half the length of the joining line and x_0, half the distance between the two minima. We do not mean that this curve represents very closely the actual potential function, but it must possess the two properties as to square root area mentioned before, and these are the only features of the potential curve which we can at present learn. The parameter x_0 is of great physical interest and it turns out that this is

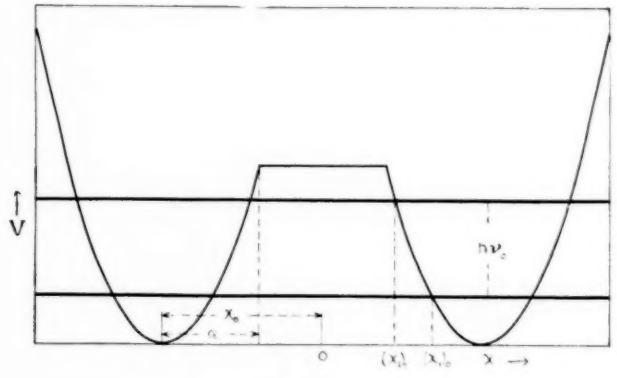

Fig. 2.

very insensitive to the exact shape of V, provided only V has the general form indicated in Figs. 1 or 2.

By use of this particular curve the quantities A and Δ may be readily computed as functions of α and x_0.

$$\frac{\Delta_n}{h\nu_0} = \left(\frac{1}{\pi}\right)\left[\frac{\alpha+[\alpha^2-2n-1]^{1/2}}{(2n+1)^{1/2}}\right]^{2n+1} \exp\left[-(2x_0-\alpha)(\alpha^2-2n-1)^{1/2}\right]. \quad (9)$$

Equating Δ_0 and Δ_1 to their observed values we obtain a transcendental equation which yields the values,

$$\alpha = 1.916$$

$$x_0 = 3.161.$$

The physical significance of these will be discussed later.

§5.

One reason for choosing the potential function illustrated in Fig. 2 is that for this particular curve we may also obtain an exact solution and thus we are able to test, for one case at least, the accuracy of the foregoing com-

putation. There are two reasons why we might doubt its validity. In the first place the W. K. B. approximation is designed to hold best for energy states where n, the quantum number is a large integer. We wish to apply the formulae however to the two lowest states where $n=0$ and 1. In the second place the W. K. B. method becomes inapplicable when the potential at the critical point is too nearly equal to the potential throughout the non-classical region. This obtains because in this case $P^{1/2}$ becomes very small and the W. K. B. expression for ψ does not satisfy the wave equation at all accurately. Fig. 2 is drawn to scale using the values for α and x_0 obtained for ammonia and it is seen that the highest critical point does not lie very far beneath the potential in the non-classical region.

The exact solution is obtained in the following manner. The wave equation may be written,

$$(d^2\psi/dx^2) + (2n + 1 - 2V/h\nu_0)\psi = 0$$

where x and $2n+1$ are proportional to the displacement coordinate q and to the energy E respectively. (n is not necessarily an integer here although it will be nearly equal to one when the potential barrier is sufficiently high.)

$$q = [h/4\pi^2\mu\nu_0]^{1/2}x, \quad E = (2n + 1)h\nu_0/2. \tag{10}$$

The potential may be expressed as follows

$$\begin{aligned} 2V/h\nu_0 &= (x - x_0)^2 \text{ from } x = (x_0 - \alpha) \text{ to } + \infty \\ &= (x + x_0)^2 \text{ from } x = (\alpha - x_0) \text{ to } - \infty \\ &= \alpha^2 \qquad \text{from } x = (x_0 - \alpha) \text{ to } (\alpha - x_0). \end{aligned}$$

In the region of the joining line, from $x=(x_0-\alpha)$ to $(\alpha-x_0)$ the differential equation is satisfied by any linear combination of a hyperbolic sine or cosine. (Assume that $2n+1<\alpha^2$.) It is known that the solutions of the total wave equation may be divided into the two classes, ψ_+ which are even functions of x and ψ_- which are odd functions. It is clear that these must just correspond to the hyperbolic cosine and sine respectively.

Thus from $x=(x_0-\alpha)$ to $(\alpha-x_0)$

$$\begin{aligned} \psi_+ &= A \cosh (\alpha^2 - 2n_+ - 1)^{1/2}x \\ \psi_- &= B \sinh (\alpha^2 - 2n_- - 1)^{1/2}x. \end{aligned}$$

Now in the region from $x=(x_0-\alpha)$ to $+\infty$, one set of solutions of the differential equation will be Weber's functions, $D_n(x-x_0)$. These functions[5] converge properly for large values of x while for small values of x (i.e., $(x-x_0)$ large and negative) we may fit them by means of the parameter n to any curve we please. Now if we join $D_{n+}(x-x_0)$ to ψ_+ or $D_{n-}(x-x_0)$ to ψ_- so that their values and first derivatives agree at the point $x=x_0-\alpha$, we shall have a complete and continuous solution to the wave equation, throughout this region. A similar process may be carried out for nega-

[5] See for example E. T. Whittaker and G. N. Watson, Modern Analysis, 4th Edition, p. 347 (1927).

tive values of x using $D_n(x+x_0)$. The conditions necessary for joining these curves will determine the n_+ or n_- and hence the energy difference Δ_n. The computation is straightforward and makes use of the asymptotic expression for $D_n(y)$ given by Whittaker and Watson, for large *negative* values of y.

$$D_{n(y)} = e^{-y^2/2}(2^{1/2}y)^n[1 - n(n-1)/4y^2 + n(n-1)(n-2)(n-3)/32y^4 \cdots]$$
$$- [(2\pi)^{1/2}e^{n\pi i}e^{y^2/2}/\Gamma(-n)(2^{1/2}y)^{n+1}][1 + (n+1)(n+2)/4y^2$$
$$+ (n+1)(n+2)(n+3)(n+4)/32y^4 + \cdots].$$

It does not seem possible to give Δ_n as an explicit function of n but the two quantities we need Δ_0 and Δ_1 have been computed,[6]

$$\begin{aligned} \Delta_0/h\nu_0 &= (2\alpha/\pi^{1/2}) \exp[-\alpha^2 - 2(x_0-\alpha)(\alpha^2-1)^{1/2}] \\ \Delta_1/h\nu_0 &= [(4\alpha^3 - 4\alpha)/\pi^{1/2}] \exp[-\alpha^2 - 2(x_0-\alpha)(\alpha^2-3)^{1/2}]. \end{aligned} \tag{11}$$

It is interesting to compare formulae (9) and (11). When x_0 and α are sufficiently large, the two values of Δ_0 agree to within 7 percent and the values of Δ_1 to within 3 percent. This result is in accord with the work of Young and Uhlenbeck[3] who found that the W. K. B. approximation for the hydrogenic wave functions was surprisingly good even for the low quantum states. The agreement of (9) and (11) for the particular values of x_0 and α found for ammonia is somewhat poorer, being about 10 percent for both Δ_0 and Δ_1. On the other hand we may equate (11) to the experimental data Δ_0 and Δ_1 when we find,

$$\alpha = 1.930 \quad x_0 = 3.182. \tag{12}$$

Thus the error in the determination of the constants α and x_0 is in each case about 0.7 percent.

We shall adopt the values (12) and from these may compute the actual distance between the two minima in the ammonia molecule. Substituting the appropriate values for ν_0 and μ, the reduced mass, into (10) we obtain $2q_0 = 0.760 \times 10^{-8}$ cm.

The moment of inertia, A, about an axis perpendicular to the symmetry axis is known from band spectrum measurements to be $A = 2.80 \times 10^{-40}$. Combining this datum with the value for q_0 we may find C, the moment of inertia about the figure axis and hence the normal distances between two hydrogen nuclei and between a hydrogen and nitrogen nucleus.

$$C = 4.42 \times 10^{-40}$$
$$H - H = 1.64 \times 10^{-8} \text{ cm}$$
$$N - H = 1.02 \times 10^{-8} \text{ cm}.$$

[6] These expressions have been calculated from the asymptotic expansion for $D_n(y)$ and are consequently only asymptotically correct. The next order term would change 2α to $2\alpha + a/\alpha^3$ and $4\alpha^3 - 4\alpha$ to $4\alpha^3 - 4\alpha + 3/4\alpha + b/\alpha^3$ in the numerators of Δ_0 and Δ_1 respectively. These corrections are insignificant in the case of ammonia.

These values for C and the molecular dimensions are of considerable importance since because of the interaction between vibration and rotation it appears to be impossible to determine them from an investigation of the fine structure of the infrared bands themselves. We feel that the value of C is accurate to within 2 percent. The chief error in its determination probably lies in the uncertainty with which Δ_0 is known.

The results we have obtained may be compared with an exact solution of a two minima problem by Morse and Rosen.[7] The potential used by them has the same general form as shown in Fig. 1 in the region between the minima. For large positive and negative values of x however the potential rapidly approaches a constant asymptote in a manner which is unlikely to represent the true curve since it would predict far too low a heat of dissociation for the molecule. In spite of this difference between their potential and the one used by us, they obtain $2q_0 = 0.73 \times 10^{-8}$ cm, a value differing from ours by only 4 percent. This agreement illustrates the qualitative result of the W. K. B. approximation, namely that the magnitude of the splitting of the levels depends only upon the potential curve between the two minima. It shows also how insensitive q_0 is to the exact form of the curve in this region providing only it has the general shape of Figs. 1 or 2 and contains a sufficient number of disposable parameters which may be used to fit the observed data Δ_0 and Δ_1 with their theoretical values.

[7] P. M. Morse and N. Rosen, Phys. Rev. **40**, 1039(A) (1932).

The Nuclear Moment of Barium as Determined from the Hyperfine Structure of the Ba II Lines*

By P. GERALD KRUGER, R. C. GIBBS AND R. C. WILLIAMS**
Cornell University and the University of Illinois

(Received June 13, 1932)

The hyperfine structure of the Ba II lines λ4934A and λ4554A has been observed. The relative intensities of the observed components of λ4554A have been measured. From these data it was possible to determine the value of the nuclear moment of $Ba^{135,137}$, if it is assumed that the barium isotopes 136 and 138 have no nuclear spin. The most probable value obtained for i is 5/2. The separation of the hyperfine levels of $6s\,^2S_{1/2}$ is 0.272 cm^{-1}, of $6p\,^2P_{1/2}$ is 0.039 cm^{-1}, and of $6p\,^2P_{3/2}$ is approximately 0.033 cm^{-1}. In all other terms the hyperfine splitting is very small. There is some evidence that there is an isotopic shift of the center of gravity of the levels of the odd isotopes with respect to the even isotopes, and it has a probable value of 0.022 cm^{-1} for the $^2P_{1/2}$ state, and 0.017 cm^{-1} for the $^2P_{3/2}$ state.

INTRODUCTION

McLENNAN and Allin,[1] S. Frisch,[2] Gibbs and Kruger,[3] and Ritschl and Sawyer,[4] have previously examined the resonance lines of Ba II for hyperfine structure. The results in the first three reports were highly discordant, but the last two agreed in all essential details. However, none of the data was complete enough to determine the value of the nuclear moment for barium.

EXPERIMENTAL

The Ba II lines were strongly excited in a metal liquid air cooled Schüler lamp. The current used varied from 1 amp. to 1.4 amp. and the He gas pressure in the lamp varied from 4 mm to 10 mm. A Fabry-Perot interferometer was used in a Zeiss triple prism spectrograph to photograph the lines. Quartz etalon plates, whose silvered surfaces at various times during the work had reflection coefficients ranging from 60 percent to 94 percent, were spaced by etalon rings 1, 3, 5, 8, 10, 13, 15, 18, 20, 21, 25, and 30 mm in thickness. The times of exposure varied from thirty seconds to three hours.

Nichols and Merritt,[5] have shown that the intensity of light coming through a slit from a continuous source is proportional to the slit width, if

* The investigations upon which this article is based were supported by grants from the Heckscher Foundation for the Advancement of Research, established at Cornell University by August Heckscher. Acknowledgment is also made of the use of spectroscopic apparatus which was in part purchased by a grant from the National Research Council.

** R. C. Gibbs and R. C. Williams, Physical Laboratory, Cornell University; P. Gerald Kruger, Department of Physics, University of Illinois.

[1] McLennan and Allen, Phil. Mag. **8**, 515 (1929).

[2] S. Frisch, Zeits. f. Physik **68**, 758 (1931).

[3] Gibbs and Kruger, Phys. Rev. **38**, 1921 (1931).

[4] Ritschl and Sawyer, Zeits. f. Physik **72**, 36 (1931).

[5] Nichols and Merritt, Phys. Rev. [I] **31**, 502 (1910).

the slit is wider than 0.06 mm. This principle was used to put intensity marks on the plates so that the intensity of the components of the lines could be compared.

A dull white cardboard was placed 10 inches in front of the slit, and was uniformly illuminated by two frosted bulb lamps, which were placed two feet away, one on each side of the collimator. Slit widths of 0.8 mm, 1.0 mm, 1.2 mm, 1.4 mm, and 1.6 mm were used.

The intensity marks were photographed on the same plate as the line and its components without removing the plate from the spectrograph, so as to take account of the variation of plate sensitivity with wave-length. The time of exposure was 60 seconds. Later the plate was microphotometered and the intensity marks recorded at wave-length of the line.

Results

Table I gives the results obtained for the Ba II lines studied, and includes for the sake of comparison the data of McLennan and Allin and of Ritschl and Sawyer. Frisch found no components to these lines so his data are omitted. The intensities of the components are given in aribitrary units, and show

TABLE I. *Hyperfine structure of Ba II lines.*

λ air	Classification	Int.	Δλ of components in A	Δν of components in cm^{-1}	Total line width in cm^{-1}	Ritschl and Sawyer's data	McLennan and Allin's data
		5	+0.0279	−0.115		+0.027A	
		5	+0.0185	−0.076			+0.043A
4934.10	$6s\ ^2S_{1/2}-6p\ ^2P_{1/2}$	75	0.0000	0.0000		0.000	0.000
		5	−0.0477	+0.196		−0.045	−0.037
4899.97	$6p\ ^2P_{3/2}-7s\ ^2S_{1/2}$		sharp		0.057		0.000
							−0.060
4554.04	$6s\ ^2S_{1/2}-6p\ ^2P_{3/2}$	7	+0.0177	−0.085		+0.018	0.000
		75	0.0000	0.000		0.000	−0.051
		5	−0.0340	+0.164		−0.034	−0.085
4524.95	$6p\ ^2P_{3/2}-7s\ ^2S_{1/2}$		sharp		0.051		
4166.02	$6p\ ^2P_{3/2}-7d\ ^2D_{3/2}$		sharp		0.062		
4130.68	$6p\ ^2P_{3/2}-7d\ ^2D_{5/2}$		sharp		0.060		

the intensity ratio between components. The estimated intensity values given the strong parent line are not accurately determined with respect to those of the components, but are given merely to indicate that the parent line is very much stronger than the components.

Fig. 1 shows the hyperfine structure term schene for λ4934 $6s\ ^2S_{1/2}-6p\ ^2p_{1/2}$, and for λ4554 $6s\ ^2S_{1/2}-6p\ ^2P_{3/2}$.

Discussion

Two of the writers published a preliminary report[3] on the structure of the barium lines, and on the basis of estimated intensity ratios between the parent line and the satellites predicted a ratio of even to odd isotopes for barium of about ten to one. About the same time Aston reported isotopes 135, 136,

137 and 138, and has since then[6] reported the respective percentage ratios to be 5.9, 8.9, 11.1 and 74.2. This makes the even to odd ratio of isotopes about five to one.

At the time the preliminary report was made the two components +0.0279A and +0.0185A of λ4934 had only been suspected because of a gradual shading in intensity on the long wave-length side of the parent line. The presence of these new components increases the intensity ratio between parent line and the satellites so that it is of the right order of magnitude to agree with Aston's work.

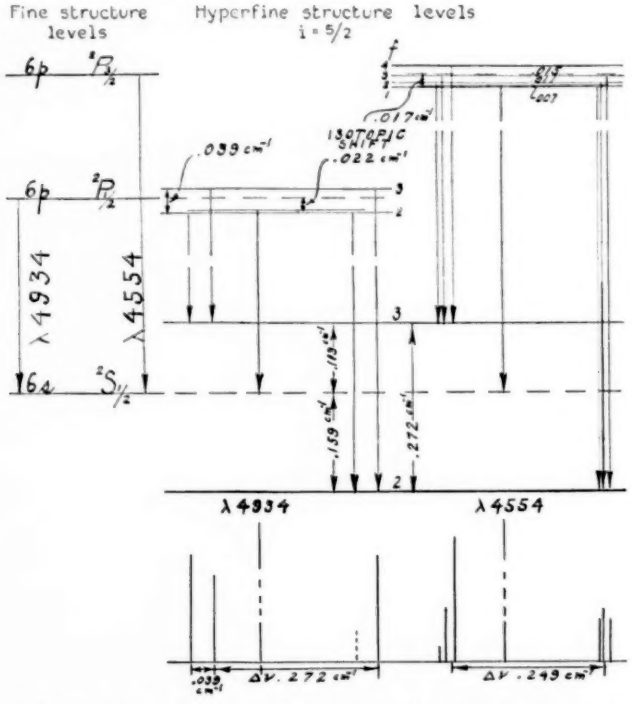

Fig. 1. Hyperfine structure energy level diagram of barium resonance lines, Ba II.

It was possible to observe these components only when using etalon spacings (25 mm), such that the −0.048A component fell on the next chief interference maximum; and (30 mm), such that −0.048A and +0.0279A fell very close to a higher order chief maximum, one on each side. This enabled accurate Δλ measurements to be made on these components, but prevented intensity measurements being made, since all the components could not be resolved on the same plate. Thus the intensities given for these components in Table I are estimated intensities. That they are all of about the same intensity can be seen from Fig. 2 which shows a microphotometer curve of λ4934. The components are unresolved, (due to the fact that the plate was taken with a 13 mm etalon separation) but are drawn in their relative positions.

Fig. 3 shows a simlar microphotometer curve for λ4554. The two com-

[6] Aston, Proc. Roy. Soc. **134**, 571 (1932).

ponents of this line are clearly resolved on the original plate but unfortunately the microphotometer does not show this. Therefore the intensity ratio of these two components was obtained in the following way. The center of the parent line was determined by bisecting the peak of the curve. Then the left side of the parent line was drawn, making it symmetrical about the center line. The right side of the -0.0340A component was projected in the same way, thus giving the shape and position of that component. The ordinates of the

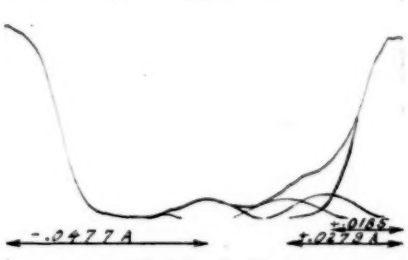

Fig. 2. Microphotometer curve of λ4934.

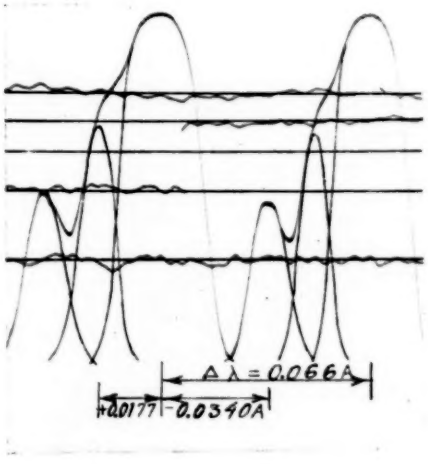

Fig. 3. Microphotometer curve of λ4554.

-0.0340A component and parent line were subtracted from the microphotometer curve to give the form and position of the $+0.0177$A component. When its position had been determined the $\Delta\lambda$ separation from the parent line was computed from measurements taken from the graph and found to agree with the measurements made on the original plate. This gives assurance that the components are correctly drawn in Fig. 3. The position of the peaks of the components may now be compared with the intensity marks (horizontal lines in Fig. 3) which were put on as described above and the intensity ratio obtained in this way. Such a calculation gives the value 1.41 to 1 for the intensity ratio of the components $+0.0177$A to -0.0340A.

A calculation of the theoretical intensities for the hyperfine components under consideration gives the following results for $i = 5/2$.

	$^2P_{1/2}$		
	f	3	2
$^2S_{1/2}$	3	28	35
	2	35	10

	$^2P_{3/2}$			
	f	4	3	2	1
	3	81	35	10	
	2		28	35	27

Thus, since the $^2P_{3/2}$ hyperfine levels separations are very small, the theoretical ratio for the components +0.0177A to −0.0340A is 1.40 to 1. This fits the above data and i has, therefore, been chosen as 5/2.

Two difficulties arise from this choice. The fourth component to λ4934A is missing. But its theoretical intensity has only a ratio of 1 to 3.5 with respect to the other components, and it is, therefore, too weak to observe. Component +0.0185A has a theoretical ratio to +0.0275A of 4 to 5, and the curves show the two about equal in intensity. This may be due to the fact that the components were unresolved on the plate from which the curve in Fig. 2 was made. It may also be added that visually, component +0.0279A appears more intense than component +0.0185 on plates taken with a 25 mm etalon separation.

If i were 7/2 the theoretical intensity ratio of components +0.0275A and +0.0185A would be about 3 to 2 and such a ratio would not fit the curve in Fig. 2. Since this ratio increases as i increases it must be concluded that i is probably less than 7/2. On the other hand, even though the experimental intensity ratio of the components of λ4554 (1:41 to 1) indicate that i is 5/2, it must be admitted that the errors involved in the method of synthesizing the curves in Fig. 3 do not eliminate entirely the possibility that i may be 2 or 3. Thus, while the data give the most probable value of i as 5/2, it may be that $3/2 \leqq i < 7/2$.

The hyperfine energy level diagram shown in Fig. 1 shows the theoretical hyperfine structure multiplets at the bottom. The observed $\Delta\nu$ separations are given. For λ4554 the two groups of three components each are unresolved and the observed $\Delta\nu$ is between the centers of gravity of the two groups. The energy level scheme has been built up from these data. The separation for the hyperfine levels of $^2S_{1/2}$ is 0.272 cm^{-1}. The unsplit $^2S_{1/2}$ level for the even isotopes, where $i=0$, has been conveniently placed at the center of gravity of the hyperfine levels. The $^2P_{1/2}$ hyperfine levels are separated by 0.039 cm^{-1}. This indicates a relative isotopic shift between the unsplit ^2P and ^2S levels for even isotopes and the center of gravity of the hyperfine levels of the odd isotopes of about 0.022 cm^{-1}.

The total widths of the hyperfine levels of $^2P_{3/2}$ is about 0.033 cm^{-1}. Here also, there is an indicated isotopic shift of about 0.017 cm^{-1}.

Other lines given in Table I were examined but no structure was found. This must mean that the hyperfine splitting in $7s^2S_{1/2}$ is very small.

All of the above mentioned etalon separations and times of exposure were used in order to make an exhaustive search for the components reported by McLennan and Allin but none were found.

The authors wish to express their appreciation for various helpful suggestions which Professor R. A. Sawyer has given them during the course of this investigation.

The Elimination of One Boundary Condition for a Sphere in Radiative Equilibrium by a Layer in Adiabatic Equilibrium

By HERMAN ROTH
Mendenhall Laboratory of Physics, Ohio State University

(Received June 21, 1932)

In a previous paper a solution of the equations for a slowly contracting or expanding fluid sphere in radiative equilibrium was obtained. In this solution, for particular values of the central pressure and temperature, a certain parameter, α, depending on the rate of contraction, determined whether or not the solution fulfilled the boundary conditions at the surface. For values of the parameter less than this critical value the solution is physically impossible. In this paper it is shown that an atmosphere in adiabatic equilibrium can be fitted to the solutions with values of α larger than the critical value. Thus the equations stating that p and T should approach zero together for some finite r and m are replaced by an inequality of which the completely radiative solution gives the limiting case. In general, the masses, radii, and luminosities, of such stars are larger, while the effective temperatures are smaller, than those of stars completely in radiative equilibrium.

I. INTRODUCTION

IN a previous paper,[1] a solution of the equations for a slowly contracting or expanding fluid sphere in radiative equilibrium with opacity given by Kramers' formula,[2] satisfying the boundary conditions at the surface, $p=0$, $T=0$, for some finite r and m, was obtained. The method used was to assume a finite pressure and temperature of stellar magnitude at the center, and then adjust a certain parameter, α, depending on the rate of contraction and the specific heat of the matter at constant volume, so that the boundary conditions at the surface were satisfied. It was found that the values of α smaller than the critical value lead to solutions which approach isothermal solutions at great distances from the center and thus have infinite mass. For values of α larger than the critical value the temperature approached zero for a finite pressure at a finite distance from the center. The suggestion was made that it might be possible to fit an atmosphere in adiabatic equilibrium to the latter case. The definite relation between the pressure and the temperature in an adiabatic atmosphere requires that the pressure and temperature approach zero at the same time. Hence the absolute value of the temperature gradient in the radiative solution with an α larger than the critical value must be larger in the outer part of the solution than the adiabatic temperature gradient. At the point where the temperature gradients are equal the entropy density determined for the radiative solution will be a maximum.[3] At points nearer the center than this point, the absolute value of the temperature gradient

[1] Herman Roth, Phys. Rev. **39**, 525 (1932). Hereafter referred to as I.

[2] Jeans, *Astronomy and Cosmogony* p. 84 (1929).

[3] This is obvious if we determine the temperature gradients from Eq. (7) and remember that the entropy is constant in an adiabatic atmosphere.

will be less than the adiabatic temperature gradient. Since the equations of adiabatic equilibrium lead to a solution fulfilling the necessary boundary conditions at the surface, the equation which states that the pressure and temperature approach zero together at the surface can be replaced by an inequality for which the completely radiative solution gives the limiting case. Thus there is the possibility of a star whose innermost portion is in radiative equilibrium and whose outer portion is in adiabatic equilibrium.[4] A large fraction of the star's mass may be contained in this outer layer as is shown by the example worked out in this paper.

II. Adiabatic Solution

The equations of radiative equilibrium for a slowly contracting or expanding fluid sphere,[1] with opacity given by Kramers' formula[2] are, with convenient units

$$dP/dm = -53.00m/r^4 \tag{1}$$

$$dT/dm = -2.793 \times 10^5 Lp/r^4 T^{7.5} \tag{2}$$

$$dp/dm = -53.00m/r^4 - 1.019 \times 10^{-2} T^3 dT/dm \tag{3}$$

$$dr/dm = 3.287T/r^2 p \tag{4}$$

$$dL/dm = \alpha T \tag{5}$$

where

$$\begin{aligned} P &= p_r + p = (\tfrac{1}{3})aT^4 + RT/\sigma \\ \alpha &= 0.6195 \times 10^{12} f'/f, \text{ for } C_v = 3R/2. \end{aligned} \tag{6}$$

It was found[1] that the critical value[5] of α was 0.172 and that the solution for $\alpha = 0.175$ leads to the temperature approaching zero before the pressure. At the point of maximum entropy density of the radiative equilibrium solution, the temperature gradient is equal to the adiabatic temperature gradient. This is the transition point from radiative to adiabatic equilibrium. The adiabatic temperature gradient is computed as follows.[6]

The entropy per unit mass of a perfect gas with radiation is given by

$$s = 4aT^3\sigma/3 + \int C_v dT/T + R \log \sigma. \tag{7}$$

The entropy is constant in any system in adiabatic equilibrium. Therefore with C_v constant and equal to $3R/2$

$$\frac{d\sigma}{dm} = -\frac{\left(4aT^2\sigma + \frac{3}{2}\frac{R}{T}\right)\frac{dt}{dm}}{\left(\frac{4}{3}aT^3 + \frac{R}{\sigma}\right)}. \tag{8}$$

[4] The telescopic appearance of the sun's photosphere suggests that the layer just below the photosphere might be in adiabatic equilibrium.

[5] In the previous paper, this was erroneously given as 0.17.

[6] These equations are implicit in the work done by Eddington, *Internal Constitution of the Stars*, p. 190 (1928). See also L. H. Thomas, Monthly Notices of Royal Astronomical Society **91**, 123 (1930).

The total pressure is given by (6) and hence

$$\frac{dP}{dm} = \left(\frac{4}{3}aT^3 + \frac{R}{\sigma}\right)\frac{dT}{dm} - \frac{RT}{\sigma^2}\frac{d\sigma}{dm}. \tag{9}$$

Eliminating $d\sigma/dm$ between (8) and (9)

$$\frac{dT}{dm} = \frac{dP}{dm}\left\{\frac{\left(\frac{4}{3}\frac{aT^3\sigma}{R} + 1\right)}{\left(\frac{4aT^3\sigma}{3R} + 1\right)^2 + \frac{4aT^3\sigma}{R} + \frac{3}{2}}\right\}\frac{T}{p}.$$

Then substituting

$$\lambda = \frac{p_r}{p} = \frac{\frac{1}{3}aT^4}{\frac{RT}{\sigma}} = \frac{aT^3\sigma}{3R}.$$

We obtain

$$\frac{dT}{dm} = \frac{dP}{dm}\left\{\frac{(4\lambda + 1)}{(4\lambda + 1)(4\lambda + 4) - 1.5}\right\}\frac{T}{p} \tag{10}$$

in a convenient form for numerical work. Eq. (10) new replaces (2) of the radiative equations while the other equations remain the same. The transition point is found to occur at the point $m = 0.9676$ of the solution I. Starting from this point, the equations were integrated in about seventy steps. The results at a few of the steps are shown in Table I.

TABLE I. *Solution of adiabatic equilibrium equations.*

$m\times10^{-33}$ gms	$p\times10^{-12}$ dynes/cm^2	$r\times10^{-11}$ cm	$T\times10^{-6}$ degrees
0.9676	2.7278	2.2382	3.9322
1.1524	2.4042	2.4130	3.7868
1.2100	2.3206	2.4642	3.7456
1.2706	2.2356	2.5194	3.7026
1.3342	2.1496	2.5739	3.6581
. . . . .	. . . . .	. . . . .	. . . . .
2.0706	1.3329	3.1653	3.1551
2.2286	1.1931	3.2880	3.0481
2.8528	0.73745	3.7803	2.6192
3.6518	0.32035	4.4900	2.0093
4.1830	0.12884	5.1097	1.5035
4.5626	0.034324	5.8086	0.97890
4.7117	0.0086333	6.3522	0.61225
4.7566	0.0026131	6.6760	0.40614
4.7768	0.0002946	7.0164	0.19924
4.7797	0.0000033	7.2652	0.055025
4.77973	0.0000020	7.3012	0.034672

Near the surface T and p vary more rapidly compared to m than compared to r. Hence more accurate results can be obtained by changing the in-

dependent variable form m to r. Further it is easily seen that with small values of T, λ is small and hence near the boundary the equation giving the temperature gradient can be replaced by

$$\frac{dT}{dm} = f(\lambda)\,\frac{T}{p}\,\frac{dp}{dm}$$

where $f(\lambda)$ approaches the value 0.4, and dP/dm approaches dp/dm. Therefore near the boundary

$$\int_0^{T_0} \frac{1}{T}\,\frac{dT}{dm} = 0.4 \int_0^{p_0} \frac{1}{p}\,\frac{dp}{dm}$$

and

$$T_0 = c p_0^{0.4}.$$

Hence near the surface a solution may be obtained in this manner. This was used to estimate the mass contained within the last few intervals of the solution.

III. Results

The mass[7] of the star completely in radiative equilibrium (for $\alpha = 0.172$) is 4.1510, while the mass of the star with an adiabatic layer (for $\alpha = 0.175$) is 4.7797, 80 percent of which is in the adiabatic layer. The luminosities are 2.3513 and 2.45 respectively and the radii are 5.3245 and 7.3012 respectively. Although the luminosity increases, r^2 has a proportionately larger increase, thus leading to a lower effective temperature. If the completely radiative solution is supposed to mark out a mass-luminosity law, then in our case we have a displacement to the side of a higher mass for the same luminosity.

The solution I represents a series of stars of the same mass but at different stages of contraction, the internal pressure, temperature and radius varying in proportions given by Lane's law. Besides these, there is a wider group with different rates of contraction which are not completely in radiative equilibrium but have an outer layer, which may contain a large fraction of the total mass of the star, in adiabatic equilibrium. In general the latter stars have more mass and also a higher luminosity.

The replacing of the equation between the parameters, stating that p and T should approach zero together at the surface in a completely radiative solution, by an inequality, for which the completely radiative solution gives the limiting case, allows a wider choice in the parameters than is possible in the completely radiative solution.

I wish to thank Dr. L. H. Thomas, for his suggestion of this problem and his assistance in its solution.

[7] In convenient units; m, 10^{33} g; r, 10^{11} cm; L, 10^{35} ergs/sec.

The Magnetic Susceptibilities of Alpha- and Beta-Manganese*

By MARY A. WHEELER
Sloane Physics Laboratory, Yale University

(Received June 6, 1932)

Pure alpha-manganese was prepared by distillation. Beta-manganese was prepared by melting a sample of the alpha-manganese in vacuum, and quenching it in water from about 1000°C. The mass susceptibilities of these two specimens were measured by a null-reading, astatic magnetometer, and found to be $9.60(10)^{-6}$ and $8.80(10)^{-6}$ respectively. These results eliminate the possibility that the ferromagnetic manganese found by some investigators is either the alpha-or the beta-crystal form.

INTRODUCTION

IN THE periodic table manganese lies in the same transition series as the ferromagnetic elements, iron, cobalt, and nickel, and adjacent to them, and also might be expected to exhibit ferromagnetism. However, although the magnetic properties of manganese have been the subject of several investigations, the results have disagreed even in such an important respect as to whether it is or is not ferromagnetic. Undoubtedly many of the discrepancies are attributable to chemical impurities, especially in the work of the early investigators. Manganese is a very active element chemically, and many of its alloys and chemical compounds are ferromagnetic. Iron as an impurity is not so important as carbon and nitrogen, as 18 percent of manganese in iron causes the iron to lose its ferromagnetism, while carbon and nitrogen, which form highly ferromagnetic compounds with manganese, are more likely than iron to be overlooked.

Honda[1] and Owen[2] found the susceptibilities of their specimens to be $10.6(10)^{-6}$ and $8.93(10)^{-6}$ respectively. Both these investigators were very careful to avoid iron. Honda and Soné,[3] and Ishiwara,[4] using similar specimens of Kahlbaum's manganese, measured susceptibilities of 9.70 and 9.66 $(10)^{-6}$. Kuh,[5] who prepared a sample electrolytically, found it to be ferromagnetic, as did Hadfield.[6] Freese[7] repeated Kuh's work, suspecting that the ferromagnetism might be due to hydrogen, since the last step in the preparation was heating a manganese amalgam in hydrogen. He also prepared specimens by sputtering in hydrogen, but found no consistent effect of the hydrogen.

* Part of a dissertation presented for the degree of Doctor of Philosophy in Yale University.

[1] K. Honda, Ann. d. Physik [4] **32,** 1027 (1910).
[2] M. Owen, Ann. d. Physik [4] **37,** 657 (1912).
[3] K. Honda and T. Soné, Sci. Rep. Tohoku Imp. Univ. [1] **2,** 27 (1913).
[4] T. Ishiwara, Sci. Rep. Tohoku Imp. Univ. [1] **5,** 53 (1916).
[5] E. Kuh, Diss. Zurich (1911).
[6] R. Hadfield, C. Chéveneau, and Ch. Géneau, Proc. Roy. Soc. [A] **94,** 65 (1917).
[7] H. Freese, Phys. Zeits. **29,** 191 (1928).

Since the magnetic susceptibilities of many substances have been found to vary in different crystal forms, the object of this research was to investigate what difference in susceptibility might exist between the alpha- and beta-crystal forms of manganese at room temperature. Manganese exists in three crystal forms, alpha, beta, and gamma. The alpha form is the low temperature modification, stable up to 742°C.[8] The beta form is stable from 742° to 1191°[9] and can be obtained in specimens quenched at room temperature from this temperature interval. Both these forms are cubic, having 58 and 20 atoms per unit cube respectively.[10] The gamma form is present in specimens prepared electrolytically, but changes back to alpha automatically in a couple of weeks. It is stable above 1191°, but has never been obtained in pure manganese by quenching.

The susceptibility of manganese as a function of the temperature was measured by Shimizu[11] who found unusually low values for his samples, which were prepared by distillation and were 99.9 percent pure. Some of his results are as follows:

Crystal form	alpha	beta	gamma
Temperature	20°C	810°C	1100°C
Susceptibility	$7.53(10)^{-6}$	$6.01(10)^{-6}$	$8.41(10)^{-6}$

None of these exhibited ferromagnetism in the temperature interval in which they were stable, but he did not investigate the high temperature forms at room temperature.

Preparation of Samples

Two samples of manganese were used for these researches, both prepared by the method of distillation, which yields manganese with a very small percentage of impurities. The first specimen was very kindly supplied by Dr. Walters of the Carnegie Institute of Technology, and was stated to have the following impurities: C, 0.009 percent; Fe, Al, Si, spectroscopic traces. Some manganese was purified similarly in an Ajax 30 KVA induction furnace. In general the method consisted in placing the crude manganese in a magnesia crucible with a second inverted crucible resting on it. The whole was placed in a silica tube which was evacuated to $(10)^{-2}$ mm. The manganese was then heated inductively to a temperature just above melting. As pure manganese is very volatile, it distilled onto the upper crucible leaving the impurities in the undistilled portion.

To obtain manganese in the beta-crystal form without impurities sufficient to vitiate magnetic measurements, it was found necessary to melt the pure distilled alpha-manganese into a lump in vacuum, then quench it in cold water, so that only the surface became impure. To do this, the manganese in a magnesia crucible was supported inside a tube of Berlin porcelain which was sufficiently nonporous at the melting point of manganese to hold

[8] M. Gayler, J. Iron and Steel Inst. **115,** 393 (1927).
[9] E. Persson and E. Öhman, Nature **124,** 333 (1929).
[10] G. D. Preston, Phil. Mag. [7] **5,** 1198 (1928).
[11] Y. Shimizu, Sci. Rep. Tohoku Imp. Univ. [1] **19,** 411 (1930).

a vacuum of $(10)^{-6}$ mm. This tube was surrounded by a carbon ring which in turn was surrounded by the coil of the induction furnace. Most of the heat was generated in the carbon ring. Ground joints between the tube and the Pyrex vacuum system were sufficiently distant from the heat to be easily water cooled. At the instant of melting the pressure rose to $(10)^{-4}$ mm, but otherwise kept down to $(10)^{-6}$ mm. When the manganese melted, argon was introduced, and then the manganese lump was quickly driven through the bottom of the tube into cold water. This lump was covered with an oxide film, which was removed by sandblasting.

No chemical analysis can as yet be obtained for this specimen. After consultation with leading authorities on the determination of gaseous impurities in metals, it appears that the errors in nitrogen determinations are as large or larger than the total amount of nitrogen probably present here. The specimen is being retained in the hope that a more precise method may soon be available. However, the susceptibility measurements are a delicate test for ferromagnetic impurities, and others cause only a small percent error. The probable impurities here would be carbon and nitrogen, both of which form ferromagnetic compounds with manganese.

X-ray Analysis

To determine the crystal structure of these samples, x-ray powder photographs were taken with Mo $K\alpha$ radiation. The value of tan 2θ for Mo $K\alpha$ was calculated from the data given in papers by Sekito[12] and Preston[10] for tan 2θ for Fe $K\alpha$, and compared with tan 2θ from these samples. (Tables I and II.)

TABLE I. *Distilled specimen compared with alpha-manganese.*

Line	Tan 2θ from Sekito	Intensity from Preston	Tan 2θ calculated from film	Estimated intensity
1	0.354	200	0.354	200
2	0.395	200	0.396	100
3	0.416	100		
4	0.435	100	0.433	75
5	0.594	40	0.593	50
6	0.624	100	0.633	50
7	0.644	200		
8	0.675	140	0.678	100
6 lines of lower intensity				
15	0.825	200	0.825	50

TABLE II. *Quenched specimen compared with beta-manganese.*

Line	Tan 2θ from Sekito	Intensity from Preston	Tan 2θ calculated from film	Estimated intensity
1	0.354	strong	0.354	very strong
2	0.374	"	0.374	strong
3	0.395	"	0.395	medium
4	0.451	"	0.454	weak
5	0.525	medium	0.541	weak
6	0.562	"		
7	0.661	very strong	0.668	fairly weak
8	0.675	medium		
9	0.712	very strong	0.710	weak

[12] R. M. Bozorth, J. Opt. Soc. Amer. **10**, 591 (1925).

In the comparison of the values for alpha-manganese with those from Sekito, it is clear that the prominent lines coincide. Preston and Sekito used cameras with circular film, and so got the lines for larger angles with relatively greater intensities. This explains the absence on our film of lines No. 9 through No. 14. The intensity maximum extending from tan 2θ 0.395 to 0.435 showed practically no structure. This was interpreted as two lines at the distances noted, but another line may have been present in the interval.

For the beta specimen, the lines coincided within the errors of measurement. The lines reflected at larger angles, No. 10 and above, were absent because of the greater distance from powder to film, as on the first film, and lines No. 5 and 6, as well as lines 7 and 8, were not resolved.

No lines which could be attributed to the gamma structure were found on either film.

Magnetometric Measurements

The magnetometer used was essentially like one described by Bozorth,[12] and was a null-reading instrument. Two small parallel magnets of equal moment were mounted horizontally, one above the other, with north poles in opposite directions, thus forming an astatic system. The specimen was placed so that each end was at the level of one of the magnets; thus each induced pole exerts the same torque on the astatic system. An equal distance from the astatic system but on the side opposite the specimen was placed a coil of proper dimensions, which, when traversed by a suitable electric current, balanced the total torque exerted on the astatic system by the specimen. The specimen was supported in a magnetizing solenoid, and the balancing coil in a similar solenoid, provided to cancel the torque on the magnets due to the magnetizing solnoid. Since the dimensions of the balancing coil and the current passing through it gave its magnetic moment, which was adjusted to be the same as that of the specimen, the magnetic moment and susceptibility of the specimen could be calculated.

The container for the specimen of powdered manganese was a glass tube cut from a 2 cm^3 hypodermic syringe of inside diameter 0.9083 cm, with ends ground flat and plugged with amber so that the inside length was 4.000 cm. The balancing coil used to counteract the torque of the specimen on the astatic system was wound on an amber spool which was so slightly paramagnetic that it deflected the magnetometer zero less than 1 mm, that being about the limit of accuracy in single readings. Two coils were wound identically, for purposes of adjustment, with two layers of 186 turns each. The winding space was 4.000 cm long, and 0.824 cm in diameter. The magnetizing solenoids were wound on brass spools 15 cm long and 1.585 cm in diameter, with 5027 turns in 20 layers. A current of air was kept constantly flowing between the specimen and the spool, and this eliminated much shifting of the wires as they heated, and also kept the specimen within a few degrees of room temperature. The adjustment was carried out as suggested by Bozorth, except that it was not found possible to hold the same adjustment for various high fields.

As the balancing coil was wound in two layers its moment was measured

magnetically by the common method of placing it in the center of a long solenoid, and measuring the charge passed through a calibrated ballistic galvanometer in series with the balancing coil and a standard mutual inductance, when a current was passed through the solenoid. From this, the magnetic moment, M, was found to be 21.62 i, with a probable error of $\frac{1}{2}$ percent, where i is the current through the balancing coil in amperes.

The average value of the field, H, in the magnetizing solenoid was calculated to be 0.982 of that of an infinite solenoid of the same number of turns per unit length. Therefore, H in gauss was found to be 413.6 I, where I is the magnetizing current in amperes; and χ, the mass susceptibility, $= M/H \cdot$ mass, or $52.27(10)^{-3}\, i/I \cdot$ mass.

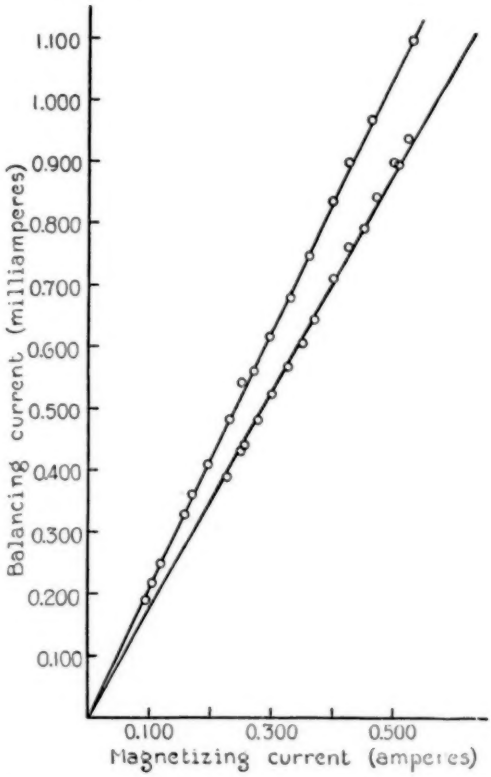

Fig. 1. Upper line, beta-manganese; lower line, alpha-manganese

The total deflection without balancing current was between 5 and 10 cm, and the limit of accuracy in each reading was about 1 mm. Since the volume susceptibility turned out to be of the order of $(10)^{-5}$, the demagnetizing effect of the poles of the specimen was neglected. With the astatic system in its zero position, the resultant field produced by its magnets on the specimen would be small. Experimentally, no change in value was noticed when the zero was changed slightly, or when the suspended system was rotated through 180°. The field on the specimen in the direction of its axis due to the second magnetizing solenoid in which the balancing coil was supported was calculated to be 1/400 that of the first magnetizing solenoid, and was neglected.

The diameter of the container was slightly larger than the average diameter of the balancing coil, but it seemed impossible that this could make a measurable change in the result, especially as the average diameter of the sample of manganese must necessarily be smaller than the container.

It is conceivable that the powdering of the manganese to place it in the container might have changed the susceptibility. Evidence would suggest that if this happened the susceptibility was increased rather than decreased by the powdering. As no change of susceptibility with field was noted, there could have been present no measurable ferromagnetic impurity, and a paramagnetic impurity would cause only a small percent error.

The results are presented in Table III and in Fig. 1 which shows the straight line relations to be expected in the absence of ferromagnetic impurities.

TABLE III. *Susceptibility measurements on alpha- and beta-manganese.*

Mass of sample, 11.307 grams			Mass of sample, 10.420 grams		
I	$i \cdot 10^3$	$(i/I) \cdot 10^3$	I	$i \cdot 10^3$	$(i/I) \cdot 10^3$
0.095	0.189	1.989	0.227	0.390	1.718
0.106	0.216	2.038	0.250	0.430	1.720
0.120	0.248	2.067	0.256	0.441	1.723
0.158	0.327	2.070	0.278	0.482	1.734
0.172	0.360	2.093	0.300	0.524	1.747
0.197	0.409	2.076	0.327	0.568	1.737
0.233	0.482	2.069	0.350	0.606	1.731
0.252	0.543	2.155	0.370	0.645	1.743
0.271	0.562	2.074	0.400	0.712	1.780
0.297	0.617	2.077	0.426	0.763	1.791
0.330	0.680	2.061	0.452	0.793	1.754
0.361	0.749	2.075	0.472	0.844	1.788
0.400	0.836	2.090	0.500	0.900	1.800
0.427	0.900	2.108	0.507	0.897	1.769
0.463	0.970	2.095	0.524	0.940	1.794
0.530	1.10	2.075			
$i/I = (2.076 \pm .006) \cdot 10^{-3}$			$i/I = (1.754 \pm .005) \cdot 10^{-3}$		
$\chi = (9.60 \pm .03) \cdot 10^{-6}$			$\chi = (8.80 \pm .02) \cdot 10^{-6}$		

CONCLUSIONS

Thus, it can be concluded that for alpha-manganese the mass susceptibility is $9.60(10)^{-6}$, and for beta-manganese, $8.80(10)^{-6}$. Considering that the specimens previously measured were probably a mixture of these two crystal structures, this result is lower than Honda's first value of $10.6(10)^{-6}$, and agrees better with his second value, $9.70(10)^{-6}$, and with that of Owen, $8.93(10)^{-6}$. The more recent work of Shimizu gave still lower values, as previously noted. For these low values no explanation can here be offered. No trace of the ferromagnetism observed in the specimens of Kuh, Hadfield, and Freese was found.

The writer wishes to extend her thanks to Dr. Walters who so kindly furnished samples of pure manganese. She also wishes to express appreciation to Professor L. W. McKeehan for suggesting the problem and for advice and criticism during its progress. The research was made possible through the grant of the Loomis Fellowship, established by Francis E. Loomis and Henry B. Loomis.

The Magnetic Susceptibility of Nitrogen Dioxide

By GLENN G. HAVENS
University of Wisconsin, Madison

(Received June 2, 1932)

A method has been developed whereby sensitivities for volume susceptibilities as high as 3×10^{-15} can be obtained. The main improvement in the method over that of other observers is in the construction of lighter test bodies and the use of smaller fibers. The method is applied to the measurement of the susceptibility of NO_2. The results agree within the limit of experimental uncertainties with Van Vleck's theoretical value for the molecular susceptibility of NO_2 namely, $\chi(NO_2)=0.375\,\chi(O_2)$. The susceptibility of N_2O_4 comes in as a second order effect and the value $\chi(N_2O_4)=-30\times10^{-6}\pm20$ percent is in fair agreement with the value $\chi(N_2O_4)=-25.8\times10^{-6}$ obtained by T. Soné.

I. INTRODUCTION

IN VIEW of the large discrepancies in the results of various observers for the magnetic susceptibilities of many gases and of the growing theoretical interest in these experimental values, it seemed advisable to carry on a series of experiments designed to increase the dependability and accuracy of the measurements. With this view the writer has designed an apparatus for the measurement of low susceptibilities for gases such as hydrogen or helium, which are fairly inert and can be readily purified.

Nitrogen dioxide is of interest both theoretically and chemically; its susceptibility should be given by the formula derived by Van Vleck,[1] namely:

$$\chi(NO_2) = 4N\beta^2S(S+1)/3kT + N\alpha$$

where $N\alpha$ is a small residual term due to high-frequency elements, β is the usual Bohr magneton, and S is the spin quantum number of the molecule and is presumably equal to $\frac{1}{2}$ for NO_2. The susceptibility of O_2 is given by the same formula. However since the ground level for this molecule is a $^3\Sigma^{-1}$ state making $S=1$, it follows that $\chi(NO_2)/\chi(O_2)=0.375$. Experimentally Soné[2] finds this ratio to be about one sixth of this value. Verhoek and Daniels[3] have worked out the dissociation constant for nitrogen tetroxide, and it is of interest to see whether the use of their value for the dissociation constant would lead to a consistent correlation of the magnetic measurements.

II. DESIGN OF THE APPARATUS

The Faraday method, whereby an oblong shaped test body is suspended in a nonhomogeneous field surrounded by the gas under investigation, was used. The method has been improved upon and used for the measurement of

[1] J. H. Van Vleck, *The Theory of Electric and Magnetic Susceptibilities*, pp. 274.
[2] Také Sóné, Sci. Rep. Toh. Imp. Univ. **11**, 139 (1922).
[3] Verhoek and Daniels, J. Am. Chem. Soc. **53**, 1250 (1931).

the susceptibility of gases by Glaser,[4] Hammar,[5] and Bitter.[6] The tube used by the writer is similar to the one used by previous workers except that the important parts of the tube were given a conducting film of gold or platinum and grounded so that there could be no electrostatic effects (Fig. 1). It was

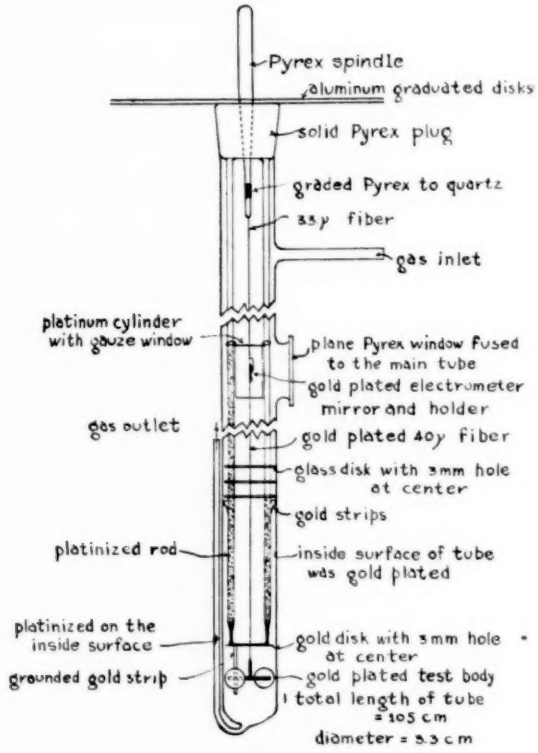
Pyrex spindle
aluminum graduated disks
solid Pyrex plug
graded Pyrex to quartz
33μ fiber
gas inlet
platinum cylinder with gauze window
plane Pyrex window fused to the main tube
gold plated electrometer mirror and holder
gas outlet
gold plated 40μ fiber
glass disk with 3mm hole at center
gold strips
platinized rod
inside surface of tube was gold plated
platinized on the inside surface
gold disk with 3mm hole at center
grounded gold strip
gold plated test body
total length of tube = 105 cm
diameter = 3.3 cm

Fig. 1. Final tube.

then found that drifts of the test body and the change in total torque from day to day were, as far as could be observed, completely eliminated after the tube and moving parts were carefully grounded.

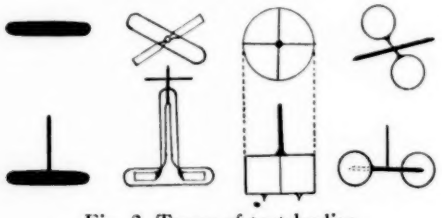

Fig. 2. Types of test bodies.

The main improvements in the method which the writer has introduced have come through the development of better test bodies and the use of smaller fibers. Four types of test bodies have been used by the writer. Fig. 2.

[4] A. Glaser, Ann. d. Physik **75,** 459 (1924).
[5] G. W. Hammar, Nat. Acad. Sci., Proc. **12,** 597 (1926).
[6] F. Bitter, Phys. Rev. **36,** 1648 (1930).

The first type is a solid ellipsoid of the type used by Hammar[5] and by Glaser.[4] The one of this form used by the writer weighs 1.8 g. The second one is a hollow quartz ellipsoid weighing less than 1 g. It has the additional advantage that the quartz compensators reduce the total torque caused by the quartz to nearly zero. The ellipsoid is evacuated and sealed off, whereas the compensators are open to the gas. These compensators not only compensate for the torque caused by the field on the material of the test body itself but also reduce the effect of temperature disturbances. The third type of test body is similar to the one designed by Bitter,[6] except that fused quartz replaced glass. It has the apparent advantage of better symmetry; but its great disadvantage is that it weighs about 7 g. The compensation resulting from symmetry is apparent rather than actual, because, even if the test body were of perfect construction, there would be total compensation for only one position in the field, and if the test body be moved even a small distance from this position, the total torque would be increased to values as great as those obtained by the use of the other types of test bodies. The test body at the right of the figure is the type finally used. It consists of two evacuated spherical bulbs attached together and compensated by a small quartz rod. The one now in use weighs less than 100 mg and has a coat of evaporated gold on the surface. By allowing the test body to rotate until the surface comes in contact with a grounded gold wire, any accumulated electrostatic charges can be removed. With this type of test body it is possible to use much smaller fibers than with the other types and it has the further advantages that the magnetic field does not have to be held so constant, and changes in temperature are not so troublesome. The following table gives approximately the sensitivity of the four different types of test bodies which were used. The volume susceptibility of hydrogen for comparison is about 2×10^{-10}.

TABLE I. *Sensitivities of test bodies.*

Type:	I	II	III	IV
Sensitivity:	4×10^{-12}	1×10^{-13}	1×10^{-12}	3×10^{-13}

The compensators of the fourth-type test body were of such diameter and length that the total torque on the test body was nearly zero when in the position indicated by Fig. 3. The angle θ was made so that one could find a position of only slightly stable equilibrium; usually θ turned out to be about 75°. The nearer θ approached the angle giving unstable equilibrium, the

Fig. 3. Position of test body in the field.

longer would be the period of vibration and thus the higher the sensitivity, limited only for a given test body by the accuracy of the torsion head. Fig. 4 shows a typical curve of the relation of the torque to the angle α of the test

body in the magnetic field. If A and B are angles of minimum and maximum torque, the difference of the torque at A and B depends upon the angle θ, and the value of the slope of the curve in Fig. 4 indicates the degree of stability, negative slopes meaning unstable equilibrium. Thus A and B are positions of neutral equilibrium and therefore high sensitivity; A on the curve would be a better angle than B because the total torque is less and therefore the fluctuations due to changes in field strength and temperature are smaller.

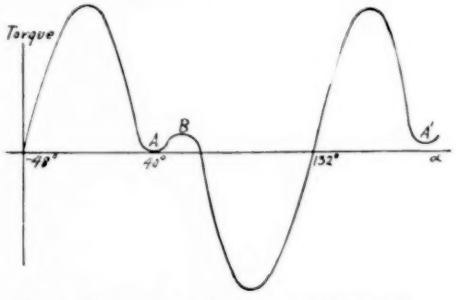

Fig. 4. Torque as a function of the angle α.

If A and B are too close together, it becomes difficult to keep the test body between these positions when the field is initially being applied; that is, while the field is rising from 0 to its final constant value. With a period of about one minute, sensitivities have been reached for which volume susceptibilities of 3×10^{-15} were observable.

The torque on a twisted fiber varies directly as the angle through which the fiber is twisted, inversely as the length, and inversely as the fourth power of the diameter. Thus for the highest sensitivities it is desirable to have a

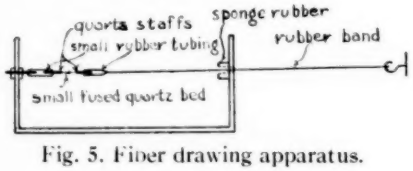

Fig. 5. Fiber drawing apparatus.

fiber of such diameter that the error in reading the torsion head will be less than that of the scale of the optical lever used to tell the position of the test body in the field. For a 3μ fiber with a 100 mg test body the torque is more than 2 revolutions of the fiber per atmosphere of hydrogen, and over 1500 revolutions per atmosphere of oxygen. The strength of this fiber is not sufficient for the heavier test bodies but is many times the strength necessary for the light test bodies.

Fibers of any diameter as low as 1μ can be readily drawn where it is not required that each end of the fiber be attached to a large staff of quartz. However, since shellac or other organic compounds could not be used in this experiment for connecting the fiber to the torsion head because of the action of NO_2, it was necessary to devise an apparatus capable of drawing a fiber of a given diameter and length from two quartz staffs without breaking the

fiber. The fiber drawing apparatus consisted merely of a stretched rubber band holding a quartz staff which would fly into a sponge rubber socket when released. (Fig. 5) At present fibers as small as 0.6μ in diameter and 50 cm long have been successfully made with this apparatus. The variation in the diameter along the entire length is less than 0.1μ, except for about 1 cm at each end. It has been found possible to draw the quartz staffs down very sharply to a 3μ to 5μ fiber. The absence of gradual tapering means that there is a definite point of contact between the staff and fiber upon which a microscope can be focused for centering purposes. The fiber is then centered very simply by heating the quartz staff in a horizontal position until its sags, due to its own weight, to the correct position. Fibers can be centered in this manner to within a radius of 5μ.

Because mercury is attacked by NO_2, a special pressure measuring device, due to Professor Daniels,[3] was used whereby the pressures of $NO_2+N_2O_4$ were measured by balancing the pressure of $NO_2+N_2O_4$ on the one side of a glass diaphragm against that of air on the other side. The pressure of air was then measured using an ordinary manometer.

TABLE II. *Taken at 20.05°C.*

Pressure of $NO_2+N_2O_4$ in cm of Hg	Torque on the fiber in revolutions	Pressure of $NO_2+N_2O_4$ in cm of Hg	Torque on the fiber in revolutions
1.94	60.752	35.58	153.558
2.99	66.000	37.69	156.727
4.18	71.995	39.55	159.998
5.28	76.087	41.66	163.079
6.28	80.991	43.51	166.254
7.49	85.925	45.89	169.988
8.67	90.080	48.20	173.728
9.89	94.182	50.00	175.675
10.92	97.082	51.52	178.165
12.64	102.429	52.64	179.648
14.42	107.522	54.23	182.272
17.03	114.623	55.91	184.382
18.43	118.358	51.09	177.673
19.87	121.720	46.72	171.678
21.21	124.827	41.53	163.694
22.68	127.988	36.55	154.603
23.94	130.814	32.25	147.338
25.36	133.585	27.89	139.090
26.91	136.580	23.52	129.947
28.10	139.135	19.28	120.088
28.72	140.170	15.56	110.64
30.55	144.195	11.76	100.05
34.01	150.414	7.85	86.791
32.25	147.659	4.54	74.148

III. RESULTS

To find the susceptibility of NO_2 it is necessary to know the dissociation constant for $N_2O_4 \rightleftarrows NO_2$ at various temperatures. The dissociation constant $k(N_2O_4)$ is given by:

$$k(N_2O_4) = p^2(NO_2)/p(N_2O_4)$$

where $p(NO_2)$ and $p(N_2O_4)$ represent the partial pressures of NO_2 and N_2O_4. Verhoek and Daniels[3] have measured this constant to about 2 percent for

the temperatures 25°C, 35°C, and 45°C. The value of $k(N_2O_4)$ can therefore be found for any other temperature from van't Hoff's equation:

$$\log \frac{k_1}{k_2} = \frac{\Delta H}{2.303R} \frac{T_2 - T_1}{T_2 T_1}$$

where ΔH is the heat of dissociation. From these equations, and a knowledge of the total pressure of the gas, the amount of NO_2 present can be readily

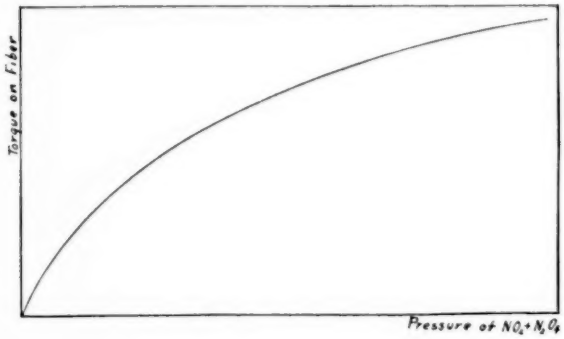

Fig. 6.

calculated. As the susceptibility of NO_2 is about 50 times that of N_2O_4, if we plot the torque on the torsion head against the partial pressure of NO_2 we

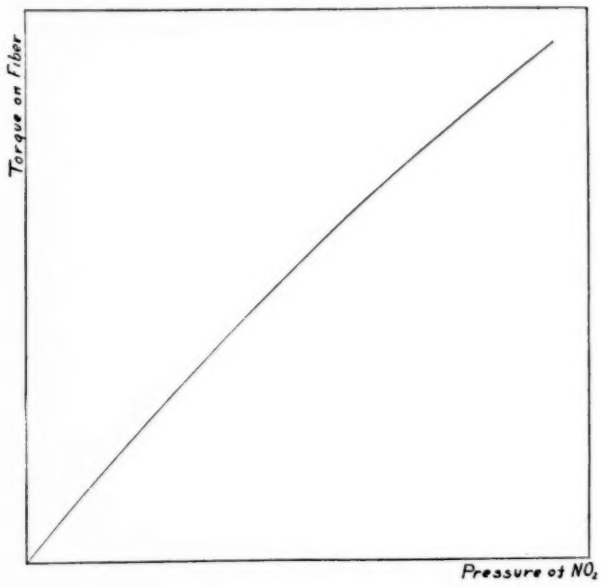

Fig. 7.

should get nearly a straight line, inasmuch as the torque due to any gas is proportional to the pressure of that gas. Fig. 6 shows a typical curve of the

observed torques plotted as ordinates and the pressures of $NO_2+N_2O_4$ as abscissas. Fig. 7 shows a typical curve of the observed torques plotted against the partial pressures of NO_2. The slight curvature is due to the fact that the

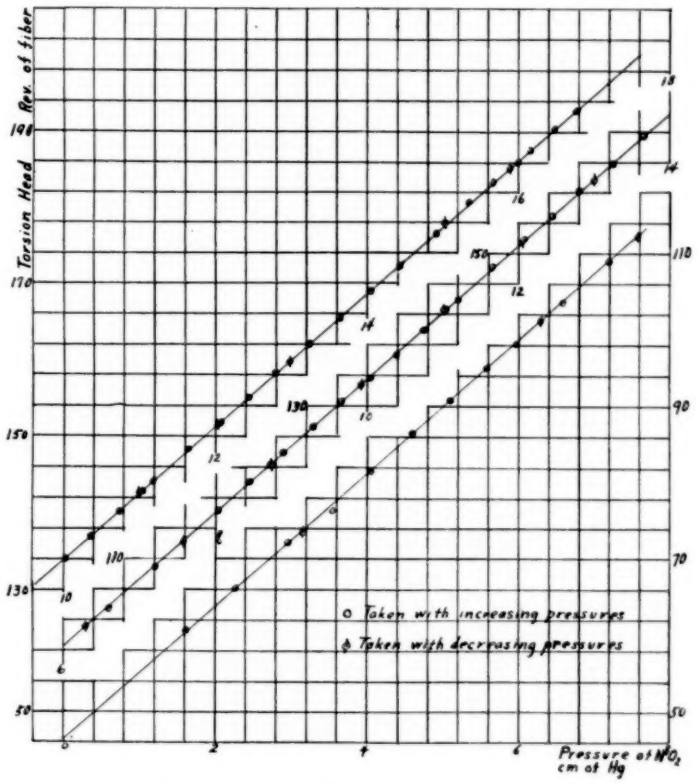

Fig. 8.

susceptibility of N_2O_4 is not zero. The curve of Fig. 8 was obtained from the data of Table III, first, by deriving from knowledge of the value of the dissociation constant, a curve of type in Fig. 7 for the susceptibility of N_2O_4 by

TABLE III. *Taken at 20.02°C.*

Pressure of Oxygen in cm of Hg	Torque on fiber in revolutions
1.63	84.34
3.75	130.66
6.73	198.70
9.62	263.51
12.25	320.50
15.08	383.63
18.30	454.65

assuming that $\chi(N_2O_4) = -2.5$ percent $\chi(NO_2)$. Fig. 8 gives the value $\chi(NO_2) = 0.390\chi(O_2)$ and is in good agreement with the theoretical value of 0.390 $\chi(O_2)$ calculated by Van Vleck,[1] which may be in error by as much as 3 percent or 4 percent because of the small neglected terms. Another factor which

might further account for the difference between this value and the theoretical value is the uncertainty in the value of $k(N_2O_4)$. The value $\chi(N_2O_4) = -30\ 10^{-6}$ agrees within the limit of error with Soné's value of -25.8×10^{-6}. Fig. 8 and three other curves at different temperatures give the values listed in Table IV. It is to be noted that the agreement with the theoretical value is

TABLE IV.

Temperature	$\chi(NO_2)/(\chi N_2O_4)$	$-\chi(N_2O_4)/\chi(NO_2)$	$\chi(N_2O_4)\times10^6$	$(\chi(O_2)=3330\times10^{-6})$
22.60°C.	0.370	2%	−25.0	
20.54	0.382	2.5%	−31.3	
20.05	0.390	2.5%	−31.3	
19.17	0.400	2.8%	−35.0	

better for the higher temperatures, which are nearer the temperatures for which $k(N_2O_4)$ was determined. Through the entire work the susceptibility of O_2 was used as a standard. Table III.

The volume susceptibility of NO_2 computed from the above relative values is $k(NO_2) = 579\times10^{-11}$. Sensitivities for k of about 10^{-12} were used, therefore the small deviations from the curves of the observed points could not be attributed to the lack of sensitivity.

An error of 0.1°C in the measurement of temperature would change the value of the dissociation constant by an amount sufficient to account for most of the deviations. However, with a thyratron tube arrangement for control, observed room temperatures was maintained constant to within 0.1°C; in addition the temperature of the tube was read to 0.01°C, on a 0.001°C thermometer, and corrections applied for each point on the curve.

IV. CONCLUSION

The results for NO_2 are entirely satisfactory and in accord with the theoretical value of Van Vleck.[1] They remove the previous very bad agreement between theory and the only existing experimental results by Soné. The results for N_2O_4, determined from the small curvature of the curves, should be correct to within 20 percent. Further work is being undertaken to determine the susceptibility of hydrogen and some other common gases.

The writer wishes to express his appreciation to Professor Mendenhall for his guidance throughout the duration of the work, to Mr. Foerst, the mechanician, for his cooperation in the construction of the apparatus, and to Mr. Verhoek and Professor Daniels for the preparation of the liquid $NO_2 + N_2O_4$.

Barkhausen Effect. III. Nature of Change of Magnetization in Elementary Domains

By Richard M. Bozorth and Joy F. Dillinger
Bell Telephone Laboratories

(Received June 24, 1932)

Transverse Barkhausen effect. It is found that the small sudden changes in magnetic moment which take place when material is magnetized, have components perpendicular as well as parallel to the direction of the magnetic field. Quantitative measurements of the transverse and longitudinal effects (changes in moment perpendicular and parallel to the direction of the field) show that the longitudinal effect is the larger when the magnetization is small and that the transverse effect is larger when the magnetization is large. Materials examined are (polycrystalline) annealed iron, hard-worked iron, and perminvar.

Domain theory of ferromagnetism. The results are interpreted in terms of the domain theory, according to which ferromagnetic materials consist of small regions or domains always magnetized to saturation. Changes in magnetization are accomplished only by changes in the *directions* of magnetization in the domains. Sudden changes from one to another of the natural directions of magnetization in the crystal give rise to the Barkhausen effect, and in general have definite transverse and longitudinal components, the former now observed for the first time. The experiments show that when the gross magnetization (that of the substance as a whole) is small, the application of an additional magnetic field causes *reversal* of the direction of magnetization in the domains for which this direction was initially nearly antiparallel to the field. Experiments on annealed iron with high gross magnetization indicate, on the contrary, that the direction of magnetization in a domain may be altered through 90°.

IN STUDYING the Barkhausen effect, experimenters have generally observed the voltage-impulses in coils encircling the material and oriented with their axes parallel to the varying magnetic field. These are ascribed to sudden changes of the magnetization of individual small domains of the metal: changes which may be either complete reversals, or rotations through angles smaller than 180°. It occurred to us that if this view is correct, voltage-impulses should appear in coils oriented with their axes at right angles to the magnetizing field; and that the study of these impulses, which we shall designate *the transverse effect*, should increase our knowledge of the elementary processes. Thus, if the transverse effect should be absent or small, it would be inferred that the magnetization in each domain affected by the field is always nearly parallel or antiparallel to the applied field. If on the other hand the transverse effect is of the same order of magnitude as the *longitudinal* effect previously observed, various other inferences can be drawn.

We have detected the transverse effect and measured it together with the longitudinal effect, on specimens of hard-worked iron, annealed iron, and perminvar. The data show that the relative importance of the two depends on the material and on the degree of magnetization of the specimen as a whole; the newly observed effect is relatively small when the magnetizing

field H is less than the coercive force, and may be equal to or greater than the longitudinal effect when the magnetization of the material approaches its saturation-value.

METHOD

The magnetic specimens examined were in the form of tubes 60 cm long and about 5 mm in diameter. For measurements of the usual (longitudinal) Barkhausen effect the tube was placed in an axial field produced by a long magnetizing solenoid as shown in Fig. 1. To measure the small changes in magnetization taking place in a direction at right angles to that of the gross magnetization (transverse effect), a current was passed through a wire coaxial with the tube, the annular field produced by it being everywhere perpendicular to the axis. The component of the change in magnetization perpendicular to the field produced an e.m.f. in the search coils placed in the same positions as they were when measuring the longitudinal effect. For both longitudinal and transverse effects the search coils were connected to the amplifier and measurements of the Barkhausen "noise" made with a thermocouple and galvanometer connected to the amplifier output.

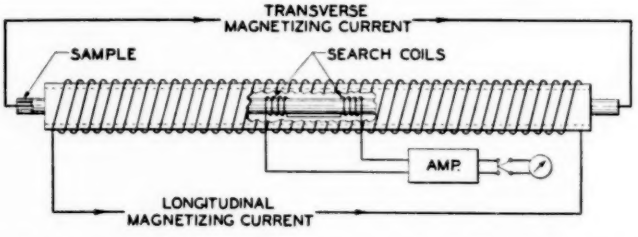

Fig. 1. Diagram of the apparatus for measuring both longitudinal and transverse effects.

As described in a previous paper,[1] the quantities measured were the slope of the B-*vs.*-H curve dB/dH, the rate at which the field was changed during measurements dH/dt, the reversible permeability μ, and the amplifier output i^2 (or the equivalent galvanometer deflection δ) which is a quantitative measure of the noise. We previously[1] derived the following expression for the average change in magnetic moment:

$$\Delta M = \frac{2(10)^{-14}\mu^{3/2}\delta}{C^2 I_s \rho^{3/2}(dB/dH)(dH/dt)} \tag{1}$$

where C is a constant of the apparatus, I_s the saturation value of the magnetization of the material under investigation, and ρ its resistivity. Since now we are dealing only with the ratio of the Barkhausen effects parallel and perpendicular to the field, it is unnecessary to determine many of the quantities in Eq. (1). The ratio of the change in magnetic moment taking place at right angles to the direction of the applied (annular) field, to the change paral-

[1] R. M. Bozorth and J. F. Dillinger, Phys. Rev. **35,** 733–752 (1930). See also the short accounts of the present work in Phys. Rev. **38,** 192–193 (1931); **39,** 353–356 (1932).

lel to the applied (axial) field, (transverse change divided by longitudinal change), is then given by

$$\frac{\Delta M_T}{\Delta M_L} = \frac{\mu_T{}^{3/2}\delta_T(dB/dH)_L(dH/dt)_L}{\mu_L{}^{3/2}\delta_L(dB/dH)_T(dH/dt)_T} \tag{2}$$

where the subscripts T and L refer to quantities measured in determining the transverse and longitudinal effects, respectively. In particular, the *transverse reversible permeability* μ_T is the ratio of the small change in induction parallel to the axis of the specimen, to the very small change in field strength applied in the same direction, when the specimen is magnetized principally annularly by the current flowing along the axis.

The rates of decay of eddy-currents caused by the discontinuities in magnetization measured, are affected by the geometry of the specimen in the same way for annular as for axial magnetization, since the search coils remain in the same position with respect to the specimen for both kinds of measurements. The eddy-currents which affect the rate of change of magnetization picked up by the search coils, are in all cases in a plane perpendicular to the axis of the specimen.

Measurements of μ, δ, dB/dH and dH/dt, were made as previously described.[1] The annular B and dB/dH were measured using an additional (third) search coil each turn of which passed inside of the tubular specimen along its length and returned on the outside. Since the cross section of magnetic material thus enclosed is relatively large, only a few turns were necessary. The axial current producing the annular magnetization was varied smoothly by means of a liquid resistance, a solution of copper sulphate into which a set of copper plates was lowered.

In a preliminary experiment the specimen was magnetized axially and the regular search coils (Fig. 1) connected to the amplifier as already described while at the same time the additional search coil wound as described above to detect the transverse change in magnetization due to an axial field, was connected to a second amplifier, the outputs of the two amplifiers being recorded simultaneously on the same moving photographic paper. It was thus observed that a single discontinuity in longitudinal magnetization was accompanied by a discontinuity in transverse magnetization. The direction of the deflection of the string recording the longitudinal effect was always the same, while the deflections of the string recording the sudden transverse changes were about half in one direction and half in the other. This showed that the average change in magnetization perpendicular to the applied field is zero, but that for any single event there was in general a change in one direction or the other. After this preliminary experiment we confined our experiments to the longitudinal effect occurring with axial field, and to the transverse effect with annular field.

Results

The materials investigated were annealed iron, hardworked iron, and annealed perminvar containing 30 percent Fe, 25 percent Co and 45 percent

Ni. No analyses of these specimens were made, but analyses of similar specimens indicate that the following impurities were present: in annealed iron, 0.1 percent C and 0.5 percent Mn; in hard iron, no impurity more than 0.02 percent; in annealed perminvar, 0.1 percent Si. The tubes were all 60 cm long. The outside diameters of the perminvar and hard iron tubes were 0.47 cm and the wall thicknesses 0.025 cm. For the annealed iron specimen the corresponding dimensions were 0.63 cm and 0.056 cm. The annealed iron was heated in vacuum for 2 hours at 1100° C and cooled 400° C per hour. The

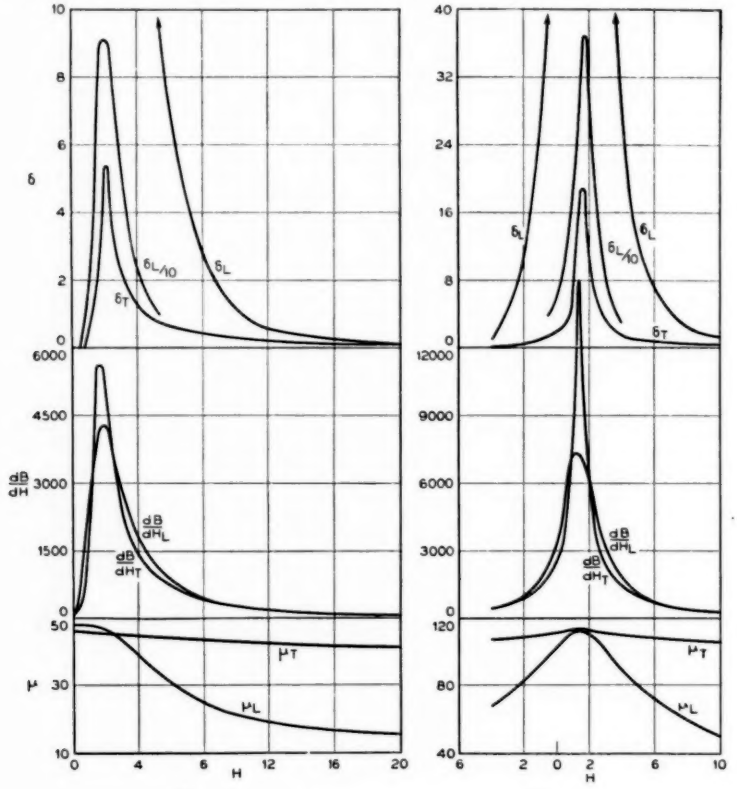

Fig. 2a Fig. 2b

Fig. 2a. Values of δ (output power of amplifier), dB/dH and μ for the magnetization curve of annealed iron, measured with transverse and longitudinal magnetizing fields. The amplifier output δ is referred to a constant value of dH/dt.

Fig. 2b. Values of δ, dB/dH and μ for the hysteresis loop of annealed iron, measured with transverse and longitudinal magnetizing fields.

perminvar was annealed for 1 hour at 875° C and cooled at a maximum rate of about 100° C per hour.

The values of dB/dH, μ, and δ for both longitudinal and transverse effects, for the hysteresis loop and magnetization curve of *annealed iron*, are shown in Fig. 2. The two hysteresis loops for annular and axial magnetization were almost identical, differing only on the steep parts of the curves where the demagnetizing factor has the greatest influence. The galvanometer deflections were observed for various values of dH/dt and from them δ_T and

δ_L were calculated for a constant value of dH/dt, using the relation $\delta \propto dH/dt$. The relative magnitudes of the longitudinal and transverse effects for the magnetization curve as shown in Fig. 3 where the average change in moment

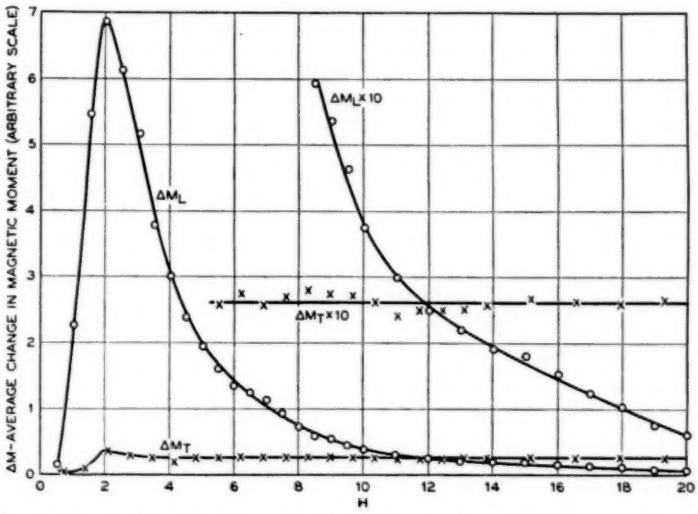

Fig. 3. Longitudinal and transverse changes in magnetic moment for the magnetization curve of annealed iron.

for each is plotted on the same scale as a function of the applied field H, and in Fig. 4 where the ratio of the effects is plotted as a function of the

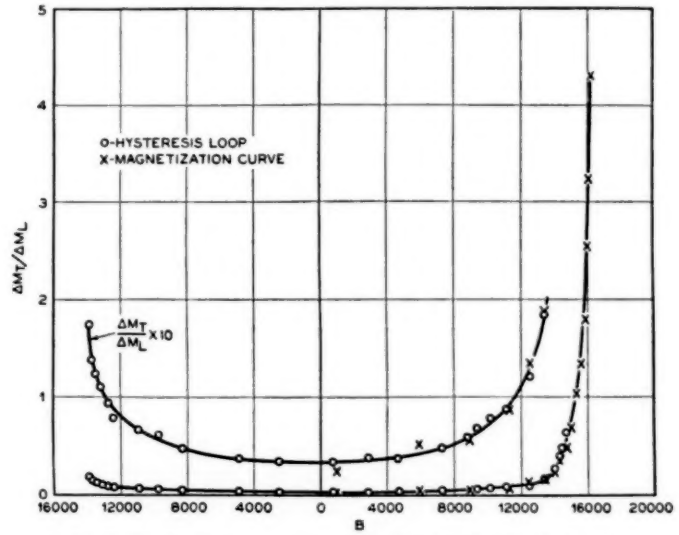

Fig. 4. Ratio of the transverse to the longitudinal change in magnetic moment in annealed iron.

induction B. Since $H \ll B$ except when B is very small, the latter is practically proportional to the magnetization. Fig. 4 shows that the change in magnetization of a domain is greater in the direction of the applied field than in direc-

tions at right angles until B is as large as 15,000. In relatively low fields, where the slope of the hysteresis loop is greatest, the direction of magnetization changes by very nearly 180°, and is antiparallel to the applied field before and parallel to it after the change. The modes of reversal of the domain will be discussed further below.

The values of dB/dH, μ, and δ for the hysteresis loop of *hard worked iron* are shown in Fig. 5. The coercive force of this material was 1.1 gauss.[2] The ratio of the transverse to the longitudinal change in magnetization in

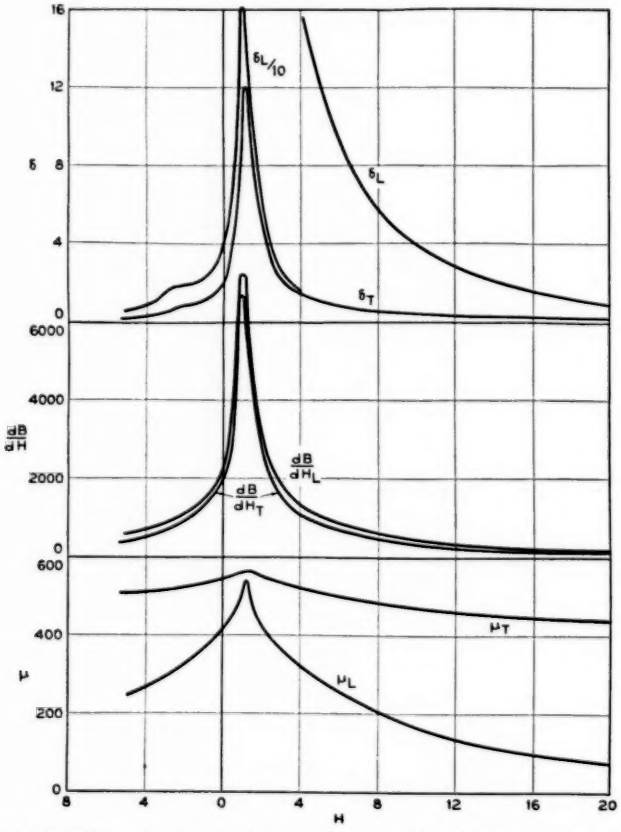

Fig. 5. Values of δ, dB/dH and μ for the hysteresis loop of hard iron, measured with transverse and longitudinal magnetizing fields.

the domains is shown in Fig. 6 as a function of B. For the same value of B, this ratio is a little larger than that for annealed iron.

The data for perminvar are shown in Fig. 7. The hysteresis loop for a maximum field strength of 4 gauss is shown in Fig. 8 because of its peculiar characteristic shape. The ratio of the transverse to the longitudinal change for this hysteresis loop is shown as a function of B in Fig. 9. No measurements were made at higher fields.

[2] Although this material is hard worked, its coercive force is about that normally found for annealed iron. This specimen was given a special treatment in hydrogen (see P. P. Cioffi, Phys. Rev. **39,** 363–367 (1932)) and if annealed would have a coercive force of about 0.1 gauss.

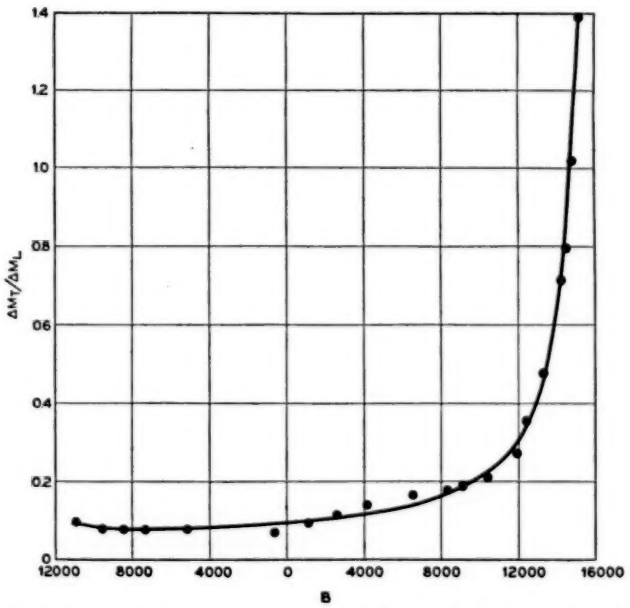

Fig. 6. Ratio of the transverse to the longitudinal change in magnetic moment in hard iron.

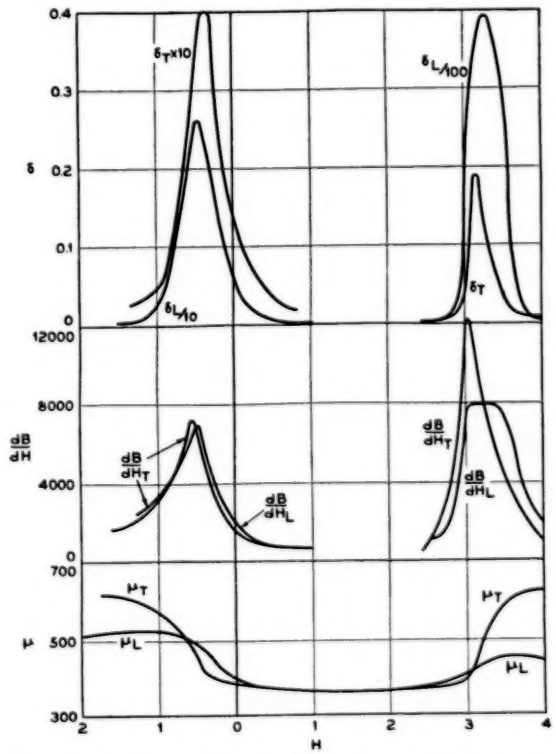

Fig. 7. Values of δ, dB/dH and μ for the hysteresis loop of perminvar, measured with transverse and longitudinal magnetizing fields.

Discussion

One of the most obvious characteristics of the curves of Figs. 4 and 6 is that when the magnetization is small the longitudinal components of the

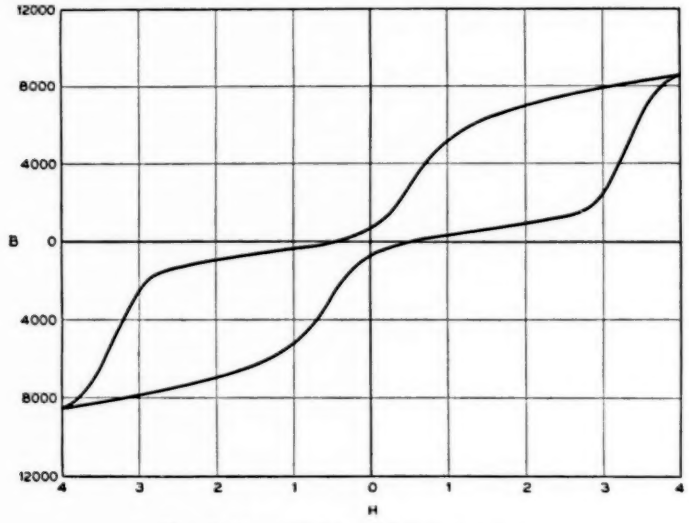

Fig. 8. Hysteresis loop for perminvar.

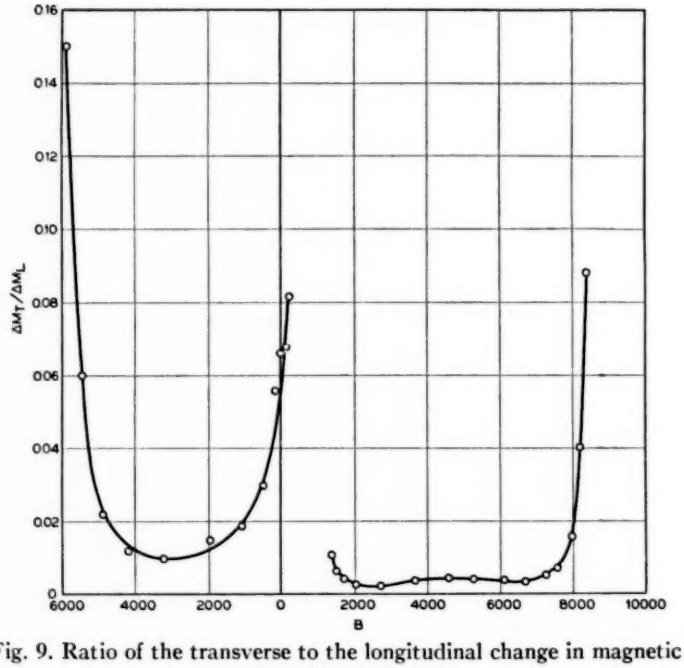

Fig. 9. Ratio of the transverse to the longitudinal change in magnetic moment in perminvar.

discontinuous changes in magnetization are larger than the transverse components, but that when the magnetization is large the transverse component is the larger. Two kinds of change of magnetization which are consistent with

this result are illustrated in two dimensions in Fig. 10. Here a shows a reversal of the magnetization-vector from the initial position (dotted line) to a final position making an angle $\theta = 15°$ with the direction of the field. In this case $\Delta M_T/\Delta M_L = 0.27$. If θ is 75° as in (b), this ratio is 3.7. In (c) and (d) the vectors rotate by 90° instead of 180° as in (a) and (b), and for final positions defined by $\theta = 15°$, the values of $\Delta M_T/\Delta M_L$ are 0.58 and 1.73 respectively. It is evident that the ratio becomes large without limit as θ approaches 90° in (b) or 45° in (d). Since we should expect that the latter changes would occur at relatively high magnetizations, and changes of kind (a) at low magnetizations, we have here a qualitative correspondence with the data as shown in Figs. 4 and 6.

Consideration of Fig. 10 (d) also shows that as θ approaches 45° the transverse change, equal to $\sin\theta + \cos\theta$, approaches asymptotically the definite limit $2^{1/2}$, taking the radius of the circle as unity. Since θ approaches 45° when

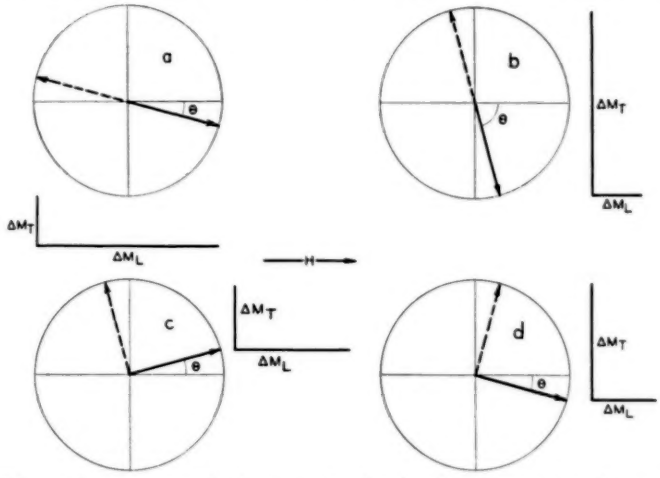

Fig. 10. Possible modes of reversal of magnetization in elementary domains, with the corresponding transverse and longitudinal components.

the magnetization is high, we should expect that then also the transverse effect should become constant. This constancy was observed as shown in Fig. 3.

The two kinds of changes shown in Fig. 10 correspond to two views of the changes which take place in ferromagnetic materials. Both are based on Weiss' idea that a ferromagnetic substance is composed of small domains, each of them initially magnetized to saturation along some direction of *natural magnetization*. According to one view (Webster's[3] and Heisenberg's[4]) which is suggested by experiments on single crystals, the directions of natural magnetization in a domain are the six <100> directions of the crystal which contains the domain; an applied field may shift the magnetization from one of these directions to another making a smaller angle with its own. According to the other view (resembling R. Becker's[5]) the directions of natural magnetization

[3] W. L. Webster, Proc. Phys. Soc. London **42**, 431–440 (1930).
[4] W. Heisenberg, Zeits. f. Physik **69**, 287–297 (1931).
[5] R. Becker, Zeits. f. Physik **62**, 253–269 (1930).

are controlled by the strains in the substance, and the only effect which an applied field can produce in a domain is a reversal of the magnetization. The changes shown in (a), (c), and (d) of Fig. 10 are compatible with the former view, (a) and (b) with the latter.

The way in which these views fit in with our results is illustrated in Fig. 11. If the directions of magnetization in the domains are controlled by the lattice of the crystal, discontinuous changes in a polycrystalline specimen can occur only until the directions of magnetization in the domains all make angles of 45° or less with the direction of the field. When this condition is attained the material is about 85 percent saturated, and the ratio $\Delta M_T/\Delta M_L$ is indefinitely large as indicated by the vertical line (a) in Fig. 11. If the control is by strain alone, the corresponding limit is designated by (b) which indicates that discontinuous processes cease when the directions of magnetization in the

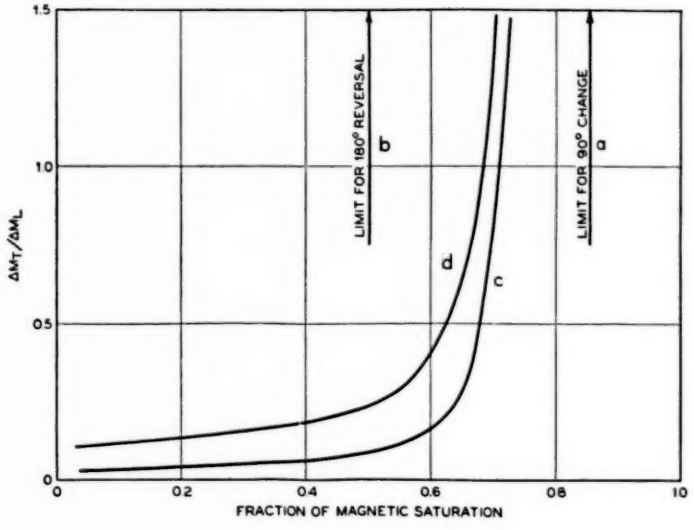

Fig. 11. Ratios of the transverse to the longitudinal change in magnetic moment in (c) annealed iron and (d) hard iron and their relation to the theoretical limits (a) for 90° changes and (b) for 180° reversals.

domains make angles of 90° or less with the direction of the field, in which case the material as a whole is only half saturated. Curves (c) and (d) represent the actual data for annealed and hard worked iron, respectively, for comparison. The curves suggest that in each material the magnetization is controlled in some of the domains by strain and in some by the lattice, the domains of the former class being increased in relative number by hard working. By interpreting the data in this way, strain has some influence even in well annealed iron, and in hard worked iron there is still a considerable amount of crystallographic control. The interpretation of the difference between the experimental curves at the lowest values of B is not yet clear; the explanation of this difference may influence the conclusions already drawn. It is intended to make a more quantitative comparison between theory and experiment in a later paper.

The curve of Fig. 9, for perminvar, is different from those for iron in that $\Delta M_T/\Delta M_L$ has relatively high values near $B=0$ as well as when B is large. This is in accord with other peculiarities of perminvar which have been regarded[6] as indicating that it is a mixture of two kinds of magnetic materials. Although the nature of the difference (if any) between these materials is yet undetermined, the data here reported are such as would be expected if about half of the material approached saturation before the other half began to change its magnetic state appreciably, and for each portion the ratio $\Delta M_T/\Delta M_L$ went through the usual changes during the cycle.

In summary, our data are in good agreement with the following conceptions: Magnetic materials are divided into small domains each of which is magnetized to saturation. In annealed materials the direction of magnetization in each domain is one of the directions of easy magnetization in the crystal which contains the domain; these, in the special case of annealed iron, are the directions of the crystal axes. With an increase in the magnetization of the material as a whole, the magnetization in each domain changes from one of these directions to another making a smaller angle with the applied field. When the net magnetization is small, most of the changes are reversals in the domains in which the initial magnetization is almost anti-parallel to the applied field. When the net magnetization is large (one half to three quarters of the saturation value), other domains are affected in which the initial magnetization is inclined at smaller angles to the field and changes of 90° occur. When saturation is almost attained a new phenomenon appears, the directions of magnetization in all of the domains cease to be controlled by the crystal lattice and approach parallelism to the applied field. This final approach to saturation is a continuous one and is not believed to be accompanied by Barkhausen effect.

[6] G. W. Elmen, J. Frank. Inst. **260**, 317–338 (1928); **207**, 583–617 (1929); U. Meyer, Phys. Zeits. **28**, 919–920 (1927); H. Kühlewein, Wiss. Veröff; Siemens-Konz. **10**, No. 2, 72–88 (1931), and Phys. Zeits. **31**, 626–640 (1930).

The Variation with Temperature of the Thermoelectric Power of Nickel and Some Copper-Nickel Alloys

By K. E. GREW
Sloane Physics Laboratory, Yale University

(Received June 9, 1932)

The thermoelectric power of pure nickel against platinum has been measured between 0°C and 500°C; similar measurements have been made on two nickel-copper alloys containing respectively 94 and 79 percent nickel. A differential method was used in which the change in thermoelectric force ΔE corresponding to a small temperature change ΔT was observed. The results are discussed in relation to Stoner's theory. Although the experimental results have the same general characteristics as those calculated, factors not considered in the simple theory are involved, even at temperatures at which the assumption that the magnetization is due to spin moments only is approximately valid.

THAT the thermoelectric properties of a ferromagnetic are in some way related to the magnetization is apparent from the sudden change in the Thomson coefficient or the "specific heat of electricity" at the Curie point.

The magnitude of this change in nickel has been deduced[1] from measurements of the thermoelectric power in the neighbourhood of the Curie point, and it is found to be approximately equal to that predicted on the quantized Weiss theory for a magnetic "carrier" for which $j=\frac{1}{2}$. This agreement in magnitude was at first regarded as implying that the carriers were free electrons, but the argument was invalidated when it was found that the specific heat of the electron increases on passing from the ferromagnetic to the paramagnetic state, whereas the "calorimetric" specific heat decreases. Stoner[2] has sought to explain this difference in sign, and on certain assumptions he has deduced an expression for the temperature variation of the thermoelectric power and the specific heat of electricity in ferromagnetics. The results of Dorfman and Jaanus[1] show considerable divergence from the theoretical values, but as they admit of a comparison over only a limited range of temperature it was thought desirable to extend the measurements.

METHOD OF EXPERIMENT

In measuring the temperature variation of the thermoelectric power it is desirable to use a direct method in which the change in thermoelectric force ΔE due to a small change in temperature ΔT is observed.

The method first adopted for the measurement of the thermoelectric power of nickel against platinum and described in a preliminary note,[3] was discarded, as it did not give consistent results at the higher temperatures; this was probably because it did not ensure that the nickel-platinum junctions were always at precisely the same temperature as the junctions of the

[1] J. Dorfman, R. Jaanus, and I. Kikoin, Zeits. f. Physik **54**, 277 (1929). J. Dorfman, R. Jaanus, K. Grigorow and M. Czernichowski, Zeits. f. Physik **70**, 796 (1931).

[2] E. C. Stoner, Proc. Leeds Phil. Soc. **2**, 149 (1931); Phil. Mag. [7] **12**, 737 (1931).

[3] K. E. Grew, Proc. Leeds Phil. Soc. **2**, 217 (1931).

couple used to measure the temperature difference. An arrangement similar to that of Dorfman and Jaanus[1] was tried, but the mica sheets used as insulation were found to become conducting at the higher temperatures.

In the method finally adopted, the nickel wire under investigation was fused to the junction of a previously calibrated platinum platinum-iridium couple, thus forming a second, nickel-platinum, couple. In series with each couple was a small resistance through which a current could be passed. The electromotive force of the couples with one junction at 0°C and the other at T°C could be almost completely counterbalanced by the potential difference across the resistances, so that the small residual potential difference could be measured on a sensitive potentiometer. The difference between this reading and a second, when the temperature had been raised to $T+\Delta T$, gave the increase in electromotive force ΔE corresponding to a change ΔT at the mean temperature $T+\frac{1}{2}\Delta T$. ΔT was calculated from the change in electromotive force of the platinum-iridium couple, and thus the thermoelectric power $\Delta E/\Delta T$ of nickel was found. This method allowed the use of a more sensitive potentiometer than would have been possible had the whole of the thermoelectric force been applied to it. It was necessary, however, in order to find the temperature T, to measure the total electromotive force of the platinum-

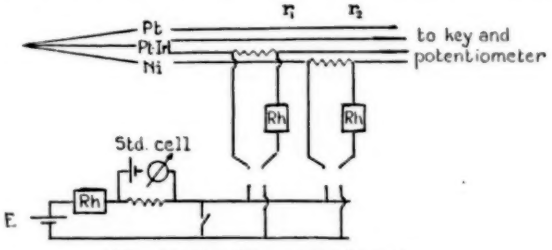

Fig. 1. The thermocouple system.

iridium couple; for this purpose the range of the potentiometer could be changed.

The circuit is shown in Fig. 1. The three wires leading to the hot junction were insulated from each other by quartz tubes. These were contained in a Pyrex tube and inserted in the furnace, which consisted of a cylindrical copper block wound with a non-inductive heating coil enclosed in a vacuum vessel; the couples passed into a hole drilled along the axis of the block. The wires emerging from the furnace were soldered to copper wires and the junctions kept in melting ice in a vacuum vessel. r_1, r_2 are the small resistances of about 1 ohm, through either of which a current from the battery E could be passed. The constancy of this current throughout a set of measurements could be checked by the standard cell and resistance; such small fluctuations as did occur were usually negligible. A key enabled (a) the platinum-iridium couple to be connected directly to the potentiometer for the measurement of the temperature T of the junction; (b) the same couple to be connected through the resistance r_1 for the measurement of the temperature difference ΔT which was usually 3 to 5 degrees; (c) the nickel-platinum couple to be connected through the resistance r_2 for the measurement of ΔE; (d) the reversal of all these connections.

To eliminate parasitic electromotive forces, it was necessary that the whole circuit with the exception of the couples themselves should be of copper. The key was constructed such that all its metal parts were of copper with no soldered connections, and as a further precaution it was enclosed in a case to avoid local heating while being operated. The small resistances were also wound from copper wire and kept at constant temperature in an ice bath on account of the large temperature coefficient of resistance of copper. Care was also taken to eliminate leakage from the heating circuit to the couple system.

The potentiometer consisted of a manganin coil wound on a marble cylinder, with a revolving contact and circular scale. By series resistances the range could be adjusted for measuring either the total electromotive force E or the small change ΔE. For the latter, 1 division on the scale corresponded to 0.075 microvolt or to a deflection of the galvanometer of 2 mm. The potentiometer was calibrated by comparison with a Wolff potentiometer. Stray electromotive forces could not be prevented in this part of the circuit, but their effect was eliminated by reversing the current and the connections to the couples.

The platinum platinum-iridium couple was calibrated between 0° and 500°C, using standard thermometers up to 200°C and the boiling points of naphthalene, benzophenone, and sulphur for the higher temperatures. The whole range was divided into 3 overlapping sections and equations of the form $T=AE+BE^2+CE^3$ were found for each. The temperatures calculated from the observed electromotive force by means of these equations should not be in error by more than 0.3°C. To calculate the change in temperature ΔT from the observed change in electromotive force ΔE it is necessary to know the temperature variation of dE/dT. This was found directly from the calibration curve.

In practice it is not possible to prevent small changes in the furnace temperature while readings are being taken. The effect of such changes, which were usually less than 0.1°C, was eliminated by taking readings at definite time intervals.

The error in individual values of the thermoelectric power is estimated at 0.7 percent.

Experimental Results

Measurements were made of the thermoelectric power of nickel and of some alloys of nickel with copper over a range from 0°C to 500°C. The nickel was drawn from rod supplied by Messrs. Hilger and was 99.97 percent pure. The copper was from the same source and of the same purity. For the preparation of the alloys and the subsequent drawing into wires I am indebted to the National Physical Laboratory, England. Melting was carried out in a crucible of china-clay and alumina, in a high frequency induction furnace using an atmosphere of hydrogen. The ingots were swaged into rods and finally drawn into wires of 0.4 mm diameter. Before measurements were made the wires were heated for some time at 800–900°C.

An obvious extension of the method allowed observations to be made on two specimens at the same time.

TABLE I. *Results for nickel and alloy A_1 (94 percent nickel).*

Temp. °C	$-\Delta_{Ni}E_{Pt}/\Delta T$	$-\Delta_{A_1}E_{Pt}/\Delta T$	Temp. °C	$-\Delta_{Ni}E_{Pt}/\Delta T$	$-\Delta_{A_1}E_{Pt}/\Delta T$
55.0	15.00	24.78	318.0	11.38	13.65
91.0	15.46	24.74	329.5	—	13.38
116.2	15.97	24.76	331.5	10.36	13.45
139.4	16.24	24.53	347.1	8.77	13.36
161.3	16.44	24.12	353.4	8.02	13.40
186.1	16.16	23.11	359.2	7.05	13.40
198.5	16.11	22.60	362.9	6.94	—
220.8	15.72	21.65	377.4	6.67	—
242.6	15.17	19.96	392.4	6.42	13.86
257.4	14.82	18.80	398.5	6.51	14.00
264.1	14.33	17.80	407.6	6.44	14.02
281.5	13.44	16.03	425.1	6.59	14.03
290.5	—	14.66	441.4	6.84	14.39
296.0	12.77	13.86	464.0	7.23	14.70
306.4	12.23	13.91	482.4	7.47	15.00

TABLE II. *Results for alloy A_2 (79 percent nickel).*

Temp. °C	$-\Delta_{A_2}E_{Pt}/\Delta T$	Temp. °C	$-\Delta_{A_2}E_{Pt}/\Delta T$
41.6	29.30	179.9	24.45
69.43	28.38	194.7	24.77
86.7	27.87	210.7	24.96
100.4	27.24	240.8	25.58
115.2	26.51	258.0	26.10
124.2	25.60	262.8	26.27
128.9	25.24	266.6	26.28
145.7	24.18	279.0	26.66
158.5	24.10	304.2	27.04
171.4	24.36		

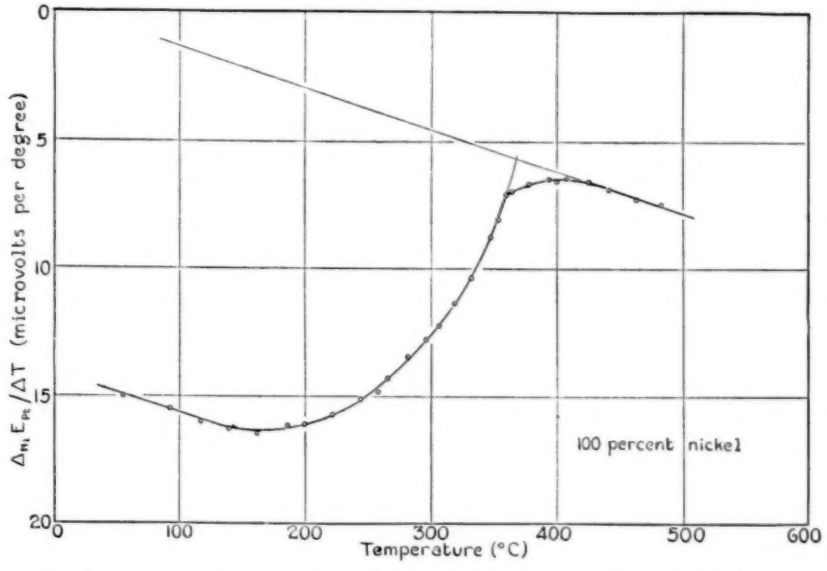

Fig. 2. The temperature variation of the thermoelectric power of nickel with respect to platinum.

The results for pure nickel and an alloy (A_1) containing 94 percent nickel are given in Table I and for a 79 percent alloy (A_2) in Table II, while they are represented graphically in Figs. 2, 3 and 4. The thermoelectric power is in microvolts per degree.

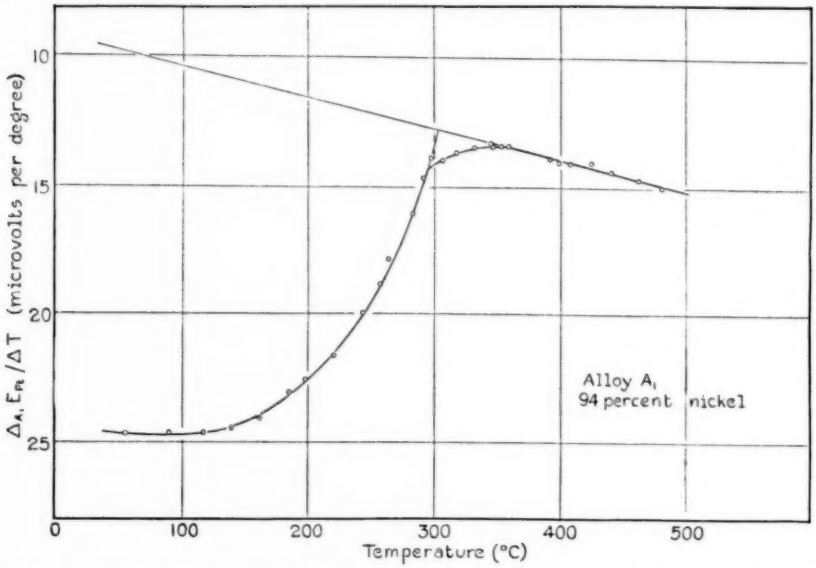

Fig. 3. The temperature variation of the thermoelectric power of a nickel copper alloy (94 percent nickel) with respect to platinum.

It will be seen that, in the case of pure nickel, the slope of the thermoelectric power curve changes abruptly at 360°C; thereafter it decreases continuously, finally assuming a constant negative value above 430°C. These changes were confirmed by the observations of the total electromotive force

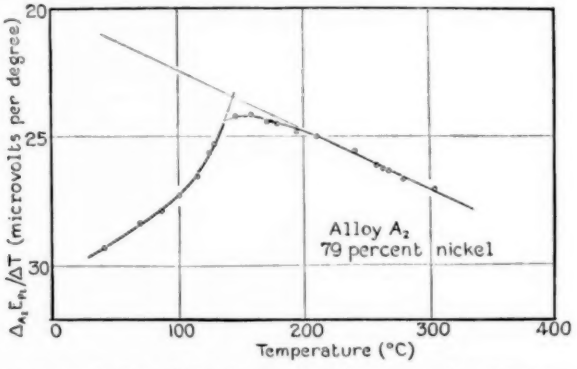

Fig. 4. The temperature variation of the thermoelectric power of a nickel copper alloy (79 percent nickel) with respect to platinum.

made concurrently, and which were in excellent agreement with those of Jordan and Swanger.[4]

The nature of the curves for the alloys is not essentially different, though the change of slope occurs at a different temperature.

[4] L. Jordan and W. H. Swanger, U. S. Bureau of Stds. Jour. of Res. **5**, 1304 (1930).

Over the limited range of temperature in which comparison is possible, the present results for pure nickel are some 4 percent greater (numerically) than those of Dorfman and Jaanus. The difference is not surprising, considering the effect of impurities and previous treatment on thermoelectric properties.

Discussion

In the papers to which reference has already been made, Stoner[2] has shown that the behavior of a ferromagnetic may be largely explained by attributing ferromagnetism to interchange interaction electrons having a spin moment $j=\frac{1}{2}$, though at temperatures approaching the Curie point it appears necessary to regard the orbital moment as being partially effective.

According to Fowler, the specific heat of electricity per electron may be defined as the increase in specific heat of the metal due to the addition of one electron. Stoner has given reasons for supposing the magnetically effective spin moments to be those of "missing" electrons, and that the addition of a free electron will neutralise one of these spins. If the contribution of each spin moment to the "magnetic" specific heat is s, and the specific heat of electricity per electron due to the magnetization is σ_e, then $\sigma_e = -s$. For the gram electron, the specific heat

$$C_E = L\sigma_e = -Ls = -S_M/q$$

where L = Avogadro's number; S_M = specific heat per gram-atom due to the magnetization; q = number of effective spin moments per atom. The thermoelectric power referred to the same units is given by

$$P_E = \int_{T/\theta}^{1} \frac{S_M/q}{T/\theta}\, d\left(\frac{T}{\theta}\right)$$

where θ is the Curie point, and P_E is the thermoelectric power of the ferromagnetic with respect to another substance without intrinsic magnetization but otherwise identical. It is zero at the Curie point, and becomes increasingly negative as the temperature decreases. Both C_E and P_E are independent of q.

These expressions refer only to the idealized ferromagnetic, in which spin moment alone is effective.

For comparison with the theoretical values, a quantity P_{obs} can be calculated from the experimental results, such that

$$P_{obs} = (\text{Ni}P\text{Pt})_T - (\text{Ni}P'\text{Pt})_T$$

where P' is the thermoelectric power at temperature T extrapolated from observations above the Curie point. P_{obs} should be comparable with P_E provided that the variation of the thermoelectric power can be regarded as the sum of the variation due to changing magnetization and a "normal" variation. Alternatively, the quantity C_{obs} can be calculated from the slope of the thermoelectric power curves and compared with the observed and calculated values of the specific heat S.

Values of P_E (taken from Stoner's paper) and of P_{obs} are plotted in Fig. 5 as functions of T/θ. The changing direction of the thermoelectric power curves above the Curie point makes the extrapolation involved in determining P_{obs} uncertain. The extrapolation has been made from that part of the

curve where the thermoelectric power is decreasing (algebraically) approximately uniformly with the temperature, this being the most favorable from the point of view of obtaining agreement between the theoretical and experimental values. The curve for iron is obtained from the measurements of

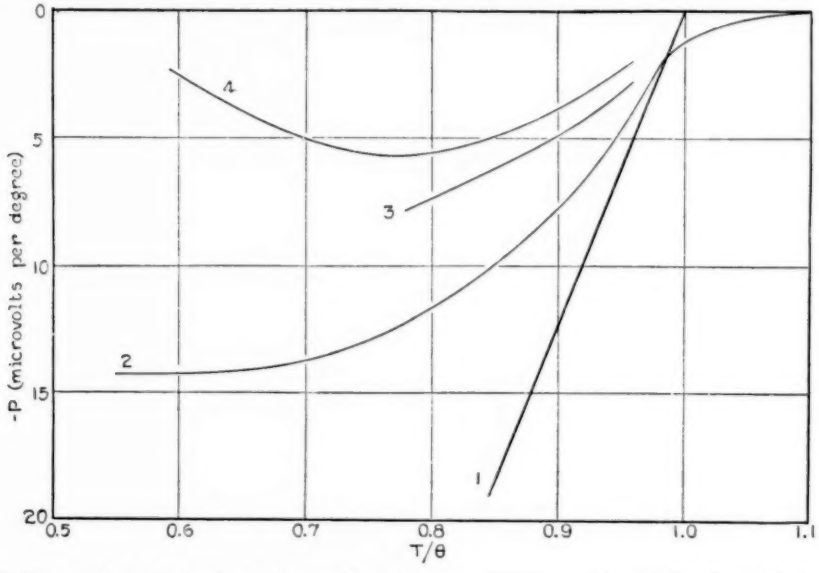

Fig. 5. Observed and calculated thermoelectric power curves. 1. P_E; 2. P_{obs} for nickel; 3. for alloy A_2; 4. for iron.

Burgess and Scott.[5] Values of P_{obs} for the alloy A_1 coincide nearly with those for pure nickel, and the curve is not shown in the figure.

In all cases, the value of P_{obs} is less (numerically) than the calculated value P_E, the divergence increasing at the lower temperatures. The ratio P_{obs}/P_E has the values found in Table III. For iron, P_{obs} actually becomes

TABLE III.

T/θ	0.9	0.8
Pure nickel	0.62	0.48
Alloy A_1	0.60	0.48
Alloy A_2	0.39	0.31
Pure iron	0.30	0.22

positive below $T/\theta = 0.5$, but the small number of observations and the probability of an effect due to the phase change near the Curie point make the justification for the extrapolation more doubtful than in the other cases.

In the case of pure nickel, it is of interest to compare the specific heat of electricity C_{obs} with the "magnetic" specific heat S given by Mme. Lapp.[6] Fig. 6 shows the variation with temperature of the observed specific heat S corrected for quantum variation, dilatation, etc.; of S_1, which Mme. Lapp calculates from the variation of the magnetization $d\sigma^2/dT$ and the molecular field constant applicable above the Curie point; and of $-C_{obs}$ derived from

[5] G. K. Burgess and H. Scott, U. S. Bureau of Stds. Bull. **14**, 15 (1917).

[6] Mme. Lapp, Ann. de Physique [10] **12**, 442 (1929).

the thermoelectric power curves. The existence of the abnormally high specific heat above the Curie point makes impossible any definite conclusion as to the relation between C_{obs} and S to be expected from Stoner's considerations. But at temperatures not too near the Curie point, where the magnetization may be attributed to spin moment alone, it would be expected that C_{obs} would be numerically greater than S or S_1, since the number of effective spin moments per atom is less than unity. This is not so, C_{obs} being less than either S or S_1 at temperatures below $T/\theta = 0.9$. Thus there is no apparent quantitative relationship between the specific heat of electricity and the "magnetic" specific heat whether one considers the values of the specific

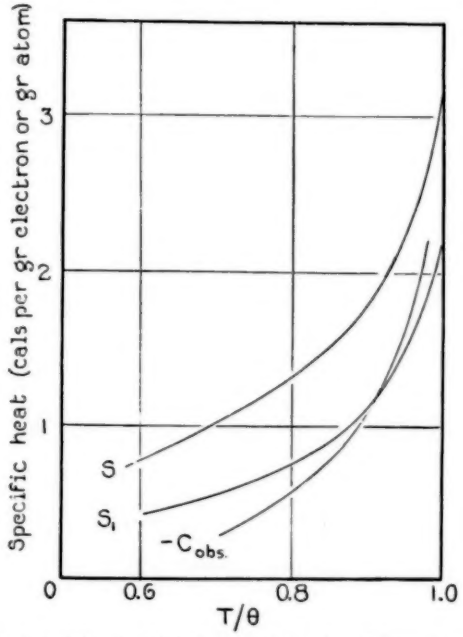

Fig. 6. Specific heat of electricity in nickel. S and S_1 after Mme. Lapp;—C_{obs} from thermoelectric power curves.

heat calculated for the idealized ferromagnetic or those experimentally determined for an actual ferromagnetic.

It appears that, although the experimental results for the temperature variation of the thermoelectric power have the same general characteristics as those calculated, factors not considered in the simple theory are involved, even at temperatures at which the assumption that the magnetization is due to spin moments only is, at least approximately, valid.

It is hoped that an investigation of other properties of the copper-nickel alloys dependent on magnetization will assist in explaining further the variation of the thermoelectric power in ferromagnetics.

This investigation was begun at the University of Leeds, England; a Commonwealth Fund Fellowship permitted of its continuation at Yale University. My thanks are due to Dr. E. C. Stoner and to Professor L. W. McKeehan for their interest and kindly criticism. I have also to acknowledge with thanks a grant from the Royal Society.

Diamond Windows for Withstanding Very High Pressures

By Thos. C. Poulter and Francis Buckley
Department of Physics, Iowa Wesleyan College

(Received June 10, 1932)

Diamond windows have been tested out and found to withstand much greater pressures than glass or fused quartz windows (up to 21,500 atmospheres), particularly when water and alcohol solutions are used to transmit the pressure to the windows.

Procedure and Results

NO HIGH pressure window up to the present time has been successfully constructed to withstand a pressure of more than 30,000 atmospheres, and then, only when the transmitting medium is a light paraffin oil or some similar material. If a material such as alcohol, water or ether is used to transmit the pressure the windows are usually fractured between 4000 and 8000 atmospheres.

This difficulty has in some cases been overcome by placing the above named liquids in a small collapsible or telescoping cell which is fitted at each end with a glass window through which one may make his observations.[1] The pressure is then transmitted to the cell by paraffin oil. Thus, the liquids which break the windows easily do not come in contact with those windows which support the pressure. By this method alcohol, ether, or water, and solutions in which these liquids are used as solvents can be observed up to 30,000 atmospheres.

The method of using a small cell inside the pressure cylinder is not completely satisfactory because some of the liquid in the cell may escape and come in contact with the pressure windows thus causing them to break. Another disadvantage in using such a cell is the fact that after the pressure has been built up to 10,000 atmospheres, or higher, and is then released, the inner surface of the cell windows are frequently fractured while in most cases the side of the window in contact with the oil is not injured. In some experiments carried out in this laboratory it was shown that diamonds showed no tendency to fracture when subjected to such conditions. This led us to believe that diamond windows should be very effective as pressure windows even though the medium used to transmit the pressure be one of those that readily breaks glass or fused quartz.

The diamond used in this investigation was 3 mm thick and 3.5 mm in diameter. It was mounted on a hard steel support polished to a mirror surface over a hole 1.5 mm in diameter and held in place in the usual manner by a small amount of liquid balsam.

[1] Thos. C. Poulter, Phys. Rev. **40**, 860 (1932); Thos. C. Poulter and Robert O. Wilson, Phys. Rev. **40**, 877 (1932); Thos. C. Poulter and Carl A. Benz, Phys. Rev. **40**, 872 (1932).

The diamond window was then surrounded by water and subjected to a pressure of 21,500 atmospheres. When the window was removed from the cylinder it was not damaged in any way. Since 21,500 atmospheres pressure is more than that necessary for the formation of ice VI, the diamond window was surrounded by a 50 percent solution of ethyl alcohol. A pressure of 21,500 atmospheres was applied. At this pressure the cylinder which contained the diamond window ruptured, thus releasing the pressure instantaneously but without damage to the diamond window.

Another cylinder was used in an attempt to test the diamond window to still higher pressures but this cylinder ruptured at about the same pressure. The diamond window used in these tests has been under pressure more than twenty times and in three cases the pressure has been released suddenly by the splitting of the cylinders. Since these windows show no ill effects from the tests which we have made thus far, it is the belief of the authors that such windows will prove very valuable in the field of optical studies at high pressures.

The Effect of Pressure on the Index of Refraction of Paraffin Oil and Glycerine

By Thos. C. Poulter, Carter Ritchey and Carl A. Benz
Physics Department, Iowa Wesleyan College

(Received June 10, 1932)

A refractometer for measuring the index of refraction of liquids under very high pressure is described. The values obtained for glycerine and a paraffin oil together with the constants for the Lorenz-Lorentz relation are tabulated.

Procedure and Results

THERE have been relatively few studies made on the change of the refractive index with pressure and those at pressures seldom, if ever, greater than 200 atmospheres.

By making use of a liquid prism which could be subjected to high pressure, the authors have constructed a refractometer for studying the effect of very great pressure upon the index of refraction of different materials.

The windows are mounted directly in contact with the hard steel disk *R* in the figure and in such a position that the liquid in the apparatus forms a 30° prism.

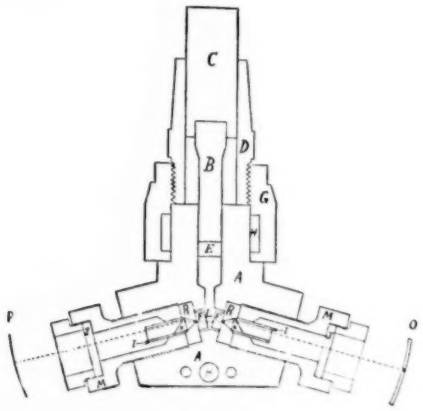

Fig. 1.

In measuring the index of refraction for different materials a much smaller opening is made in the window support than had been used in the ordinary type of pressure cylinder. This serves as a slit system to run the light through parallel to the base of the prism.

This window support is held firmly against the shoulder of the pressure cylinder by the steel plug *M* which screws down tightly against it. On the outer end of this plug is a safety window *J*, held in place by another steel plug. Because of the large shift in the light beam this safety window must be larger than the triple safety window usually used so that the light beam can be easily followed.

Since the position of the prism L formed by the liquid in the pressure cylinder would bend the light up, it is necessary to place two small correction prisms K in the cylinder to direct the beam of light from the light source O, through the liquid prism L and out onto the screen P. These two correction prisms are mounted in brass tubes which enable one to adjust their positions readily.

The space between the pressure windows and the small correction prisms is filled with a liquid of nearly the same index of refraction as the glass, so as to correct for the lens effect of the pressure windows.[1] Knowing the angle of the prism L, the pressure that is developed, and by measuring the angle of minimum deviation, it is possible to study the effect of pressure on the index of refraction of different liquids.

The liquids used were a paraffin oil, merasol, a product of the Standard Oil Company and glycerine. This oil is used for transmitting pressures in various other experiments and for this reason it was desirable that we know the effect of pressure upon its index of refraction.

The expression $n=(\sin \frac{1}{2}(R+D))/(\sin \frac{1}{2}R)$ gives the index of refraction n when the prism angle R and the angle of minimum deviation D of a transmitted beam is known. By measuring the change in deviation of the transmitted yellow light, the change in n was determined with each increase of pressure. The densities for the oil were measured by the piston travel in a cylinder designed for such measurements, while that for the glycerine was taken from data obtained by P. W. Bridgman.[2]

Tables I and II give the values for the refractive index n and density e at the pressures designated, together with the constant K for the Lorenz-Lorentz relation:

$$\frac{n^2-1}{n^2+2}\cdot\frac{1}{d}=K$$

TABLE I. *Refractive index and density of paraffin oil.*

pressure (atm.)	density (gm/cc)	n	K
1.	0.8706	1.4749	0.324
2697.	0.954	1.5340	0.325
5394.	1.006	1.5659	0.324
8091.	1.031	1.5895	0.326
10789.	1.052	1.6008	0.324
13585.	1.069	1.6039	0.324

TABLE II. *Refractive index and density of glycerine.*

pressure (atm.)	density (gm/cc)	n	K
1.	0.987	1.4722	0.282
1803.	1.025	1.4858	0.279
3703.	1.054	1.4962	0.278
4510.	1.078	1.5103	0.279
7212.	1.100	1.5210	0.279

From these values of K it can be seen that the value for the Lorenz-Lorentz relation is constant within the limits of experimental error up as far as measurements were made.

The authors wish to express their appreciation for the assistance in the form of a grant from the National Research Council.

[1] Thos. C. Poulter and Carl A. Benz, Phys. Rev. **40**, 872 (1932).

[2] P. W. Bridgman, Proc. Amer. Acad. Arts and Sci. **67**, 1–27 (1932).

LETTERS TO THE EDITOR

Prompt publication of brief reports of important discoveries in physics may be secured by addressing them to this department. Closing dates for this department are, for the first issue of the month, the twenty-eighth of the preceding month; for the second issue, the thirteenth of the month. The Board of Editors does not hold itself responsible for the opinions expressed by the correspondents.

Probable Values of e, h, e/m and α. A Reply to R. T. Birge

The Physical Review of April 15th contains a paper[1] (and a letter) by R. T. Birge on "Probable Values of $e, h, e/m$ and α." Throughout the paper Birge uses a method of estimating e and h (the electronic charge and Planck's constant) which I suggested and used.[2] Whilst adopting my method, Birge disagrees with various details of my work, and I wish to reply briefly to his criticisms.

(I) Any one of the usual methods of estimating h involves the experimental determination of a quantity A_n, which occurs in an equation of the form $h=A_n e^n$. I assumed an arbitrary value for e, plotted the values of $A_n e^n$ against n, and fitted a linear graph to the observations. From this graph estimates of e and h were deduced, which do not depend on any direct determination of e (such as Millikan's).

The probable errors may be estimated from the residuals with the help of the equation

$$r=0.6745\left(\frac{\sum(pvv)}{s-q}\right)^{1/2}$$

where r is the probable error of an observation of unit weight. I assumed, in effect, that s is the number of observations (36) and q the number of variables (2). Birge, however, (reference 1, p. 237), uses collectively all the observations of A_n for each particular value of n, obtaining three unequally weighted "points" (at $n=1$, $1\frac{1}{3}$, and $1\frac{2}{3}$). Then $s=3$, $q=2$, and his estimates of the errors are about twice my estimates (though there is no disagreement as to the line itself). Birge's explicit criticism of my method is: "That his procedure cannot be correct is immediately evident from the fact that if all observed h_n values correspond to the same value of n (giving only one point), no solution at all would be possible."

Let us suppose that the only data were 12 estimates of A_1 in the equation $h=A_1 e$. Then "no solution at all would be possible" as regards estimating e and h (and their errors); my method gives no solution. But Birge's statement needs qualifying; the slope of the line is indeterminate but its intercept on the line $n=1$ is determinate, giving an estimate of h/e. My method yields a reasonable estimate of the probable error of this value of h/e, but Birge's method gives the error in the indeterminate form $0/0(1-2)^{1/2}$. This is an absurd estimate of the probable error of the mean of 12 experimental determinations of what we designate (h/e), and I think this is sufficient to show that Birge's method of estimating the probable errors is incorrect.

(II) In the letter in the same number of the Physical Review, Birge explains that he had overlooked my statement that "By assuming a value of h, and plotting all the deduced values of e against $1/n$, the direct estimates of e could also be plotted at $1/n=0$. The increase in accuracy would, however, be negligible." This accounts for Birge referring in his paper to this method as "the essential extension of Bond's method." It also explains his statement that I had not carried my method to its logical conclusion. I deliberately did not use this second method at the start, for the same reason as Birge (reference 1, p.

[1] Birge, Phys. Rev. **40**, 228–261 and 319–320 (1932).

[2] Bond, Phil. Mag. **10**, 994 (1930) and **12**, 632 (1931). See also Proc. Phys. Soc. of London **44**, 374–382 (1932).

232), viz., I wished to show that an accurate estimate of e could be made, which was *independent* of any direct estimate, but which confirmed Millikan's value.

(III) Birge's chief disagreement with my work is in his adopting as the value for e/m (1.761 ± 0.001) or $(1.759\pm0.001)\times10^7$ e.m.u., and consequently disagreeing with both Eddington's theoretical numbers 137 and 1847.6. This estimate of e/m is the *only* experimental evidence against *either* of Eddington's theories. I would point out that, though e/m has now been measured for 35 years, it is only during the last three years that any appreciable number of physicists have accepted the value Birge advocates. Moreover, I understand from Sir Arthur Eddington that the discovery of the neutron makes it seem likely that the equations used in deducing the spectroscopic estimates of e/m are in error.

(IV) In section 4 of Birge's letter he speaks of the probable error of an estimate of e that I had given as being much larger than the error he estimates. I believe Birge's estimate must be wrong, as it would make his estimate of e ten times more accurate than the data from which it is obtained.

W. N. Bond

Department of Physics,
University of Reading, England.
May 11, 1932.

The Relation of Relative Humidity to the Absorption of Supersonic Waves in Various Mixtures of CO_2.

A sputtered quartz crystal with a frequency of 4.096×10^5 vps was used as source for supersonic waves. The absorption of these waves by a column of air mixed with different percentages of CO_2 was measured with an acoustic radiometer of the torsion vane type. A constant relative humidity of 10 percent for one set of runs was maintained with P_2O_5, 15 percent relative humidity for another set was obtained using LiCl and 35 percent for the remaining runs was obtained using CrO_3 as a dryer.

Curves plotting log of deflection (log D_x) against height (x) of radiometer from crystal face were plotted from the data and values for the absorption constant (k) were obtained by taking the slope of the straight lines thus plotted.

The following values of k were taken from these curves:

	10% R.H.	15% R.H.	35% R.H.
5% CO_2	0.053	0.09	0.11
50% CO_2	0.51	0.64	0.69
95% CO_2	0.97	1.19	1.29

These values indicate that relative humidity has a very marked and important effect upon the absorption in CO_2 or in air containing large percentages of CO_2.

Henry H. Rogers

Pennsylvania State College,
May 26, 1932.

Constants of the N_2O Molecule

In a recent paper on N_2O[1] the vibration frequencies as indicated by infrared absorption bands were correlated, and the anharmonic coefficients determined, employing an equation developed by Dennison for linear triatomic molecules. It now appears that this relation is too limited in its application, and should have been written in the more general form

$$W_l = V_1\nu_1+V_2\nu_2+V_3\nu_3+x_{11}V_1^2+x_{22}V_2^2 +x_{LL}L^2+x_{33}V_3^2+x_{12}V_1V_2+x_{13}V_1V_3 +x_{23}V_2V_3+A$$

[1] Barker, Phys. Rev. **38**, 1827 (1931).

Table I.

ν observed	transition	anharmonic coef. symbol	value	ν^0	ν computed
1285.4	$(0\rightarrow1)V_1$	x_{11}	-3.3	1288.7	1285.4
2564.2	$(0\rightarrow2)V_1$				2564.2
589.0	$(0_0\rightarrow1_1)V_2$	x_{22}	-2.2	588.3	589.1
579.5	$(1_1\rightarrow2_0)V_2$	x_{LL}	$+3.0$		578.7
590.5	$(1_1\rightarrow2_2)V_2$				590.7
1167.3	$(0_0\rightarrow2_0)V_2$				1167.8
2224.1	$(0\rightarrow1)V_3$	x_{33}	-13.8	2237.9	2224.1
4420.7	$(0\rightarrow2)V_3$				4420.6

e pressing in first approximation the dependence of the vibration terms upon the various quantum numbers, A being a common constant. As a consequence it is necessary to revise the values of ν^0 and of certain of the coefficients, the results being more consistent than before. Table I supercedes parts of Tables IV and V in our report. The values of x_{13} and x_{23} remain unchanged. Those of x_{12} are somewhat modified, but as before fail to agree well among themselves.

The original report also contained a regrettable error in the value of the moment of inertia of the N_2O molecule, which should have been given as 66.0×10^{-40}.

E. F. BARKER

University of Michigan,
June 30, 1932.

Raman Effect of Methyl Acetylene

The Raman spectrum of methyl acetylene ($CH_3\cdot C\vdots CH$) has been studied and ten lines have been found as shown in Table I. A mercury light source was employed in the usual way and was used both unfiltered and with $\lambda=4358$A reduced by 2 mm of a solution of iodine in carbon tetrachloride. The photographs were taken on a Steinheil spectrograph. The expected Raman frequencies of the monosubstituted acetylene $C\vdots C\cdot$ bond (2128 cm^{-1}) and the $\vdots C\cdot H$ bond (3306 cm^{-1}) were found and are in agreement with the values of Bourguel and Daure.[1] Furthermore, lines for the aliphatic $C\cdot H$ bond (2928 cm^{-1}) and the $C\cdot C$ bond (618, 931 cm^{-1}) were found for this molecule. Some lines in Table I are not yet identified, although they also appear in other hydrocarbon molecules.[1] The ten lines mentioned are quite definite, but others are possible and it is expected to extend the work by using monochromatic excitation.

TABLE I. *Raman lines in methyl acetylene.*

Frequency cm^{-1}	Intensity	Frequency cm^{-1}	Intensity
310	weak	2871	medium
618	weak	2928	strong
931	medium	3144	medium
1384	weak	3207	weak
2128	strong	3306	weak

The methyl acetylene was made available through the kindness of Dr. G. B. Heisig of this laboratory.

GEO. GLOCKLER
H. M. DAVIS

University of Minnesota,
Minneapolis, Minn.,
July 1, 1932.

[1] Bourguel and Daure, Comptes Rendus **190,** 1298 (1930); and Bull. Soc. Chim. **47/48,** 1365 (1930).

Structure of Atomic Nuclei

For some time, there has been speculation as to whether or not the atomic nucleus can be regarded as consisting of shells of protons, just as the external structure is known to consist of shells of electrons. The writer has recently pointed out[1] that the experimental evidence seems to demand a modification of this view, in that s, p, d (etc.) shells do exist, but that a closed shell of azimuthal quantum number l consists of $2l+1$ protons and $2l+1$ neutrons. It was shown that the facts are well represented for elements of mass number (M) less than 36. It is of interest to inquire if this scheme is capable of extension to elements of higher mass number.

Detailed questions of stability must be left until later, but a qualitative analogy proves to be of help. In the outer atom, the normal state with one electron missing from a closed shell is of the same symmetry character as the normal state with just one electron in the closed shell. In the p shell, for instance, the ground states are ^2P, ^3P, ^4S, ^3P, and ^2P. There is symmetry about the middle element, which corresponds to a half-completed shell. If we make the hypothesis that such a symmetry exists for nuclei, then it is to be expected that this symmetry will be of a two-dimensional character, when the number of neutrons is plotted against the number of protons (or better, when the excess of neutrons over protons is plotted against the number of protons). For the s shell, H^3 is missing, and one cannot say very much about the symmetry. For the p and d shells, symmetries of an elementary type exist. The f shell, corresponding to the mass range 37 to 64, shows some symmetry, but so many points are missing that it is difficult to decide on the location of the center of symmetry. Either $M=50$ or $M=52$ will serve the purpose, the excess of neutrons over protons being four. The g shell corresponds

[1] J. H. Bartlett Jr., Nature (in press).

to a mass range 65 to 100 and should be symmetrical about the point of mass 82. Similarly, the h shell should be symmetrical about the point $M=122$. Barton[2] has called attention to the fact that two "clusters" of nuclei having two-dimensional symmetry do exist, the centers of symmetry being at $M=84$ and at $M=124$, respectively. An examination of the diagram leads one to conclude that the points 82 and 122 would serve equally well. In the first case, the center of symmetry is for protonic number 36.

The above evidence seems to indicate quite clearly that, for $M<144$, the picture of closed shells of protons and neutrons is in agreement with the facts. (It may be similar for heavier elements, but the information is as yet quite insufficient). Furthermore, it seems that Russell-Saunders coupling holds, and that nuclei occupying positions symmetrical about the half-completed shells will have the same resultant orbital angular momentum, but not necessarily the same total angular momentum.

Evidently, the reason why the principal quantum number does not play an important part, if any, is that the central field is a non-Coulomb one, as in molecules. No restriction is placed on the value of the azimuthal quantum number, which may increase until centrifugal force causes disruption. For the same principal quantum number, one would expect the binding energy of the protons and electrons to be approximately constant with increasing mass. The evidence indicates this to be so.[3]

The occurrence of s, p, d (etc.) symmetry is to be expected if the equations describing the system are invariant under a rotation of axes, which is so when there is no preferred direction.

While the above model probably gives many of the essential symmetry features, there remains the problem of setting up the equations of motion in order to determine the energy levels. This may require more knowledge about the law of interaction between a proton and a neutron.

JAMES H. BARTLETT, JR.

Zürich,
July 3, 1932.

[2] H. A. Barton, Phys. Rev. **35**, 408 (1930).

[3] L. Strum, Zeits. f. Physik **50**, 555 (1928).

The Becquerel Effect as a Special Case of the Barrier-layer Photoelectric Cell

The observation of E. Becquerel,[1] that illumination of one of two identical electrodes immersed in an electrolyte develops an electromotive force, marked the inception of a continuous series of investigations on this and related phenomena. The paucity of general conclusions available from these researches however,[2] furnishes a marked contrast to the rigor and elegance which have attended the development of the "Hallwachs" effect. And it is thus fortunate that a new avenue of approach to the solution of this problem has been opened by the advent of the barrier-layer cell of Lange[3] and Schottky,[4] whose formal similarities to the Becquerel cell (e.g., the circumstance that neither requires an auxilliary e.m.f. in order to operate, and a characteristic reversal of polarity with increase of wave-length[5]) almost immediately suggested their essential identity.[6,7] It is the object of this note to adduce some quantitative evidence in support of this view, which we have accumulated in an extended investigation of the subject.

The careful studies of Schottky and his coworkers[8] have established several fundamental relationships governing the behavior of the barrier-layer cell. Among others, it was demonstrated that:

a. the short-circuit current is strictly proportional to the light intensity,

b. the short-circuit current, and not the open-cuircuit e.m.f., is fundamental, and

c. the direction of electron-flow in the cell is determined by the location of the barrier-layer ("Hinterwandeffekt or Vorderwandeffekt").

[1] E. Becquerel, Comptes Rendus **9**, 144, 561 (1893).

[2] A. L. Hughes and L. A. DuBridge, "Photoelectric Phenomena" McGraw-Hill Co., New York, 1932. pp. 5–6.

[3] B. Lange, Phys. Zeits. **31**, 139, 964 (1930).

[4] W. Schottky, Phys. Zeits. **31**, 913 (1930).

[5] A. Garrison, J. Phys. Chem. **27**, 601 (1923).

[6] E. Duhme, Zeits. f. Elektrochemie **37**, 682–4 (1931).

[7] H. Simon and R. Suhrman, "Lichtelektrische Zellen und ihre Anwendung" Julius Springer, Berlin 1932, pp. 54–55.

[8] O. v. Auwers and H. Kerschbaum, Ann. d. Physik **7**, 129 (1930).

In our experiments—of which a more complete account will be published in the near future—uniform and adherent layers of cuprous oxide were formed on copper plates of approximately 40 sq. inches area by heating to about 1000°C in an electric furnace and quenching rapidly. The reverse sides of the electrodes were covered with black lacquer, followed by an insulating and water-proof coat of paraffine. Cell elements of these dimensions enable one to draw heavy photoelectric currents for low levels of illumination, and hence to minimize polarization phenomena. In this case unfiltered radiation from a small tungsten-filament lamp at a distance of five feet produced photocurrents of the order of one-half milliampere.

For constant light intensity, additions of increasing amounts of electrolyte increased the photocurrent in accord with the expression:

$$i = i_0 R_0/(R_T + R_0)$$

where i_0 is the maximum current for a given light intensity, R_T the resistance of electrolyte plus resistance of meter and leads, and R_0 the resistance of Cu-Cu_2O electrode system (assumed approximately constant for a given light intensity).

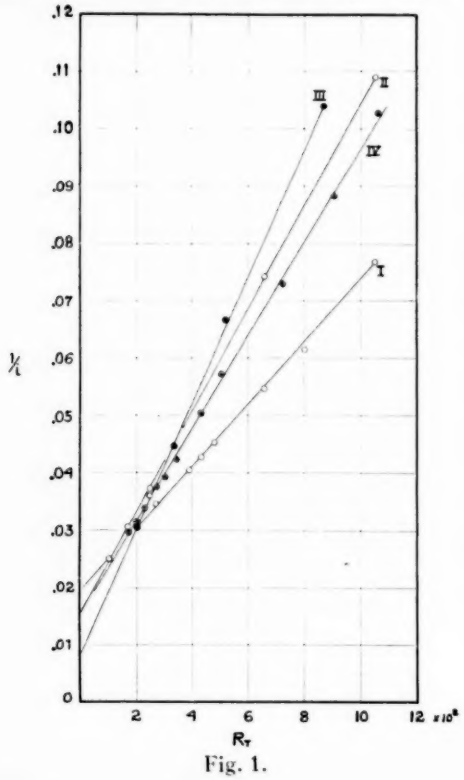

Fig. 1.

The results are exhibited in curves I, II (NaCl), and III (KCl) of Fig. 1. Since these are not superimposed it might be inferred that the electrolyte resistance is not the sole determining factor. It will be observed however that straight line functions were always obtained, although the slope and intercept varied continuously. That this must be occasioned by some secular change in the sensitive surface was demonstrated by repeating the measurements with a mixture of the two electrolytes (curve IV) a procedure which permits one to avoid the disturbing effect of progressive changes in the electrodes.

The equation predicting our results is identical with that of Auwers and Kerschbaum[8] for the network equivalent to a barrier-layer cell, save for a second term inserted by them to correct for the non-ohmic character of the internal resistance. The simplified expression, however, satisfactorily accomodates our results, and indeed, precisely accounts for the photocurrent in the barrier-layer cell as a function of external resistance, provided the resistance range is of the order encountered in the electrolytic cells.

It follows therefore that the primary function of the electrolyte is to act as conductor for the photoelectric current. That secondary chemical effects may arise is not only possible but practically inevitable. For this reason it is imperative to secure instantaneous values for the short-circuit current. Whenever such complications could be avoided the short-circuit current was found to be proportional to the light intensity. Furthermore the temperature coefficient for the Becquerel effect is accurately reproduced by combining the known thermal contributions to the barrier-layer current and the electrolyte conductivity.

If, as seems the case, the Becquerel effect arises from a Lange cell whose behavior is frequently obscured by a host of electrochemical, and possibly photochemical, complications, it seems wisest to direct more attention to the simpler phenomenon—which promises so much of practical and theoretical interest.

R. H. MÜLLER
A. SPECTOR
Washington Square College,
New York University,
July 5, 1932.

A Note on the Hyperfine Structure of Beryllium Lines

The identification of the neutron by Chadwick[1] has developed a keen interest in the value of the nuclear moment of beryllium. For this reason the beryllium lines given in Table I have been examined for structure with the aid of a Fabry-Perot interferometer. The interferometer plates were spaced 2, 3, 5, 8 and 10 mm apart. The spectrum was excited in a metal liquid air-cooled Schüler lamp so that the Doppler effect should be small.

The only line showing a definite structure was the Be II line λ4673A. $3\,^2D-4\,^2F$ transition. The wave-length separation here corresponds to a $\Delta\nu$ difference of 0.480 cm^{-1}, which is the $3\,^2D_{3/2}-3\,^2D_{5/2}$ separation.

TABLE I.

line	λ	classification	structure
Be I	8254	$2\,^1P-3\,^1S$	sharp
Be II	4673	$3\,^2D-4\,^2F$	one component at −0.105A
Be I	4572	$2\,^1P-3\,^1D$	sharp
Be II	3130	$2\,^2S-2\,^2P_{1/2,3/2}$	sharp
Be I	2348	$2\,^1S-2\,^1P$	line width about 0.030A

The term "sharp" in Table I means that no structure was found. In the case of λ3130 the two lines $^2S_{1/2}-{}^2P_{1/2}$ and $^2S_{1/2}-{}^2P_{3/2}$ are 0.648A apart and were unresolved by the prism instrument used. It was, therefore, necessary to make one line fall on the first chief maximum of the other line in the interferometer pattern so that the intervening space would be free to show any components. Even so, no components were found.

The only indication of possible structure lies in the fact that λ2348A has a line width of about 0.030A.

This negative result does not necessarily mean that $i=0$ for Be and it is hoped that an examination of the Be III and IV lines with the 21 ft. grazing incidence vacuum spectrograph which is now being set up in this laboratory will show a beryllium structure comparable with that of lithium.

P. GERALD KRUGER
R. C. WAGNER
Department of Physics,
University of Illinois,
July 5, 1932.

[1] T. Chadwick, Nature **129,** 312 (1932).

Newton's Rings in Transparent Metallic Films

In attempting to produce a film of manganese on glass by cathodic sputtering from a piece of pure manganese only 2.5×1.5 cm in area, a series of colored fringes were observed in the film by reflected light. These fringes are undoubtedly similar to those observed by Bockstahler and Overbeck[1] who reported some observations on sputtered tin. In order to make a closer study of these fringes, a mica screen having a circular opening of 1.5 cm diameter, was placed about one mm in front of the manganese cathode. Due to the intense heating, a Pyrex glass plate was used to receive the film. Manganese sputters very slowly. With a current of about 10 milliamperes, hydrogen being the residual gas, some ten hours were required to produce a film in which was visible, by reflected light, a series of brilliant Newton's rings. During the period of sputtering these rings gradually increased in size, other rings forming within, until the outermost ring had a diameter of almost 5 cm. The order of colors appearing was as follows: yellow, light brown, reddish brown, purple, blue, green, and back to yellow. This seems to be about the same as that reported by Edwards[2] who made some observations on films of copper deposited on aluminum and nickel.

The glass directly underneath the center of the circular opening in the mica, was found to be free of any metallic deposit, due doubtless to the intense heating of the glass plate produced by the cathode rays. The film was thus of variable thickness, being a maximum just under the edge of the circular opening in the mica screen, and diminishing to zero both towards the center and the edges of the glass plate. Hence a cross section of the film taken across the center of the glass plate would be like a vertical cross section of a volcanic mountain, the center of the film corresponding to the crater of the volcano.

It seems quite likely that the colored fringes are due to the interference of light between the front and rear surfaces of the transparent manganese film, confirming the

[1] L. I. Bockstahler and C. J. Overbeck, Phys. Rev. **37,** 465 (1931).

view taken by Edwards.[2] These rings enable one to test this assumption, for whatever phase differences in light that might be introduced as the result of reflection and refraction at the front and rear surfaces of the film, it must be true that adjacent rings of identical color are located at points in the film differing in thickness by one half of a wave-length as measured in the metal. This serves as a step by step method for evaluating the thickness of the film at various points. Accordingly the film was illuminated normally by monochromatic light, and the positions of the various black interference rings measured by means of a short focus cathetometer. Reflection from the rear of the glass plate was eliminated by attaching a glass prism to the rear of the plate by means of cedar oil.

There is some question as to the thickness of the film at the first or outermost black ring. Allowing for the phase differences due to reflection and refraction at the surfaces of the film, the thickness of the film at this point was estimated to be not over one tenth of a wave-length. By plotting two cross sections of the film taken at right angles to each other, the mean thickness of the film was evaluated graphically. The maximum thickness of the film was found to be 8.1×10^{-5} cm.

Assuming the film as having a circular area of 2.5 cm in diameter, the weight of the film was computed by means of the expression $\pi r^2 dN\lambda/2n$, where r is the radius of the film; d, the density of manganese; n, the refractive index of manganese as obtained previously[3] for this sample forming the cathode; λ, the wave-length in air; and N the number of black fringes which serves as a measure of the mean thickness of the film. The weight of the manganese film so computed was 0.0045 gr from measurements made on the black rings as viewed in mercury green light, and 0.0042 gr as viewed in yellow sodium light. By actual weight of the glass plate before and after sputtering, the weight of the manganese film was found to be 0.0040 gr. The results are sufficiently in agreement to justify the conclusion that the phenomenon observed is one of interference.

J. B. NATHANSON
Carnegie Institute of Technology,
Pittsburgh, Pa.,
July 8, 1932.

[2] H. W. Edwards, Phys. Rev. **38,** 166 (1931).

[3] J. B. Nathanson, J. O. S. A. **20,** 593 (1930).

Total Secondary Electron Emission from Metal Faces

It is well known that in experiments relating to the emission of secondary electrons from metal faces due to an incident beam of primary electrons, the ratio R of the total secondary to the primary current increases almost linearly with the potential from about 30 volts, attains a broad maximum (almost similar to a saturation effect) at some potential and then decreases slowly and linearly as the applied potential is increased. The energy at which the maximum occurs depends on the nature of the target and also for any particular metal, on the nature of the crystal face bombarded.[1,2] The reason why the secondary electron curve bends round and decreases at higher potentials has so far been obscure.

Copeland[3] has recently made the interesting suggestion that if the rate of fall of R with potential be divided by the actual value of R in the region, the ratio for various metals gives a fairly linear graph when plotted against the densities of the targets. The aim of this note is to draw attention to the further interesting observation that this ratio for any particular metal probably depends also on the grating constant of the crystal face presented for bombardment. Experiments on polycrystalline nickel targets[1] and on the 100[2] and 110 faces of large nickel single crystals, conducted by the writer in Prof. O. W. Richardson's laboratories in King's College, London, show that the ratio dR/RdV varies almost linearly with the grating constants of the faces.

These observations suggest that the decrease of R at higher potentials is probably due to the absorption of the primary electrons and to a much larger extent of the secondary electrons. As the potential is increased, the depth of penetration of the primary electrons within the metal increases and as a result, there is much greater absorption of the slower

[1] S. R. Rao, Proc. Roy. Soc. **A128,** 41 (1930).

[2] S. R. Rao, Proc. Roy. Soc. **A128,** 57 (1930).

[3] P. L. Copeland, Phys. Rev. **40,** 122 (1932).

secondary electrons. This absorption can itself account for the decrease in the value of R under consideration. It is also instructive to find out the variation of the ratio dR/RdV with the atomic number instead of with the density. The kind of absorption in this case may be due to the collisions of the outgoing secondary electrons with the bound orbital electrons within the atoms, while that part of the absorption depending on the grating constant may be due to the collisions of the secondary electrons with the free or valency or structure electrons.[4] The grating constant may be taken as a measure of the probability of the collisions of the secondary electrons with those mentioned above. The experiments of Davisson and Kunsman and later of Davisson and Germer[5] suggest that the largest secondary emission is in the direction of the primary beam when the incidence is normal.

These considerations indicate that the decrease of R at higher potentials is mainly due to the absorption of the secondary electrons due to their collisions with the bound or partly bound or free electrons. The efficiency of production of the secondary electrons would therefore be a constant after a certain potential is reached (this potential depending on the nature of the metal and the crystal surface) if there were no absorption of the secondary electrons.

The results mentioned above derive additional support from the fact that adsorption of gases by the crystal surface increases the ratio $dR/R\,dV$ considerably. This was found to be the case with the 110 face of a nickel crystal.

Also careful experiments by Nakaya[6] show that a similar saturation effect exists in the photoelectric efficiency curves for soft x-rays at voltages in the neighborhood of 3000 volts for ordinary metals. It is highly probable that if the potentials are carried much higher, these curves may also show a similar fall in value due to the absorption of the photoelectrons in the medium of the photoelectric target.

More accurate work on the secondary electron emission from different metals and crystal faces is necessary to settle these interesting questions.

S. Ramachandra Rao

Annamalai University,
Annamalainagar, S. India,
June 8, 1932.

[4] O. W. Richardson, Proc. Roy. Soc. **A128,** 63 (1930).

[5] C. J. Davisson and L. H. Germer, Phys. Rev. **30,** 705 (1927).

[6] U. Nakaya, Proc. Roy. Soc. **A124,** 616 (1929).

A Theory of the Ozone of the Lower Atmosphere and Its Relation to the General Problem of Atmospheric Ozone

The observed failure of radiation in the region 2200–2000A to penetrate the earth's atmosphere has made it of considerable interest to identify the substances which are responsible for the stopping of this radiation lying between the ultraviolet absorption of ozone and that of oxygen. The absorption of light by the molecule O_4[1] in the earth's atmosphere can account for the removal of the greater part of this radiation. That this is the case may be shown in an approximate way by using the absorption coefficient of O_4 and its dissociation constant computed in Ref. 1, and an oxygen distribution in the atmosphere given over the heights 0 to 11 km by the expression $n=5.38\times10^{18}\ e^{-1.12\times10^{-6}z}$ molecules /cc, and above 11 km by the expression $n=1.57\times10^{18}\ e^{-1.73\times10^{-6}z}$ molecules/cc, where z, the height, is in centimeters, this distribution resembling closely that given in Table 2, p. 393, Vol. I, International Critical Tables. These quantities lead to an intensity at the earth's surface of a little less than 1 percent of the initial intensity outside the atmosphere. The absorption will, however, be greater than this, for it was shown by Warburg,[2] on whose experimental work rests the quantitative measurement of the absorption, that in air this unusual oxygen absorption was greater for the same amount of oxygen than in pure oxygen. This was briefly discussed in Ref. 1. The use of Warburg's data on air leads, in much the same way as was done for pure oxygen in Ref. 1, to an equilibrium constant of approximately $K_p=0.6$ gm/cc for the dissociation of O_4, if the molecular absorption coefficient is

[1] Wulf, Jour. Am. Chem. Soc. **50,** 2596 (1928); Proc. Nat. Acad. Sci. **14,** 609 (1928).

[2] Warburg, Berl. Ber., p. 230, 1915.

taken to be unchanged. The atmosphere is approximately a 79% N_2 and 21% O_2 mixture over the altitudes of appreciable O_4 absorption. Carrying out the same calculations as mentioned above, with the same distribution of oxygen but with this O_4 dissociation constant appropriate to air, one finds that radiation in the vicinity of 2100A will be reduced to roughly 10^{-5} of its original value. At a height of 4 km the intensity proves to be a few percent of the original, this being mentioned here because experiment has shown that no detectable radiation of these wavelengths occurs even at this height.[3] Qualitatively these calculations do not, of course, depend upon the interpretation of this absorption as being due to the molecule O_4, it being sufficient that there is this density-dependent absorption in oxygen, that is, this absorption which does not follow Beer's Law. The above is not intended to imply that O_4 is the only absorbing substance, but simply that its absorption cannot be entirely neglected. Ozone and the molecule O_2 undoubtedly also absorb weakly in this region.

At the same time this absorption accounts, at least in part, for the ozone in the lower atmosphere recently measured by Götz and Ladenburg.[4] For the absorption of this radiation leads to photochemical ozone formation as also has been shown by Warburg.[5] This ozone formation from O_4 occurs chiefly in the troposphere, because the greater part of the absorption lies in these relatively low altitudes. This ozone is in a singular position photochemically, being protected from radiation most active in its decomposition by the ozone formed at higher altitudes from O_2. In view of the observation that no detectable radiation in the region 2200–2000A reaches even a height of 4 km, the photochemical formation of this ozone of O_4 origin apparently occurs for the most part at moderate heights. No inconsistency enters here with the observations on the ozone content of the atmosphere close to the earth, however, since the troposphere is a stirred atmosphere, convection distributing the ozone more or less uniformly throughout it. The formation of ozone from O_4 depends evidently upon atmospheric density, not merely upon the total oxygen in the path, and hence will be related to latitude and weather conditions. The above considerations are obviously related to the general problem of atmospheric ozone, especially to its distribution, though further work is required to determine the quantitative importance of these relations.

OLIVER R. WULF
Bureau of Chemistry and Soils,
U. S. Department of Agriculture,
Washington, D. C.,
July 14, 1932.

[3] Lambert, Dĕjardin and Chalonge, Compt. Rend. **177,** 757 (1923).

[4] Götz and Ladenburg, Die Naturwissenschaften **19,** 373 (1931); see also Fabry and Buisson, Comp. Rend. **192,** 457 (1931).

[5] Warburg, Berl. Ber. p. 746; 1911, p. 216; 1912, p. 872; 1914; Z. Elektrochem. **26,** 54 (1920); **27,** 133 (1921).

The Raman Spectra of Two Liquid Phases of Nitrobenzene

M. Wolfke and J. Mazur have found an irregularity in the heating curve[1] and also abrupt temperature variation of the dielectric constant and density[2,3] of mononitrobenzene, at a temperature of 9.5°C, i.e., slightly above the freezing point. Their results seem to imply a definite intra-molecular energy change in the liquid state at 9.5°, and, therefore, presumably the Raman spectrum should be modified at that transition temperature. An attempt was made to find such a modification, but exposures taken above and below 9.5° failed to show any evidence of one.

Three types of modification of the Raman spectrum were looked for: (1) shift of one or more of the lines, (2) intensity changes, (3) disappearance of one or more of the lines in one or the other phase.

Shifts of the order of 0.2A could have been observed in the region of the Raman lines but no shift of any line was found.

At the lower temperatures, a marked increase in the intensity of all the lines in the blue end of the spectrum was observed but, by several other experiments, this was found to be due to a large but continuous change in the absorption coefficient of nitrobenzene with temperature.

Exposures up to one and a half hours were taken at 6.0°C and room temperature but

[1] M. Wolfke and J. Mazur, Nature **127,** 741 (1931).

[2] J. Mazur, Nature **126,** 993 (1930).

[3] J. Mazur, Nature **127,** 893 (1931).

these plates show no line appearing at one temperature and not at the other. No longer comparison exposures were made since a fourteen hour exposure at room temperature brought out only one line that the one and one half hour exposure did not show.

Our plates show a number of lines which Kohlrausch does not report[4] for nitrobenzene, but, pending further study, we cannot say whether these lines belong to nitrobenzene, nitrothiophene (which may have been present at least as a trace), or some other impurity. These unidentified lines occur at wave-number separations approximately equal to: 675, 1025, 1080, 1175, 1385, 1415, 1755, 1805, 2450, 2690, and 2830 cm^{-1}.

The sample used was C. P. mono-nitrobenzene which had been washed first with dilute Na_2CO_3 and then many times with distilled water, dried a week or more over $CaCl_2$, and triply distilled under about 1 mm of Hg pressure. The original sample had shown the presence of a trace of nitrothiophene and it may be that the distillation did not completely remove this impurity.

The spectra were taken with a Hilger constant deviation spectrograph with dispersion of about 20A/mm at 4358A. The General Electric Company Raman Outfit was used for irradiating the sample, with a 220 volt hot cathode mercury arc along one focus of the elliptical reflector and the sample tube along the other focus. Highly distilled nitrobenzene has still a slight yellow color and absorbs strongly the exciting radiation we used (4358A). Therefore the sample tube was made conical, and of such a taper as to just fill the spectrograph aperture. This arrangement greatly increased the intensity of the Raman spectrum. A glass walled cooling system was placed in contact with the whole length of the sample tube. In a final 18 hour exposure at room temperature, the cooling system contained distilled water with enough potassium chromate to absorb completely the 3650, 4046 and 4078 lines. The sample itself aided in this complete absorption. All of the lines on the final plate must have been excited by the 4358 line and its two companions or have been anti-Stokes lines due to 4916 line or those of longer wave-lengths. Computations, however, proved that none of the lines was an anti-Stokes term.

Eastman 40 and Ilford Golden Iso Zenith (H and D 700 and 1400) plates were tried but the Eastman 40 plates were selected because much less trouble was had from fogging during development with this type. The slightest fog covered up many weak lines.

A. M. THORNE
P. L. BAYLEY

Lehigh University,
Bethlehem, Pa.,
July 14, 1932.

[4] K. W. F. Kohlrausch, Der Smekal-Raman Effect. Julius Springer, Berlin, 1931.

A New Band System of Barium Hydride in the Infrared

With the aid of the new Eastman Infrared Sensitive plates the writer has discovered an intense band system of BaH in the infrared with principal heads at about 9020A and 10,000A, degraded to the red. The experimental conditions were identical with those used by Fredrickson and Watson[1] in photographing the $^2\Pi \rightarrow {}^2\Sigma$ BaH bands in the visible red region. The bands in the infrared are also $^2\Pi \rightarrow {}^2\Sigma$, the two systems having a common final $^2\Sigma$ state, but with considerably different spin multiplet spacing in the $^2\Pi$ states. For the spacing between the two groups of branches in the infrared band is about 1000 cm^{-1}, whereas $A = 462$ for the red system previously investigated.

The shorter wave-length group of branches from 8920A to about 9250A has been photographed at high dispersion with good intensity using the Infrared Sensitive plates A, but with the new Eastman Infrared Sensitive plates B only the strongest lines of the branches beyond 10,000A have been registered even with long exposure.

This is the first instance among the diatomic hydride molecules for the alkaline earths of a second $^2\Pi$ state, and the nearness of these two $^2\Pi$ levels in BaH is undoubtedly to be correlated with the fact that only for Ba is the ^3D level found below ^3P. But $A = 832$ for the lowest ^3P levels of the Ba atom, and so no definite assignment of either of the observed $^2\Pi$ levels of BaH to the ^3P level of Ba seems possible. Rather, as now seems even more evident,[1] these molecular levels must come from a forcing together of the ^3P and ^3D levels of the Ba atom. This point will be discussed and the data on this infrared BaH system presented in a later communication.

WILLIAM W. WATSON

Sloane Physics Laboratory,
Yale University,
July 15, 1932.

[1] W. R. Fredrickson and W. W. Watson, Phys. Rev. **39**, 753 (1932).

Zeeman Effect and Perturbations in the CO Angstrom and the N_2^+ Bands

Rosenthal and Jenkins[1] have described an interesting example of multiple perturbations in the $^1\Sigma \rightarrow {}^1\Pi$ Angstrom CO bands, particularly in the (0, 0) band at 4511A, for which they give the undoubtedly correct quantum analysis. Spectrograms recently taken by the writer show additional faint lines which extend their "resonance" curves at several of the perturbations and which emphasize the occurrence of two lines for each J value around the perturbation points. The correctness of the quantum assignments of all these lines is attested by the $\Delta_2 F'(J)$ combination relations and by the Zeeman effect observed in the present investigation. The existence of large, irregular Zeeman effects for certain lines was first noted by Crawford[2] in his work on the regular Zeeman effect in these CO bands.

As pointed out by Rosenthal and Jenkins, the fact that these perturbations are multiple would indicate that the perturbing state is not a singlet state, and the different types of Zeeman effects observed at the several perturbations bear this out. In general, the greater the displacement of the perturbed line the larger its Zeeman effect, and the effects increase rapidly with increasing field strength. The regular Zeeman effect for lines with these intermediate and high J values for this type of electronic transition is so small as to leave the unperturbed lines totally unaffected by the magnetic field. At the first perturbation point, however, the line $P_b(8)$ for example is symmetrically broadened at low field strengths and becomes a wide asymmetrical doublet with broad components at high field strengths (30,000 gauss). The effect of the field on the Q branch lines around $J=12$ is just to increase the magnitude of the perturbation, the shift of $Q_a(14)$ at $H=26{,}000$ gauss being $+0.96$ cm^{-1}, while that of $Q_b(11)$ on the other branch of the "resonance" curve is -0.55 cm^{-1}. Those Q lines having the maximum perturbation are shifted the most, but the field lines are quite sharp, there being no indication of any shading towards the no-field position. The lines $P_a(16)$ and $R_b(16)$ near the maximum of the next perturbation, on the other hand, are merely much broadened by the magnetic field at all field strengths, the uniform broad block of radiation being not quite symmetrical about the no-field line. Some of the P, R and Q lines at the perturbation around $J=28$ in the (0, 1) band as well as in this (0, 0) band become very sharp doublets, with the two components of different intensity, for the line on the one side of the perturbation point, while a line on the other side of the perturbation is uniformly broadened.

These differences in Zeeman pattern indicate that the state perturbing this $^1\Pi$ state is multiple, in violation of one of Kronig's rules that the two perturbing states must have the same multiplicity. However, this rule need not be expected to hold strictly here, for singlet-triplet combinations do occur in CO. The $d(^3\Pi?)$ level which lies just 0.09 volts below this $^1\Pi$ state may be the level whose rotational terms are responsible for these perturbations. The differences in the spread of the magnetic sublevels in the three spin components, together with the rule that only levels of the same M value perturb each other, could account for the variations in field patterns observed for these perturbed lines. An analysis of the Merton-Johnson triplet bands in the red which arise from this d level should be made to find these corresponding perturbations.

The N_2^+ bands which are a $^2\Sigma \rightarrow {}^2\Sigma$ transition are present on some of the writer's CO spectrograms. A perturbation similar to those in the $^2\Sigma \rightarrow {}^2\Sigma$ CN tail bands occurs in this system[3] in all bands with $v'=1$ for $J=13\frac{1}{2}$. All of the lines except those displaced near the center of the perturbations are insensitive to the magnetic field, whereas these perturbed lines are either shifted or become rather sharp doublets. A more detailed description of these peculiar Zeeman effects in both of these band systems, together with the possible explanations, will be submitted in the near future for publication in this journal.

WILLIAM W. WATSON

Sloane Physics Laboratory,
Yale University,
July 15, 1932.

[1] J. E. Rosenthal and F. A. Jenkins, Proc. Nat. Acad. Sci. **15**, 896 (1929).

[2] F. H. Crawford, Phys. Rev. **33**, 341 (1929).

[3] M. Fassbender, Zeits. f. Physik **30**, 73 (1924).

The Rôle of Gas Adsorption in Counting Chambers*

Recently in Naturwissenschaften (vol. **20,** p. 315), W. Schulze briefly outlines experiments with Geiger-Müller tube counters which indicate, according to his interpretation, that gas adsorption on metallic surfaces can have no influence on the abruptness of the interruption of the current pulse when these devices are functioning properly as counters. He is probably correct in assuming that both point counters and tube counters are dependent upon the same fundamental physical conditions, in spite of marked differences in behavior. However, the mere fact that widely different electrode treatments, in the case of tube counters, yield no noticeably different operating conditions, does not in itself justify the conclusion that gas adsorption plays no role in the operation of the counter. It is a well established fact that the surface of the point electrode in the point counter does require special and careful preparation, especially when operated at or near atmospheric pressure. It is also true that the inner surface of the tube counter can be given such treatment that it will fail to function as a counter at any pressure whatever. It is difficult to reconcile these facts with the view put forth in Schulze's communication mentioned. The adsorption of gas by solid surfaces is one of the most common occurrences with which we have to deal since gases are adsorbed under a great variety of conditions. Moreover, when, as is usual, the tube is the negative electrode, the arrangement is such that intense electric fields do not exist near the inner surface of the tube and it is not to be expected that the surface conditions would be as important as in the case of the point counter used with the point as the negative electrode.

I should like to point out that it seems questionable to try to draw any general conclusions regarding the principles underlying the operation of counters from observations only in hydrogen at reduced pressures as Schulze has done. For under such conditions adsorption of gas undoubtedly does occur and it would appear very difficult to prepare any kind of electrode surface which would not have its properties modified by such adsorption. As clearly demonstrated with a point counter, the effects of such adsorption are most evident when the kind of gas in the counter is changed while it is in operation, the pressure remaining constant. When a counter with a prepared copper point is counting with hydrogen at atmospheric pressure slowly streaming through it, the introduction of a few percent of CO into the flowing hydrogen immediately causes the counter to cease functioning. This is very difficult to explain on any basis of an effect existing only in the gas discharge in the counter but its explanation becomes relatively simple when the adsorption properties of CO on "catalytic" copper are considered.

L. F. Curtiss

National Bureau of Standards,
Washington, D. C.
July 15 1932.

* Publication Approved by the Director of the Bureau of Standards of the U. S. Department of Commerce.

BOOK REVIEWS

Graphische Darstellung in Wissenschaft und Technik, M. PIRANI. Pp. 149, figs. 71. Walter de Gruyter and Co., Berlin, 1931. Price RM 1.80.

This little booklet of the Sammlung Göschen is well up to the standard set for the series. It provides a self contained, easily understood, concise and trustworthy treatment of the matter chosen for consideration. The selection of material is good. Chapter 1, 31 pages, is an elementary and detailed discussion of the principles and methods involved in presenting graphically the information contained in a table of two variables. It is excellent reading for freshmen technical students. Chapter 2, 36 pages, presents various methods for exhibiting graphically the relationship between two variables connected by a known equation. Thus the method of reducing the graph to a straight line by constructing suitable rectangular scales is given, and with this a neat and useful central projection method of constructing scales for the linear fractional transformation. Chapter 3, 67 pages, discusses graphical representations of equations of three variables, the topographical method followed by a concise and excellent treatment of the construction of alignment charts. Throughout the text specific references to more extended treatments are made and an appendix contains a bibliography and a table of functional relationships with related suggestions as to suitable choices of graphical methods.

HENRY E. HARTIG
University of Minnesota

Vector Analysis, with Applications to Physics. RICHARD GANS. Translated from the sixth German edition by Winifred M. Deans. Pp. 163. Blackie and Son.

This is a concise and very clear introductory account of vector analysis, and of its applications to mechanics, hydrodynamics, electrodynamics, and optics, including crystal optics. Some 45 exercises are given, and the methods of solution of these are collected at the end of the book.

The treatment brings out very forcibly not only the fact that one of the reasons for the usefulness of vectorial methods in stating and solving a large class of physical problems lies in the conciseness of the notation, but also, and in the reviewer's opinion this is far more important, that vector methods allow the writing of various physical relationships in a manner which exhibits the physical content of these relationships in a most natural and lucid way.

Tensors are introduced by means of linear vector functions. The treatment is very understandable.

Incidentally, the reader must be careful to combine the remarks about vectors on page 1 with those made in Section 3 on the addition of vectors, in order to obtain a satisfactory definition of a vector.

The English translation of Professor Gans' book was made from the sixth German edition. (A Spanish translation appeared in 1926.) It should do a good service to those who wish to become acquainted with the fundamental ideas of vector analysis, and with their applications.

V. ROJANSKY
National Research Fellow
Princeton University

Ergebnisse der Exacten Naturwissenschaften, P. TEN BRUGGENCATE. Vol. X. Die Veränderlichen Sterne.

In this 80 page article ten Bruggencate gives a very useful, critical compilation of the principal contemporary knowledge of variable stars. After a brief introduction and description of a system of classification, the lion's share of the space—65 pages—is taken up by a detailed study of the cepheids and the long-period variables, both of which groups are treated ex-

haustively, especially from the more physical aspects of astronomy. Furthermore a large amount of detailed information concerning individual stars and light curves is added and discussed, which discussion becomes enhanced because of the author's extensive experience in this aspect of variable star work. Contrasted to this the treatment of the semi-regular and irregular variables appears somewhat summary, and not in proportion to their importance. As another slight criticism may be offered that no historical introduction precedes, but that the subject is considered to have begun around 1850.

W. J. LUYTEN
University of Minnesota

Interferometer Methods in Astronomy. F. G. PEASE. Vol. X.

The pamphlet begins with a short historical summary of the early attempts to apply the interferometer to astronomical measurements, then reviews Michelson's work in adapting the interferometer to the 100 inch reflector. A table is given with the measured diameters of seven stars, thus condensing into such a modest space what might well be called the most phenomenal astronomical observations of the century. A detailed description of the new and more powerful 50 foot interferometer recently constructed at Mt. Wilson, forms the closing paragraphs. The only criticism that might be offered is that instead of attributing the first calculations of stellar diameters to Eddington and Russell, Hertzsprung should have been mentioned, who predicted the diameter of Arcturus in 1905, many years before the rest of the astronomical world had become conscious of the existence of giant stars.

W. J. LUYTEN
University of Minnesota

Die dynamische Theorie der Roentgenstrahlinterferenzen in neuer Form. M. v. LAUE. Sonderabdruck aus Vol. X der Ergebnisse der exakten Naturwissenschaften, Pp. 25. Julius Springer, Berlin, 1931.

This reprint deals with a simplified presentation of the dynamic theory of x-ray interference, which is, as the author states, "one of the master works of mathematical physics of all time." However, it is incorrect to refer to this theory as Ewald's, for the results were derived several years earlier by C. G. Darwin. Darwin's work is not even mentioned in this paper. The theory as worked over by Laue presents a considerable simplification over Ewald's treatment. Nevertheless it is assumed that the reader is familiar with the wave-kinematical theory of the Laue interference as developed with the aid of the reciprocal lattice. Of course, this is usually the case. The effectiveness of the presentation is considerably marred by the several misprints in the final results.

JOSEPH VALASEK
University of Minnesota

Kerr-Effekt, Lichtzerstreuung und Molekülbau. H. A. STUART.

This is a chapter of 48 pages from Vol. X of "Ergebnisse der Exakten Naturwissenschaften." Particular attention is given to the calculation of the three principal polarizabilities of a molecule from combination of measurements on the Kerr effect and on the depolarization of light. Information obtained in this way forms an interesting supplement to the more familiar determination of dipole moments from dielectric constants. Dr. Stuart has done considerable original experimental work on depolarization and on the Kerr effect, including the difficult measurements of the latter in gases. Consequently one has the assurance that the chapter is written by an author thoroughly conversant with the field. The article properly stresses the fact that the depolarization is often difficult to measure with precision. In particular, the depolarization found by Strutt in helium seems to be in flat contradiction with quantum theory, unless imputed to experimental error.

J. H. VAN VLECK
University of Wisconsin

Die Lichtausbeute bei Stossanregung. W. HANLE AND K. LARCHÉ. Pp. 285–324, figs. 16. Ergebnisse Der Exakten Naturwissenschaften, Herausgegeben von der Schriftleitung Der "Naturwissenschaften" Vol. X Verlag von Julius Springer, Berlin, 1931.

Numerous investigators have been interested in the various processes responsible for the light emitted in a gaseous discharge. This article is a review of the literature pertaining to these processes, in particular to the intensity relations between lines and the probability of excitation of certain lines by collisions between electrons and atoms as a function of the speed of the electrons. The authors have prepared graphs of the *excitation functions* of many of the lines in the arc and spark spectra of Hg, Cd, Zn, He, and Ne, from experimental data. The positions of the maxima of the excitation functions are also given in tabular form. A brief resume of the theory of excitation by electron impact in included in the discussion.

The remainder of the article is concerned with the light yield resulting from collisions between ions and atoms, *collisions of the second kind*, and from the bombardment of solids with mass particles.

P. T. SMITH
University of Minnesota

Zur Quantenmechanik der Multipolstrahlung (Dissertation, University of Utrecht), H. C. BRINKMAN. Pp. 60. Noordhoff N. V., Groningen, 1932.

This work is divided into three chapters, of which only the last is accurately described by the title. The first chapter contains an excellent exposition of the powerful symbolic method developed by Weyl and Kramers for handling problems involving angular momentum; the second is a discussion of the classical electromagnetic radiation from a system of electrons, and its resolutions into *multipole radiations* of different orders.

The mathematical physicist will undoubtedly find the first chapter of greatest interest. Dr. Brinkman's exposition of the symbolic method of evaluating matrix elements is concise and comprehensive. The principal feature of this method is the representation of a wave function ψ_{nlm} as a symbolic product, $\xi^{l+m}\eta^{l-m}$, the factors ξ and η being treated as complex numbers and called the components of a spin vector. The coordinates, and in general the components of any vector or vector operator, are represented symbolically as

$$x = (\xi^2-\eta^2)/2,$$
$$y = (\xi^2+\eta^2)/2i,$$
$$z = -\xi\eta.$$

This notation may be heuristically derived from the fact that in certain cases the $=$ is an actual numerical equality. Its deeper significance originates in the theory of invariance under the rotation group.

The procedure is to make the required matrix elements appear as the coefficients of an invariant homogeneous polynomial in the components of one or more spin-vectors (ξ, η). Such polynomials form a very restricted class; in the case of a single vector they all have the form $c(|\xi|^2+|\eta|^2)^{2l}$. The coefficients of the polynomial are at first unknown, but simple considerations always suffice to identify it with an invariant whose coefficients are easily calculated by purely algebraic means. As only the ratios of the coefficients of an invariant are fixed, only the ratios of the matrix elements are determined in this way.

Chapter II deals with classical electromagnetic radiation, the treatment being based on the Hertzian vector. The expansion of the field in a series of spherical harmonics is discussed in a detailed manner. The terms of this series are classified as electric dipole, electric quadrupole, magnetic dipole, and in general, multipole radiation. The contribution of the magnetic properties of the electron to the magnetic dipole radiation is discussed briefly, but it is pointed out that contributions to the higher orders of radiation are also to be expected.

The last chapter is concerned with the reinterpretation of the results of Chapter II by the correspondence principle and the calculation of the matrix elements by means of the methods developed in Chapter I. From the nature of these methods, it follows that no calculations of

the absolute probability of a *forbidden* transition are attempted. The goal is a generalization of the Goudsmit-Kronig-Hönl relative intensity formulae, selection principles included.

The final results may be listed as: (1) The selection principles and intensity rules for the multipole radiation of any order emitted by an atom with Russell-Saunders coupling. (The Kronig-Hönl formulae are special cases.) (2) The Rubinowicz formulae for the relative intensties of the Zeeman components of quadrupole radiation. (3) Formulae for the relative intensities of the Zeeman components of magnetic dipole radiation, taking the magnetic moment of the electron into account.

CARL ECKART
Palo Alto

PROCEEDINGS
OF THE
AMERICAN PHYSICAL SOCIETY

MINUTES OF THE NEW HAVEN MEETING, JUNE 23–25, 1932

The 179th meeting of the American Physical Society was held in New Haven, Connecticut on Thursday, Friday and Saturday, June 23, 24 and 25, 1932, upon invitation from Yale University. The registration for the meeting numbered 194. The scientific sessions were held in the Sloane Physics Laboratory and in the Osborn Zoological Laboratory. The presiding officers were W. F. G. Swann, President of the Society, Paul D. Foote, Vice-president, Karl K. Darrow, Bergen Davis, Herbert E. Ives, George B. Pegram and S. R. Williams.

Thursday morning was taken up with four parallel sessions of contributed papers, abstracts of which appear in these Proceedings. Thursday afternoon there were two informal conferences, one on Definitions and Units presided over by Leigh Page, and one on The Atomic Nucleus presided over by Henry A. Barton.

Friday morning was devoted to a symposium of four invited papers on "X-rays," abstracts of which are included in these Proceedings.

Saturday morning was given over to a joint session with the Applied Mechanics Division of the American Society of Mechanical Engineers which was meeting at Yale during the same three days. This joint meeting was a symposium on "Plasticity." Abstracts of the papers appear in these Proceedings.

The local committee provided very complete arrangements for the comfort, entertainment and enjoyment of the visitors throughout the meeting. The Physical Society dinner was held at the New Haven Lawn Club on Thursday evening with 145 guests present. There were no after dinner speakers and the dinner was followed by a complimentary presentation at the University Theatre of A. A. Milne's "The Perfect Alibi" by the Yale Dramatic Association. This was thoroughly enjoyed by every one.

On Friday afternoon the members were taken to a picnic at Double Beach, a delightful place on the shore where there were sea bathing, sports and dinner. Some members, who did not attend the picnic, went to the Boat Race at New London. Throughout the three days there were special teas, trips through the museums and the Sterling Library and sightseeing trips through the city provided for the visiting ladies and any others who wished to take advantage of them.

On Saturday afternoon there was a short meeting of the Physical Society at which President Swann and others discussed for the information of the membership some of the problems relating to publications and finance to which the Council has been giving much attention.

At the close of the joint session of the two societies on Saturday morning there was a unanimous rising vote of thanks given to Yale University and the local committee and to the Yale Dramatic Association for the splendid arrangements and entertainment provided for the visiting Societies during the three days of their meetings in New Haven.

Meeting of the Council. At its meeting on Friday, June 24, 1932, the Council elected one person to fellowship. Fourteen candidates were elected to membership. *Elected to fellowship:* Harold Pender. *Elected to membership:* H. E. Banta, John E. Davis, Georges Dejardin, G. W. Heitkamp, G. B. Kistiakowsky, Shoji Makishima, Ralph E. Nusbaum, Walter J. Osterhoudt, Tokutaro Sawai, Walter Soller, S. R. Toh, C. M. Van Atta, Juanita Witters and Stephen A. Zieman.

The regular scientific program of the Society consisted of forty-three contributed and seven invited papers. Numbers 7, 8, 9, 10, 21, 23, 33 and 39 were read by title. Number 12 was withdrawn at the request of the author and therefore the abstract does not appear in the Proceedings. The abstracts of the papers are given in the following pages. An *Author Index* will be found at the end.

W. L. SEVERINGHAUS, SECRETARY

1. Theory of variation of paramagnetic anisotropy among different salts of the iron group. J. H. VAN VLECK, *University of Wisconsin.*—Experimentalists find that nickel salts are magnetically isotropic to about one percent, but that those of cobalt have anisotropy amounting to around 30 percent. A theoretical explanation is given for this difference, which at first sight is puzzling because both the Ni^{++} and Co^{++} ions have F ground terms (respectively $d^8\ ^3F$ and $d^7\ ^4F$). Suppose the crystalline potential of the form $Ax^2+By^2-(A+B)z^2+D(x^4+y^4+z^4)+f(r)$ where the rhombic or second order terms are small compared to the "cubic" or fourth order ones, as indicated by the recent investigations of Jordahl, Penney, and Schlapp (Phys. Rev. May 15, (1932)). Then by joint adaptation of the Bethe group theory of crystal Stark effect and the Goudsmit-Slater method of diagonal sums it is shown that the energy diagram connected with the splitting in the crystal field is inverted for Co^{++} as compared to Ni^{++}, so that a state which is nearly isotropic magnetically is the ground state for Ni^{++}, whereas an anisotropic one is the normal level for Co^{++}. The inversion phenomena are also discussed in connection with other ions of the iron group in which it appears. The nearly perfect isotropy of manganous salts is trivial, as Mn^{++} is in an S state.

2. Monocrystal Barkhausen effects in rotating fields. F. J. BECK AND L. W. MCKEEHAN, *Yale University.*—The directions of Barkhausen effects in a single crystal disk of silicon steel, held stationary in a magnetic field rotating slowly in the plane of the disk, have been determined. Search coils at right angles picked up impulses proportional to selected rectangular components of the changes in magnetization. Measurements on an oscillographic record were made at two values of induction: 1480 and 645. Values of the angle Φ between the change in magnetization ΔI and the corresponding variation in the applied field, $(d\boldsymbol{H}/dt)\Delta t$ are determined for various positions of the applied field relative to the crystallographic axes. The normal to the disk made angles of 30°, 60°, 90° with these axes. For these low values of induction the effects are mainly transverse and are more nearly transverse for the greater value of induction. The average value of Φ is about 20° (ΔI lagging) for the lower value of B and is less than 5° for the higher value. Individual values of Φ for one setting differ by as much as 30°. The average magnetization apparently lags the applied field and makes a small angle with it. The direction and frequency of effects seemed unaffected by changing the direction of $\boldsymbol{H}$ in the plane of the disk.

3. Mechanical hardness influenced by magnetism. S. R. WILLIAMS, *Amherst College, Amherst, Mass.*—About a year ago, Herbert published a most interesting article on "magnetic hardening of metals," (American Machinist **74,** 967, 1931). Not only did he find that rotating a ferromagnetic substance in a magnetic field changes the hardness but that the same thing occurred for substances which are not ferromagnetic. This work of Herbert's confirms some observations on steel rods, made by the writer in 1924, (Williams, Trans. A. S. S. T., p. 362, 1924). The work of 1924 has been repeated and confirmed on a series of high carbon steel rods of different drawing temperatures. The study has been extended to a series of steel rods of different carbon content and hardness. The effect seems to be very clearly shown. Magnetostrictive effects have been the means for studying the changes in hardness due to magnetic fields.

4. The dielectric constant of liquid sulphur. H. J. CURTIS, *Yale University.*—The dielectric constant and power factor of liquid sulphur was measured by a bridge method at four different audiofrequencies and over the temperature range 118°C to 350°C. The dielectric constant was found to be independent of frequency and equal to 3.520 ± 0.010 at 118°C. The specific polarization is independent of temperature between 118°C and 158°C and equal to 0.2528 ± 0.0008 cm^3g^{-1}. Above 158°C the polarization decreases directly as the reciprocal of the absolute temperature, showing that molecular association occurs with very strong binding forces between the molecules. This shows that liquid sulphur is definitely nonpolar. A method was developed for differentiating between that part of the power factor which is due to conductivity and that which is due to molecular friction. The former was found to be very large, especially at high temperatures, and the latter very small at all temperatures. This is a further confirmation of the fact that sulphur is nonpolar. The infrared spectrum of liquid sulphur contains definite absorption bands, which shows that its molecules are polar. It is difficult to understand this contradiction, since both measurements seem to give conclusive results.

5. Dielectric constant and particle weight. J. W. WILLIAMS, *University of Wisconsin.*—Svedberg has been successful with the determination of the size and weight of colloidal particles by observing their linear velocities when subjected to a centrifugal field. A similar result should follow from a study of their rotational velocities in an alternating electrical field. The method, an application of the dipole theory of Debye, depends upon the fact that owing to the frictional resistance of the medium to the rotation of the suspended particles a finite time is required for their orientation in the field. If the frequency dependence of the dielectric constant is determined for a system composed of electrically dissymetrical particles supended in a liquid medium there will be found to be a region in which the dielectric constant decreases as the frequency is increased. The theory expresses the size, and therefore the weight, of the suspended particle in terms of the observed critical frequency and the "viscosity" of the medium. The available data are as yet insufficient for the exact determination of the particle size because the systems involved fail to conform to the assumptions underlying either the law of Stokes or the Clausius-Mosotti relation. Nevertheless, calculations from them indicate that once it becomes possible to evaluate the true inner friction constant of the system important results may be obtained. The method readily distinguishes monodisperse and polydisperse sols.

6. Surface charge of large particles in liquids. HAROLD A. ABRAMSON, *Columbia University, and* HANS MUELLER, *Massachusetts Institute of Technology.*—It is proposed that an advance in the study of the constitution of the solid-liquid and liquid-liquid interfaces may be made by calculation of σ, the surface density of electric charge, in addition to the analysis of the potential difference, ζ, between the movable phases. For large particles σ can be readily calculated by an extrapolation of the Debye theory. This has been done for the negatively charged surfaces of graphite, glass, cellulose, "collodion" and paraffin oil, in the case of ions (valence 1:1; 1:2; 2:1; 1:4) not producing reversal of sign of charge. Although the ζ-concentration curves are rather complex, the σ-concentration curve in every case yields a simple curve resembling typical adsorption with an initial steep slope and with saturation at salt concentrations of about 0.01 molar. Curves of this type have been predicted by Stern. The character of the curves is determined by both ions. The slope at zero concentration varies markedly, particularly with the nature and valence of the anion; e.g., for glass in the order $I > Br > Cl$, the

differences diminishing as saturation approached. The method of calculation employed here to ascertain the nature and magnitude of the forces involved in adsorption of ions by "inert" surfaces at the liquid interface is justified by previous theory and experiment of the authors.

7. Some remarks on the physical constants of cells in connection with their size and shape. N. RASHEVSKY, *Westinghouse Research Laboratories, East Pittsburgh.*—In a paper presented at the Cambridge meeting, (Physics **2,** 303, 1932) a formula was deduced, giving the size of a cell in terms of its physical constants, such as, the coefficient of diffusion for oxygen, permeability, surface tension and rate of metabolism. From values for the diffusion coefficient D as found for muscle tissue, values of the order of magnitude of 10^{-3} cm for the size were found. Bacteria, however, are much smaller, and in order to account for their size, values for D about 1000 times as small must be assumed. It is interesting, that in a recent investigation Professor R. W. Gerard arrived at a similar conclusion from an entirely different point of view; namely, from the study of oxygen consumption. He discarded, however, the assumption of such a small D, as being not supported by any other facts, and interpreted his experimental results otherwise. Questions as to the possible reason of such a small D in bacteria are discussed in the present paper. Furthermore, some applications of the author's foregoing studies to the problem of shape of certain cells are made.

8. Electric phase angle of cell membranes. KENNETH S. COLE, *Columbia University.*—From the theory of an electric network containing any combination of resistances and a single variable impedance element having a constant phase angle independent of frequency, it is shown that the graph of the terminal series reactance against the resistance is an arc of a circle with the position of the center depending upon the phase angle of the variable element. If it is assumed that biological systems are equivalent to such a network, the hypotheses are supported at low and intermediate frequencies by data on red blood cells, muscle, nerve, onion membrane and potato. For some tissues there is a marked divergence from the circle at high frequencies, which is not interpreted.

9. A theory of surface conductance at an electrolyte-solid interface. KENNETH S. COLE, *Columbia University.*—An expression has been derived on the basis of the Maxwell-Boltzmann distribution and Poisson's equation for the tangential surface conductance of an electrolyte in contact with a charged plane surface. One part of this expression is analogous to the result given by Smoluchowski for a Helmholtz double layer, while the second part arises from the movement of the ions in the diffuse ion cloud under the applied electric field. The theory shows qualitative agreement with the data of Briggs for the conductance of univalent chloride solutions at a cellulose surface. For all but the most dilute solutions, the Smoluchowski term is negligible and the surface conductance is proportional to the charge density on the surface. The theory does not agree with the data for different anions and it is suggested that the decrepancy may be due to adsorption phenomena. There may be a movement of the adsorbed ions or of a diffuse ion cloud resulting from the presence of adsorption potentials at a distance from the interface.

10. Photographic reciprocity and intermittency defects near the long wave-length limit of plate sensitivity. BRIAN O'BRIEN AND VERNON L. PARKS, *Institute of Optics, University of Rochester, N. Y.*—Previous work on compensation of reciprocity failure in photographic spectrophotometry by intermittency defect imposed on light beam of higher intensity by interrupted exposure [Phys. Rev. **33,** 640 (1929), Phys. Rev. **37,** 471 (1931)] has been extended to the long wave-length limit of plate sensitivity (λ10,000A for one emulsion) where both defects become large. The four emulsions used, Eastman Process, Process Panchromatic, Contrast Bromide, and Infrared Sensitive 3Q, all exhibit large reciprocity failure. A tungsten incandescent source was maintained constant within 1/4 percent, and mounted on a carriage with range of movement of 50 meters for varying intensity. Fixed sectors were used with aperture ratios of 1/40 to 1/1212, running 28 flashes per second. Errors in measurement of sector apertures and exposure timing were less than 1/2 percent. Although reciprocity failures were as great as 0.92 in density, the difference in density produced on adjacent areas by continuous

low intensity and interrupted high intensity exposure (for It=const.) in no case amounted to a difference in log exposure greater than 0.012, and average difference was less than 0.004. Although just within the limit of measurement this appears to be a systematic difference with reciprocity defect greater than intermittency defect, but difference, if real, is so small that it may be neglected in photographic photometry.

11. The absorption spectrum of sulfur dioxide. J. A. DUNCAN, *Columbia University* (*Introduced by Harold C. Urey*).—The absorption spectrum of sulfur dioxide has been photographed in the region λλ2165–2410A with a Hilger E185 quartz spectrograph having a dispersion of about 1A per mm. The bands are partially resolved into rotational band lines. In this work an effort has been made to analyze the rotational structure rather than the vibrational structure, since Chow (Bull. of the Am. Phys. Soc. Vol. 7 No. 2, 19, April 12, 1932) using lower dispersion is working on the latter problem. The more intense lines of some bands can be classified into branches having approximately constant second differences. These bands appear to fall roughly into two classifications; (1) bands consisting of only one branch resembling a Q branch; (2) bands consisting of two or more branches. It is found to be possible to include in this way nearly all the strong lines of these bands.

12. The alternation of intensities in the sodium bands. JOSEPH JOFFE, *Dept. of Chemistry, Columbia University*. Withdrawn at author's request.

13. The continuous absorption spectrum of chlorine. G. E. GIBSON AND NOEL S. BAYLISS, *The University of California, Berkeley, California*.—A photographic method was used to investigate the continuous absorption spectrum of chlorine at six different temperatures. The effect of increasing the temperature is to decrease the absorption coefficient at the maximum and to broaden the region of continuous absorption. The results were analyzed to obtain the individual contributions of the first two vibrational levels of the normal electronic state to the total absorption. Plotted against wave number, the absorption from the lowest level, ($v''=0$), has a form similar to that of a Gauss error curve, and the absorption from the next level, ($v''=1$), has two maxima. The results are in qualitative accord with a theory of continuous absorption developed by Gibson and Rice.

14. The origin of the mercury bands at 2480A. J. GIBSON WINANS, *University of Wisconsin*.—The mercury bands near 2480A were photographed under different excitation conditions with the purpose of determining their origin. A discharge through mercury vapor was produced in a quartz tube through external electrodes by a low voltage Tesla coil. A photograph of the 2476 band in the third order of a 21-ft. grating checked that of Miss Brozowska, (Zeits. f. Physik **63,** 557 (1930)). Five different tubes containing distilled mercury showed the entire group of eight bands. These bands were weakened by heat. From these observations the origin is some form of mercury molecule, the most probable being Hg_2 or Hg_2^+. Six lines of evidence favor Hg_2^+ over Hg_2: (1) observations on fluorescence, (2) comparison of intensities in mercury arc and electrodeless discharge, (3) comparison of the intensities of the 2476 and 2345 bands under strong and weak field excitation, (4) abscence of other bands of similar character in the mercury spectrum and the observation by Rayleigh that these bands do not appear in absorption, (5) classification of these bands as sequences $v'-v''=0\pm1\pm2\pm3$ which leads to a value for $D>0.5$ volts; (6) observed emission from state $v'=41$ corresponding to very high temperature molecules.

15. Observations on the fluorescence spectra of cadium vapor. W. CRAM AND J. G. WINANS, *University of Wisconsin*.—A broad band in the fluorescence of cadmium vapor has been previously observed between the limits 3050−2288A. Kapuscinski found that monochromatic light of wave-length in this band was absorbed and reemitted by the vapor. In the present experiment fluorescence was excited in cadmium vapor by light from a copper spark. The band was found to extend from 3050 to 2212A. Lines in the exciting light, of wave-length below 2288A, were reemitted by the vapor in the same manner as those observed by Kapuscinski. The spectrum of the electrodless discharge showed this same band but with different intensity distribution. These observations can be explained by the use of potential energy-

nuclear separation curves which correspond closely to those given by Winans to interpret the absorption spectra of cadmium vapor.

16. Rotational Raman effect of gases. CHARLTON M. LEWIS, *California Institute of Technology.*—The study of the Raman effect of gases has been extended to the pure rotation of the simpler hydrocarbons. Acetylene shows the same pattern of alternating intensities that was found by Hedfeld and Mecke in absorption. Ethane and ethylene, which have the form of the symmetrical and asymmetrical top, respectively, show more complicated fine structure; but in neither case is there evidence of more than one moment of inertia. The pure rotation spectrum of methane appears to be missing, or at least of a lower order of intensity than the rotation-vibration band already found by Rasetti. The P and R branches of this band are not very much weaker than the Q branch, while another mode of vibration, which yields an extremely intense Q branch, shows no P and R branches. These characteristics are largely in agreement with what is to be expected from an extension to the rotational Raman effect of Placzek's method of treating the vibration lines.

17. Raman effect in crystalline NH_4Cl. F. T. HOLMES, *Lehigh University.*—Schaefer, Matossi, and Aderhold (Zeits. f. Physik **65,** 289 (1930)) have reported two broad Raman lines for NH_4Cl at 3155 and 3035 cm^{-1}. The author has found that in addition to these lines most of the characteristic frequencies found by Reinkober (Zeits. f. Physik **5,** 192 (1921)) in the infrared appear in the Raman spectrum as rather broad lines. However the line at approximately 1700 cm^{-1} is very sharp. In addition to these, a set of four very weak lines has been observed in the region near 3155 and 3035 cm^{-1}. In consideration of the prediction by Pauling (Phys. Rev. **36,** 430 (1930)) of rotation of the ammonium ion in this substance at room temperature, it seems possible to regard the members of this set as vibrational-rotational lines. Intensity considerations indicate that they may be associated with the 3035 cm^{-1} vibrational shift. Making these assignments, and assuming $\Delta j = \pm 2$ with no "missing lines," the moment of inertia of the rotating group is calculated to be approximately 2.0×10^{-40} gm cm^2.

18. Zeeman effect in the $^2\prod$ $^2\sum$ CaH bands. W. PEYTON CUNNINGHAM, *Yale University.* (*Introduced by W. W. Watson.*)—The Zeeman effect in the λ7000, $^2\Pi$ $^2\Sigma$ CaH band has been investigated at field strengths of 10,500, 18,200 and 30,000 gauss. For the Q branches the patterns are in excellent agreement with the predictions of Hill's formulas for doublet states. In the lines of the R and P branches, however, marked departures from these predicted patterns occur in the region of intermediate and high K levels. It is shown that the inclusion of the magnetic moment due to ρ, the sizeable component of l perpendicular to the internuclear axis is the Π_d levels, gives quite closely the needed corrections for these patterns. Calculation shows that for all these lines of high K values one block of components becomes so wide and diffuse as to be unobservable. Interesting variations with ρ and H in the observed narrower block of components for the region just above the crossing of the Π_d levels are discussed.

19. Zeeman effect of Pb III. J. B. GREEN AND R. A. LORING, *Ohio State University.*—The Zeeman effect of Pb III has been studied at fields of about 40,000 gausses with the newly completed 30,000 line 21-ft. Paschen-Runge concave grating set-up at this laboratory, and the same general type of vacuum box used in our work on Sn. Of particular interest in this spectrum is the $6s6p$ configuration, which seems to violate all the rules laid down by the theory. The coupling is practically j-j in type, and accurate measurements of the four lines involved in the transition $6s6p - 6s7s\ ^3S_1$ indicate that (1) the Pauli g-sum rule for the $^3P_1 + {}^1P_1$ is not accurately obeyed, the experimental value being 2.53 against the theoretical 2.50; (2) the g-value of $^3P_2$ which should be unaffected by coupling (taking into account perturbations within its own configuration) is 1.35 (exp) against 1.50 (theo.). The abnormal g-value must be attributed to perturbations by the neighboring $6p^2$ or $6s6d$ configurations.

20. Theory of quantum defect due to polarization, with application to multiplet anomalies in Al II. N. G. WHITELAW AND J. H. VAN VLECK, *University of Wisconsin.*—The formula $\Delta = (\alpha e^2 n^3 / 4chR)\overline{1/r^4}$ for the quantum defect Δ due to polarization is usually derived by introducing a model in which the atom-core is given *ad hoc* a polarizability α. Instead a derivation

is given by perturbation theory in which inter-electronic interaction is considered explicitly. The above formula for Δ is found to be valid only if exchange terms are neglected and if the absorption lines ν(A.C.) of the atom-core are large compared to those ν(V.E.) representing transitions of the valence electron. The calculation enables one to determine the "perturbations," i.e., deviations from the formula, when there is close resonance between ν(A.C.) and ν(V.E.). The theory is applied to the $3smf\,^3F$ series of Al II, which Langer, Shenstone, and Russell have noted is perturbed by a $3p3d\,^3F$ term. The widening of the multiplets in the vicinity of the perturbation is caused by a partial robbing of the intruders wide structure, and can be calculated from the observed displacement of the multiplet centroids from hydrogenic values. The calculated over-all widths for the successive members are 5.1, 10.8, 37.2, (58.2 for intruding $3p3d$), 20.8, 7.3, 3.7, . . . against observed 4.9, 12.3, 40.4, (58.1), 17.8, 5.7, 2.4. The discrepancies may be diminished by the further consideration of higher order approximations.

21. A theorem on spectroscopic stability. R. M. LANGER, *University of Minnesota.*—Recent spectroscopic observations, especially some of the rare gas spectra (e.g., E. Rasmussen, Zeits. f. Physik **75,** 695, 1932) bring out symmetries in the oscillations of the term values of similar series. They suggest a connection between the departures of related terms from Ritz formulae. In fact such a connection can be deduced theoretically. The rare gas series exemplify one of several possible types of behavior. The usual calculations of energy levels assuming separate configurations lead to multiplet separations and smooth series which often disagree with experimental data. Since these incomplete solutions for discrete spectra differ from the correct ones by a unitary transformation the sum of the energies of mutually perturbing configurations is correctly given by the incomplete solutions. This leads to the very useful theorem that the displacements of interacting levels from their expected positions on smooth series curves must add up to zero. The power of this stability theorem depends on narrowing down the set of levels under consideration. It will help in estimating certain large displacements of terms in series which are not well marked and will also help calculate constants for irregular series. Probably the most helpful application of the theorem will be the criterion it gives for deciding whether one has all of the set of levels which are affecting one another. The important but difficult case of continuous spectra has not been considered.

22. The escape of imprisoned resonance radiation from a gas. CARL KENTY, *General Electric Vapor Lamp Co. Hoboken, N. J.*—Theoretical considerations lead to the view that a large concentration of resonance quanta diffusing through a gas would, on the basis of Doppler broadening only, give rise to a distribution function for excited atoms, with respect to atomic speed, which would lie between two limiting distribution functions: (1) Maxwell's distribution function, namely

$$f_1(S)dS = [4/(\pi)^{1/2}](S^2/w^3)\exp\,-(S^2/w^2)dS$$

where S is the speed of an atom and w is the most probable speed; and (2) a distribution function expressing a lower relative excitation of the high speed atoms, namely

$$f_2(S)\,dS = 2(S/w^2)\exp - (S^2/w^2)dS.$$

On the basis of either (1) or (2) the diffusion coefficient as well as the average square free path are found to be infinite provided the volume of gas is infinite; otherwise, the *apparent* values of these quantities will depend on the volume, increasing therewith without limit because of the importance of extremely long free paths. Coupling or other broadening occuring at higher pressures will presumably accentuate the effect of abnormally long free paths. The results are in qualitative agreement with imprisonment experiments of Zemansky and of Webb and Messenger, in Hg, and with the experiments of Found and Langmuir and of Kenty in Ne (in print).

23. Yield of fluorescent x-rays from the *K* shells of various elements. DONALD K. BERKEY, *University of Cincinnati.*—The fluorescent yield w from the K shells of an aggregate of atoms is defined as the ratio of the number of characteristic K quanta emitted to the number of quanta photoelectrically absorbed in the K shells. The author has measured this ratio by comparing the total intensities of the primary and fluorescent rays from various substances, using the

ionization method devised by A. H. Compton (Phil. Mag. **7**, 961, 1929). The following results were obtained:

Element		w	Element		w
27	Cobalt	0.38	42	Molybdenum	0.78
28	Nickel	0.39	47	Silver	0.73
29	Copper	0.43	48	Cadmium	0.72
30	Zinc	0.46	50	Tin	0.67
33	Arsenic	0.53	51	Antimony	0.64
34	Selenium	0.56	52	Tellurium	0.60
38	Strontium	0.72			

These results show that the fluorescent yield increases to a maximum for elements in the neighborhood of molybdenum, beyond which it decreases. It is planned to continue this investigation for elements of higher atomic number than tellurium.

24. Fine structure in the x-ray *K* absorption edge of calcium in compounds. VOLA P. BARTON, *Goucher College, and* GEO. A. LINDSAY, *University of Michigan.*—The fine structure of the Ca *K* edge has been examined in several calcium compounds. A quartz crystal was used and the calcium compound was ground to a fine powder and suspended in a collodion film for an absorbing screen. In cases where the calcium compound could be used as reflecting crystal and at the same time as absorber, the results were found to be the same as with screens. Calcite and aragonite, the same chemically, show markedly different fine structure, thus indicating that not the chemical compound, but rather the crystal form, is the determining factor. This is in accordance with Kronig's theory. Dolomite, Ca $Mg(CO_3)_2$, and ankerite, (Ca, Mg, Fe)CO_3 have the same crystalline form as calcite, and show the same fine structure for Ca, but the appearance for Fe in ankerite is different. This is not so satisfactory for the theory, for the iron and calcium atoms are similarly placed in the same crystal, and the ejected electron in passing through the crystal should experience the same variation in potential.

25. Further experiments on x-ray reflections from quartz crystals oscillating piezoelectrically. J. M. CORK, *University of Michigan.*—By both the Bragg method and the Laue method, quartz crystals at rest and oscillating piezoelectrically have been further studied. Starting with a relatively thick crystal and using a finely collimated x-ray beam the structure of the Laue spots could be readily observed. For oscillating crystals and also for polished crystals at rest the spots are double in structure. Etching the crystal with H Fl results in single spots for the non-oscillating crystal. The perfection of the surface is revealed by observing line breadth and intensity when the crystal is employed in a Siegbahn vacuum spectrograph at a wave-length of 5.5A; and for short x-ray wave-lengths on a Bragg spectrometer of 55 cm radius. In no case was line breadth or intensity sensibly altered by piezoelectric oscillation of the crystal. Results obtained are compatible with the elastic vibrational theory already proposed, (Fox and Cork. Phys. Rev. **38,** 1420 (1931)).

26. X-ray wave-lengths by ruled grating. R. B. WITMER AND J. M. CORK, *University of Michigan.*—With a ruled glass grating, measurements have been made of the wave-lengths in the *L* series emission spectra for elements from Ti (22) to Zn (30); and in the *K* series for elements from C (6) to Si (14). The grating employed (whose constant was $d=0.00166309$ mm) was ruled by Siegbahn on his new machine and gave excellent reflections. The experimental arrangement was identical with that employed in the precision determination of the *L* series wave-lengths of molybdenum (Cork, Phys. Rev. **35,** 1456, (1930)). This method has the important advantage that for the complete series of plates the position of the grating is in no way altered. The results obtained for the shorter wave-length lines are greater by about 0.3 percent than the corresponding wave-length measurements obtained by the crystal method. Crystals that have been employed for the longer wave-length range are mica, sugar, and palmitic acid. The individual results obtained with these crystals are shown to be so eratic that a comparison with the results obtained with the grating method is meaningless. The change in the relative intensity and the form of the α_1 line with change in atomic number is shown. Additional data

using different incident grazing angles are being taken to observe any possible variation in wave-length with angle of incidence. (Prins and Hanawalt, Nederlandsch Tijdschrift voor Naturkunde **12,** 1 and 15, 1932).

27. Additional theory of plane gratings for x-rays. ROY C. SPENCER, *University of Nebraska.*—The positions of the diffracted virtual images of a source as seen in a plane grating placed at a distance L are given by $L' = L \sin^2\theta/\sin^2 i$ where i and θ are the grazing angles of incidence and diffraction. For use with x-rays the incident beam is confined between two equal slits of width S distant L apart with the grating close to the second slit. The diffracted beam produced backwards appears to be confined between two slits of width S' and distance L' apart where $S' = S \sin\theta/\sin i$ and L' has the value given above. The intensity of a cross section of the diffracted beam is a trapezoid, the constant part having a width S' and each side an angular width S'/L'. The former varies directly as $\sin\theta$, while the latter varies inversely. Assuming a parallel beam, the angle between the maximum and the first diffraction minimum is λ/S'. The ratio of this diffraction width to the geometrical side width is $\lambda L'/S'^2 = \lambda L/S^2$, a constant of the slit system. This should not exceed unity. The combined effect of geometric and diffraction widths may be studied using a sodium flame and two slits.

28. The gamma-ray spectrometer. M. C. HENDERSON, *Yale University.*—The method first used by Rutherford and Andrade (Phil. Mag. **27,** 854, 1914; **28,** 263 (1914)) to measure the wave-lengths of the radium gamma-rays and later adapted by Steadman (Phys. Rev. **36,** 460 (1930)) to the Geiger point counter has been improved and some preliminary results obtained. The Geiger-Müller tube counter has been adopted as the detector. It has proved easily possible to resolve and measure the 20 and 35 x.u. radium B and C gamma-rays. With 30 mg of radium, the 35 x.u. line causes 4.7 discharges per minute out of a total of 16.5. All counting is automatic and runs 24 hours a day. The resolving power is low but it will be possible to resolve lines about 5 x.u. apart without further changes in the apparatus. The lower limit of wave-length that can be measured without disturbance from the central beam is about 20 x.u. The interrelated effects of source thickness, slit width, crystal setting and slit setting upon the theoretical gamma-ray intensity transmitted through the slit can be plotted as a series of three-dimensional models, which will be shown. The method of coincidences, so successfully applied to cosmic rays, has been tried to record gamma-rays, with encouraging results and it is being further developed. Steadman's results (loc. cit.) are not confirmed.

29. The threshold counting voltage of the Geiger-Müller tube and some related phenomena. D. COOKSEY AND M. C. HENDERSON, *Yale University.*—The voltage at which a Geiger-Müller tube begins to count is determinable to 0.1 percent. The dependence of this threshold voltage upon chamber and wire dimensions, material and nature of the surfaces, temperature of the wire, and pressure and kind of gas has been investigated. It is found that the threshold voltage for proper counting is independent of the wire and wall materials. For any chosen pressure and wire size the threshold voltage so varies with the chamber diameter that the field at the surface of the wire remains constant. This threshold field depends on the gas and its pressure, passing thru a minimum at low pressures in a similar manner to the sparking potential. Knowing the threshold field, the formula: field = voltage/(a log b/a), where a and b are the radii of the wire and chamber respectively, enables the counting voltage to be calculated for any desired dimensions and gas pressure. For small wires, less than 0.075 mm diameter, the threshold field is inversely proportional to the diameter but diminishes less rapidly than this for larger wires. Raising the temperature of the wire while counting lowers the threshold voltage. One iron wire continued to count in air up to a dull red, above which temperature spurious discharges masked the proper counts.

30. New determinations of the ranges of α-particles from polonium, uranium I and uranium II. F. N. D. KURIE, *Yale University.*—The cloud chamber method described by the author in the abstracts of the New Orleans meeting (1931) has been used to determine the ranges of α-particles from polonium, uranium I and uranium II. The experiments on polonium were undertaken to test the method, but the results are in such good accord with previous values that

they may stand alone. The range of polonium α particles at 0°C and 760 mm pressure is 3.690 $\pm$0.005 cm. A graphical method has been devised for separating the number-distance curves of the two uraniums, which consists in plotting the data on probability paper. The plot then becomes three intersecting straight lines, the midpoint of the short connecting line giving the relative proportions of the two kinds of particles. The ranges of the uranium particles at 0°C and 760 mm pressure are respectively: $R_{U\,I}=2.58\pm0.015$ cm, $R_{U\,II}=3.11\pm0.01$ cm. The polonium range is derived from 335 tracks, the uranium ranges from 594 tracks. The uranium ranges are in complete agreement with the results of Laurence (Phil. Mag. **5**, 1027 (1928)), got by methods more likely to be in error than those used here.

31. Generalization of wave mechanics suggested by higher order terms in the classical electrodynamic equation of motion, and its influence on β-particles ionization for velocities approaching that of light. W. F. G. SWANN AND A. BRAMLEY, *Bartol Research Foundation of The Franklin Institute.*—Classical electrodynamics gives, for small velocities, an equation of electronic motion of the form

$$\frac{e}{6\pi ac^2}\ddot{x}-\frac{e}{6\pi c^3}\dddot{x}+\text{etc.}=E+\frac{[uH]}{c} \tag{1}$$

where a is the classical electronic radius. In the present paper, the equation is solved and for the cases which are relevant gives rise to

$$\frac{e^2}{6\pi ac^2}\dddot{x}=E+\frac{[uH]}{c}+f(D)E \tag{2}$$

where $f(D)$ is a determined function of the operator d/dt. We now build a Schroedinger equation for ψ with the right-hand side of (2), replacing $E+[uH]/c$ as used in the ordinary developments, but with d/dt replaced by ∂/dt, which for the field of a high-energy β particle of velocity v becomes $-v\Delta$. The perturbation, instead of involving only the scalar and vector potentials ϕ, and U, which can be expressed in terms of it, involves also a series of spatial derivatives of ϕ. Application to the ionization of an atom gives for q the number of ions per centimeter of path, an expression which, with increasing β-particle energy, first diminishes, then increases, and finally diminishes towards zero. The first decrease followed by increase corresponds to the conclusions of Oppenheimer, as yet apparently unpublished. The final decrease comes from the new features introduced. It predicts a decrease of ionization for β-particle energies greater than about 10^{10} volts.

32. An interpretation of cosmic-ray phenomena. THOMAS H. JOHNSON, *The Bartol Research Foundation of the Franklin Institute, Swarthmore, Pa.*—Schindler's measurements form the basis for a more specific theory of the process of ionization by cosmic rays than had hitherto been possible. To explain his data the following assumptions are made. (1) The primary rays contribute nothing *per se* to the ionization but produce secondary rays such as electrons and protons from the material through which they pass, the production coefficient β_m being a characteristic of the medium. (2) The absorption of the primary rays can be represented by a single exponential function with a coefficient ν_m characteristic of the medium. (3) The absorption of the secondaries can be represented by an exponential function, with a coefficient $\mu_m{}^n$ which is characteristic of both the absorbing medium m and the medium n in which the secondary ray was produced. The ionization at distance x behind the interface nm is given by

$$I=\frac{A\beta_m}{\mu_m{}^n-\nu_m}(e^{-\nu_m x}-e^{-\overset{m}{\mu_m} x})+Be^{-\overset{n}{\mu_m} x}.$$

The constants have been determined to bring agreement with the data in the case of the air to lead, air to iron, iron to lead, and lead to iron transitions. The absorption coefficients of the secondary rays determined in this way agree with the energies measured by Millikan and Anderson. The relation of these ideas to other experiments is also discussed.

33. Study of getter action of phosphorus. HENRY J. MILLER, *Emporium, Pa.*—The clean-up of commercial 50 watt 230 volt vacuum incandescent lamps by phosphorus has been investigated and compared with the clean-up in lamps of the same type evacuated by laboratory methods by means of a third external electrode measuring the ratio of positive ions to electrons flowing to this electrode while the filament voltage is gradually raised from zero to a value somewhat above normal rating. The clean-up initiated by the thermionic current flowing between filament terminals progresses with maximum efficiency at filament potentials which, for lamps with getters, agree with the volt value of maximum ionization efficiency of 150 volts found by Mayer for air and nitrogen (Ann. d. Physik **45,** 1 (1914)). Commercial lamps without getters do not clean up. Lamps without getters evacuated by laboratory methods clean up but at higher potentials than the corresponding lamps with getters (175 to 200 volts). The clean-up curves of lamps with getters and without getters suggest the interpretation of the observed clean-up as "chain-reaction" according to Bodenstein. (*Preuss. Akad. Wiss. Phys. Math. Kl.* 1928, p. 490).

34. The Kerr electro-optical effect in carbon dioxide. C. W. BRUCE, *University of Virginia,* (*Introduced by J. W. Beams*).—Measurements have been made on the variation with density of the Kerr electro-optical effect in CO_2 using a method similar to that of Stevenson and Beams (Phys. Rev. **38,** 133 (1931)). The measures were taken at a constant temperature of 34.6°C. The density was varied from 0.05 to 0.288 gm/cc and was computed from pressure readings by use of Amagat's data. The results of Stevenson and Beams were confirmed for the range (0.08−0.18) over which they worked. A comparison made between the variation of the Kerr constant as determined experimentally and as computed from the relation $B \propto [(n^2+2)^2 (\epsilon+2)^2]/n$, taken from the Langevin-Born theory, shows good agreement. The data for the index of refraction used in the above relation were that of Phillips (Proc. Roy. Soc. **A97,** 225 (1920)), and for the dielectric constant was that of Keyes and Kirkwood (Phys. Rev. **26,** 754 (1930)).

35. The initiation of electrical discharges in effectively ion free gases. J. W. BEAMS AND JOHN W. FLOWERS, *University of Virginia.*—A study is made of the factors that initiate the discharges described by Street and Beams (Phys. Rev. **38,** 416 (1931)). In carefully dried and filtered gases (air, hydrogen, nitrogen, helium) at atmospheric pressure, it is possible to apply 5×10^5 volts per cm between spherical brass electrodes for 10^{-6} sec. without electrical breakdown, provided the gas is kept "swept" as free as possible of ions by auxiliary fields. However, when ultraviolet light falls upon the cathode a field of 4×10^4 volts per cm starts the discharge in less than 10^{-7}sec. The maximum field depends upon the conditions of the surface of the electrodes and is of the same order of magnitude as that required to produce breakdown in a vacuum, which is known to be started by field currents from the cathode (Wood, Phys. Rev. **5, 1** (1897); Hull and Burger, Phys. Rev. **31,** 1121 (1928); Snoddy, Phys. Rev. **37,** 1678 (1931)). When a steel point and plane were substituted for the brass spheres in the above experiment the field at the surface of the point could be made at least 10^7 volts per cm for 10^{-6} sec. without breakdown if the point was positive. However, breakdown started in less than 10^{-6} sec. if the point was made the cathode and the field raised to only 10^6 volts per cm. In a vacuum fields of 8×10^7 volts per cm were applied to the pointed steel or tungsten anode for 10^{-7} sec. without breakdown. Similar results were obtained with gaseous pressures less than 0.01 mm.

36. Ionization of helium, neon and argon under impact of their own positive ions. CHARLES J. BRASEFIELD, *Yale University.*—The number of electrons liberated from neutral rare gas atoms under impact of their own positive ions was measured as a function of the kinetic energy of the ions. It was found that helium was ionized at 100 equivalent volts; neon at 90 and 130 volts; and argon at 55 and 95 volts. It is thought that the higher ionizing potentials in the case of neon and argon are the result of impacts of doubly charged ions. The error in these measurements is hard to estimate but is thought to be within ±10 volts. If we assume (1) that half of the kinetic energy of the impacting ion is available for ionization and (2) that the energy required to liberate an electron is approximately the sum of the energies necessary to liberate it

separately from its own core and from that of the impacting ion, we might expect ionization of the rare gases under impact of their own positive ions to occur at approximately the following values: in helium at 98 volts, in neon at 86 and 125 volts and in argon at 63 and 87 volts.

37. New devices for recording Kennelly-Heaviside layer reflections. HARRY R. MIMNO AND P. H. WANG, *Harvard University.*—Two new pieces of apparatus for layer height measurement have been built and tested. The first device is merely an improved form of the "long film" type of oscillograph, ordinarily used in pulse transmission experiments. In order to increase the resolving power without wasting or tearing the photographic paper tape, the oscillograph has been constructed with a magnetic clutch, shock absorber, and magnetic brake. The second device is a high speed chronograph, designed to give an accurate record of layer heights over an extended period of time. A complete history of the reflections produced by 2000 successive pulses is recorded in compact form on a strip of photographic paper, 90 cm long and 12 cm wide. The time scale may be varied from 5 minutes to 24 hours. The received pulses modulate a glow lamp, producing a small, sharply-defined dot on the moving paper. The resolving power appears to be somewhat better than that obtained with the best galvanometer oscillographs. A cathode-ray oscillograph is used to monitor the reception. The high speed chronograph has other applications, outside of the radio transmission field.

38. A new type of vacuum or circulating pump. E. L. HARRINGTON, *University of Saskatchewan.*—A new type of vacuum or circulating pump employing a helical tube made to rotate about the axis of the helix is described. Its action depends on a pumping liquid which fills the lower bends of the helix and crowds out the gas being pumped as the helix is rotated. There is a provision for the return of the pumping liquid to the first coil of the helix as the latter continues to rotate. The liquid may be chosen to suit the work at hand. Among the advantages claimed for the pump are the following: mercury vapour is not employed, heating and cooling elements are not required, adapted equally well to corrosive and non-corrosive gases, vapors and liquids, constant personal attention is not needed, it may be started or stopped instantly without the use of stop-cocks, and its action is reversible.

39. The form of potential barrier at the surfaces of conductors. A. T. WATERMAN, *Yale University.*—The method of treatment described by the writer (Phys. Rev. **38,** 1497–1505 (1931)) has been used to investigate the form of potential barrier inside as well as outside the surface of a conductor in equilibrium with its electron atmosphere, assuming continuity of potential and electric intensity at the boundary. The results indicate that there is a sharp rise in the barrier of about 4 or 5 volts within a distance of several Angstrom units in the immediate neighborhood of the surface (assumed plane), about one fifth of the rise occurring inside the conductor. The rest of the potential curve rises more gradually. Similar treatment for the form of barrier between plane parallel electrodes shows this to consist of a potential "plateau." To be consistent with contact potential as defined by the Kelvin experiment, on bringing the electrodes together there is a flow of electrons into the less electropositive metal, the potential barrier becomes a "hill" of decreasing height, until it disappears in a point of inflection at contact. Similarly the potential "trough" within a thin conducting film flattens out and disappears as the thickness of the film approaches zero. The case of a thin film deposited on base metal is difficult to solve, but gives promise of accounting for some of the peculiarities observed in such cases.

40. The caesium-oxygen-silver photoelectric cell. C. H. PRESCOTT, JR. AND M. J. KELLY, *Bell Telephone Laboratories Inc.*—The active cathode surface of the caesium-oxygen-silver photoelectric cell appears to be a film or surface concentration of caesium of atomic dimensions adsorbed upon a matrix of caesium oxide and silver containing free caesium and a small amount of silver oxide. The spectral characteristics of the photoelectric response depend largely upon the thickness of the surface film of free caesium. This film thickness is determined by the caesium concentration in the underlying matrix and is maintained by a diffusion equilibrium. Variations in the amount of caesium upon the surface were made either by exposing the standard finished cathode to small amounts of oxygen and allowing the response to recover

by diffusion of free caesium from the underlying material, or else by allowing small amounts of additional caesium to deposit upon the standard surface. With increasing thickness of the caesium surface film the characteristics of the spectral response appear to vary continuously from a low response (with amounts of surface caesium far below the normal) which decreases with wave-length (from 6000A to 10,000A) to a high response for the normal surface with a selective maximum at 7500A−8000A, and finally to a low response with a maximum approaching 6000A.

41. Some photovoltaic properties of Cu:Cu_2O | $Pb(NO_3)_2$ solution | Cu:Cu_2O photocells. WILBUR E. MESERVE, *Cornell University* (*Introduced by Ernest Merritt*).—The light sensitive electrodes were prepared by chemical methods which produce a uniform coating of copper oxide of any desired thickness. Two identical electrodes were placed in a 1 percent solution of $Pb(NO_3)_2$, the back of the light exposed electrode being insulated from the electrolyte. Measurements were made of the photo-e.m.f. produced by the cell when illuminated by sinusoidally interrupted light of variable frequency. By impressing the output of the cell on a resistance coupled amplifier of proper design, which takes no current from the cell and thus reduces polarization and internal chemical changes to a minimum, the frequency response was determined with the use of the stabilized cathode-ray "oscilloscope." The spectral sensitivity of the cells was determined with sinusoidally interrupted light from a monochromator and checks with that which has been determined with steady illumination. The angle of phase shift of the photo-e.m.f. with respect to the interrupted light was also measured and was found to first increase and then decrease with frequency, the maximum angle occurring at about 500 cycles. The internal capacity of the cell as an electrolytic condenser was found to nearly double when one electrode was illuminated by strong sunlight.

42. The isotopic weight and packing fraction of H^2. K. T. BAINBRIDGE, *Bartol Research Foundation*.—The mass of neutral H^2 is 2.01353 ± 0.000064 obtained from comparison of the mass of $(H^1H^1H^2)^+$ with He^+ on fourteen spectra secured with the mass-spectrograph recently described. The eqivalent packing fraction of H^2 is 67.6. On the assumption that the nucleus is composed of two protons and one electron the energy of binding is approximately 2×10^5 electron-volts but if the H^2 nucleus is made up of one proton and one Chadwick neutron then the binding energy of these two particles is 9.5×10^5 electron volts. $(3H^1)^+$ and He^+ provided the dispersion measurements for these spectra and the presence of $(H^1H^2)^+$ can only introduce a negligible correction. Lines of mass 4.0285 on the spectra were attributed to $(H^1H^1H^2)$ ions because (1) no lines of comparable intensity appeared in this position when commercial hydrogen was used, (2) under the conditions existing in the discharge tube the probability of formation of $(2H^2)^+$ was much less than for $(H^1H^1H^2)^+$, (3) the mass is less than the mass of $(4H^1)^+$ by an amount outside of the limit of error. The two enriched samples of hydrogen used were prepared by Brickwedde, both had been tested spectroscopically by Urey and Murphy and one was a sample of Bleakney's.

43. The isotopes of uranium. T. B. WILKINS AND W. M. RAYTON, *University of Rochester*.—The existence of an isotope of uranium (AcU_I) of shorter life than U_I as the parent of the actinium series was predicted in 1926 (Wilkins, Nature **117,** 719 (1926)). An alpha-ray range of 3.2 cm and period 2.5×10^8 yrs., then assigned, were confirmed by Rutherford's interpretation of Aston's mass-spectrogram of lead. (Nature **313,** 1929.) A mass-spectrogram of uranium failed to reveal even U_{II}. In the present work the alpha-rays from a thin sputtered film of uranium fell on a special photographic emulsion. The number of grains in individual tracks was counted. Two main peaks are indicated in the frequency curve at 9 and 11 grains and clearly marked humps at 13 and 16. The peak at 11 is slightly higher than at 9. Polonium gave a smooth curve with peak at 13. Hence Laurence's ranges of U_I and U_{II} are confirmed (Phil. Mag. **5,** 1027 (1928)), but two and possibly three additional isotopes of a less active series are indicated. The study of the relative activities of these two series may lead to a simpler method of determining the ages of rocks.

Nos. 44 to 47 are abstracts of invited papers which made up a symposium on x-rays.

44. The spectrum of scattered radiation. J. A. GRAY, Queen's University.—It is generally assumed that, when homogeneous x-rays are scattered through an angle θ, the modified band has both an average wave-length and a wave-length of maximum intensity given by the equation

$$\lambda_m = \lambda + h/mc\,(1-\cos\theta) \quad \ldots\ldots\ldots \quad (1)$$

So that if $\lambda+\delta\lambda$ = average wave-length of scattered rays

$$\delta\lambda = (R/R+1)\cdot h/mc\,(1-\cos\theta)$$
$$- (R/R+1)\times 0.0243\,(1-\cos\theta)\text{A}.$$

where R = ratio of integrated intensity of modified band to that of the unmodified line.

I have carried out experiments at different times since 1913 to obtain values of $\lambda+\delta\lambda$, but always with heterogeneous rays. A brief description of the method follows. The primary rays passed through two slits and fell on the radiator, the scattered rays passing through a second set of slits into an ionization chamber where their intensity was measured. Three readings were taken, the first with no absorber, the second with an absorber in the path of the primary rays, position A say, and the third with an absorber in the path of the scattered rays in position B say. It is essential that the ratio of the two last readings should be determined as accurately as possible. This ratio will be called A/B.

An analysis of some results obtained in 1922 is given in Table I, the average value of θ being $\pi/2$.

TABLE I.

Abs.	A/B	P	P'	μ/ρ	μ'/ρ	λ	$\delta\lambda$
0.304	1.13	0.327	0.289	3.68	4.08	0.63	0.023
0.608	1.24	0.152	0.123	3.09	3.44	0.59	0.022
0.912	1.32	0.079	0.0598	2.79	3.09	0.57	0.021
1.216	1.40	0.043	0.0307	2.59	2.86	0.56	0.020

The first column gives the mass of the aluminum absorber in g/cm². When the absorber is placed at A, the ionization is P times as great as it is with no absorber; when placed at B, P' times as great. From P and P' the values of μ/ρ and μ'/ρ are obtained. From μ/ρ, λ is obtained from tables. It is given to two figures. $\delta\lambda$ is obtained from relative values of μ/ρ and μ'/ρ' by assuming that μ/ρ varies as λ^3.

It will be seen that $\delta\lambda$ is less than 0.024A, the value it should apparently have if all the scattered radiation is modified.

The radiator was paraffin wax, 1 inch square in cross section. Assuming a value of $R=8$, $\delta\lambda$ should be of the order 0.021A, if the primary rays are homogeneous. As the table shows these rays are not homogeneous. The effect of using heterogeneous rays is shown in Table II. A primary beam has been assumed to consist of rays of wave-lengths 0.4, 0.5, 0.6, 0.7, 0.8 and 1A respectively, the scattered rays ($\theta=\pi/2$), having wave-lengths 0.424, 0.524 etc. and relative intensities 0.05, 0.20, 0.25, 0.25, 0.20,and 0.05 respectively. This assumed beam has similar properties (absorption coefficients) to the one with which the results of Table I were obtained.

TABLE II.

Abs.	A/B	P	P'	μ/ρ	λ	$\delta\lambda$
0.304	1.11	0.318	0.286	3.77	0.63	0.020
0.608	1.20	0.138	0.115	3.23	0.60	0.020
0.912	1.27	0.0693	0.0543	2.92	0.58	0.019
1.216	1.35	0.0380	0.0282	2.69	0.56	0.018

It will be noticed that $\delta\lambda$ decreases as the thickness of the absorber is increased. A comparison of the figures in the two tables indicates that $\delta\lambda$ for homogeneous rays of wave-length 0.6A is about 0.026A for the radiator used, and, if we assume $R=8$, that the average wave-length of the modified rays is 0.029A greater than λ and not 0.024A, the value given by Eq. (1).

In later experiments, I have attempted to see if $\delta\lambda$ varied with the thickness of the radiator, using heterogeneous rays. One set of results is given in Table III.

TABLE III.

Abs.	Radiator	A/B	P	P'			
0.303	1 sheet	1.20	0.220	0.183	5.00	0.7	0.028
0.303	2 sheets	1.18	0.220	0.187	5.00	0.7	0.025
0.303	12 sheets	1.16	0.220	0.190	5.00	0.7	0.023

The radiator consisted of sheets of filter paper soaked in paraffin wax, the mass of the former being 0.07 g/cm² and of the latter 0.10 g/cm². For $\theta=\pi/6$, A/B was found to be equal to 1.01.

The variation of $\delta\lambda$ with thickness of absorber is again shown in Table IV, the radiator being one sheet of waxed filter paper.

TABLE IV.

Abs.	A/B	P	P'	λ	$\delta\lambda$
0.067	1.07	0.538	0.503	0.86	0.032
0.134	1.14	0.330	0.293	0.80	0.030
0.268	1.18	0.250	0.216	0.70	0.026

It will be noted that $\delta\lambda$ decreases as the thickness of the radiator and of the absorbing material increases. It is concluded that a thorough spectroscopic examination, both photographic and electrical, must be made of the radiation scattered by thin radiators. It is recommended that all such measurements should be verified by the above absorption method, and that this method be applied to gases, particularly hydrogen, helium and other rare gases, the two former as they give us the nearest approximation to free electrons. It is also of great importance to determine the ratio R accurately.

45. X-ray evidence for high electron momenta in atoms and in solid bodies. J. W. M. DUMOND, *California Institute of Technology.*—The work of the author in collaboration with H. A. Kirkpatrick, furnishes evidence for the interpretation of the breadth and structure of the modified line in the spectrum of scattered x-rays as a Doppler broadening caused by the momenta of the electrons in the scattering body. A test of the correctness of this interpretation was made by studying the variation in the shifted line breadth at half maximum as a function of the primary wave-length and also as a function of the scattering angle. The behavior of the shifted line breadth with both these variables is shown to be entirely consistent with the doppler interpretation of its origin. Very sharply defined homogeneous scattering angles could be obtained thanks to the geometry of the multicrystal spectrograph used in this work. The wave-lengths tested covered a range from 700 x.v. to 200 x.v. The Doppler interpretation of the broadening of the shifted line is shown to be in good accord with quantum mechanics. The profile of the Compton line can be interpreted as a distribution curve expressing the relative probability of scattering by electrons of component momentum, px, resolved along on axis, x, which very nearly bisects the angle formed by the incident and scattered beams of radiation. The distribution of electrons in linear momentum has been obtained by this method for carbon and beryllium scatterers and appears to be entirely consistent with the distribution to be expected quantum-mechanically as computed from formulae of Pauling and Podolsky for hydrogenic momentum distributions. The application of these hydrogenic distributions by the introduction of screening factors gives of course only a rough approximation to the momentum distribution in the free carbon atom. It gives nevertheless a distribution curve very similar to that deduced from the experiment save that the maximum of the curve occurs at somewhat lower momenta in the theoretical curve for the free carbon atom than in the experimental curve for a solid carbon scatterer. This is exactly what is to be expected since in solid carbon the proximity of neighboring atoms requires higher momenta of the outer electrons than they would possess in a free atom.

46. Status of x-ray wave-lengths. J. A. BEARDEN, *The Johns Hopkins University.*—The determination of x-ray wave-lengths by crystal gratings requires a knowledge of the constancy of the grating constant of crystals from various sources, and as precise a determination of this constant as is possible. Recent measurements (Phys. Rev. **38,** 3089, (1931)) have shown that the grating constant of calcite crystals from various sources varies less than 1 part in 200,000. The average true value of the grating constant was found to be $d=3.02810$A at 18°C, and the effective value for the first order diffraction $d_1=3.02769$A.

The most precise methods of measuring the diffraction angles appear to be the photographic and double crystal spectrometers. For true symmetrical lines it can be shown that the two methods should give results of the same order of precision. In the case of asymmetrical lines the double crystal method has a distinct advantage in that measurements can be made on the peak of the lines, or from the shape of the lines corrections can be applied to take into account the close components. The importance of measuring x-ray wave-lengths by the double crystal method is shown by the results obtained on the K series of copper and iron where most of the lines are asymmetrical.

Since the ruled grating measurements of x-ray wave-lengths are about 0.25 percent higher than the crystal values it is important to know which value is correct. Studies of the diffraction by ruled grating when used for measuring x-ray wave-lengths have as yet given no explanation of the observed difference. However, the following facts appear to support the crystal value rather than the ruled grating results. (1) Allison (Am. Phys. Soc. Washington 1932) has examined calcite crystals which gave the theoretical rocking curve width and diffracted intensity for a perfect crystal. (2) Tu (Phys. Rev. **40,** 662 (1932)) finds no evidence for mosaic structure. (3) The agreement between Planck's constant h determined by the limit of the continuous x-ray spectrum and other methods. (4) Inconsistency of fundamental constants if the grating wave-lengths were accepted as absolute. (5) Dispersion of x-rays.

47. Fine structure in x-ray absorption spectra. J. D. HANAWALT, *The Dow Chemical Co., Midland, Mich.*—The fine structure in x-ray absorption spectra which extends over a region of several hundred volts to the short wave-length side of the principal absorption edges of many elements has been explained in terms of the simultaneous transitions of two or more electrons due to the absorption of a single quantum. However, this interpretation is not consistent with the experimental facts which are brought out by a study of the effects of the physical and chemical state of the absorbing atom on the fine structure, and by a study of the effect of temperatures changes on the fine structure. These facts are: (1). The fine structure of a polyatomic vapor and of the same material in the solid state are usually similar, though the solid exhibits an additional structure not seen in the vapor spectrum. (2) The fine structure of a polyatomic vapor may differ from that of the solid. (3) Fine structure of more than a few volts separation from the main edge is not observed for any monatomic vapor. It is important to note that the structure which is exhibited by monatomic vapors if of such small energy value as to be satisfactorily explained by the Kossel theory of the transitions of the ejected electrons to various of the virtual orbits of the atom. (4) Fine structure is not observed in the spectra of the polyatomic vapors Se_8 and AsH_3. (5) The fine structure exhibited by Hg in $HgCl_2$ in solid and in vapor forms has the same energy separations from the principal edges in both its L_{III} and its L_{II} spectra. (6) An element in different chemical compounds may show different types of fine structure. (7) In the series As, $AsCl_3$, As_2O_3, As_2O_5, AsH_3 the principal edge has the same wave-length for the vapors, while there are shifts of 5.5 ± 1.5 volts for the solids. (8) The fine structure in the K absorption spectra of Fe becomes fainter as the temperature is raised and at 800°C has almost entirely vanished. (9) There is a shift of the fine structure discontinuities in the direction of longer wave-lengths as the temperature is raised. For a change from 20°C to 800°C the magnitude of this shift is 5.0 ± 2 volts at a point 115 volts from the K edge. Statements 8 and 9 are illustrated in Fig. 1.

Kronig has shown that the principal experimental facts concerning fine structure may be understood from the theory of the quantum mechanics of electrons in crystal lattices. The theory shows that not every value of velocity is possible to the motion of electrons traveling through a crystal lattice, but rather that there exists an energy spectrum consisting of alter-

nating zones of permitted and forbidden energies. In the case of the isolated atom the electron is ejected from the atom and in addition might be given *any* value of kinetic energy. However, in a crystal lattice the x-ray quantum can only eject an electron from the atom and thereby become absorbed if it gives the electron such a value of kinetic energy as to bring it into one of the permitted energy zones. Thus one will expect variations in the absorption coefficient on the short wave-length side of the main edge related to this sequence of permitted and forbidden energy zones. Kronig shows that for a one-dimensional sequence of periodic potential barriers the forbidden levels fall together with the energy values $W_n = n^2h^2/8ma^2$, where n takes integer values, h is Planck's constant, m is the electronic mass, and a is the distance between successive potential barriers. From this equation, if the lattice constant a increases through thermal expansion the energy zones shift toward the zero level. The magnitude of this shift for Fe agrees with that experimentally observed. Also, the greater distorsion of the periodicity in the lattice at high temperature causes a smearing of the sharp boundaries between permitted and forbidden energy zones and so causes the vanishing of the fine structure.

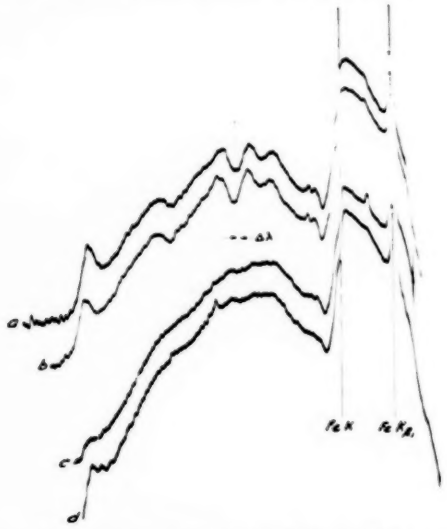

Fig. 1. Microphotometer traces of the K absorption spectra of Fe.
(a) 20°C, (b) 20°C, (c) 770°C, (d) 840°C.

The reciprocal lattice constant squared form of the energy has since been verified in other ways. Lindsay has shown that the fine structure of K in the crystals KCl, KBr, and KI has the same character for each crystal but that the energy separations from the main edge of the corresponding discontinuities in the three spectra are inversely proportional to the squares of the lattice constants. Coster and Veldkamp have demonstrated this same principle by a comparison of the F-C cubic metals Cu, Au, and Pt. They have also found by a study of a Au-Cu mixed crystal that the fine structure discontinuities of the Au L_{III} spectra have shifted to higher energies and the discontinuities of the Cu K spectra have shifted to lower energies by just such amounts that in the mixed crystal they have the same values. They have also shown many interesting facts concerning the intensity of the fine structure.

Recently Kronig has extended his theoretical considerations by investigating in how far it is possible to relate the individual minima of the fine structure, similarly as the lines of an x-ray powder diagram, to the various reflections of the electrons on the lattice planes, and has shown that a decisive agreement between theory and experiment is not obtained in this way.

Nos. 48 to 50 are abstracts of papers which made up a symposium on plasticity.

48. On the problem of the solid state. F. ZWICKY, *California Institute of Technology.*—A discussion will first be given of these particular questions which constitute the problem of the

solid state. One of the most characteristic phenomena exhibited by real crystals is a peculiar coexistence of perfection in certain respects and imperfection in others. This behavior of crystals may be traced back to the fact that the properties of crystals can roughly be divided into two groups, structure insensitive and structure sensitive, of which the latter group is responsible for hysteresis effects.

The problem of the solid state essentially consists in understanding the coexistence of structure sensitive and structure insensitive properties. After it was realized that the theory of the ideal lattices had nothing to offer in the way of a rational explanation of these phenomena, two different attempts were made in order to arrive at a solution.

The first attempt is based on the observation that in general crystals during their growth and existence are very severely affected by certain disturbing effects, such as thermal and mechanical stresses, liberation of dissolved gases, etc., which hinder the formation of ideal crystals. These facts suggest the assumption that all structure sensitive properties are due to *accidental imperfections*. Although this view has many points to recommend itself it cannot be regarded as a solution of the problem of the solid state. The main objection to the *imperfection theory* is that as we grow the crystals more and more carefully the less their structure sensitive properties conform with those which we derive from the theory of ideal crystal lattices.

The second attempt is based on the observation that the physical properties which are peculiar to the crystalline state are extending over distances far greater than the effective action radii of individual atoms and molecules. They therefore suggest the existence of certain *cooperative effects* which are exhibited only if atoms and molecules are present in very great numbers. With this observation in mind the author has undertaken a systematic study of cooperative phenomena whose physical origin is essentially related to forces depending on the distances as $1/r^2$, $1/r^3$, and $1/r^4$ and also on the exclusion principle. Mathematically speaking we are confronted with the problem of conditionally convergent series. If we consider ideal crystals only, intrinsic equations of state for crystals can not exist, as the mentioned cooperative effects introduce effects of the boundaries, no matter how large the crystals are. For this and other reasons a *secondary structure* of crystals is tentatively introduced. The conception of the secondary structure resolves many of the difficulties encountered by the older theories. It also allows us to draw many new conclusions and to predict a great number of phenomena as yet unknown. Finally theoretical and experimental work which has been done so far on the secondary structure will be discussed; special consideration will be given to the problems related to the mechanical and electrical strength of crystals. It also will be shown that the secondary structure, if its exists, will necessitate a generalization of the classical theory of elasticity inasmuch as it renders insufficient the representation of strains and stresses by tensors.

49. Magnetism and plasticity. FRANCIS BITTER, *Westinghouse Research Laboratories, East Pittsburgh, Pa.*—It is the purpose of this paper to show how the above phenomena may be used to throw light on each other. To a first approximation the magnetization of a ferromagnetic sample depends on four factors: the shape of the sample (including such geometrical details as cracks, grain boundaries, etc.), the magnitude of the applied field, its orientation with respect to the crystallographic axes, and the nature of the lattice distortions. If three of these factors are known, the fourth is calculable from the magnetization.

As an illustration the experiments of F. Schmidt (Dissertation Dresden 1931) are discussed. This author measures the induction in iron alloys in a constant field as a function of elongation up to the breaking point. He finds that the induction has a maximum during the elastic expansion, another when the material begins to flow, and a third just before rupture. These maxima indicate either a very peculiar dependence of induction on lattice distortion in iron (which is being further investigated theoretically), or an irregular dependence of lattice distortion on total elongation. Either conclusion would have interesting consequences. Once a satisfactory relationship between lattice distortion and magnetization is established, it becomes possible to make strain analyses with magnetic tools, even during the processes of flow. Becker and Kersten (Zeits. f. Physik, **71,** 553 (1931); **64,** 660, (1930)) have done important work in this direction.

The second part of the paper shows that the unsatisfactory magnetic properties of the outside layers of rolled samples results at least in part from the peculiar distribution of stresses and fibering along the surfaces just under the rolls.

50. Internal dissipational resistance to distortion in solids and its correlation with other physical properties. R. L. WEGEL AND H. WALTHER, *Bell Telephone Laboratories.*—Measurements of two internal dissipation coefficients expressed as equivalent viscosities have been made on samples of a variety of solids including glass, hard rubber, relatively pure metals and alloys. The resonant bar method was used, observing elongational and torsional vibrations within the frequency range 500 to 50,000 cycles per second, and at strain amplitudes 10^{-6} to 10^{-8} cm/cm. At these amplitudes *viscosity* is independent of strain amplitude but not of frequency. In two samples of glass viscosity is inversely proportional to frequency for both extension and torsion, which shows the energy loss per cycle to be independent of frequency and that according to current terminology the mechanism is *hysteretic*. On the assumption that the material is isotropic and that dissipation is associated only with shear, the usual expression for Young's modulus, generalized for vibrations to include viscosity, is $E+ie=9k(N+in)/(3k+N+in)$ in which the imaginary components in each case are products of viscosity and radial frequency. The imaginary components of each elastic coefficient are found experimentally to be very small compared with the real parts, from which it follows that

$$E/N = 2\,(1+\sigma); \qquad e'/n = 4\,(1+\sigma)^2/3$$

in which σ is Poisson's ratio which has a negligible imaginary part. In the glass samples these ratios should be different but experimentally turn out to be equal, suggesting the likelihood that dissipation (nonthermodynamic) is associated with compression to the same extent as with shear. In high purity aluminum samples viscosity varies with frequency to the power $-4/3$ approximately and in nickel to the power $-1/2$ approximately. Other materials follow similar power laws lying between these limits in the frequency range investigated. This suggests that in all except perhaps glass there are within the samples, owing to their structure, relaxation mechanisms having relaxation times of the order of magnitude 10^{-3} to 10^{-5} seconds. The gross plastic relaxation time is usually minutes or hours or more. It is convenient to regard the internal dissipation coefficient of a solid as a complex viscosity, each component of which in general varies with frequency as it does in the case of a gas or a liquid.

Viscosity of solids at room temperature increases with extreme rapidity with temperature, a trend opposite to that in liquids. In steel alloys tested viscosity increases slowly with hardness (Rockwell) up to about the point of brittleness, after which the increase is enormous. During the aging process of lead alloys viscosity changes rapidly. In Pb-Ca (0.04 percent) the increase is over 300 percent, while the electrical conductivity changes by a matter of only 10 percent. In one sample over a year old the change is still in process. With the same heat treatment high purity lead decreases about 20 percent in a week or so, and then remains constant. A test of viscosity should be a useful guide in connection with the development of special alloys when better correlation with other physical properties is available.

AUTHOR INDEX TO ABSTRACTS OF NEW HAVEN MEETING

Abramson, Harold A. and Hans Mueller—No. 6

Bainbridge, K. T.—No. 42
Barton, Vola P. and Geo. A. Lindsay—No. 24
Bayliss, Noel S.—See Gibson
Beams, J. W. and John W. Flowers—No. 35
Bearden, J. A.—No. 46
Beck, F. J. and L. W. McKeehan—No. 2
Berkey, Donald K.—No. 23
Bitter, Francis—No. 49
Bramley, A.—see Swann
Brasefield, Charles J.—No. 36
Bruce, C. W.—No. 34

Cole, Kenneth S.—Nos. 8 and 9
Cooksey, D. and M. C. Henderson—No. 29
Cork, J. M.—No. 25
——— see R. B. Witmer
Cram, W. and J. G. Winans—No. 15
Cunningham, W. Peyton—No. 18
Curtis, H. J.—No. 4

Du Mond, J. W. M.—No. 45
Duncan, J. A.—No. 11

Flowers, John W.—see Beams

Gibson, G. E. and Noel S. Bayliss—No. 13
Gray, J. A.—No. 44
Green, J. B. and R. A. Loring—No. 19

Hanawalt, J. D.—No. 47
Harrington, E. L.—No. 38
Henderson, M. C.—No. 28
——— see Cooksey
Holmes, F. T.—No. 17

Joffe, Joseph—No. 12
Johnson, Thomas H.—No. 32

Kelly, M. J.—see Prescott
Kenty, Carl—No. 22
Kurie, F. N. D.—No. 30

Langer, R. M.—No. 21
Lewis, Charlton M.—No. 16
Lindsay, Geo. A.—see Barton
Loring, R. A.—see Green

McKeehan, L. W.—see Beck
Meserve, Wilbur E.—No. 41
Miller, Henry J.—No. 33
Mimno, Harry R. and P. H. Wang—No. 37
Mueller, Hans—see Abramson

O'Brien, Brian and Vernon L. Parks—No. 10

Parks, Vernon L.—see O'Brien
Prescott, C. H., Jr., and M. J. Kelly—No. 40

Rashevsky, N.—No. 7
Rayton, W. M.—see Wilkins

Spencer, Roy C.—No. 27
Swann, W. F. G. and A. Bramley—No. 31

Van Vleck, J. H.—No. 1
——— see Whitelaw

Walther, H.—see Wegel
Wang, P. H.—see Mimno
Waterman, A. T.—No. 39
Wegel, R. L. and H. Walther—No. 50
Whitelaw, N. G. and J. H. Van Vleck—No. 20
Wilkins, T. R. and W. M. Rayton—No. 43
Williams, J. W.—No. 5
Williams, S. R.—No. 3
Winans, J. Gibson—No. 14
——— see Cram
Witmer, R. B. and J. M. Cork—No. 26

Zwicky, F.—No. 48

CURRENT LITERATURE OF PHYSICS

Extracts from the Tables of Contents of Some of our Contemporaries

NATURE

VOL. 130, NO. 3270 — JULY 2, 1932

Short Reviews:

World Structure and the Expansion of the Universe. By **E. A. Milne** 9

Letters to the Editor:

Mass-Spectra of Helium and Oxygen. By **F. W. Aston** 21

Velocity of Light. By **Olin C. Wilson** 25

Spectrographic Observations of Infrared Lines in the Auroral Spectrum. By **H. Hamada** . 26

NATURE

VOL. 130, NO. 3271 — JULY 9, 1932

Short Reviews:

Professor Planck and the Principle of Causality in Physics. By **Allan Ferguson** 45

Letters to the Editor:

New Evidence for the Neutron. By **Irène Curie and F. Joliet** 57

Concentration of Slow Neutrons in the Atmosphere. By **P. B. Moon** 57

Rectilinear Propagation and Diffraction of Electrons. By **Henry de Laszlo and V. E. Cosslett** 59

Influence of Light on Paramagnetic Susceptibility. By **C. J. Gorter** 60

Infrared Bands in the Aurora. By **Joseph Kaplan** 60

ZEITSCHRIFT FÜR PHYSIK

VOL. 76, NOS. 7 AND 8 — JUNE 20, 1932

γ-Radiation Excited in Boron and Beryllium. By **H. Becker and W. Bothe** 421

Interpretation of the Ramsauer Effect for Symmetrical Diatomic Molecules. By **H. Chr. Stier** 439

Non-Diagram Lines of the $K\,\alpha$-Radiation of Aluminum. By **Erik Carlsson** 471

On a New Form of Light Source for the Excitation of Resonance Fluorescence of Metal Vapors, in Particular of Mercury Vapor. By **F. G. Houtermans** 474

Splitting of Absorption Spectra by Decrease in Temperature. By **W. Kasperowicz** 481

Investigations on Electron Counter Tubes. By **J. N. Hummel** 483

Magnetic Analysis of Internal Stresses. By **M. Kersten** 505

Disaccommodation with Time of Small Symmetrical and Unsymmetrical Hysteresis Loops. By **H. Atorf** 513

Distribution of Intensities in the $N_2\alpha$ and the $NO\beta$ Bands. By **F. Cavalloni** 527

Mechanism of Plasticity. By **N. Seljakow** 535

Dispersion Theory in Metallic Conductors. By **Y. Fujioka** 537

Infrared Characteristic Frequencies of Alkali Halide Crystals. By **Max Born** 559

Some Fundamental Remarks on the Experiments with Cosmic-Ray Coincidences. By **L. Tuwim** 561

DIE NATURWISSENSCHAFTEN

VOL. 20, NO. 26 — JUNE 24, 1932

Deflection of Light in the Gravitation Field of the Sun. By **A. Kopff** 486

Electron Radius and the Collision of Particles. By **E. Guth** 490

On the Disintegration of Matter by Radiation. By **E. G. Steinke and H. Schindler** 491

Procedure to Separate Isotopes in Gaseous Mixtures. By **G. Hertz** 493

DIE NATURWISSENSCHAFTEN

Vol. 20, No. 27 — July 1, 1932

Recognition of the True Nature of Optical Imagery and its Influence on the Understanding of Optical Apparatus in General. By **Moritz v. Rohr** 496

Short Original Communications :

Half-Value Time of Protactinium. By **Aristid v. Grosse** 505

Remarks on the Above. By **Otto Hahn** 505

New Measurements of Cosmic Radiation at High Altitudes. By **G. A. Suckstorff** 506

Contribution to Crystal and Contact Layer Photoeffect. By **W. Bulian and H. Schreiber** . 506

PHYSIKALISCHE ZEITSCHRIFT

Vol. 33, No. 10 — May 15, 1932

Concerning the Influence of α-Radiation on the Electrical Breakdown of Crystals. By **G. Jaffe** 393

Calculation of the Dipole Moments of Molecules with Multiple Axes of Free Rotation. By **C. T. Zahn** 400

On the Multiplex Interference Spectroscope. By **E. Pauls** 405

Torsion Model of Nickel at High Temperatures under Simultaneous Magnetization. By **W. Möbius** 411

Visual Observation of High-Frequency Oscillations by Means of Electrodeless Glow Discharge. By **F. Herold** 418

General Vapor Pressure Apparatus. By **R. Mohr** 419

PHYSIKALISCHE ZEITSCHRIFT

Vol. 33, No. 11 — June 1, 1932

Heat Transfer under Free Convention. By **R. Hermann** 425

New Way to Investigate the Elastic and Plastic Deformation of Polycrystalline Metals by Röntgenographic Processes. By **F. Regler** 435

On the Intensity of the Infrared Water Absorption Bands with the Addition of LiCl- or $LiNO_3$. By **M. Neunhoeffer** 439

Inelastic Scattering of Cathode Rays. By **Ph. M. Morse** 443

On the Absorption of Short Electric Waves in Ionized Gases, an Investigation to Detect a Long Wave-length Region in the Spectrum of Hydrogen Atoms. By **H. Klumb** . 445

Practical Helps on the Building Up and Operation of High Vacuum Apparatus. By **G. Mönch** 447

Demonstration of Standing Electric Waves with the Help of a Simple Receiver. By **R. Ramshorn** 451

On the Streaming of Gases at Low Pressures. By **H. Ebert** 453

PHYSIKALISCHE ZEITSCHRIFT

Vol. 33, No. 12 — June 15, 1932

Cathode Region of the Glow Discharge. By **E. W. Pike** 457

Thermoremanence and Spontaneous Magnetization. By **J. Koenigsberger** 468

Generalized Spinor Calculus and the Dirac Equation. By **L. Infeld** 475

Influence of the Salts on the Minimum Potentials. By **W. Gräwe** 483

COMPTES RENDUS

Vol. 194, No. 23 — June 6, 1932

On the Non-turbulent Rule Beyond a Criterion of Alternate Vertices. By **C. Camichel, P. Dupin, M. Teissie-Solier** 1997

On the Differential Invariants of Groups in Relativity. By **J. Le Roux** 2019

General Theory of the Elastic Suspension of Pendulums. By **J. Haag** 2021

On the Measure of the Resistance Caused by a Viscous Medium to the Movements of a Body. By **G. Siadbei** 2023

Problem Concerning Cylindrical Vertices of a Small Cross Section. By **J. Rossignol** 2026

Magnetic Susceptibility of Sulphur Vapor. By **L. Neel** 2035

Attempt to Coordinate the Infrared Absorption Bands of Some Ring Hydrocarbons. By **J. Lecomte** 2037
Sulphur Phosphorescents: Extinctive Action of the Metals of the Iron Group. By **Maurice Curie and Jean Saddy** 2040
On the Interpretation of a Magneto-Optical Effect. By **Marcel Cau** 2042
On a Partial Solution of the Photographic Integral. By **Jacques de Lassus Saint-Genies** 2045
Goniometric Researches on the Atmosphere. By **R. Bureau** 2073

COMPTES RENDUS

VOL. 194, NO. 24 — JUNE 13, 1932

Simple Relations between the Molecular Spectrum and the Structure of the Molecule. By **H. Deslandres** 2093
Similarity of Hydrodynamical Systems of the Same Order but Without Similar Linear Dimensions. By **C. Camichel and L. Escande** 2105
Intrinsic Form of the Laws of Motion in a Plane. By **Pierre-Ernest Mercier** 2122
Concerning the Role of Rotation of Material Particles in the Evolution of the Universe. By **Emile Sevin** 2124
On Very Thin Crystals Having Curved Contours. By **Lew Kowarski** 2126
Molecular Surfaces and Volumes in Superficial Solutions. By **D. G. Dervichian** 2129
New Optical Properties of Liquids Subjected to Ultrasonic Waves. By **R. Lucas and P. Biquard** 2132
Rules Concerning Polarization of Raman Lines from Crystals. By **Jean Cabannes** 2134
Influence of the Temperature on the Natural and Magnetic Rotation Dispersion of Three Pinens, By **Constantin Salceanu** 2136

COMPTES RENDUS

VOL. 194, NO. 25 — JUNE, 20, 1932

Multiple Point Motion Corresponding to Schrödinger's Equation for the Case of a Single Point. By **A. Buhl** 2195
Direct Measurement of the Magnetic Susceptibility of Liquids by the Curie-Cheneveau Magnetic Balance. By **C. Courty and C. Cheneveau** 2197
Realization of a Black Body at the Boiling Point of Metals. By **T.-N. Panay** 2198
Variation of Wave-length of Rays Emitted by a Very Intense Copper Arc. By **J. Gilles** 2200
Possibility of a Compton Effect in Optics. By **F. Wolfers** 2202
Interpretation of the Magneto-Optic Experiments of Pogany; Influence of Thickness. By **Marcel Cau** 2204
Magnetic Spectrum of β-Rays Emitted by $ThC+C'+C''$. By **S. V. Sze** 2206
Some Experiments on the Radiations Excited by α-Rays in Light Elements. By **Irene Curie, F. Joliot and P. Savel** 2208
Possible Emission of Demi-Helium in the Case of Certain Induced Radioactive Processes. By **Francis Perrin** 2211

LE JOURNAL DE PHYSIQUE

VOL. III, SERIES VII, NO. 5 — MAY, 1932

Diffraction of Electrons by Single Crystals. By **J.-J. Trillat and T.-V. Hirsch** 185
Anomalies in the Viscosity of Solutions in Gelatine. By **M. Pichot** 205
On the Physical Significance of the Groups of Transformations. By **M. Mariani** 219

HELVETICA PHYSICA ACTA

VOL. V, NO. 3

Application of Optics of Turbid Media to the Illumination of the Atmosphere. II. Simplified Expressions for Calculating the Brightness of the Atmosphere. By **P. Gruner** 145
On the Cathode Fall in the Arc Discharge. By **P. Bächtiger and M. Wehrli** 161
Remarks on the International Weston Element. By **E. König and F. Büchmuller** 166
On an Efficient Light Filter for Raman Investigations. By **R. Bär** 174
Dirac's Wave Equation for the Electron and Geometrical Optics. By **W. Pauli** 179

Temperature Effect of Molecular Polarization in Some Gases and Vapors. By **R. Sänger, O. Steiger and K. Gächter** 200
Kipp Apparatus for Electrical Stimulation of Nerves. By **H. König** 212
New Method for Investigating the Diffraction of Very Slow Electrons. By **A. Bühl** 214
New Method to Measure the Einstein-de Haas Effect. By **F. Coeterier and P. Scherrer** .. 217
On the Mechanical Interpretation of the Coercive Phenomena Connected with Spontaneous Magnetization Applied to Various Phenomena. By **A. Perrier** 223
On Electron Collisions in the Arc Discharge. By **W. Pauli** 233

JOURNAL OF THE FRANKLIN INSTITUTE

VOL. 214, NO. 1 JULY, 1932

Microscope-Centrifuge and Some of Its Applications. By **E. Newton Harvey** 1
Transmission of Electrons by Thin Films; An Historical Resume. By **Mildred Allen** 25
Experimental Work on the Transmission of Electrons by Thin Gold Films. By **Mildred Allen** 43
Evidence for the Constitution of the Ether. By **James MacKaye** 73
Rittenhouse Diffraction Grating. By **Thomas D. Cope** 99
Quantum Phenomena in the Biological Effects of Radiant Energy. By **E. U. Condon** 105

JOURNAL OF THE OPTICAL SOCIETY OF AMERICA

VOL. 22, NO. 7 JULY, 1932

Lorentz Double Refraction in the Regular System. By **E. U. Condon and F. Seitz** 393
Intensity, Area, and Distance of Visual Stimulus. By **Ellis Freeman** 402
On the Penetration of Daylight into the Sea. By **E. O. Hulburt** 408
Trichromatic Colorimeter. By **J. Zernike** 418

THE REVIEW OF SCIENTIFIC INSTRUMENTS

VOL. 3, NO. 7 JULY, 1932

Design of Temperature Control Apparatus for Piezo Oscillators. By **Victor J. Andrew** ... 341
Machine for the Graphical Study of the Composition of Simple Harmonic Motions. By **Theodore Soller** 352
Reciprocal Lattice Projecting Ruler and Chart. By **Lucien J. B. LaCoste** 356
Vibrating Reed Oscillograph. By **F. J. Shollenberger** 365
New Method of Measuring Contact Potential Differences in Metals. By **W. A. Zisman** .. 367
Determination of Quality as a Basis for Commodity Standards. By **F. W. Reynolds** 371
Method of Frequency Measurement with the Cathode-Ray Oscillograph. By **Lawrence A. Wood** 378
X-Ray Reflection Spectrograph. By **H. Kersten** 384
New Mercury Vapor Lamp for Laboratory Use. By **Isay Balinkin and D. A. Wells** 388

THE REVIEW OF SCIENTIFIC INSTRUMENTS

VOL. 3, NO. 8 AUGUST, 1932

Field Intensity Meter. By **G. H. Brown and Glenn Koehler** 403
One-Tube Balanced Circuit for D. C. Vacuum Tube Amplifiers of Very Small Currents. By **Walter Soller** 416
Small Experimental Electromagnet. By **S. R. Williams, W. W. Stifler and T. Soller** 423
Cathode Sputtering of Beryllium and Aluminum in Helium. By **P. D. Kueck and A. Keith Brewer** 427
Further Development of the Rotary Voltmeter. By **Paul Kirkpatrick** 430
Improved Device and Method for Adjusting the Cylindrical Camera of the Bernal Universal X-ray Photogoniometer and Similar Instruments. By **Harold P. Klug** 439
Simple Manometer Utilizing a Nonvolatile Liquid of Low Density. By **C. G. Malmberg and Warren W. Nicholas** 440
Foucault Pendulum with Maintained Amplitude and the Measurement of its Apparent Rotation. By **William C. Baker** 444

PHYSICS

VOL. 3, No. 1 JULY, 1932

Amplifier-Oscillograph Applied to the Study of Dielectrics with Continuous Potentials. By **Sigmund K. Waldorf** 1
New Low Noise Vacuum Tube. By **G. F. Metcalf and T. M. Dickinson** 11
Preliminary Note on a New Magnetometer. By **C. A. Heiland** 18
On the Role of the Electric Wind in Electrical Precipitation in Gases. By **Evald Anderson** 23
Eötvös Torsion Balance. By **Donald C. Barton** 29
Application of the Reflection Seismograph. By **Eugene McDermott** 39

REVIEWS OF MODERN PHYSICS

VOL. 4, No. 3 JULY, 1932

Optical Dispersion. By **S. A. Korff and G. Breit** 471
Quantum Theory of Dispersion. By **G. Breit** 504
Quantum Mechanics of Collision Processes. By **Philip M. Morse** 577